JULY · 1953

Proceedings of the I·R·E

A Journal of Communications and Electronic Engineering

Volume 41 Number 7

IRE WESTERN CONVENTION

San Francisco Convention and Tourist Bureau

The Civic Auditorium, shown above, will be the scene of the 1953 Western Electronic Show and Convention to be held in San Francisco, Calif., on August 19-21. For further details, see page 940.

IN THIS ISSUE

TABLE OF CONTENTS INDICATED BY BLACK-AND-WHITE MARGIN, FOLLOWS PAGE 64A

The IRE Standards on Electron Devices: Methods of Measuring Noise appears in this issue.

The Institute of Radio Engineers

for *Stock* Hermetically Sealed Components

For over fifteen years UTC has been the largest supplier of transformer components for military applications, to customer specifications. Listed below are a number of types, to latest military specifications, which are now catalogued as UTC stock items.

RCOF CASE

Length 1 25/64
Width 61/64
Height 1 13/32
Mounting 1 1/8
Screws .....4-40 FIL.
Cutout .....7/8 Dia.
Unit Weight .....1.5 oz.

MINIATURE AUDIO UNITS...RCOF CASE

Type No.	Application	MIL Type	Pri. Imp. Ohms	Sec. Imp. Ohms	DC in Pri., MA	Response ± 2db. (Cyc.)	Max. level dbm	List Price
H-1	Mike, pickup, line to grid	TF1A10YY	50,200 CT, 500 CT*	50,000	0	50-10,000	+ 5	$16.50
H-2	Mike to grid	TF1A11YY	82	135,000	50	250-8,000	+21	16.00
H-3	Single plate to single grid	TF1A15YY	15,000	60,000	0	50-10,000	+ 6	13.50
H-4	Single plate to single grid, DC in Pri.	TF1A15YY	15,000	60,000	4	200-10,000	+14	13.50
H-5	Single plate to P.P. grids	TF1A15YY	15,000	95,000 CT	0	50-10,000	+ 5	15.50
H-6	Single plate to P.P. grids, DC in Pri.	TF1A15YY	15,000	95,000 split	4	200-10,000	+11	16.00
H-7	Single or P.P. plates to line	TF1A13YY	20,000 CT	150/600	4	200-10,000	+21	16.50
H-8	Mixing and matching	TF1A16YY	150/600	600 CT	0	50-10,000	+ 8	15.50
H-9	82/41:1 input to grid	TF1A10YY	150/600	1 meg.	0	200-3,000 (4db.)	+10	16.50
H-10	10:1 single plate to single grid	TF1A15YY	10,000	1 meg.	0	200-3,000 (4db.)	+10	15.00
H-11	Reactor	TF1A20YY	300 Henries-0 DC, 50 Henries-3 Ma. DC, 6,000 Ohms.					12.00

RC-50 CASE

Length 1 5/8
Width 1 5/8
Height 2 5/16
Mounting 1 5/16
Screws .....#6-32
Cutout .....1 1/2 Dia.
Unit Weight .....8 oz.

COMPACT AUDIO UNITS...RC-50 CASE

Type No.	Application	MIL Type	Pri. Imp. Ohms	Sec. Imp. Ohms	DC in Pri., MA	Response ± 2db. (Cyc.)	Max. level dbm	List Price
H-20	Single plate to 2 grids, can also be used for P.P. plates	TF1A15YY	15,000 split	80,000 split	0	30-20,000	+12	$20.00
H-21	Single plate to P.P. grids, DC in Pri.	TF1A15YY	15,000	80,000 split	8	100-20,000	+23	23.00
H-22	Single plate to multiple line	TF1A13YY	15,000	50/200, 125/500**	8	50-20,000	+23	21.00
H-23	P.P. plates to multiple line	TF1A13YY	30,000 split	50/200, 125/500**	8 BAL.	30-20,000	+19	20.00
H-24	Reactor	TF1A20YY	450 Hys.-0 DC, 250 Hys.-5 Ma. DC, 6000 ohms . . . 65 Hys.-10 Ma. DC, 1500 ohms.					15.00

SM CASE

Length 11/16
Width 1/2
Height 29/32
Screw .....4-40 FIL.
Unit Weight .....8 oz.

SUBMINIATURE AUDIO UNITS...SM CASE

Type No.	Application	MIL Type	Pri. Imp. Ohms	Sec. Imp. Ohms	DC in Pri., MA	Response ± 2db. (Cyc.)	Max. level dbm	List Price
H-30	Input to grid	TF1A10YY	50***	62,500	0	150-10,000	+13	$13.00
H-31	Single plate to single grid, 3:1	TF1A15YY	10,000	90,000	0	300-10,000	+13	13.00
H-32	Single plate to line	TF1A13YY	10,000****	200	3	300-10,000	+13	13.00
H-33	Single plate to low impedance	TF1A13YY	30,000	50	1	300-10,000	+15	13.00
H-34	Single plate to low impedance	TF1A13YY	100,000	60	.5	300-10,000	+ 6	13.00
H-35	Reactor	TF1A20YY	100 Henries-0 DC, 50 Henries-1 Ma. DC, 4,400 ohms.					11.00

The *impedance ratings* are listed in standard manner. Obviously, a transformer with a 15,000 ohm primary impedance can operate from a tube representing a source impedance of 7700 ohms, etc. In addition, transformers can be used for applications differing considerably from those shown, keeping in mind that impedance ratio is constant. Lower source impedance will improve response and level ratings . . . higher source impedance will reduce frequency range and level rating.

* 200 ohm termination can be used for 150 ohms or 250 ohms, 500 ohm termination can be used for 600 ohms.
** 200 ohm termination can be used for 150 ohms or 250 ohms, 125/500 ohm termination can be used for 150/600 ohms.
*** can be used with higher source impedances, with corresponding reduction in frequency range. With 200 ohm source, secondary impedance becomes 250,000 ohms . . . loaded response is —4 db. at 300 cycles.
****can be used for 500 ohm load . . . 25,000 ohm primary impedance . . . 1.5 Ma. DC.

United Transformer Corp.
150 VARICK STREET • NEW YORK 13, N. Y.
EXPORT DIVISION: 13 EAST 40th STREET, NEW YORK 16, N. Y. CABLES: "ARLAB"

Changes of address (with advance notice of fifteen days) and communications regarding subscriptions and payments should be mailed to the Secretary of the Institute, at 450 Ahnaip St., Menasha, Wisconsin, or 1 East 79 Street, New York 21, N. Y.

PROCEEDINGS OF THE I.R.E.®

Published Monthly by

The Institute of Radio Engineers, Inc.

VOLUME 41 — *July, 1953* — NUMBER 7

PROCEEDINGS OF THE I.R.E.

INSTITUTE NEWS AND RADIO NOTES SECTION

John R. Ragazzini

DIRECTOR, 1953–1954

John R. Ragazzini, Director of Region 2, was born on January 3, 1912, in New York, N. Y. He received the B.S. and E.E. degrees in 1932 and 1933 from the College of the City of New York, and the A.M. and Ph.D. in 1938 and 1941 from Columbia University.

After a brief association as an engineering aide with one of the New York City departments, Dr. Ragazzini joined the teaching staff of the School of Technology of the College of the City of New York, remaining until 1941. He then joined the faculty of the School of Engineering of Columbia. He is now professor of electrical engineering, in charge of all university courses in electronics and feedback control systems.

During World War II Dr. Ragazzini served as a technical aide on the National Defense Research Committee and as an official investigator in the Division of War Research at Columbia, supervising research contracts in the fields of ultra-high-frequency transmitters and receivers, electronic analogue computers and control systems.

Since 1951 Dr. Ragazzini has again been on partial leave of absence to act as director of the recently established Electronics Research Laboratories of the Department of Electrical Engineering of Columbia. He has also been active as a consultant to industrial organizations and government agencies since 1946.

Dr. Ragazzini joined the Institute as an Associate in 1941, became a Member in 1946, a Senior Member in 1952, and was elected a Fellow in 1953. He has been active in section activities and is a member of numerous IRE committees.

Dr. Ragazzini is a member of the American Institute of Electrical Engineers, the American Society for Engineering Education, Phi Beta Kappa, Tau Beta Pi, Sigma Xi, and Eta Kappa Nu.

Spectrum Utilization

EDWARD W. ALLEN, JR.

The "gold in the hills" of radio communication is the frequency spectrum. Unfortunately, the supply of channels which it offers is strictly limited, and the demands are increasing and insatiable.

The methods used by the United States Government to meet this situation are clearly set forth by a skilled and experienced worker in this field, who is a Fellow of the Institute, and Chief Engineer of the Federal Communications Commission.—*The Editor.*

Within the past few years there has arisen an increasing interest in the effective utilization of the radio spectrum. While there still remains much to be learned about the detailed behavior of radio waves, together with the physical causes thereof, enough has been known for several years to make a general appraisal of applications for which various ranges of the spectrum are suited.

The rapid developments between 1941 and 1945 opened large new reaches of the spectrum, but they also made it clear that the new bands would not provide some of the radio services required by industries which had expanded rapidly within the same period. Then, as now, the greatest congestion arose in the bands suited to long distance communication. Thus there was need for revised service allocations in these bands and new allocations in the newly opened bands, so that the orderly development of services could continue.

The Radio Technical Planning Board was organized by the industry to study the problem and recommend to the Federal Communications Commission bands of frequencies to be allocated to various services. The allocations were completed in 1945 and were incorporated in the International Radio Convention of Atlantic City in 1947. Agreement was reached at the Extraordinary Administrative Radio Conference at Geneva in 1951 as to a procedure for moving existing services into bands allocated at Atlantic City; these moves, requiring several years, are in progress.

It is expected that the general pattern of allocations will be retained for many years, but it is equally to be expected that changes will be made in response to the development of new techniques and new services, and the changing demands of existing services. If the spectrum is to yield the maximum of utility and the changes are to be made smoothly and with a minimum of impact upon emerging and existing services, a vigorous program of spectrum management must be maintained. Continuous surveillance is required to assure that the bands are used to the best advantage by the services to which they are allocated, and to anticipate changes in allocation between services.

The organization necessary to accomplish these ends has already been completed. The Joint Technical Advisory Committee has published its first report on the subject, "Spectrum Conservation." JTAC is now engaged in a study of spurious radiations which constitute a nonproductive spectrum occupancy, and of ways and means for their reduction or elimination. The benefits of these and further studies and recommendations will be made available to those with whom rests final responsibility for determining the nature of spectrum utilization, both nationally and internationally.

The Office of the Telecommunications Advisor to the President fills a need which has been recognized for some years, providing a unified responsibility for the planning of the use of the spectrum and a consolidation and justification for channel requirements by agencies of the Federal Government. The responsibility of the TAP for representing all Government interests in spectrum management should prove to be a significant advance over the former IRAC system, in which each Government agency using radio had a voice.

The resulting dual responsibility, the TAP for Federal Government uses of radio and the FCC for other uses, while perhaps not ideal, can be made to function well. As in any co-operative venture, its success will depend to a large extent upon the determination to make it succeed, upon the mutual recognition and respect of the rights and responsibilities of each party, and upon the support which it receives from those who will be affected by its decisions.

Electronics and the Engineer*

DAVID SARNOFF†, FELLOW, IRE

Introduction

TO BE THE FIRST RECIPIENT of the Founders Award of the Institute of Radio Engineers is a distinction to be cherished. I am profoundly grateful for this significant honor conferred by the world's outstanding group of radio engineers, and accept it with a deep sense of pride.

It has been my pleasure to know the founders of the IRE and many of the engineers who throughout the years have contributed to the growth and renown of the Institute. They have been men of high principle, fervently interested in all phases of radio. The character of the Institute reflects their vision and steadfast adherence to the purposes for which the IRE was founded in 1912.

Early Days of the IRE

As a member of the Institute since its inception, I have always been greatly interested in its activities. I was Secretary of the IRE from 1915 to 1917, and was elected a Fellow of the Institute in 1917.

Our first meetings were held in the days when wireless telegraphy was the inspiration for the presentation of technical papers and discussions. In those days meetings were often looked upon as "ham sessions," for the majority who attended were wireless amateurs—almost everyone had his own station and knew the code. Among them were Hogan, Marriott, Goldsmith, Weagant, Simon, Binns, Godley, Pacent and many others whose names today are recognized throughout the industry as pioneers and leaders.

Imbued with a fraternal spirit that sprang from amateur wireless, the Institute grew in stature. It became a great educational factor in the field of electric communications. As time went on it achieved international prominence, attracting to its platform scientists, engineers and inventors from around the world.

New advances were disclosed in lectures by Marconi, De Forest, Pupin, Hammond, Alexanderson, Beveridge, Hazeltine, Langmuir, Pickard, Kennelly, Armstrong, Zworykin, and a host of others who made history by their revelations in discovery and invention.

There were years, however, when the annual banquet of the IRE was a small and intimate affair and was held in a small room. At the outset there were only 109 members. Today there are 33,000 members. Their diverse interests reveal how radio engineering has broadened in scope and impact within the past decade.

I know of no engineering organization which has contributed more to the advance of radio, television and electronics than this Institute. The topics covered in engineering papers presented in issues of the IRE PROCEEDINGS reflect the measure of radio-electronic expansion.

We find such subjects as klystrons, cyclotrons, synchrotrons, graphechons, magnetrons and orthicons as well as fluorescent materials, microwave relays, ceramics, radioheat, guided missiles, printed circuits and ultra-high frequencies, to mention only a few—a new world of technology and a new vocabulary. All are related to the parent radio. Like the art itself, the Institute has vastly widened its domain.

Under able leadership the Institute has kept abreast of progress. It has recognized the achievements of its members impartially and regardless of competitive considerations.

The IRE is not an organization of old men. It is enlivened by the spirit of young engineers. And even those of us who have been members since the early days of wireless like to think of ourselves as veterans with youthful vision. Youth is to this Institute what the electron is to the science of communications and related fields.

The wireless spark was the signal that brought the pioneers of IRE together. When Robert Marriott was elected first President of the IRE in 1912, radiotelephony was but a hope. Broadcasting was an elusive idea. And television was not even mentioned.

Now the pioneers have a right to smile when they see electronic communications returning to the crystal detector stage via the transistor. These new speck-like crystals not only detect, but amplify and oscillate. What a fantastic idea that would have been in 1912! Those of us who operated crystal detectors—silicon, galena and carborundum—can well marvel at the wonders of germanium and the revolutionary effects that the transistor is destined to create. It is a new tool and the key to vast opportunities.

A Challenging Art

On an occasion such as this it is tempting to conjure up the old days of wireless that live in memory and compare them with the Electronic Age in which we now live. But this is no time for nostalgia. It is in the nature of our life's work to look forward not backward, except to pay tribute to those pioneers who made it possible for us to meet here in 1953 as members of this great Institute.

The latest advances in microwaves and color television, in electron tubes and transistors now attract you to study and discussion. These potential developments brighten your destiny and the future of the Institute. At no time have radio and electronic engineers been in greater demand. Today they are soldiers of science, defenders of the flag. They are in the front line that bulwarks progress and prosperity.

It is fitting that we salute today's engineer who is being led into new dominions of science and industrial accomplishment by the challenge of the electron. His is a future that is fascinating and promising. Even our wildest dreams cannot encompass all the possibilities open to the radio-electronic engineer in the years ahead.

The future is in your hands and those of the engineers who will follow in your footsteps as we have followed the signposts erected by Marconi, De Forest, Fessenden, Armstrong, Zworykin, DuMont, Farnsworth—and others who have marched to fame in the IRE's great cavalcade of science and engineering.

New Fields

Between now and 1960—and that is only seven years away—great changes in industry will take place as a result of developments in solid-state electronics. Indeed, the vacuum tube is approaching its 50th anniversary confronted by a mighty competitor—the transistor.

Present day electronic devices, instruments and systems will be transistorized. This new tool of science will widen the usefulness of electronics. It will spread its applications into many fields which the electron tube has not been able to serve.

Household Products

Within these next few years we should not be surprised to see electronic appliances find their way into the home. Air-conditioners, using electronics, eliminating motors, blowers and compressors, and therefore noiseless in operation, may lead a mighty procession of household products to new markets.

Business Machines

Industrial electronics offers many opportunities for substantial development and expansion. It will revolutionize many phases of business, especially within large organizations. For example, electronic computers can translate, process, compute, store and print pertinent facts and information. They simplify the task, greatly increase the efficiency and perform the functions of an accounting system with utmost speed and accuracy.

Electronics will change clerical operations, relieve men of routine and drudgery and effect enormous savings in time, money and materials. The world of business machines is ripe for electronics.

Inspection Devices

Electronics can also serve in other directions. It promises new aids to health, safety and better living. There are countless applications for the development of inspection methods to insure the highest purity in liquids, vaccines, drugs and all bottled beverages, including milk. Electronics becomes the foe of impurity and contamination in all bottled, packaged or canned products.

Aviation

Another important area for further development and expansion of electronics is aviation, especially in communication and radar. Electronics is the pilot of the robot plane and the hand that guides the missile. Recently the Army exhibited a new rapid-fire radar controlled anti-aircraft gun, which is an electronically guided artillery weapon that searches out and hits with deadly accuracy a hostile aircraft in any weather and destroys it at altitudes up to four miles.

* Decimal classification: R060 × R090.1. Presented, Annual IRE Banquet, New York, N. Y.; March 25, 1953.

† Chairman of Board and Chief Executive Officer RCA, 30 Rockefeller Plaza, New York, N. Y.

Industrial Television

In a few short years we have seen television develop into a major factor in American life. Its extraordinary potentialities for political education, cultural instruction and entertainment have been amply demonstrated. However, many other applications of television's basic function—extension of human sight—are ready for practical use.

Thus far, the phenomenal growth of broadcast television has overshadowed these other applications which operate over closed-circuit systems and constitute the growing field of industrial television. The opportunities for expansion of television in this field are wide.

Wherever danger, remoteness or discomfort preclude the presence of a human observer, the industrial television camera can take his place. Handling of explosives, pouring of castings, watching the operations of furnaces and remote power sub-stations are examples of television's usefulness to industry.

As yet only a negligible fraction of the potential of industrial television has been tapped. The major obstacle has been cost. That obstacle is being overcome by lightweight equipment using the vidicon camera tube. The dimensions of industrial television may surpass the growth in broadcast television we are now witnessing.

At this IRE convention, we will demonstrate a much simplified closed-circuit television system, which provides a vidicon camera attachment for a standard home television receiver. The simple attachment is connected as easily to a television receiver as a record-player and does not affect the normal use of the receiver in any way. With the addition of this camera unit every one of the 23,000,000 television receivers now in use becomes potentially a closed-circuit system for schools, the home and other places.

Schools, in which television sets are becoming more and more a standard classroom fixture, may employ their TV sets to bring talks and demonstrations to the entire school or to selected classes, without the loss of time or the confusion attendant upon a call to assembly. On college campuses the linking of the lecture halls by television will permit exchange of instruction between departments, adding to the variety and interest of the courses. In biological research and technical education, this form of television has proved a valuable tool.

The availability of a simple closed-circuit system will put the television microscope as a new instrument for instruction within reach of every high school and college in the country.

Until now industrial television has been utilized mainly by larger business and industrial organizations, but the reduction in cost brings it within reach of thousands of small businesses.

Many uses are also foreseen for closed-circuit TV in hotels, department stores and other business establishments. A visual intercommunication system between offices for checking papers and documents, between office, factory and warehouse, can now be realized economically.

One of the largest fields ahead for the use of closed-circuit television is the home itself. Closed-circuit sound systems are familiar to Americans. We think nothing of voice communication between rooms in the same house, between offices in the same building, between upstairs and downstairs. We are destined, I believe, to become equally familiar with closed-circuit systems of sight transmission.

When the cost of the camera attachments is sufficiently low to permit their use in the average home they may make the television receiver truly the control center of the home. The snap of a switch will turn the receiver from the broadcast program to view the children asleep in the nursery or at play in the yard, or the cooking on the kitchen range. The housewife will not only hear but see the caller at the door before she opens it.

All the new vistas opening up in electronics cannot be covered in our discussion here. But this much seems certain—As the science of electronics continues to unfold, new discoveries will be made, new inventions will be created and new products and services will be developed. This will steadily increase the size of the electronics industry, its importance for national defense and its value to the public.

Competition Spurs Progress

The United States is fortunate in having a radio-electronic industry made up of so many competent organizations of which the membership of the IRE is representative. The keen competition in research and engineering as well as manufacturing spurs continued effort on the part of all and stimulates scientific and economic advances matched by no other country. Our industrial machine is unequalled anywhere.

Where the interests of the nation and the public are concerned, engineers from the various organizations cooperate effectively. We see an outstanding example of this in the work of the National Television System Committee, comprised of leading engineers of the industry. Through extensive field tests they are today formulating signal standards to be recommended to the FCC for commercial broadcasting of compatible color television with all its inherent advantages.

Through the individual efforts of competing organizations the United States has achieved preeminence in radio, television and electronics. For national defense, the industry of which you as engineers are such a vital part, provides superior equipment developed and produced by American ingenuity and craftsmanship. The finest radio-television instruments and services in the world, and at the lowest cost, are made available to the American home. In achieving this, the industry provides employment for hundreds of thousands of people and contributes vitally to the high standards of living enjoyed in America.

Science and Human Progress

We are reminded by a British philosopher that science as a dominant feature in determining the beliefs of educated men has existed for only about 300 years, and as a source of economic technique for about 150 years. As radio-electronic engineers you therefore belong to a relatively young profession, which the philosopher describes as "an incredibly powerful revolutionary force."

Indeed, as engineers, you have great responsibilities, for through your work you can change living habits, expand knowledge, speed commerce, strengthen national security, disseminate education, spread religion, improve standards of living, and add to the health, comforts, and pleasures of your fellowmen.

These achievements, of course, presuppose that your accomplishments are applied for useful and not destructive purposes. For the ultimate test of the value of new knowledge that scientists discover, of new tools that engineers develop, is in the use which man makes of the new instrumentalities.

I do not subscribe to the theory, occasionally heard, that science has given us machines beyond our moral ability to control. The true spirit of science, it seems to me, is to create not to destroy. We may use our technological knowledge to turn back the clock of civilization, or we can use the forces of science as master keys to wind that clock so that its hands will move continually toward a brighter future for all mankind.

But man must be the master, not the slave of the machine. For the machine has neither mind, nor soul, nor sense of moral values. In the spiritual crusade for a free and peaceful world, science is our strongest ally. Science can help greatly to deter the aggressor from attacking the nations he seeks to conquer or destroy. It may even prevent another world war. Or, if the conflict cannot be averted, science can thwart the enemy's designs and help us immeasurably to win it. Today the research laboratory is a vital part of our national security and progress.

A Memorable Day

On numerous occasions I have been invited to our laboratories to see an invention or new scientific principle demonstrated.

Usually the laboratory is arrayed with all sorts of gadgets, meters, intricate apparatus and a maze of wires that all lead to some focal point of interest—the invention. Sometimes one wonders how in the world all that complex circuitry can be simplified and made to function in a small cabinet suitable for the home. That is where the engineer enters the scene. It is his job to make the invention practical, simple and saleable at a reasonable price.

I shall always remember the day when our research men told me they had something new to show me in television. I went to our Princeton laboratories and the men made good. They turned on two television sets, side by side, and both produced pictures. Then they snapped a switch and one of the sets showed pictures in color!

"This is wonderful," I exclaimed, "when can we demonstrate it to the industry? What you have demonstrated to me proves that all-electronic color television can be made compatible with existing black-and-white sets so that the advent of color will not make them obsolete."

I could see that my enthusiasm and impatience were not exactly in tune with the patience of the research men, for they said it might be six months or a year before they would be ready to stage a general demonstration.

They threw up their hands when I asked, "How about next week?"

Well, to make a long story short, we compromised and within a month members of the industry witnessed all-electronic color

television. And since that time, with impatience prodding patience, the engineers have made miraculous strides in adapting and perfecting compatible color TV for the home.

Today, a color television set in outward appearance is the same as a black-and-white set, but several years ago the equipment needed to receive color was a crate full of gadgets and controls. Thanks to the engineer, color TV now is not far from the home.

Faith and Facts

I have frequently remarked to our scientists and engineers that I have greater faith in them than they have in themselves. But I have been warned on occasion that my faith was stimulated by "an imagination unrestrained by sufficient knowledge of scientific facts." Well, there is ample warrant for that indictment and I plead guilty. But I appeal to this fair and competent jury of scientists and engineers and ask you—Are there not some extenuating circumstances that may lessen in your eyes the size of my sins?

Is it not also a scientific fact that what seemed to be true yesterday is sometimes proved by new knowledge to be false today? For example—Maxwell's theory of the ether as a medium for propagation of light, heat and electric waves, eventually was discarded by the scientific world as "a supreme paradox of Victorian science and yet a triumph of the scientific imagination." It did, however, help the world to understand wireless.

Originally—and this is a classic in the field of communications—Hertz, Marconi and other earlier experimenters used tiny waves. But as wireless developed it was found that long waves more easily covered greater distances. A theory developed that short waves were strictly limited in range. But during World War I commercial experimenters as well as American wireless amateurs were amazed to discover that short waves were more efficient for communication across the hemispheres. It was found that the short waves were reflected from the Kennelly-Heaviside layer, popularly referred to as the "radio mirror" high in the sky. So superior were the results that the early theory was proved fallacious. As a result, short waves became the backbone of world-wide radio.

On more than one occasion theories formulated to help explain a new discovery have proved to be convenient but no more real than the equator of the geographers.

The realm of science with its fact, and sometimes fiction, has always held great fascination for me. Therefore, you as engineers can understand how deeply I was touched in September, 1951, when the men of our Laboratories commemorated my 45 years of service in radio by naming the RCA Laboratories "The David Sarnoff Research Center." After expressing my appreciation perhaps I should have sat down. But the faith I have in scientists, research men and engineers, inspired me to ask them to invent three presents for my 50th radio anniversary, in 1956.

I asked them for an inexpensive tape recorder of television pictures, an electronic air-conditioner, and a true amplifier of light.

Presents Are Under Way

Less than two years have passed, and now I will let you in on a secret. Recently I was given a preview at our Laboratories of some preliminary steps toward my 1956 anniversary presents!

I was surprised at the demonstration I saw of a television program coming from New York and being simultaneously recorded on tape in the Princeton Laboratories 45 miles away. The recording was played back instantly. The quality of the recorded picture still needs improvement—but even its present performance convinced me that I will have the television tape recorder before the time I specified.

Tape recordings will obsolete the use of film for television and reduce over-all costs. Small degradations which mark the various steps in the production of a film, creating a cumulative effect in the final print, will be eliminated. This new method will revolutionize the entire art. As a simpler and cheaper process, it will extend into color television. And it may extend into the motion-picture industry as well.

As you all know, the recording of sound on magnetic tape already has reached a high degree of perfection. When recorded sound has served its purpose it can be wiped off and the tape used over again. I believe that we now stand on the threshold of the same service for sight.

The second present I asked for—an all-electronic air-conditioner—is still in the embryonic stage, but I saw signs of life!

The third present I asked for—a true amplifier of light—is the toughest problem to solve. As you know, the present method is first to convert the light into electricity, next to amplify it, and finally to convert the electricity back into light. Most limitations of television now are due to this complicated and inefficient method of handling light.

I still believe that one of these days we shall learn how to amplify light directly.

Science and Freedom

I hold to the conviction that if we intelligently accept the challenges that spring from our opportunities, the wonders we have witnessed in the past fifty years will be dwarfed. Indeed, the advances of the next half century will make those of our generation pale into insignificance. Our great hope for continued advance stems from the fact that the sum total of our knowledge of science and nature is but a drop in the ocean of knowledge that spreads to the far distant shores of the future.

All of you, as engineers, have a right to take special pride in the fact that America, supremely the land of Liberty, is also supremely the land of science. This is no accident, my friends, but a matter of cause and effect. Freedom is the oxygen without which science cannot breathe. At their best, at their most creative, science and engineering are attributes of liberty—noble expressions of man's God-given right to investigate and explore the universe without fear of social or political or religious reprisals.

Without freedom there can be no genuine research, which is the uninhibited pursuit of truth no matter where it may lead. In the final analysis science is a search for the truth about the natural laws governing the universe.

The task of engineering is to translate those findings into products and services to enrich man's life. The role of radio engineers in this dynamic enterprise has been great. It is destined to be even greater.

Colorimetry in Color Television*

F. J. BINGLEY†, FELLOW, IRE

Summary—**This paper considers the relations between the colorimetric quantities of the system and the electrical signals into which they are encoded for transmission. The type of system considered specifically is that in which the complete video signal comprises a monochrome component together with a color carrier, which collaborate to transmit all of the information necessary for a subjective reproduction of a colored scene. However, the colorimetric equations derived in the paper are quite general, and would apply to any system of color reproduction.**

* Decimal classification: R583×535.6. Original manuscript received by the Institute, May 1, 1952; revised manuscript received January 5, 1952. First part of manuscript presented at the 1951 IRE National Convention, New York, N. Y.; second part presented at the Toronto, Canada, meeting, October, 1951.

† Philco Corp., Philadelphia 34, Pa.

Introduction

THE SCIENCE of colorimetry has developed largely in the environment of the dye, paint, printing, and photographic industries. The fundamentals, which have been so well established by the many pioneer workers in the field of colorimetry, may be extended and applied to color television. It is the purpose of this paper to show how this may be done. Particular reference will be made to a compatible color-television system. The paper will constitute a sequel to an earlier paper by the author[1] to which reference is

[1] F. J. Bingley, "The application of projective geometry to the theory of color mixture," PROC. I.R.E., vol. 36, no. 6, p. 709; June, 1948.

made since many of the techniques disclosed in that paper will be applied in the present instance.

The fundamental quantities of colorimetry, as established by the Commission Internationale de l'Eclairage (usually referred to as CIE), are

$$X = \int E_\lambda R_\lambda \bar{x} d\lambda$$

$$Y = \int E_\lambda R_\lambda \bar{y} d\lambda$$

$$Z = \int E_\lambda R_\lambda \bar{z} d\lambda,$$

where the integrations are taken through the visible region of the spectrum. These quantities are referred to as tristimulus values.

In these equations, the function E_λ represents the power distribution of the illuminant in which the colored object is viewed. The function R_λ represents the reflectance characteristic of the object, that is, the proportion of incident light which is reflected, expressed as a function of wavelength. The three functions $\bar{x}$, $\bar{y}$ and $\bar{z}$ describe the psychophysical characteristics of a standard observer as established by experiments conducted by CIE; they are shown in Fig. 1. It may be noted here that CIE chose the ordinate scale for these quantities so that the areas under them are all equal. As a consequence of this, when the illuminant is equal energy white and the object is uniformly reflecting, the three integrals above become equal, so that $X=Y=Z$ for this case.

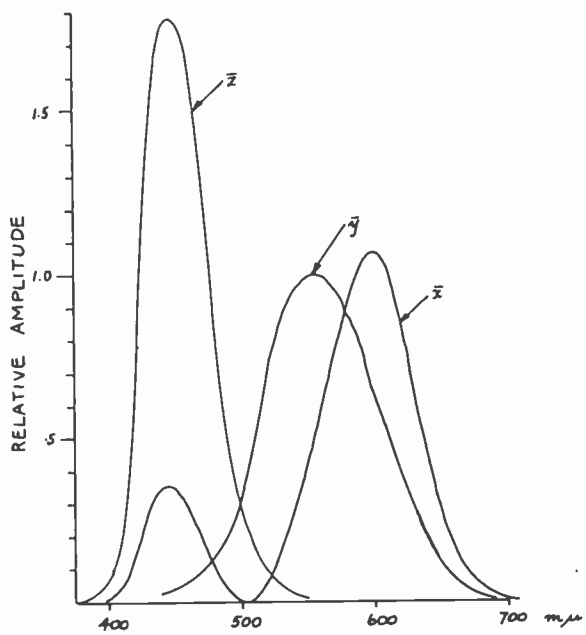

Fig. 1

Using the tristimulus values as fundamentals, other related quantities called "chromaticity co-ordinates" have been defined, namely,

$$x = \frac{X}{X+Y+Z}$$

$$y = \frac{Y}{X+Y+Z}.$$

The quantity $T=X+Y+Z$ is the total tristimulus value. Obviously, it may be written that

$$T = X+Y+Z = \frac{X}{x} = \frac{Y}{y} = \frac{Z}{z}.$$

The tristimulus values express the psychophysical assessment of a color by a standard observer whose characteristics have been established by subjective tests of a number of observers. The chromaticity coordinates provide a convenient method of mapping colors on a chromaticity diagram. A familiarity with this technique will be assumed.

It has been established by experiment that in a mixture of colors the three individual tristimulus values, which describe each of the colors, are individually additive to give the three tristimulus values of the mixture. That is to say, in a mixture of two colors specified by X_1, Y_1, Z_1, and X_2, Y_2, Z_2, the mixture color has tristimulus values X, Y, Z such that

$$X = X_1 + X_2$$
$$Y = Y_1 + Y_2$$
$$Z = Z_1 + Z_2.$$

This leads directly to a fundamental property of the chromaticity diagram, namely, that the point representing a mixture of two colors is at the center of gravity of masses $(X_1+Y_1+Z_1)$ and $(X_2+Y_2+Z_2)$ located respectively at the chromatic points of the two constituent colors. The analogy with mechanics is complete because the total tristimulus value of the mixture color is also the sum of the six tristimulus values which describe the two constituent colors.

For a complete discussion of colorimetric fundamentals reference may be made to the literature, some of which is listed in the references appended to this paper.[2,3]

Reproduction of Colors by Mixtures of Primaries

The philosophy of the preceding paragraph can be extended to cover the mixture of three colors, each specified by its respective set of tristimulus values. These three colors can be mixed to provide a wide gamut of colors, and when so used are referred to as "primaries." The primaries may each be represented by a point on the chromaticity diagram, thus defining what may be called "the triangle of primaries." Any mixture of the three primary colors will produce a color located within the triangle of primaries.

[2] W. T. Wintringham, "Color television and colorimetry," Proc. I.R.E., vol. 39, p. 1135; October, 1951.
[3] W. D. Wright, "Measurement of Color," Adam Hilger, Ltd., London, England; November, 1944.

The Fundamental Colorimetric Equation

The reproduction of a given color by a color-television system implies control of the outputs of at least three separate light sources or primaries at the receiver. These light sources have specified colors generally described as "red," "green," and "blue." Their respective colors may be defined by the appropriate pairs of chromaticity co-ordinates $x_R y_R$, $x_G y_G$, and $x_B y_B$. Their outputs can well be specified by the respective total tristimulus values T_R, T_G, and T_B.

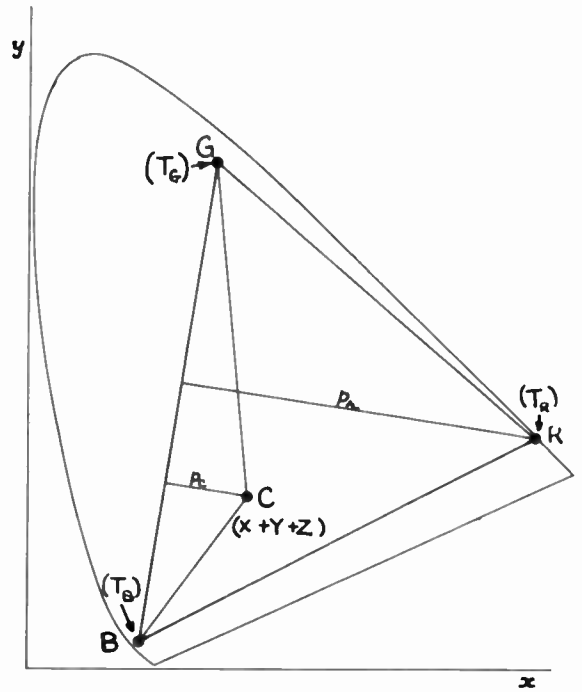

Fig. 2—Fundamental equation for red primary. $T_R \cdot P_r = (X_c + Y_c + Z_c)P_c$; that is, $T_R \cdot \Delta = (X_c + Y_c + Z_c)\Delta_1$, where Δ = area of $\triangle RGB$ and Δ_1 = area of $\triangle CGB$.

Consider a color being produced by a mixture of three primaries. The colorimetrics involved are illustrated in Fig. 2. The primaries are indicated at points R, G, and B. The total tristimulus values which the three primaries are putting out are, respectively, $T_R (= X_R + Y_R + Z_R)$, $T_G (= X_G + Y_G + Z_G)$, and T_B $(= X_B + Y_B + Z_B)$. Because of the mechanical analogy we may, for example, take moments about the line GB, and obtain the fundamental equation given in the caption of this figure. Here p_r and p_c are the perpendicular distances from the red primary and the mixture color C, respectively, to the line GB. The transformation to areal co-ordinates is readily made by multiplying both sides of the equation by $\frac{1}{2}GB$, resulting in the equation shown.

The development of this equation in terms of the chromaticity co-ordinates of the three primaries, which of course are constants for a given receiver, may be carried out as follows: We have, from Fig. 2,

$$T_R \Delta = (X + Y + Z)\Delta, \tag{1}$$

where T_R is the output of the red primary measured in terms of total tristimulus value.

Now the area of a triangle may be simply stated in terms of the co-ordinates of its vertices, leading to the following for Δ and Δ_1:

$$2\Delta = \begin{vmatrix} x_R & x_G & x_B \\ y_R & y_G & y_B \\ 1 & 1 & 1 \end{vmatrix} \tag{2}$$

$$2\Delta_1 = \begin{vmatrix} x & x_G & x_B \\ y & y_G & y_B \\ 1 & 1 & 1 \end{vmatrix}, \tag{3}$$

where x_R, y_R; x_G, y_G; x_B, y_B; and xy are the co-ordinates of the points R, G, B and C, respectively.

By substituting for Δ_1 in (1) and expanding the determinant, there is obtained

$$\begin{aligned} 2\Delta T_R = {} & [y_G(1 - x_B) - y_B(1 - x_G)]X \\ & + [(1 - y_G)x_B - (1 - y_B)x_G]Y \\ & + [x_G y_B - x_B y_G]Z. \end{aligned} \tag{4}$$

There are two similar equations for T_G and T_B

$$\begin{aligned} 2\Delta T_G = {} & [y_B(1 - x_R) - y_R(1 - x_G)]X \\ & + [(1 - y_B)x_R - (1 - y_R)x_B]Y \\ & + [x_B y_R - x_R y_B]Z \end{aligned} \tag{5}$$

$$\begin{aligned} 2\Delta T_B = {} & [y_R(1 - x_G) - y_G(1 - x_B)]X \\ & + [(1 - y_R)x_G - (1 - y_G)x_R]Y \\ & + [x_R y_G - x_G y_R]Z. \end{aligned} \tag{6}$$

There is thus very simply derived a relation between the total tristimulus value put out by the red primary and fixed fractions of the X, Y, and Z tristimulus values of the mixture color. These same fractions hold no matter what the mixture color is, so long as the chromaticity co-ordinates of the three primaries are given stated values. Two similar equations exist for the total tristimulus values T_G and T_B of the green and blue primaries, respectively.

The three fundamental equations may be rewritten

$$T_R = \frac{a_1}{2\Delta}X + \frac{b_1}{2\Delta}Y + \frac{c_1}{2\Delta}Z \tag{7}$$

$$T_G = \frac{a_2}{2\Delta}X + \frac{b_2}{2\Delta}Y + \frac{c_2}{2\Delta}Z \tag{8}$$

$$T_B = \frac{a_3}{2\Delta}X + \frac{b_3}{2\Delta}Y + \frac{c_3}{2\Delta}Z, \tag{9}$$

where Δ is the area of the receiver primary triangle

$$= \tfrac{1}{2}[(x_R - x_B)(y_G - y_B) - (x_G - x_B)(y_R - y_B)]$$

by expanding the determinant in (2) and where

$$\begin{aligned} a_1 &= y_G(1 - x_B) - y_B(1 - x_G) \\ a_2 &= y_B(1 - x_R) - y_R(1 - x_B) \\ a_3 &= y_R(1 - x_G) - y_G(1 - x_R) \\ b_1 &= (1 - y_G)x_B - (1 - y_B)x_G \\ b_2 &= (1 - y_B)x_R - (1 - y_R)x_B \end{aligned}$$

$$b_3 = (1 - y_R)x_G - (1 - y_G)x_R$$
$$c_1 = x_G y_B - x_B y_G$$
$$c_2 = x_B y_R - x_R y_B$$
$$c_3 = x_R y_G - x_G y_R.$$

The coefficients a_1, b_1, c_1, and so on may thus be represented by fixed areas on the chromaticity diagram.

Equations 7, 8, and 9 may be represented more compactly by the following:

$$T_R = \alpha_1 X + \beta_1 Y + \gamma_1 Z \quad (10)$$
$$T_G = \alpha_2 X + \beta_2 Y + \gamma_2 Z \quad (11)$$
$$T_B = \alpha_3 X + \beta_3 Y + \gamma_3 Z, \quad (12)$$

where X, Y, and Z specify the reproduced color, and where the nine coefficients α_1, β_1, γ_1, and so on are functions of the six chromaticity co-ordinates of the three receiver primaries. The values of the coefficients for the NTSC primaries are given in Fig. 3, which also contains a tabulation of other useful numerical coefficients.

The fundamental equations relate the color produced at the receiver to the tristimulus outputs required of each of the receiver primaries. If the system represents a reproducer producing colorimetric fidelity, then the values of X, Y, and Z refer not only to the output color but also to the input.

Useful variations of these equations may be set down. For example, since $Y = yT$, we may write

$$Y_R = y_R T_R = \alpha_1 y_R X + \beta_1 y_R Y + \gamma_1 y_R Z \quad (13)$$
$$Y_G = y_G T_G = \alpha_2 y_G X + \beta_2 y_G Y + \gamma_2 y_G Z \quad (14)$$
$$Y_B = y_B T_B = \alpha_3 y_B X + \beta_3 y_B Y + \gamma_3 y_B Z, \quad (15)$$

where Y_R, Y_G, and Y_B represent the respective luminance contributions of the red, green, and blue primaries.

Two other sets of equations may be written—one set based on the relation $X = xT$, the other based on the relation $Z = (1-x-y)T$. These are of less general use than the luminance equations just written.

Another useful variant is represented by the set

$$T_R = (\alpha_1 + \beta_1 + \gamma_1)Y + \alpha_1(X - Y) + \gamma_1(Z - Y) \quad (16)$$
$$T_G = (\alpha_2 + \beta_2 + \gamma_2)Y + \alpha_2(X - Y) + \gamma_2(Z - Y) \quad (17)$$
$$T_B = (\alpha_3 + \beta_3 + \gamma_3)Y + \alpha_3(X - Y) + \gamma_3(Z - Y). \quad (18)$$

We may also write

$$R = \frac{T_R}{\alpha_1 + \beta_1 + \gamma_1} = Y + p_1(X - Y) + q_1(Z - Y) \quad (19)$$
$$G = \frac{T_G}{\alpha_2 + \beta_2 + \gamma_2} = Y + p_2(X - Y) + q_2(Z - Y) \quad (20)$$
$$B = \frac{T_B}{\alpha_3 + \beta_3 + \gamma_3} = Y + p_3(X - Y) + q_3(Z - Y), \quad (21)$$

where

$$p_1 = \frac{\alpha_1}{\alpha_1 + \beta_1 + \gamma_1}, \qquad q_1 = \frac{\gamma_1}{\alpha_1 + \beta_1 + \gamma_1},$$
$$p_2 = \frac{\alpha_2}{\alpha_2 + \beta_2 + \gamma_2}, \qquad q_2 = \frac{\gamma_2}{\alpha_2 + \beta_2 + \gamma_2},$$
$$p_3 = \frac{\alpha_3}{\alpha_3 + \beta_3 + \gamma_3}, \qquad q_3 = \frac{\gamma_3}{\alpha_3 + \beta_3 + \gamma_3}.$$

From the above set of equations, (19), (20), and (21), when equal energy white is the reproduced color, then $R = G = B$ because, in this case, $X = Y = Z$. The colorimetric quantities R, G, and B are directly related to the channel voltages in a television system. In a linear system, the channel voltages may be derived from R, G, and B by a single dimensionalizing constant relating voltage to tristimulus value; and the channel voltages are often referred to as R, G, and B.

Each primary contributes to the luminance of the mixture color, the total luminance being the sum of the contributions of each primary. The contribution of each primary to the luminance can be expressed by

$$Y_R = y_R(\alpha_1 + \beta_1 + \gamma_1)R \quad (22)$$
$$Y_G = y_G(\alpha_2 + \beta_2 + \gamma_2)G \quad (23)$$
$$Y_B = y_B(\alpha_3 + \beta_3 + \gamma_3)B. \quad (24)$$

One thing clearly brought out by the above equations is that the fundamental building blocks of color are the three tristimulus values by which it is specified. It appears that, if it is required faithfully to reproduce a color, we must have exact knowledge of X, Y, and Z, and must use this knowledge to control the values T_R, T_G, T_B at the receiver. This is true no matter what the receiver primaries are, the only requirement being that we use

	x	y	a	b	c	2Δ
Red	0.670	0.330	0.5474	−0.1526	−0.0826	0.3164
Green	0.210	0.710	−0.2574	0.5226	−0.0074	
Blue	0.140	0.080	0.0264	−0.0536	0.4064	
	$\alpha=\frac{a}{2\Delta}$	$\beta=\frac{b}{2\Delta}$	$\gamma=\frac{c}{2\Delta}$	$\alpha+\beta+\gamma$	p	q
Red	1.7301	−0.4823	−0.2611	0.9867	1.7534	−0.2646
Green	−0.8135	1.6517	−0.0234	0.8148	−0.9984	−0.0287
Blue	0.0834	−0.1694	1.2845	1.1985	0.0696	1.0718

Fig. 3—Values of coefficients for NTSC primaries.

this knowledge in accordance with the coefficients specified in the fundamental equation for the receiver primaries in use.

Encoding of Colorimetric Values

The information concerning the values of X, Y, and Z may be given directly or indirectly. The indirect information may take the form of three independent linear combinations of X, Y, and Z typified by

$$P = lX + mY + nZ,$$

where l, m, and n are constants. Three such equations are necessary, and they must be independent. Such an equation will be referred to as representing a "color package" or "tristimulant." The coefficients l, m, and n may be positive, negative, or zero. The nine values involved (three for each of three color packages) constitute the transmission code.

A typical television system is shown in Fig. 4. For simplicity, wire connections have been shown to enable the fundamentals to be discussed. The matter of packaging information for radio transmission will be discussed later. Here we show the pickup system giving information in the form of three channel voltages proportional to X, Y, and Z. All three of these voltages are fed to the inputs of three separate matrix or mixing units. Each of these matrix units has the function of applying the appropriate coefficients to the three channel voltages entering, so that the output voltage of a given matrix has the same set of coefficients as the corresponding fundamental equation. This will be observed in the equations describing output voltages noted on each of the three output lines, one for each matrix.

The receiving mechanism will be assumed to be a direct-view unit, having three picture tubes, with red, green, and blue fluorescent screens, respectively. The chromaticity co-ordinates defined by the screens determine the coefficients in the fundamental equation, as shown previously. It will be assumed that the tubes are linear in their relation between total tristimulus value and grid voltages. Their assumed characteristics are as shown in the lower part of Fig. 4.

By introducing amplifiers having the gains specified (one between the output line of each matrix and its corresponding red, green, or blue tube) the required output will be produced from each tube to match the input color, since colorimetric quantities exactly appropriate to give correct reproduction have thus been developed.

The system is capable of exact color reproduction within certain limitations. The limitation arises from the fact that certain of the coefficients in the fundamental equation are negative. When the input color has values of X, Y, Z so that a resultant matrix output voltage is negative, the corresponding tube or tubes is incapable of producing an appropriate response. This will be found to occur *whenever the input color lies outside the receiver primary triangle.* Widening the receiver primary triangle to encompass the input color—of course accompanied by the proper readjustment of coefficients as dictated by the fundamental equation—will enable the color to be reproduced accurately. In other words, the information picked up by the camera in the method described is complete and accurate. Any limitation of color-reproduction fidelity is imposed only by the receiver itself.

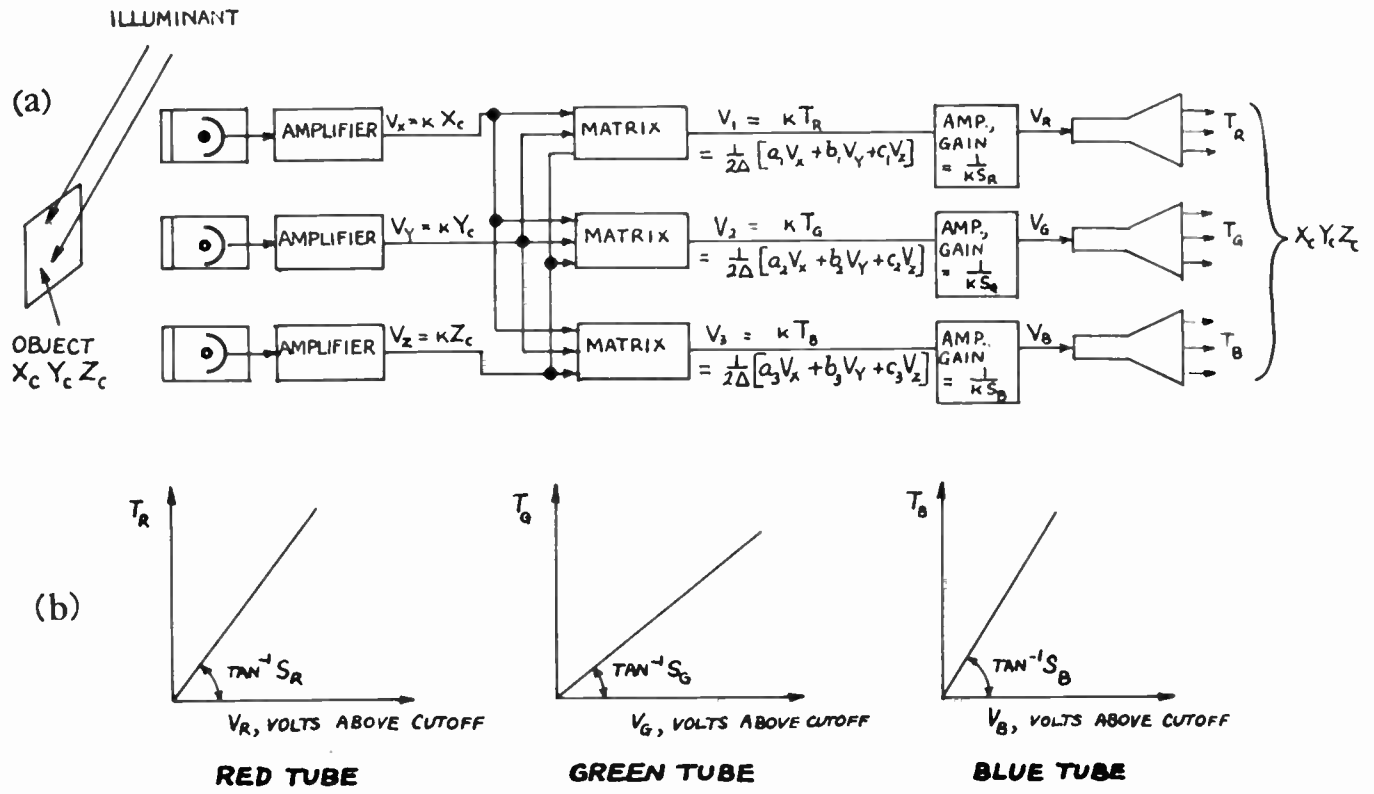

Fig. 4—(a) Diagram of complete system. (b) Characteristics of picture tubes.

Signal Packaging

By this is meant the manner in which the colorimetric information is put together for shipment over the ether. Packaging must be such as to protect the information from significant damage in shipment but no more robust than necessary.

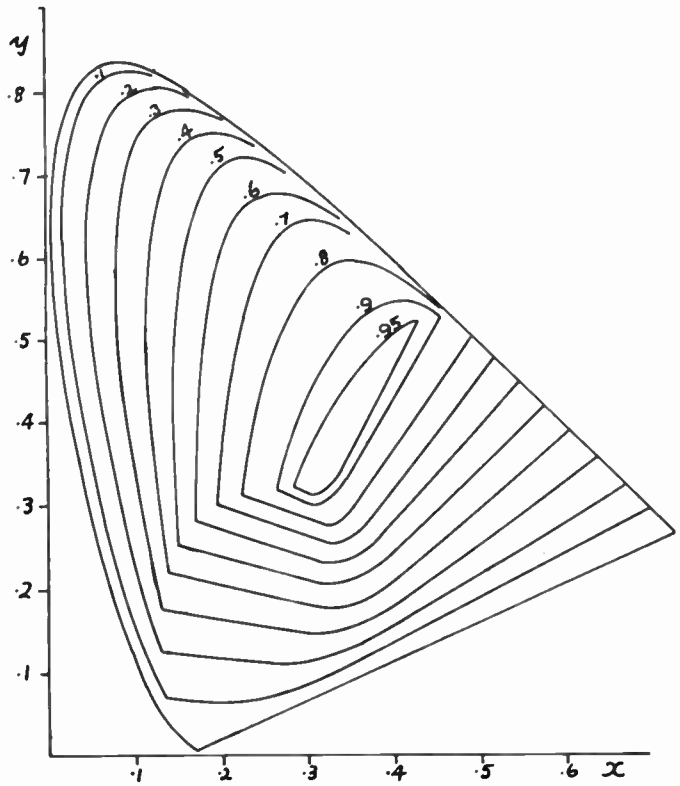

Fig. 5—Maximum demand for Y. Adapted from curves of maximum visual efficiency of colored objects.[4]

An important property of the television system is illustrated in Fig. 5. Briefly, it shows how much luminance a television system may be required to transmit, based on a unit value for a 100-per cent reflectance white object as unity. This will represent the maximum brightness the system will need to handle. As the color of the objects before the camera is changed, less brightness will be required. A stated value of relative brightness defines a contour in the chromaticity diagram—the appropriate decimal values are indicated. These curves were first derived by MacAdam.[4] The curves indicate what any television system (including monochrome) will have to deal with in the way of brightness for input objects of various colors. As was pointed out in the previous paper,[1] the demand values so derived can be exceeded by the presence of self-luminous sources or fluorescent materials in the original scene. Use of spot lights can make similar excess demands occur.

A given point on the chromaticity diagram, once Y is also given, determines unique values for X and Z. Thus similar demand curves can be drawn for X and Z. These are shown in Figs. 5, 6 and 7, respectively. The contour markings indicate the maximum values that the system can be demanded to reproduce at any given point on the chromaticity diagram.

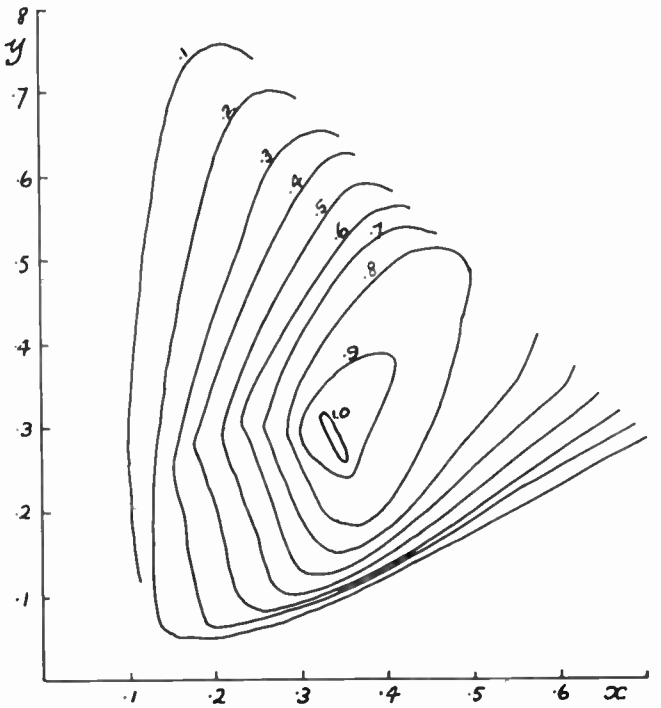

Fig. 6—Maximum demand for X.

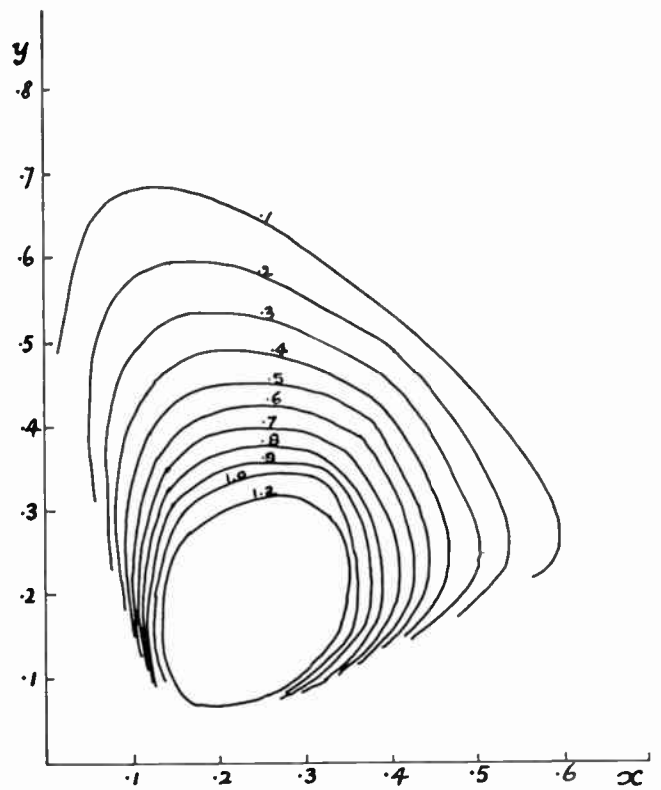

Fig. 7—Maximum demand for Z.

A color-television system with which we have had considerable experience transmits information in packages containing Y, $X-Y$, and $Z-Y$, or rather voltages proportional to these quantities. It is, therefore, interesting to examine the demands for $X-Y$ and $Z-Y$.

[4] D. L. MacAdam, "Maximum visual efficiency of colored materials," *Jour. Opt. Soc. Amer.*, vol. 25, pp. 249–361; 1935.

Demand curves for $X-Y$ are shown in Fig. 8. It may be noted that $X-Y$ and $Z-Y$ are both zero on white. We also note the straight line which is the locus of colors for which $X-Y$ is zero. It divides the chromaticity diagram into two areas. In one of these areas, the quantity $X-Y$ is negative; in the other, positive. Note $X-Y$ has demand values that range from $+0.4$ to -0.4.

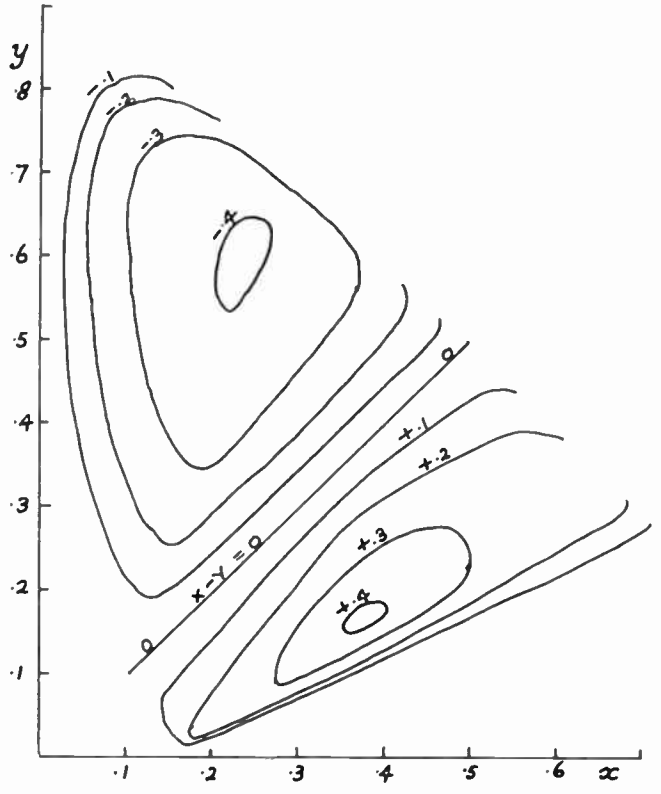

Fig. 8—Maximum demand for $X-Y$.

The corresponding demand curves for $Z-Y$ are shown in Fig. 9. Here is observed another straight line along which $Z-Y$ is zero, which divides the diagram into two parts, one of which has all positive values of $Z-Y$, the other, all negative. The range of $Z-Y$ demand is from $+1$ to -0.8.

In the system referred to, the exact method of packaging is as follows: The luminance information, Y, is transmitted directly over the normal picture carrier, using present monochrome television standards so as to render the system compatible. The balance of the information is placed upon a subcarrier, referred to as a "color carrier." The quantities $Z-Y$ and $X-Y$ are used to amplitude modulate two color-carrier vectors which are in quadrature. The resultant color carrier, which is then both phase and amplitude modulated, is added to the normal Y signal, and the complete signal is transmitted on the normal picture carrier. The color-carrier frequency is chosen to have minimum visibility. Because both $X-Y$ and $Z-Y$ vanish for white input pictures, there is no color carrier on white. This is important since it improves compatibility by ensuring that there is color carrier present only when necessary to transmit color. For the same reason, colors near white have only small carrier amplitudes. This brief description is sufficient to discuss the colorimetrics involved.

The matter of color-carrier demand is obviously very important, for it must share amplitude range with the luminance signal, because the color carrier is superimposed upon it at all times. To examine this, let us look at Fig. 10. This shows the amplitude demanded or the

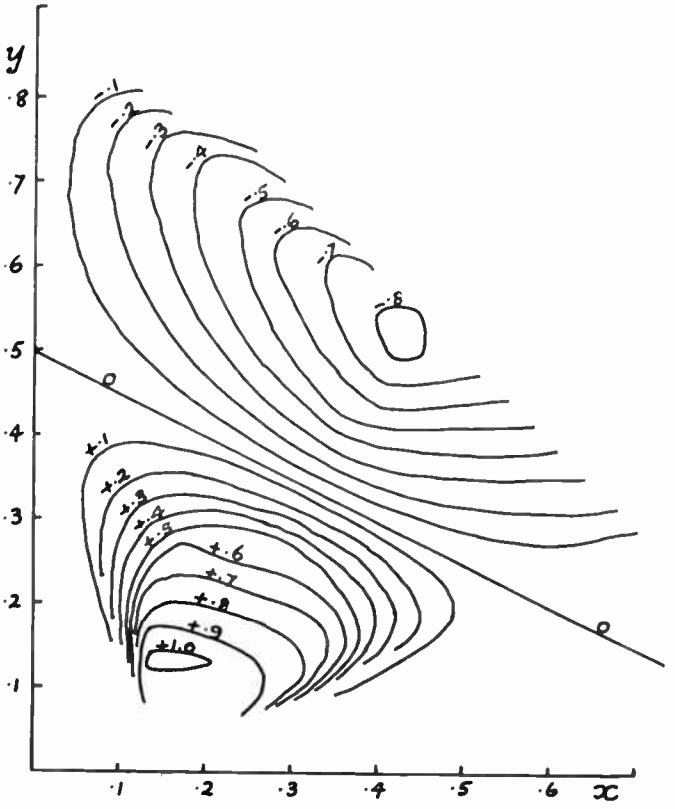

Fig. 9—Maximum demand for $Z-Y$.

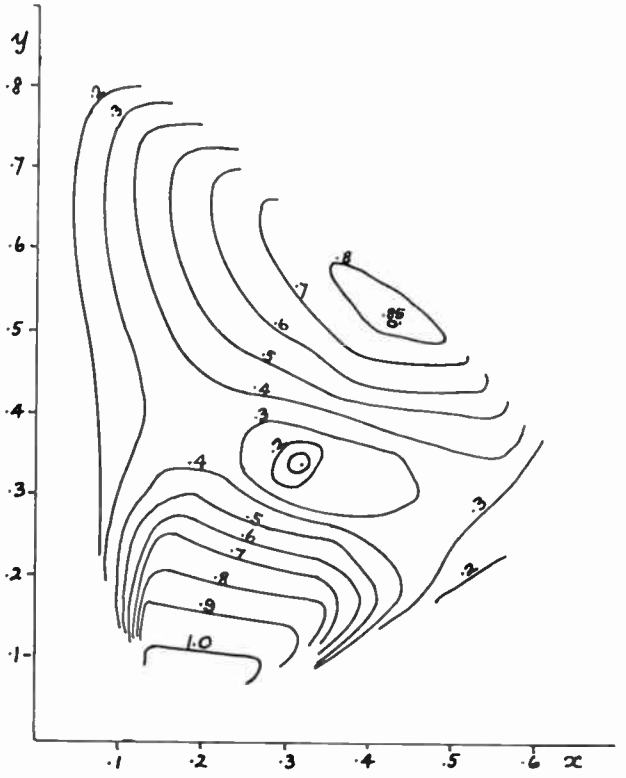

Fig. 10—Color-carrier amplitude at maximum demand. Color-carrier vectors $X-Y$ and $Z-Y$.

$$C = Y_D\sqrt{\left[\frac{X-Y}{Y}\right]^2+\left[\frac{Z-Y}{Y}\right]^2}.$$

color carrier at various colors, for the case that the carrier vectors are related to $X-Y$ and $Z-Y$ by the same constant. The demand is high at 0.85 in the yellow, and also high in blue with a value of 1.0. The color carrier is measured by its peak value on these curves.

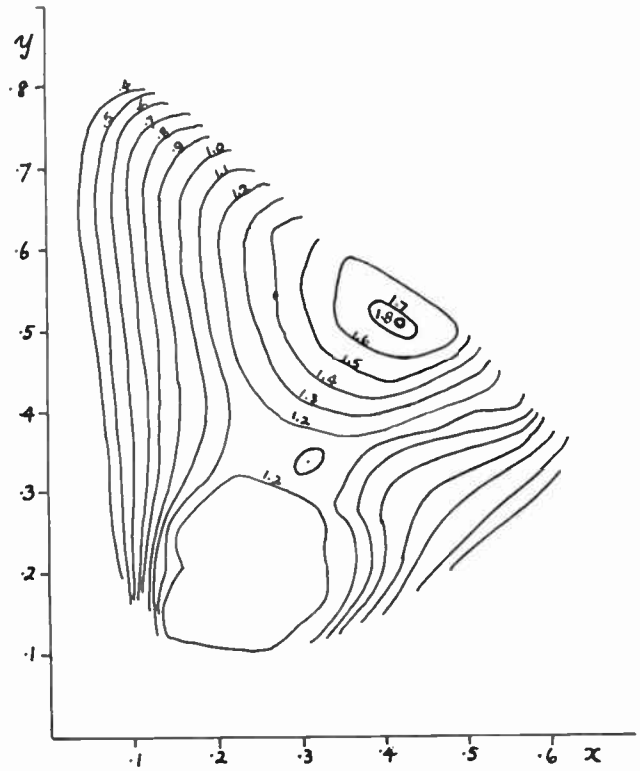

Fig. 11—Peak value of video signal at maximum demand. Color-carrier vectors $X-Y$ and $Z-Y$.

$$V_{peak} = Y_D\left[1+\sqrt{\left[\frac{X-Y}{Y}\right]^2+\left[\frac{Z-Y}{Y}\right]^2}\right].$$

Another set of curves can be drawn assuming that the same constant of proportionality relates the luminance signal to Y as relates to subcarrier vector to $X-Y$ and $Z-Y$. This set of curves is obtained by adding the color-carrier vector to the luminance signal (Y demand curves) to give a mapping of the contours of peak video signal at maximum demand. Fig. 11 shows the result. It shows that the maximum peak signal can occur in the yellow, at 1.8 times the signal at white maximum demand, for which the color carrier vanishes because both $X-Y$ and $Z-Y$ are zero.

Similarly, by subtracting the subcarrier vector from the luminance signal, we can obtain a mapping of trough values at maximum demand; the result is shown in Fig. 12. Note the substantial negative regions, indicating that the subcarrier has dipped down below black level. The maximum negative value is -0.9, a substantial amount of negative swing for which room will have to be provided.

These facts led us to inquire whether a better relative weighting of $X-Y$ and $Z-Y$ could be found. It was determined from colorimetric literature that the eye was much less sensitive to changes in $Z-Y$ than to equal changes in $X-Y$, by a factor of about one-third. It seemed appropriate, therefore, to scale down the $Z-Y$ vector by a factor of one-third, thereby reducing the subcarrier amplitude substantially without materially affecting the performance of the system.

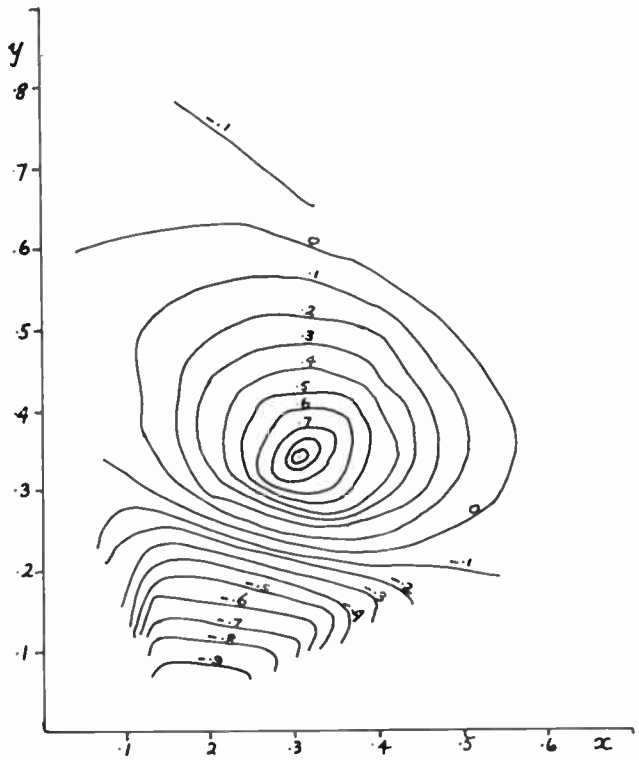

Fig. 12—Trough value of video signal at maximum demand. Color-carrier vectors $X-Y$ and $X-Y$.

$$V_{trough} = Y_D\left[1-\sqrt{\left[\frac{X-Y}{Y}\right]^2+\left[\frac{Z-Y}{Y}\right]^2}\right].$$

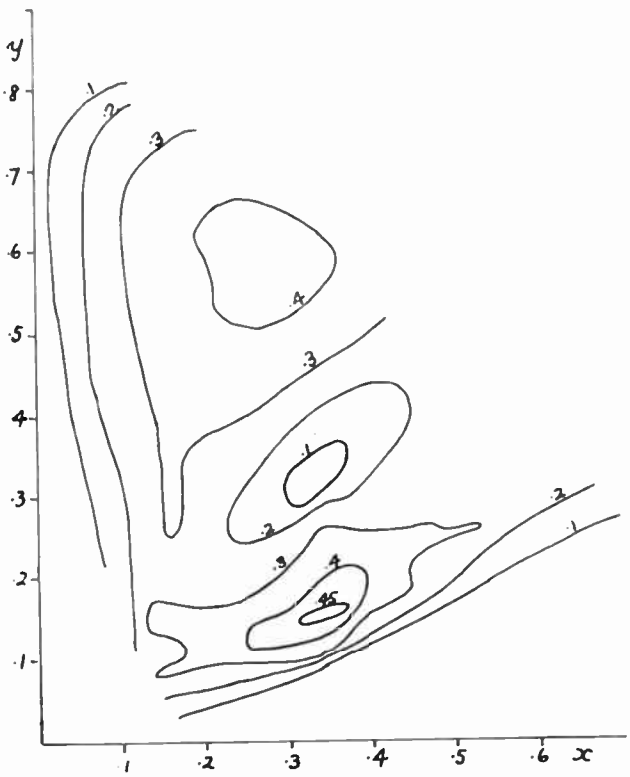

Fig. 13—Color-carrier amplitude at maximum demand. Color-carrier vectors $X-Y$ and $(Z-Y)/3$.

$$C = Y_D\sqrt{\left[\frac{X-Y}{Y}\right]^2+\frac{1}{9}\left[\frac{Z-Y}{Y}\right]^2}.$$

The corresponding color-carrier amplitude at maximum demand is shown in Fig. 13. The peak values are about half those previously shown for equal weighting and the hills have been moved away from the vulnerable yellow and blue regions.

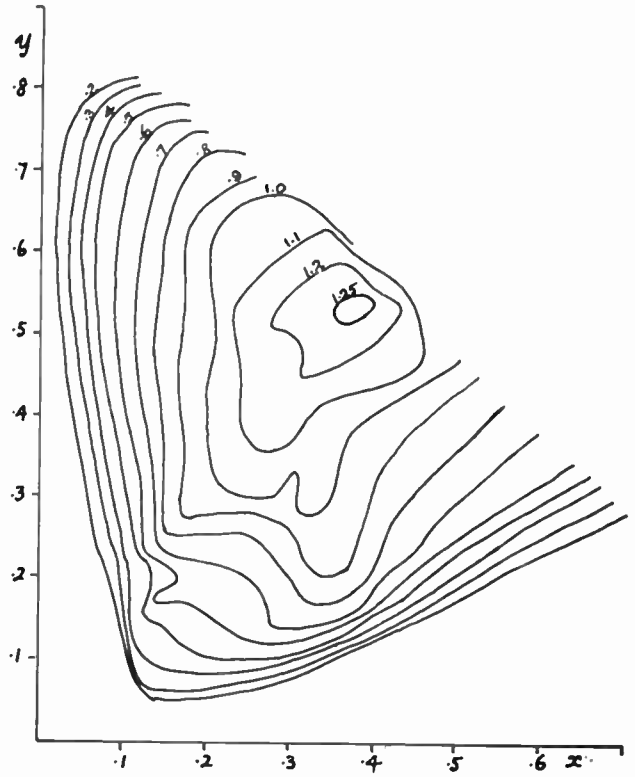

Fig. 14—Peak value of video signal at maximum demand. Color-carrier vectors $X-Y$ and $(Z-Y)/3$.

$$V_{peak} = Y_D\left[1+\sqrt{\left[\frac{X-Y}{Y}\right]^2+\frac{1}{9}\left[\frac{Z-Y}{Y}\right]^2}\right].$$

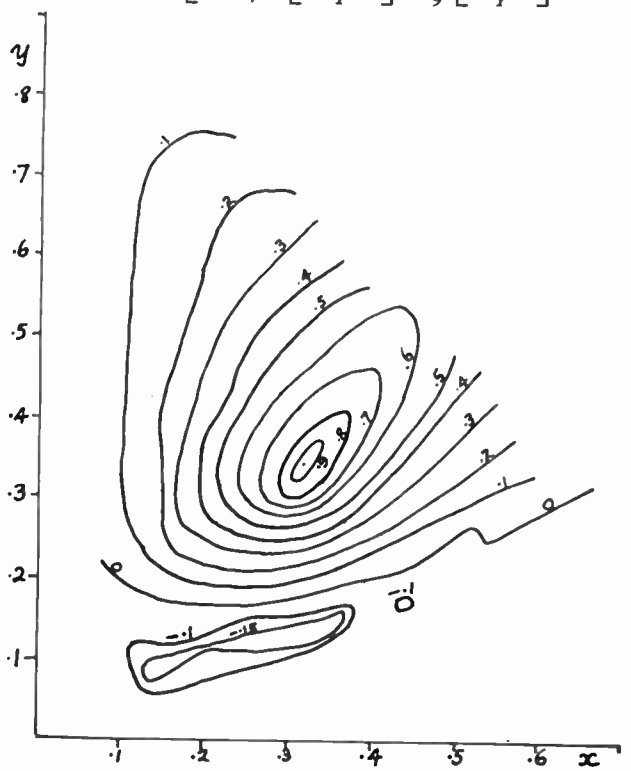

Fig. 15—Trough value of video signal at maximum demand. Color-carrier vectors $X-Y$ and $(Z-Y)/3$.

$$V_{trough} = Y_D\left[1-\sqrt{\left[\frac{X-Y}{Y}\right]^2+\frac{1}{9}\left[\frac{Z-Y}{Y}\right]^2}\right].$$

The improvement in the peak value of video signal at maximum demand is very definite, as Fig. 14 shows. Likewise, Fig. 15 showing the trough value at maximum demand is very greatly improved, the maximum negative excursion being only 0.15.

The degree of improvement is further illustrated in Fig. 16 which shows, for the two cases just discussed, the video signal for certain colors determined to be critical from the signal maps previously shown. It shows that, given equal signal weighting for the carrier vectors, there is required a maximum signal range of the channel 2.6 times that needed for the luminance signal alone under maximum demand conditions. On the other hand, it shows that if the $Z-Y$ vector is reduced by a factor of one-third, the maximum signal range required is only 1.4 times that required for luminance alone.

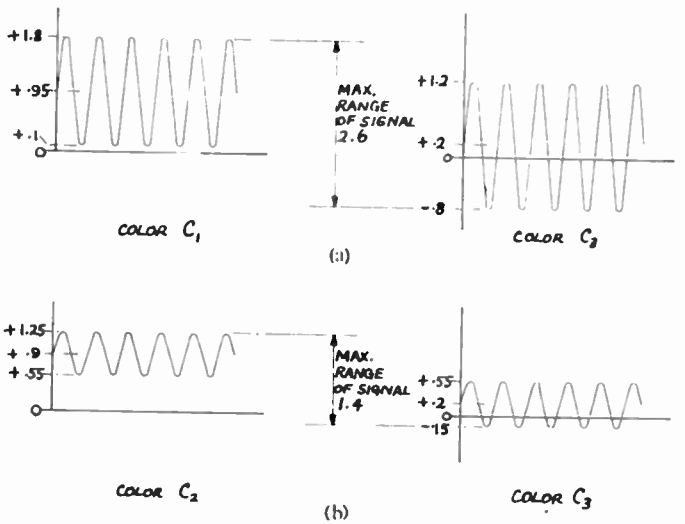

Fig. 16—Video signals at critical colors. (a) Color-carrier vectors $X-Y$ and $Z-Y$. (b) Color-carrier vectors $X-Y$ and $(Z-Y)/3$.

Control of Luminance in a Color-Television System

The control of luminance in a color-television system will now be discussed. Referring to previous equations 22, 23, and 24, these may be added to obtain the total luminance, with the following result:

$$\begin{aligned} Y_R + Y_G + Y_B = {} & (\alpha_1 y_R + \alpha_2 y_G + \alpha_3 y_B)X \\ & + (\beta_1 y_R + \beta_2 y_G + \beta_3 y_B)Y \\ & + (\gamma_1 y_R + \gamma_2 y_G + \gamma_3 y_B)Z. \end{aligned}$$

It will be found that, identically,

$$\alpha_1 y_R + \alpha_2 y_G + \alpha_3 y_B = \gamma_1 y_R + \gamma_2 y_G + \gamma_3 y_B = 0 \quad (25)$$

and

$$\beta_1 y_R + \beta_2 y_G + \beta_3 y_B = 1, \quad (26)$$

so that the equation becomes

$$Y_R + Y_G + Y_B = Y.$$

This equation says that the sum of the luminances of the three primaries equals that of the reproduced color; and further that the values of X and Z exercise no control over luminance. This should be the case, but the calculation provides an interesting check of the fundamental equations.

Luminance equations based on (16), (17), and (18) may be written as follows:

$$Y_R = y_R(\alpha_1+\beta_1+\gamma_1)Y+\alpha_1 y_R(X-Y)+\gamma_1 y_R(Z-Y) \quad (27)$$

$$Y_G = y_G(\alpha_2+\beta_2+\gamma_2)Y+\alpha_2 y_G(X-Y)+\gamma_2 y_G(Z-Y) \quad (28)$$

$$Y_B = y_B(\alpha_3+\beta_3+\gamma_3)Y+\alpha_3 y_B(X-Y)+\gamma_3 y_B(Z-Y). \quad (29)$$

The quantities $X-Y$ and $Z-Y$ belong to a class of tristimulants often called "color differences."

Adding these three equations and making use of identities (25) and (26) we find that

$$Y_R + Y_G + Y_B = Y.$$

It is seen that in performing the summation, the coefficients of $X-Y$ and $Z-Y$ have become zero in virtue of identity (25) above, while the coefficient of Y has become unity in virtue of identities (25) and (26). Thus it is seen that $X-Y$ and $Z-Y$ can exercise no control of luminance.

The Monochrome Signal

In the practice of color television of the type to which this paper refers specifically, one of the tristimulants is transmitted analogously to the main video signal of a monochrome television system. Appropriately this signal is referred to as the monochrome signal.

Two forms of monochrome signal will be considered. The contents of the tristimulant corresponding to these two forms are (1) Y, and (2) $\frac{1}{3}(R+G+B)$, respectively.

We may rewrite the fundamental equations 3 to obtain

$$R = \frac{T_R}{\alpha_1+\beta_1+\gamma_1} = \frac{\alpha_1}{\alpha_1+\beta_1+\gamma_1}X + \frac{\beta_1}{\alpha_1+\beta_1+\gamma_1}Y + \frac{\gamma_1}{\alpha_1+\beta_1+\gamma_1}Z \quad (30)$$

$$G = \frac{T_G}{\alpha_2+\beta_2+\gamma_2} = \frac{\alpha_2}{\alpha_2+\beta_2+\gamma_2}X + \frac{\beta_2}{\alpha_2+\beta_2+\gamma_2}Y + \frac{\gamma_2}{\alpha_2+\beta_2+\gamma_2}Z \quad (31)$$

$$B = \frac{T_B}{\alpha_3+\beta_3+\gamma_3} = \frac{\alpha_3}{\alpha_3+\beta_3+\gamma_3}X + \frac{\beta_3}{\alpha_3+\beta_3+\gamma_3}Y + \frac{\gamma_3}{\alpha_3+\beta_3+\gamma_3}Z. \quad (32)$$

Thus, by addition

$$\tfrac{1}{3}(R+G+B) = \lambda X + \mu Y + \nu Z, \quad (33)$$

where

$$\lambda = \frac{1}{3}\left[\frac{\alpha_1}{\alpha_1+\beta_1+\gamma_1}+\frac{\alpha_2}{\alpha_2+\beta_2+\gamma_2}+\frac{\alpha_3}{\alpha_3+\beta_3+\gamma_3}\right]$$

$$\mu = \frac{1}{3}\left[\frac{\beta_1}{\alpha_1+\beta_1+\gamma_1}+\frac{\beta_2}{\alpha_2+\beta_2+\gamma_2}+\frac{\beta_3}{\alpha_3+\beta_3+\gamma_3}\right]$$

$$\nu = \frac{1}{3}\left[\frac{\gamma_1}{\alpha_1+\beta_1+\gamma_1}+\frac{\gamma_2}{\alpha_2+\beta_2+\gamma_2}+\frac{\gamma_3}{\alpha_3+\beta_3+\gamma_3}\right]$$

and where, obviously,

$$\lambda + \mu + \nu = 1.$$

If we write M for the monochrome signal, then for one case to be considered we have

$$M_1 = Y$$

and for the other case

$$M_2 = \lambda X + \mu Y + \nu Z.$$

The type of receiver display unit will determine the form in which the monochrome signal must be fed to it. For example, if the receiver display is of direct view, it is convenient to feed the monochrome signal directly to all three grids, which are connected together for the purpose. It is customary to have this signal representative of luminance because several receiver advantages are achieved. If the monochrome component of the complete video signal transmitted is M_2, then a conversion must be accomplished at the receiver in order to obtain a monochrome signal proportionate to luminance. The nature of the conversion required may be derived in the following manner:

If

$$M_2 = \tfrac{1}{3}(R+G+B),$$

then

$$M_2 = \lambda X + \mu Y + \nu Z \equiv Y + \lambda(X-Y) + \nu(Z-Y)$$

since

$$\lambda + \mu + \nu = 1.$$

Thus

$$Y = M_2 - \lambda(X-Y) - \nu(Z-Y). \quad (34)$$

This shows that the luminance signal is assembled at the receiver, subtracting pieces of color-difference information obtained from the color carrier. Thus we see that, when the monochrome signal is $\frac{1}{3}(R+G+B)$, this conversion is required. It introduces control of luminance by $X-Y$, $Z-Y$, which we have seen is colorimetrically unnecessary.

The Color Carrier

The complete video signal includes, as noted previously, the monochrome signal and a color carrier. Let us consider now the makeup of the color carrier itself.

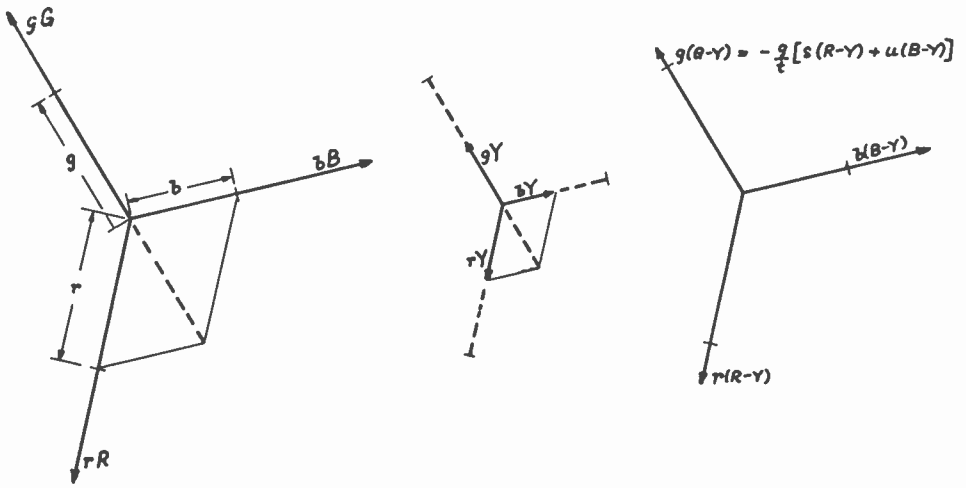

(a) (b) (c)

Fig. 17—(a) Given set of vectors—balanced when $R=G=B$. (b) A set of balanced vectors. (c) Set of vectors equivalent to original set. $Y=sR+tG+uB$, so that since $s+t+u=1$, $-t(G-Y)=s(R-Y)+u(B-Y)$.

Only two quantities are necessary to specify the color carrier completely. These two quantities may be thought of in a variety of ways, but for our immediate purposes they will be thought of as two vectors of specified and fixed phases. These vectors, by their amplitudes, will respectively carry information in the form of voltages proportional to two independent color packages, which together with the first package, the monochrome signal, will completely specify the color being transmitted.

It has appeared advantageous to have color carrier vanish on white, and this leads to a natural choice of $X-Y$ and $Z-Y$ as ingredients from which the two tristimulants controlling the color-carrier vectors are composed. An alternative philosophy of the color carrier considers it to be made up of three vectors whose values are respectively proportioned to R, G, B. If the system is arranged so that the angles between the vectors and the relative magnitudes are so interrelated that when $R=G=B$ the color carrier vanishes, the desired result will also have been achieved.

It is interesting to construct vector diagrams representing the color carrier. These diagrams can be used to display the interconnection between the philosophies involved. For this purpose, Fig. 17 is shown. This indicates at (a), a set of vectors proportioned to R, G, and B with constants of proportionality r, g, b. The geometric relations necessary to insure that this system of vectors is balanced or in equilibrium at white is shown on this figure in the following manner: Lengths representative of the constants r, g, and b have been marked off along the arms of the vector framework. These lengths are indicated on the diagram by dimension lines and witness marks placed at the appropriate points along the vector arms. The condition that the vectors are at equilibrium at white is stated geometrically, simply by completing the parallelogram whose sides are r, b. The diagonal of this parallelogram indicated by the dash line, must then equal g, and must furthermore be collinear with it. The witness marks, denoting the terminal points of lengths r, g, b along the vector framework, will be repeated in succeeding figures. Fig. 17(b) shows a set of balanced vectors which may be constructed on the same angular framework. Here we have chosen to multiply the proportionality constants by the luminance value Y. Obviously, a system of equilibrium vectors results.

This set of balanced vectors may now be subtracted from the original set to obtain a set of color-difference vectors. This is illustrated in Fig. 17(c). Since only two vectors are necessary to specify the color carrier, there is an interrelation between the three vectors which is given by the equation shown on this figure. This interrelation expresses the fact that the luminance is made up of contributions from the red, green, and blue primaries in accordance with the equations previously developed. For brevity we have used the symbols s, t, and u to represent the luminance contribution coefficients.

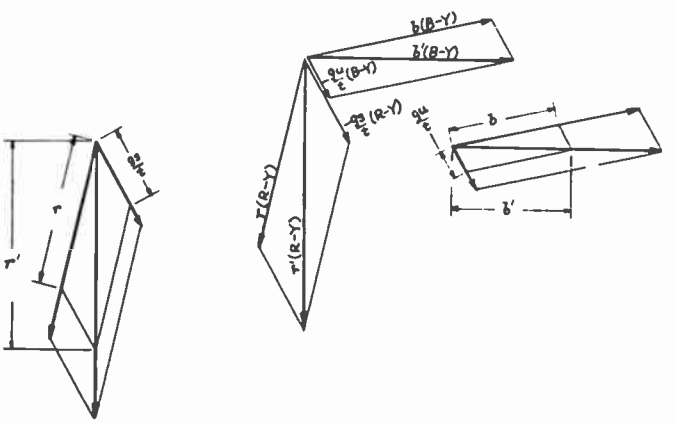

Fig. 18—Original set transformed to two vectors proportional to $B-Y$ and $R-Y$.

Using this interrelation, we may remove one of the vectors by substituting its value in terms of the other two. This is shown in Fig. 18, which shows the color carrier finally reduced to a pair of vectors proportional to $B-Y$ and $R-Y$. The mechanism of the substitution involved is shown in this diagram from which the vector $g(G-Y)$ has been removed by substituting for it its

equivalence in terms of $B-Y$ and $R-Y$. Completion of the vector parallelograms give the resultant $B-Y$ and $R-Y$ components of the complete color-carrier signal. To emphasize the geometry involved, the two individual vector diagrams referred respectively to $B-Y$ and $R-Y$ have been shown in exploded form to the right and left of the main diagram.

As an interesting example of the representation of the color carrier in terms of several sets of vectors, Fig. 19

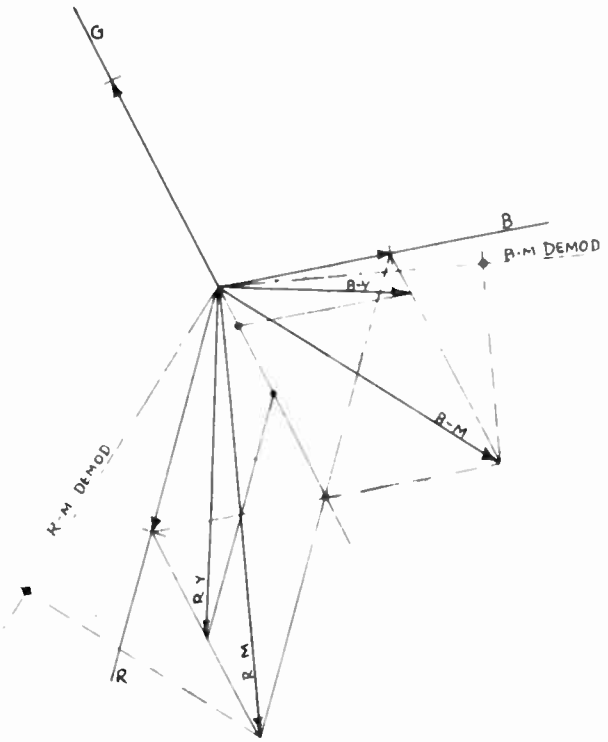

Fig. 19—Composite vector diagram.

is presented. Here we see (a) the original vectors proportioned to R, G, and B, (b) a pair of vectors proportioned to $B-Y$ and $R-Y$ derived by the construction just indicated, which are equivalent to the original set of three vectors, (c) a pair of vectors $B-M$ and $R-M$ derived by a similar construction, which may also be used as a pair of vectors equivalent to the original three vectors, and (d) the demodulation angles which must be used to abstract $B-M$ and $R-M$ information together with the relative amplitudes in which this information will be obtained. It will be seen that by using the methods outlined, a complete graphical analysis of color-carrier representation is provided.

Returning momentarily to the analytical approach, we can develop equations representative of the relations between the various color-difference quantities.

Referring to (19), (20), and (21), we may rearrange them to show that

$$R - Y = p_1(X - Y) + q_1(Z - Y) \tag{35}$$

$$G - Y = p_2(X - Y) + q_2(Z - Y) \tag{36}$$

$$B - Y = p_3(X - Y) + q_3(Z - Y). \tag{37}$$

Thus the signals $R-Y$, $G-Y$ and $B-Y$ are functions only of $X-Y$ and $Z-Y$.

Now let us find the values of $R-M$, $G-M$ and $B-M$. We have from (19), (20), (21), and (33)

$$\begin{aligned} R - M &= Y + p_1(X - Y) + q_1(Z - Y) \\ &\quad - (\lambda X + \mu Y + \nu Z) \\ &= (p_1 - \lambda)[X - Y] + (q_1 - \nu)[Z - Y] \\ &\quad + Y(1 - \lambda - \mu - \nu). \end{aligned}$$

Since $\lambda+\mu+\nu=1$, then must

$$R - M = (p_1 - \lambda)[X - Y] + (q_1 - \lambda)[Z - Y] \tag{38}$$

and, similarly,

$$G - M = (p_2 - \lambda)[X - Y] + (q_2 - \lambda)[Z - Y] \tag{39}$$

$$B - M = (p_3 - \lambda)[X - Y] + (q_3 - \lambda)[Z - Y]. \tag{40}$$

Thus $R-M$, $G-M$, and $B-M$ are functions only of $X-Y$ and $Z-Y$.

We have seen that the color carrier can be represented in terms of the values of $X-Y$ and $Z-Y$. It is possible to derive, from this equivalence, families of loci on the chromaticity diagram which represent the loci of colors for which the color-carrier amplitude per unit of luminance has a constant value. These curves are ellipses, and Fig. 20 shows a set of the curves derived for a pair of orthogonal color-carrier vectors representative of

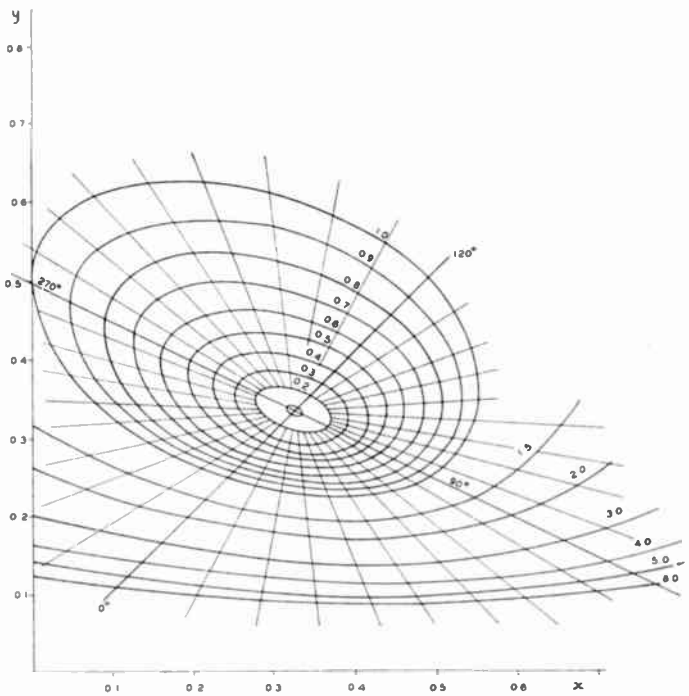

Fig. 20—Locus of colors for which the color-carrier voltage per unit luminance is constant. Color-carrier vectors $X-Y$ and $Z-Y$.

$$\sqrt{\left[\frac{X-Y}{Y}\right]^2+\left[\frac{Z-Y}{Y}\right]^2}=l.$$

Values of parameter l indicated on curves.

$X-Y$ and $Z-Y$, respectively. Also, it shows the loci of constant color-carrier phase. These are straight lines through the white point, as may be proved geometrically. Thus the diagram enables one to define a given color in terms of color-carrier amplitude and phase.

The next figure shows a similar diagram covering the case where the color-carrier vectors are proportioned to $X-Y$ and $\frac{1}{3}(Z-Y)$ (Fig. 21). Here again, the curves of constant color carrier per unit luminance are ellipses, and the lines of constant color-carrier phase are straight lines through the white point. Notice that the phase change per unit distance on the diagram is smallest in the yellow and blue regions, indicating a better compromise particularly in the blue region of the diagram, where it is well known that the eye is very sensitive to small changes in chromaticity.

The National Television Systems Committee has recently adopted a color signal in which the color-carrier vectors are $X-0.98Y$ and $0.30(Z-1.18Y)$ at an included angle of 119°. The color packages represented by these vectors do not vanish on equal energy white, but instead have been selected to vanish on illuminant C. An alternative expression for these signals would be in terms of vectors $B-Y$ and $R-Y$, where these vectors are composed of combinations of color packages $(X-0.98Y)$ and $(Z-1.18Y)$, so that they will vanish

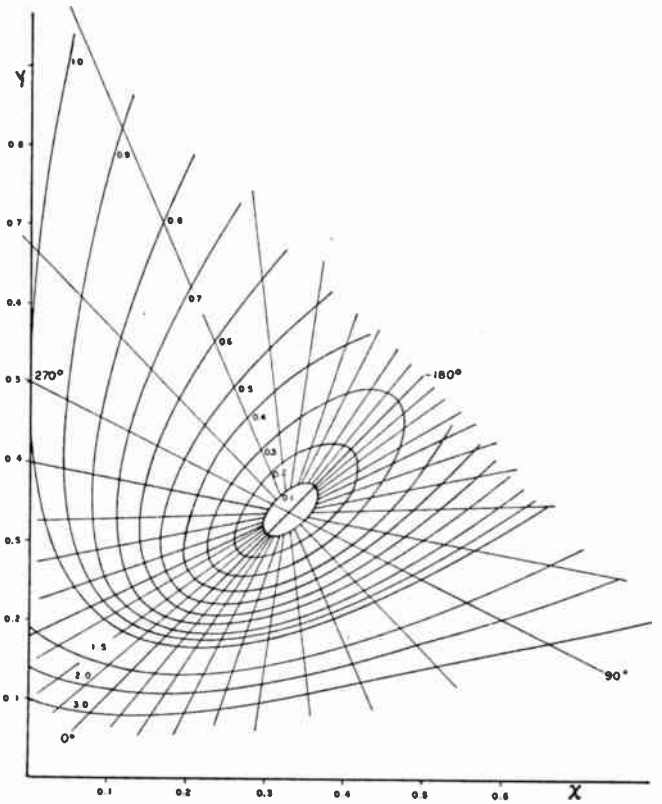

Fig. 21—Locus of colors for which the color-carrier voltage per unit luminance is constant. Color-carrier vectors $X-Y$ and $(Z-Y)/3$.

$$\sqrt{\left[\frac{X-Y}{Y}\right]^2+\frac{1}{9}\left[\frac{Z-Y}{Y}\right]^2}=l.$$

Values of parameter l indicated on curves.

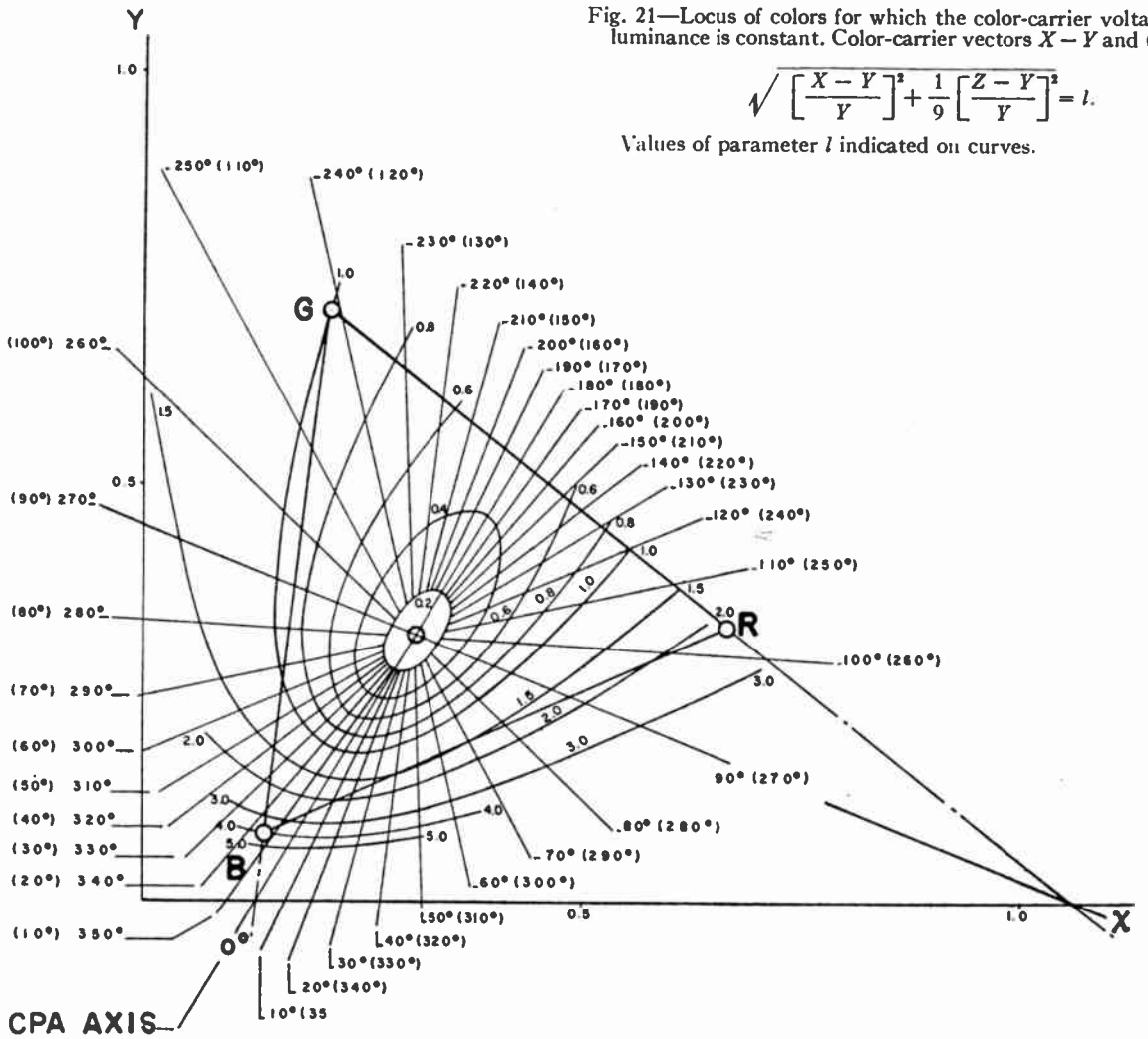

Fig. 22—Color-carrier amplitude per unit luminance, for NTSC color signal. Showing loci of colors corresponding to constant color-carrier phase. Phase lines angular values in parentheses correspond to even fields; other values to odd fields.

on illuminant C. It is possible to draw a similar diagram showing loci of colors having constant color-carrier amplitude and to show on this diagram also the loci of colors having constant color-carrier phase. Because the original proposal made use of CPA, which reverses the phase of the vector proportional to $R-Y$ in successive fields, a given color-carrier phase corresponds, in general, to a different color locus in odd and even fields, respectively. Such a diagram is presented as Fig. 22. The phase reference for this figure is that phase corresponding to positive values of the vector representing $B-Y$. The color synchronizing signal phasor leads this phase by 90°, thereby corresponding to positive values of the $R-Y$ vector in odd fields. A recent modification omits CPA, and changes the phase of the color synchronizing phasor to be that of $-(B-Y)$.

It will be noticed that the ellipses of Fig. 22 are somewhat similar to those of Fig. 21. Also, the closer spacing of the equiphase lines in the yellow and blue regions of the diagram is a feature shared by these diagrams. This similarity arises because the two signals represented on the two figures, respectively, are each intended to recognize the fact that the eye is less sensitive to changes in $Z-Y$ than it is to changes in $X-Y$ and that, therefore, the relative amplitudes of the color-carrier vectors should be suitably proportioned if the best transmission compromise is to be achieved.

Conclusion

It is hoped that the analytical methods described will be found useful in setting up color-television system standards.

The PDF Chromatron—A Single or Multi-Gun Tri-Color Cathode-Ray Tube*

ROBERT DRESSLER†, ASSOCIATE, IRE

Summary—**Described in this paper is a single gun and three gun version of a simple color cathode-ray tube developed by Chromatic Television Laboratories, Inc., based on the ideas of Dr. Ernest O. Lawrence of the University of California. Both types utilize post deflection focusing (PDF) and acceleration as will be discussed in the body of this paper. The principles described are quite general and may be applied to other cathode-ray tube and camera tube designs. The single and three gun types discussed below will operate with any of the presently proposed color television transmission systems.**

The Chromatron

DURING THE PAST few years, considerable attention has been given to the development of various color cathode-ray tubes. The tube described in this paper has been named the Chromatron, a completed picture of which is shown in Figure 1. The shape of this single gun variety is essentially that of a standard metal cathode-ray tube, the only difference being that the cone is made in two sections and welded together to permit the insertion of the color structure after face-plate sealing.

The Color Structure

The color structure is basically the same for both the single and multi-gun tube types, with the exception of the color-phosphor sequence. The current structure consists of a grid of closely spaced wires built up on a frame, the support for which is the color-viewing or image plate on which the phosphors are deposited in parallel strips. Fig. 2 shows a possible color sequence for a single gun tube. The phosphors are deposited on the image plate using conventional screen-printing techniques, after which the phosphors are aluminum-backed.

* Decimal classification: R583.6×R138.31. Original manuscript received by the Institute, August 21, 1952; revised manuscript received February 26, 1953.

† Director of Research and Development, New York Laboratory, Chromatic Television Laboratories, Inc., New York, N. Y.

Directly behind the image plate is a wire grid whose wires run parallel to the phosphor lines. Their placement with respect to the phosphor strips is determined by equation 1.5 and will be discussed more fully later.

Fig. 1—Completed 22-inch Chromatron.

For now, it is sufficient to indicate that the wires fall behind or are related to each red and blue phosphor strip none behind the green.

In the single-gun type, all of the wires that fall behind the red phosphor strips are electrically tied together and are brought out to a single terminal at the side of the tube. Likewise, all of the wires behind the blue phosphor strips are tied together and brought out to an external terminal. In addition to the wire-grid electrodes, there is a third terminal connecting to the aluminum backing on the phosphors.

Between the electrical center of the wire grid and the aluminum coating, a focusing and accelerating potential is applied, which makes a series of converging-cylindrical electron lenses in the front section of the tube. As

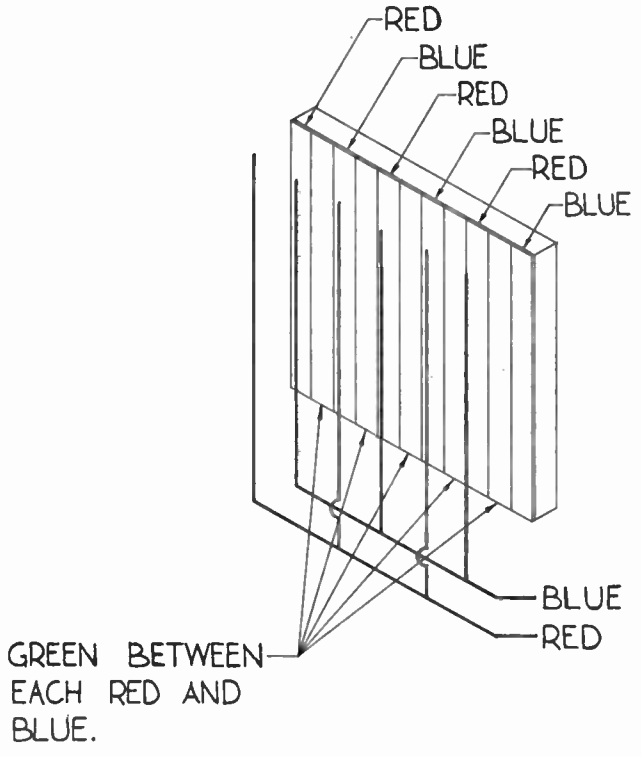

Fig. 2—Schematic representation of the phosphor sequence and placement for the single-gun tube.

electrons travel down the length of the tube from a gun perpendicular to the image plate, they are sharply focused by the series of electrostatic lenses to the green

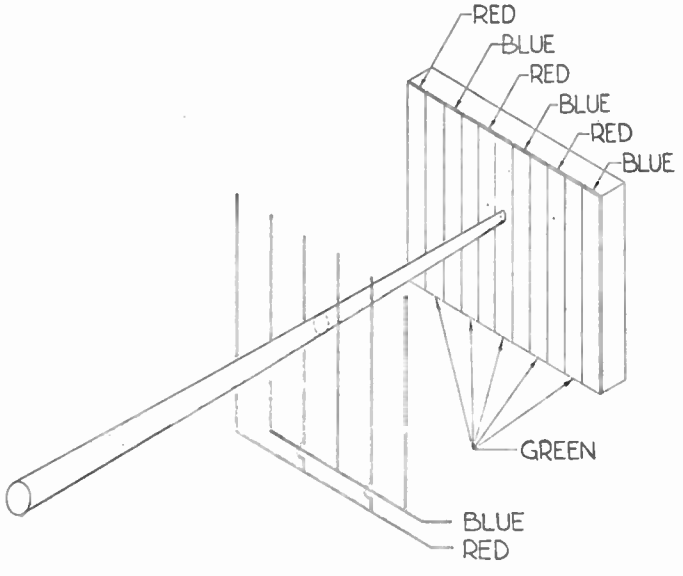

Fig. 3—Sketch showing the focusing action of the electrostatic cylindrical lens.

strips between each red and blue strip, when there is zero potential between the red and blue terminals of the wire grid, as shown in Fig. 3. Thus, a green raster appears on the image plate. Now, a potential difference may be applied between the sets of wires to deflect the focused beam in the direction of the positive wires. This voltage can be made of such a magnitude that the beam will strike a phosphor strip adjacent to the green, thus rendering a red or blue raster on the image plate, depending on which set of wires was positive. Separate colors, therefore, can be displayed by simply switching the potential of these wires. With a color-switching device of this type, the color displayed depends only on the potential of the wires, so that no color distortion or contamination can result from nonlinear sweeps or minor inaccuracies in gun position. In addition, the cylindrical lenses up front focus the beam of electrons into a spot so fine as compared with phosphor-strip width, that the placement of wire behind the phosphors need not be extremely critical.

With the structure just described, it is also possible to have a number of electron guns, each exciting one given set of phosphors. This allows a particular color to be excited by applying the signal voltage directly to the grid of the gun that excites a particular phosphor, as Fig. 4 shows. In this multigun version, no color switch-

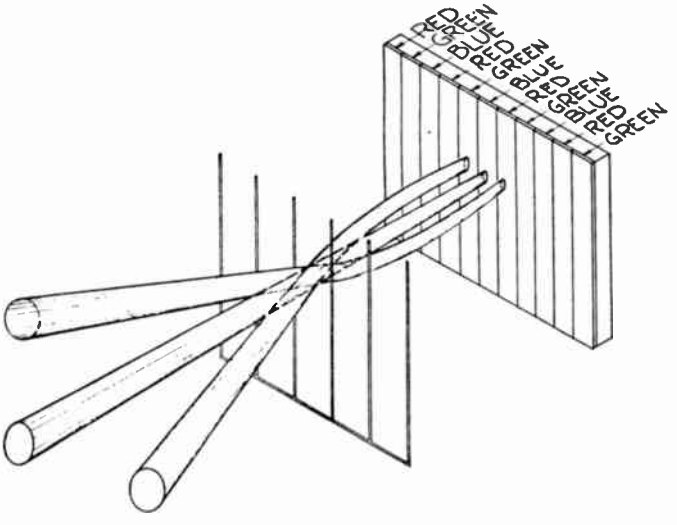

Fig. 4—Sketch of the phosphor sequence and beam focusing action for a 3-gun Chromatron.

ing is required, and the color grid remains at a chosen fixed potential. This potential provides the post-deflection focusing field for the electron lenses. The phosphor sequence for a multi-gun version is red, green, blue, red, green, blue, . . .

As determined from (1.5), electrons that enter the cylindrical lens at different angles are displaced by different amounts on the screen. Therefore, two guns of the three may be slightly inclined, physically or electrically, to the axis perpendicular to the phosphor plate and the electrons from these guns will strike different phosphor strips. The three phosphors are excited simultaneously. Here the beams simply enter a cylindrical lens and are separated out at very high efficiency, allowing smultaneous or rapid switching of the colors. In the three-gun tube, there is no switching required up front since the electron-striking position is determined

by the electron's angle of entry into the electrostatic cylindrical lens. Excellent color purity has been obtained using these methods.

Physical Constants and Drive Requirements

In terms of the potentials applied and the geometry of the tube, the physical constants and the drive requirements for tubes of this type will be derived. The defining symbols for the physical dimensions and potentials are

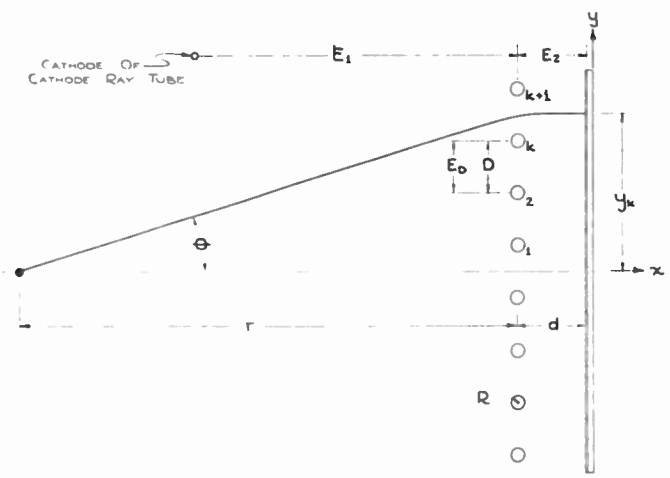

Fig. 5—Schematic cross section of the Chromatron showing relative positions of the various elements. (Complete list of symbols is given in Appendix I.)

shown in Fig. 5. The reciprocal of the mean velocity in the region between wire-grid and aluminum backing at any angle θ is

$$\frac{1}{\bar{v}_x} = \sqrt{\frac{m}{e\,10^7}}\sqrt{\frac{2E_1}{E_2^2}} \cdot \cos\theta\left[\sqrt{1+\frac{E_2}{E_1\cos^2\theta}}-1\right]^1. \qquad (1.1)$$

Defining v_y as the velocity of the electrons parallel to the grid in the same region as above, then

$$\Delta y = \frac{v_y}{\bar{v}_x}\,d \qquad (1.2)$$

is the displacement on the phosphor screen due to v_y, no matter what the cause of v_y.

Evaluating the "y" direction-spot displacement on the screen *due to scanning*, the y component is

$$v_{y_1} = \sqrt{\frac{e\,10^7}{m}}\sqrt{2E_1}\sin\theta,^2 \qquad (1.3)$$

therefore

$$\Delta_{y_1} = d\sqrt{\frac{e\,10^7}{m}}\sqrt{2E_1}\sin\theta\sqrt{\frac{m}{e\,10^7}}\sqrt{2\,\frac{E_1}{E_2^2}} \cdot \cos\theta\left[\sqrt{1+\frac{E_2}{E_1\cos^2\theta}}-1\right], \qquad (1.4)$$

[1] Appendix II.

or simplifying,

$$\Delta_{y_1} = d\,\frac{E_1}{E_2}\sin 2\theta\left[\sqrt{1+\frac{E_2}{E_1\cos^2\theta}}-1\right]. \qquad (1.5)$$

This relationship tells where an electron will strike the screen if it has been deflected by an angle θ, or simply if it arrives at the electrostatic lens at the angle θ. This equation is used to determine the phosphor placement for the single-gun tube. Also, if grid-wire spacing is uniform, this equation is used to determine the electron-arrival angle required for three-gun version of this tube. Equation (1.5) may be rewritten in a form which indicates the electron-strike position for any color cell "k" as follows:

$$y_k = kD + \Delta_{y_1}$$

and

$$\sin\theta_k = \frac{kD}{\sqrt{r^2+k^2D^2}}$$

$$\therefore\quad y_k = kD + \left[\frac{2dE_1Drk}{E_2(r^2+k^2D^2)}\right] \cdot\left[\sqrt{1+\frac{E_2(r^2+k^2D^2)}{E_1r^2}}-1\right]. \qquad (1.55)$$

In actual practice, the phosphor strips are laid down with a constant pitch slightly larger than the distance between wires of the wire grid. A constant chosen with care is an approximate solution to (1.5). If the value of the constant pitch is obtained by substituting $k=1$ in (1.55), (the other parameter specified judiciously) the solution gives tolerable errors to deflection angles of 48 degrees. If a modified pitch is used, say the pitch required for the 142nd wire ($k=142$), then a 74-degree deflection angle is permissible before errors cause color change. In the practical case, considering defocusing at wide-deflection angles, deflection angles between 66 and 69 degrees can be realized without varying the pitch. Curves showing the pitch variation with angle, and the error growths for using the constant pitches indicated above are included in Appendix III as Figs. 10, 11, 12 and 13.

Focus Potential Requirement

The voltage ratio required for focusing the electron beam on the phosphor screen is determined from the electron velocity parallel to the grid. That is

$$v_y = \frac{e\,10^7}{m}\int E_y dl = \frac{e\,10^7}{m}\int \frac{E_y}{v_x}\,dx. \qquad (2.1)$$

In the vicinity of the wire grid, v_x is given as

$$v_x = \sqrt{\frac{2e\,10^7}{m}}\sqrt{E_1}\cos\theta. \qquad (2.2)$$

[2] The subscript 1 denotes that scanning is the cause of the v_{y_1} component.

So

$$v_y = \sqrt{\frac{e\,10^7}{2m}}\,\frac{1}{\sqrt{E_1}\cos\theta}\int E_y dx, \qquad (2.3)$$

therefore

$$\Delta y = \frac{d}{E_2}\left[\sqrt{1+\frac{E_2}{E_1\cos^2\theta}}-1\right]\int E_y dx \qquad (2.4)$$

All that remains is to evaluate $\int E_y\,dx$.

Since all wires are at the same potential, and all lines of force from the wires end on the screen, the deflection for an electron passing midway between two wires is zero by symmetry. For an electron passing at a distance y_0 from the center, $\int E_y\,dx$ can be evaluated by applying Gauss' theorem to an integral of the normal component of the field taken around the following path. The integrals from A to B and from B to C are zero since along these paths, E_y and E_x are zero, respectively. The integral from D to A has the value y_0E_2/d since E_x is approximately equal to E_2/d at the screen. Having evaluated this and noting that the total charge inside this path is zero, it follows that

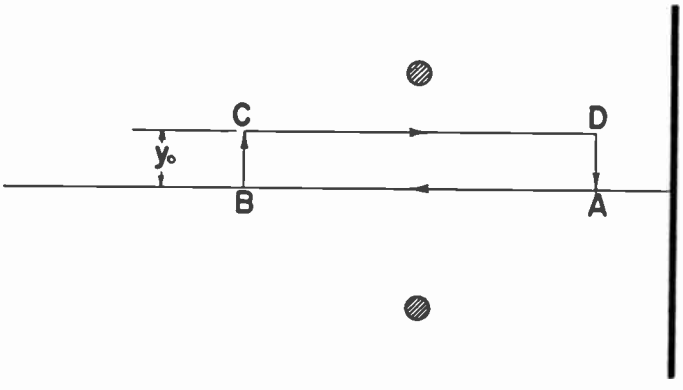

Fig. 6—Path of integration to evaluate $\int E_y dx$ to determine the electron displacement at the striking surface due to the focusing action of the cylindrical lens.

$$\int E_n d\Sigma = \int_{AB=0} + \int_{BC=0} + \int_{CD\ \text{Req'd Integral}} + \int_{DA=\frac{y_0E_2}{d}} = 0$$

$$\therefore \quad \int E_y dx = \frac{-y_0E_2}{d}. \qquad (2.5)$$

Therefore, displacement or focusing effect is given by

$$\Delta y_f = -\left[\sqrt{1+\frac{E_2}{E_1\cos^2\theta}}-1\right]y_0. \qquad (2.6)$$

For perfect focusing $\Delta y_f = -y_0$, therefore

$$\sqrt{1+\frac{E_2}{E_1\cos^2\theta}}-1=1 \text{ or } 1+\frac{E_2}{E_1\cos^2\theta}=4$$
$$\therefore \quad \frac{E_2}{E_1\cos^2\theta}=3. \qquad (2.7)$$

The required ratio is a function of θ. If the voltages are set so that $E_2=3E_1$, the focusing is perfect at $\theta=0$ degrees and fails to be perfect by 4.5 per cent of the phosphor-strip width or 0.67 mils at $\theta=30$ degrees. By a small change in E_2, this error can be divided so that about half appears at $\theta=0$ degrees and half at $\theta=30$ degrees. In this manner, focusing is obtained with negligible defocusing with a flat screen over the complete angular range from 0 to 36 degrees for the half angle.

Color Switching Potential Requirement

The preceding relationships are useful for both single or three-gun tubes. The last expression to be derived will indicate the required color-switching potential for the *single-gun tube* in terms of its geometry; that is, the voltage required to deflect the electron beam from the green-phosphor strip to either a red or blue. Obviously, no switching voltage is required for the three-gun tube. With this derivation, the problem again resolves itself into evaluating $\int E_y\,dx$ but over a different path. Neglecting the accelerating potential since its effect is known, the focusing region of the tube with a potential E_d placed between the grid wires can be examined. All lines of force due to the deflecting potential begin and end on grid wires. The deflecting force is found by applying a modified Gauss' theorem to the following path. Let each wire bear a charge of $-q$ and $+q$ coulombs per unit length. If the region considered is not too close to the end of the grid, E_y along AB is zero by symmetry. E_x along BC and DA are zero; therefore

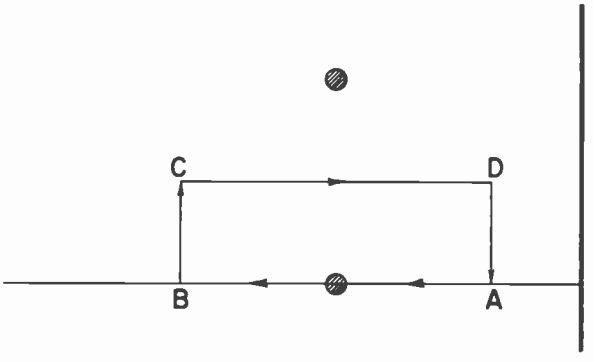

Fig. 7—Path of integration to evaluate $\int E_y dx$ to determine the potential difference required between the wire grids to switch the electron beam from one colored phosphor to the next.

$$\int E_y dx = \frac{4\pi}{\mathcal{E}}Q \text{ inside} = \frac{4\pi q}{2\mathcal{E}}. \qquad (3.1)$$

Since the electric field due to the deflecting potential is zero along BC and DA, there is no difference in deflection for any two paths through the same gap between wires.

The charge q is equal to CE_D where C is the capacity between wires per unit length of wire. So

$$\int E_y dx = \frac{2\pi CE_D}{\mathcal{E}}, \qquad (3.2)$$

and

$$v_y = \sqrt{\frac{e\,10^7}{2m}}\,\frac{2\pi C E_D}{\mathcal{E}\sqrt{E_1}\cos\theta}. \qquad (3.3)$$

Therefore, the displacement at the screen is

$$\Delta y_D = \frac{d}{\mathcal{E}F_2}\left[\sqrt{1+\frac{E_2}{E_1\cos^2\theta}}-1\right]2\pi C E_D, \qquad (3.4)$$

Setting $E_2=3E_1$ and $\theta=0$,

$$\Delta y_D = \frac{2\pi C d}{\mathcal{E}}\,\frac{E_D}{E_2} = \frac{2}{3\mathcal{E}}\,\pi C d\,\frac{E_D}{E_1}. \qquad (3.5)$$

The angular variation here is much the same as in the case of focusing. With a compromise accelerating voltage, the displacement can be held to within 4.5 per cent of phosphor-strip width for an angular range from 0 to 34 degrees. For a fixed-beam displacement, the switching potential required varies inversely as the capacity; for higher-definition tubes where the wires are closer together, the deflection voltage and therefore the driving-power requirement is actually diminished. To express this potential completely in terms of the geometry of the tube, the capacity between wires per unit length is shown approximately as

$$C = \frac{\mathcal{E}}{4\ln\dfrac{D}{R}}. \qquad (3.6)$$

To switch colors the beam must be deflected $1/3D$. So

$$E_D = \frac{2E_1}{\pi}\,\frac{D}{d}\ln\frac{D}{R}. \qquad (3.7)$$

This is the required color-switching voltage in terms of the geometry of the tube.

To give some idea of the actual numbers that comprise a complete design, note: for a tube with the wires placed 320 mils behind the phosphor screen, a distance between wires of 30 mils, wire diameter 6 mils, the accelerating potential $E_1=4{,}000$ volts, the switching potential required is $E_D=540$ volts. The electrons striking the screen are 16-kv electrons, due to the post acceleration obtained by the focusing potential. The total capacity of a grid for a screen size of 12×16 inches is approximately 1,200 $\mu\mu$f. The width of a three-color cell at the phosphor surface, as determined from (1.5) using the 125th pitch as constant for the entire image plate is 30.74 mils. No correction from this constant pitch is required for deflection angles to 69 degrees. If wider-deflection angles are desired, the phosphor centers can easily be distributed about 2 or 3 mean values. Error growth curves for the various pitches are shown in Appendix III, as noted earlier.

The displacement formula given as (1.5) results in some distortion of the "barrel" type. This would tend to make the straight lines slightly curved. In the practical case, this line fails to be straight by only 4 mils over the 12 inches. With the error divided left and right, greatest deviation is only 2 mils. Distortion is negligible.

Number of Phosphor Lines and Definition

The number of phosphor lines when positioned at right angles to the direction of scan determine the horizontal resolution of the tube. If a television source is used, the number of changes along the horizontal line for a given bandwidth is

T_a = Active time per trace.

$H_{TV} = 2T_aF_{max}$

F_{max} = Maximum freq. transmitted.

Each element thus defined along the horizontal line should have the possibility of being multi-colored. That is to say, within the diameter of this element there must be all three: red, blue and green fluorescent materials. So, the number of distinct phosphor lines per inch is

$$\frac{6T_aF_{max}}{W} \qquad W = \text{Width in inches.}$$

For a 60-field standard, a 16-inch picture width and an information bandwidth of 4.2 mc, the tube requires 84 lines per inch. The Chromatrons being manufactured at present[3] have 15-mil phosphor strips and will resolve 270 black and white elements per horizontal line, when the phosphor strips are held vertically.

It should be noted that the phosphor strips also may be held horizontally. In this case, there is no tube limitation on horizontal definition. The number of strips required is about the same as above so as not to impair vertical resolution. Actually, this mode of operation is very appealing psychologically since people already are used to seeing horizontal lines on their television-picture tubes when viewing the picture within the critical-viewing distance.

These tubes have been operated with the phosphor strips in both of the above mentioned directions. Of considerable interest is the fact that when the strips are oriented in the same direction as scanning lines, the moire pattern produced may be reduced to negligible intensity and is not observed at ordinary viewing distances.

With respect to line coarseness for the calculated spacing, the eye will see a line structure of 33 lines per inch in a single color. Considering the average television receiver to be interlaced 75 per cent of the time, the horizontal structure due to the scanning lines for a picture 12-inches high, with 483-active lines is approximately 30 lines per inch. So, the structure is not objectionable and in many cases invisible at ordinary viewing distances. For close viewing, say twice the height of the picture-tube screen, lines are visible but not as individual colors. Rather, one sees a complete color picture which has that familiar television-line discontinuity.

Phosphors

To obtain proper color reproduction, it is necessary to have phosphors whose spectral characteristics are

[3] During time elapsed for publication of this paper experimental 10 Mil phosphor strip tubes have been satisfactorily tested.

such that they can reproduce primaries at least as saturated as those being transmitted. At the transmitter, gelatin filters or dichroic mirrors provide excellent color saturation in all of the primaries. Phosphor development has not attained the goal of being able to produce colors as saturated as filters in the red region of the spectrum. However, highly acceptable subjective results have been obtained with presently available phosphors. A color trichromatic diagram is drawn in Fig. 8 to show how

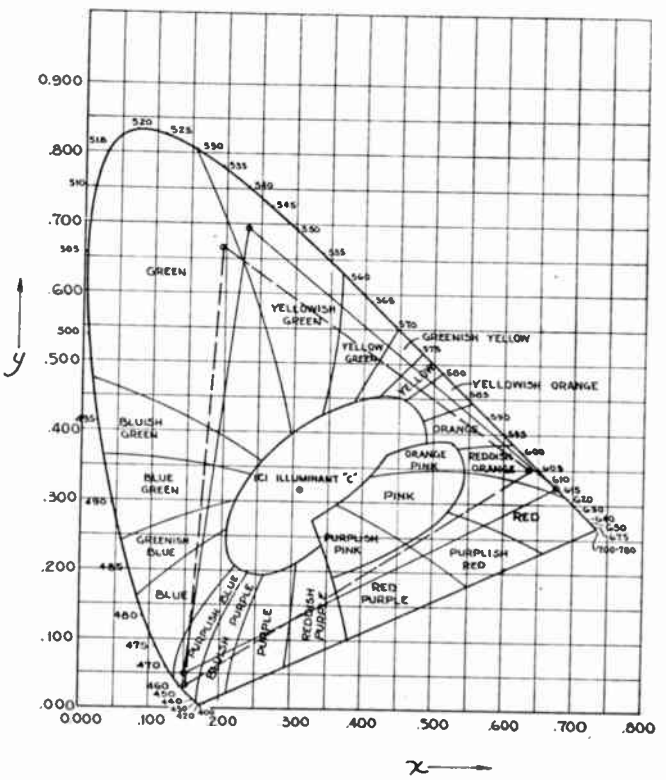

Fig. 8—ICI coordinates for the present phosphors as compared with the best filters for additive color reproduction work. (Solid lines connect the filter ICI coordinates.)

the reproducing phosphors compare with the transmitting filters. (The solid lines connect the filter primaries.) Fig. 9 shows curves as spectral response versus wave length for the phosphors used at the present time. These are Red (Zn Phosphate:Mn), Blue (CaO MgO 2Si O_2:Ti), Green (Zn_2 Si O_4:Mn). The thickness of the phosphors on the image plate for maximum-light efficiency depends on their chemical makeup. This problem has been studied in great detail by H. Bethe and others. The silk-screening method allows each phosphor to be laid down at its optimum thickness.

Secondary Emission

In tubes of this type, secondary-emission effects resulting from wire emission may be reduced by biasing the wire grid slightly with respect to the shell. In this manner, all secondaries are urged to the shell leaving the fields, as set up by the circuits, relatively unchanged.

Persistence Effects

When using a rotating disc to reproduce colors with a field-sequential color system, it is necessary that the phosphor-light output decay quite rapidly so that only a negligible trace of light appears after a single-field interval. With a direct view tube of the type being discussed, each color is excited separately. Therefore, it is practical to use phosphors with a persistence characteristic $2\frac{1}{2}$ to 3 times longer than is possible with a disc method of color reproduction. The use of longer-persistence phosphors greatly increases resistance to flicker and color breakup.

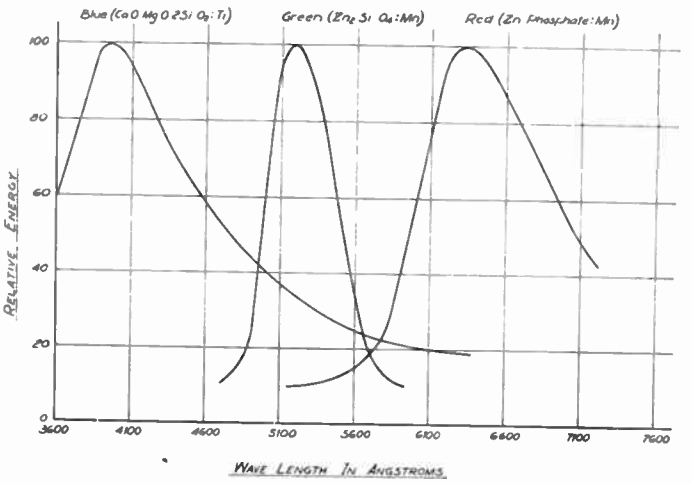

Fig. 9—Spectral-energy distribution of the phosphors in the present Chromatron.

It is also possible to make a direct-view tube of this type with long-persistence phosphors, allowing military displays of various kinds of information.

Driving Circuits

The color switching circuits for the single gun Chromatron depend upon the type of color television transmission system used. To reproduce color television pictures from a simultaneous compatible system, it is only necessary to convert the video information into sequential form at the receiver. One approach which has been successfully demonstrated involves switching of the three simultaneous color signals at the subcarrier rate used by the NTSC, namely, 3.58 MC. This technique permits the use of an inductance in parallel with the color grid, the combination being tuned to the desired switching frequency.

The high frequency switching voltage applied to the color grid causes the electron beam to move in rapid sequence over the color phosphor strips as the raster is scanned. A gating circuit is incorporated to control the intensity of the beam in proportion to the related color video signal.

To display the NTSC signal, the input power to the oscillator driving the color grid structure was approximately 50 watts. Here the color grid capacity was resonated with a coil outside of the tube. It is possible to place a high efficiency toroid coil inside of the tube in which case only the power losses for the resonated circuit must be supplied through the tube terminals, permitting a computed power reduction to approximately 15 watts.

Other methods of switching single gun Chromatrons are in development and a detailed paper is being prepared for publication later this year.

Of course, for a field sequential or low switching color transmission system, a rectangular switching wave form is generated to move the beam to the proper color phosphor position. In these frequencies there is only approximately 1/10th of a reactive watt circulated in the color grid structure.

Conclusions

The tubes described have many advantages as color-picture tubes. They make use of post acceleration to aluminum backed phosphors, giving a bright-color picture as well as a black and white picture without loss of television detail. The single-gun tube will operate on field-sequential color from conventional-adapted receivers with the addition of only three tubes for color switching. New components and circuit developments in progress may permit a practical solution to the problem of using the single-gun type with high-frequency switching or simultaneous-color-television systems.

The three-gun tube will operate in the conventional manner from both high-switching rate or simultaneous-color-television systems. Because of the post focusing and the small spot size thus obtained, the registration problem of wire and phosphors has been greatly minimized. There is no objectionable masking loss. In these tubes, the lens wires absorb approximately 14 per cent of the incident electrons. Allowing, 86 per cent of the electron beam to be turned to useful light output. The tube design permits wide-deflection angles making it possible to produce color tubes which are no longer than conventional black and white tubes. The viewing angles for these tubes are exactly the same as a conventional black and white cathode-ray tube. All of these features permit substantial economics in manufacture.

Acknowledgments

The author gratefully acknowledges the helpful suggestions and criticisms of Dr. Ernest O. Lawrence, Director of Radiation Laboratory, University of California and Dr. Edwin M. McMillan of the University of California.

Appendix I

Definition of Symbols:

r—the distance between the center of deflection of the electron beam and the plane of the grid wires.

d—the distance between the grid wires and the aluminum backing of the phosphor screen.

R—wire radius.

D—distance between the center of adjacent wires of the wire grid.

E_D—the potential difference required between the two sets of wires to switch colors.

x and y—directions are shown on Fig. 5.

θ—deflection angle.

y_k—the distance from the axis of the cathode-ray tube that a particle will strike if deflected through an angle θ.

E_1—the potential difference between the cathode of the cathode-ray tube electron gun and the electrical center of the color-structure wires.

E_2—the potential difference between the electrical center of the color-structure wires and the aluminum backing of the phosphor screen.

v_x—the velocity of a particle as it approaches the color structure wires perpendicular to the plane of the grid wires.

V_x—the perpendicular-striking velocity of particle as it strikes phosphor surface of tube.

$\bar{v}_x$—the average velocity in the region between the grid wires and the phosphor surface.

$$\bar{v}_x = \tfrac{1}{2}[v_x + V_x]$$

m and e—the mass and charge of particle in question.

Appendix II (See Fig. 5)

Derivation of Equation (1.1)

From an energy consideration

(1) $\tfrac{1}{2}mv_x^2(1 + \tan^2\theta) = eE_1$

also

(2) $\tfrac{1}{2}m(V_x^2 + v_x^2\tan^2\theta) = e(E_1 + E_2)$,

since

$$\frac{v_y}{v_x} = \tan\theta \qquad v_y = V_y = v_x\tan\theta$$

from (1)

$$\tfrac{1}{2}mv_x^2 = \frac{eE_1}{1 + \tan^2\theta} = eE_1\cos^2\theta$$

or

$$\boxed{v_x^2 = \frac{2e}{m}E_1\cos^2\theta}\,.$$

Substituting in 2)

$$\tfrac{1}{2}m\left(V_x^2 + \frac{2e}{m}E_1\cos^2\theta\tan^2\theta\right) = e(E_1 + E_2)$$

or

$$\tfrac{1}{2}m\left(V_x^2 + \frac{2e}{m}E_1\sin^2\theta\right) = e(E_1 + E_2),$$

so

$$V_x^2 = \frac{2e}{m}[(E_1 + E_2) - E_1\sin^2\theta]$$

$$\boxed{V_x^2 = \frac{2e}{m}[E_2 + E_1\cos^2\theta]}\,.$$

Since v_x and V_x are positive

$$\bar{v}_x = \frac{1}{2}\sqrt{\frac{2e}{m}}\,[\sqrt{E_1}\cos\theta + \sqrt{E_2 + E_1\cos^2\theta}]$$

or

$$\bar{v}_x = \frac{1}{2}\sqrt{\frac{2e}{m}}\left[\sqrt{E_1}\cos\theta\left(1 + \sqrt{1 + \frac{E_2}{E_1\cos^2\theta}}\right)\right].$$

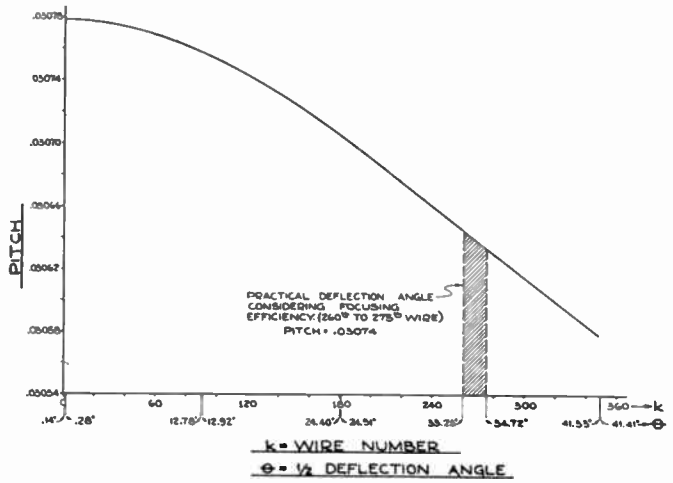

Fig. 10—Required pitch variation with deflection angle.

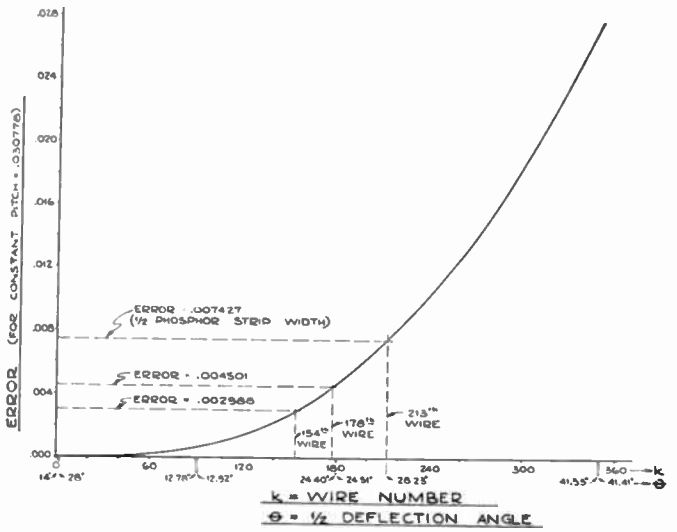

Fig. 11—Wire-placement error versus deflection angle using as constant pitch value, the value obtained when $k=1$ in equation (1.55).

Appendix III

Fig. 10 shows the required pitch variation with wire number for the 15-mil phosphor-strip tube. Silk screens can be made whose pitch varies in accordance with the given curve. However, it is interesting to note that choosing certain constant pitches allows large deflection angles without color shift. Figs. 11, 12, and 13 indicate the errors for choosing particular constant pitches. The

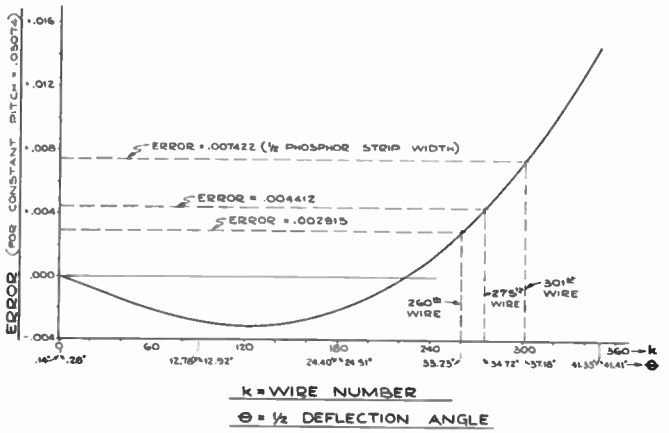

Fig. 12—Wire-placement error versus deflection angle using as constant-pitch value, the value obtained when $k=125$ in (1.55).

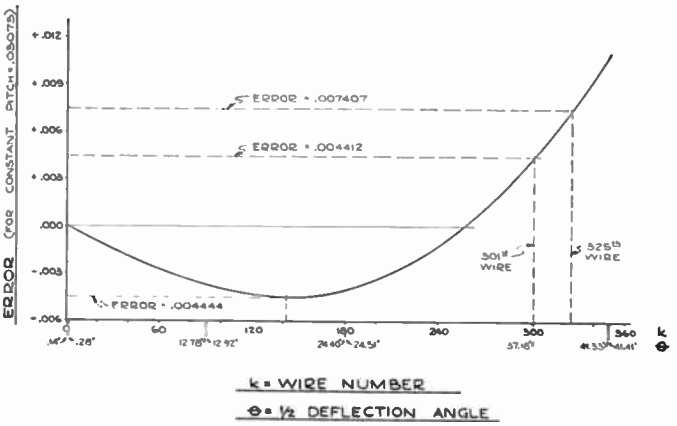

Fig. 13—Wire-placement error versus deflection angle using as constant-pitch value, the value obtained when $k=142$ in (1.55).

errors allowed for the 15-mil phosphor-strip tube lie between 0.0030 inch and 0.0045 inch. The error curves show the deflection angles which may be obtained using either one of these errors as a basis for the constant pitch required. Practical variation in tubes which have been manufactured indicate that these tubes will operate between 66 and 69 degree deflection angles.

Bibliography

1. D. B. Judd, "Colorimetry," U. S. Dept. of Comm., *Nat. Bur. Stand., Cir.*, no. 478; March 1, 1950.
2. O. D. Kellogg, "Foundations of Potential Theory," Frederick Ungar Pub. Co., New York; 1929.
3. K. L. Kelly, "Color designations for lights," *Jour Res. Nat. Bur. Stand.*, vol. 31, research paper 1565; July–December, 1943

Pulse-Code Modulation Systems*

A. J. OXFORD†

Summary—**Following a review of the principles of pulsed transmission of information, the method of pulse-code modulation (PCM) is discussed. Two different experimental systems for performing this function are described.**

Introduction

ALTHOUGH the use of short radio pulses for transmitting speech has been contemplated for a number of years, it is only comparatively recently that much attention has been paid to the production of working systems. For example, some of the earliest suggestions for time-multiplexed telephony date back to the beginning of the century, and Heising described a method for transmitting speech by pulse-length modulation in 1924.

There are several reasons why these ideas appear to have lain undeveloped until the early years of World War II, when the first practical systems were demonstrated. There is no doubt that a great incentive was given to this work by the development of the art of waveform manipulation which was required for television and developed so intensively for radar. Progress in these applications also gave the technician valves which would stand impulsive modulation and an ever-increasing range of very-high-frequency bands in which to operate. Meanwhile, frequency-multiplex systems of multichannel operation, which depended on different circuit techniques, were being adopted extensively for telephone systems. There is evidence that the incompatibility of the two systems of multiplexing has been partly responsible for the lack of interest hitherto shown in pulse communication by many authorities. It has been demonstrated, however, that for many applications, the use of pulse systems with time multiplexing can result in smaller and lighter equipments which meet the same specifications and have important advantages compared with frequency-multiplex systems.

Time Sampling

There are several methods of achieving pulse transmission of speech or music, but all depend on the principle of time sampling. By this process we imply that instead of transmitting continuously to the receiver information about the instantaneous amplitude of the input waveform, we only require to take periodic measurements of this quantity so long as we do so sufficiently frequently. In fact, it can be shown that we must take our samples at a rate which is at least twice the highest frequency required to be transmitted. This is so because two samples per cycle are required to define a sine wave. If this is done, then no harmonic distortion is introduced by the sampling process and cross modulation does not occur due to the presence of more than one modulating frequency in the input.

For speech transmission the sampling process involves some form of electronic switch, but for clarity of explanation the diagram of Fig. 1 shows an electromagnetic device, such as a relay, carrying out the sampling function and storing the information so derived in the condenser C. The switch contacts may be closed for as short a period as desired, so long as the storage capacity can be charged to the new value in this time. We have, therefore, available the whole of the time interval between one sampling instant and the next to transmit to the receiver the information regarding the instantaneous-input amplitude. This information may be transmitted by a chain of pulses whose amplitude, length, phase, or frequency is modulated to carry it. Systems operating on these principles have been demonstrated and used in various applications.[1,2]

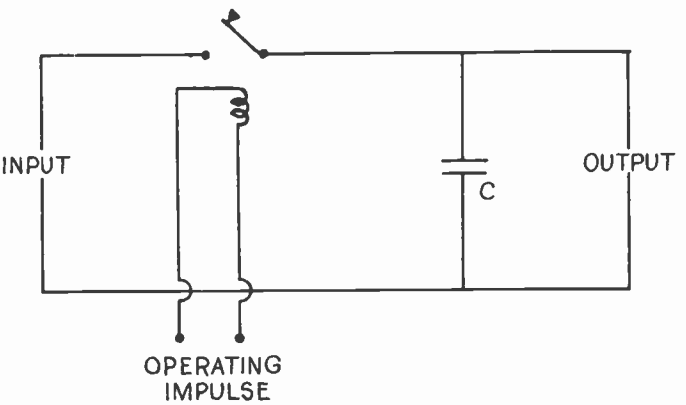

Fig. 1—Sampling process.

Multiplexing

If we restrict the time taken to transmit the instantaneous amplitude to $1/n$ of the time between samples, then we can interlace the information contained in a total of n-speech channels. This process is usually done by collecting in a multiway switch samples from all the speech channels in turn and then passing the complex-video waveform to the modulating device (Fig. 2). An important advantage of this arrangement is that during the process and after use of suitable time constants is sufficient to ensure the absence of cross talk between channels; nonlinearity is relatively unimportant.

Bandwidths and Noise

The various methods of modulating a train of pulses so as to carry the sample information have been listed

* Decimal classification: R148.6. Original manuscript received by the Institute, February 10, 1953. Reprinted from *Proc. I.R.E.* (Australia), vol. 13, pp. 281–287; July, 1952.

† Superintendent, Electronics Research Laboratory, Adelaide, S. Australia.

[1] D. G. Reid, "A 60-centimetre multi-channel system employing pulse-position modulation," *Jour. IEE* (London), vol. 94, pt. IIIA, p. 573; 1947.

[2] "Multi-channel pulse modulation," *Wireless World*, vol. 52, p. 187; 1946.

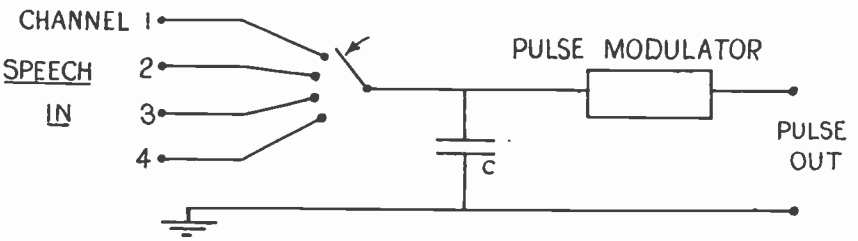

Fig. 2—Multiplying process.

above and described elsewhere in the literature.[3,4] It is not intended to deal here with these methods except to point out that they all convert the speech into a form requiring extended frequency allocation, in return for which they give, in varying degree, an improved signal-to-noise ratio. In other words, the conversion to pulse modulation gives us an opportunity to trade bandwidth for signal-to-noise ratio. It is important for us to make certain that when we use this trading system we take advantage of the most favorable rate of exchange.

(a) *Hartley's Law*

In 1928 Hartley[5] stated a law which enabled the efficiency of communication systems to be assessed. It was that the amount of information that any system can transmit it proportional to both bandwidth and time. When, however, the newly invented system of frequency modulation was described by Armstrong, it became evident that he was increasing the bandwidth required without apparently increasing the capacity of the system to transmit information. He had, in fact, gained in signal-to-noise ratio, his exchange rate being one octave of bandwidth for 6 db of signal-to-noise ratio. Subsequent mathematical work has shown that this is not the best exchange rate and that it should be possible to double the signal-to-noise ratio (in decibels) per octave of bandwidth.

In other words, if we have a system giving 25-db signal-to-noise ratio for 20-kc bandwidth, then 40-kc bandwidth should give 50 db not 31 db as would be the case in a frequency-modulated system.

In order to extend the meaning and usefulness of Hartley's Law, it was restated by Shannon[6] as follows:

$$M = \left(1 + \frac{P}{N}\right)^{TW}$$

where

M = number of independent message items identified time T
W = bandwidth
P = signal-to-noise ratio in power
N = units.

[3] D. Cooke, Z. Jelonek, A. Oxford, and E. Fitch, "Pulse communication," *Jour. IEE* (London), vol. 94, pt. IIIA, p. 83; 1947.
[4] E. M. Deloraine and E. Labin, "Pulse time modulation," *Elec. Comm.* (London), vol. 22, p. 91; 1944.
[5] R. L. Hartley, "Transmission of information," *Bell Sys. Tech. Jour.*, vol. 7, p. 535; July, 1928.
[6] C. E. Shannon, "A mathematical theory of communication," *Bell Sys. Tech. Jour.*, vol. 27; July and October, 1948.

Pulse-Code Modulation (PCM)

Pulse-code modulation gives us the opportunity to take advantage of this theoretically optimum method of exchanging bandwidth for signal-to-noise ratio. It is at the present time the only system known which approaches the theoretical limit.

It depends on taking a still further liberty with the speech signals after they have been time sampled. We then proceed to carry out a quantizing process on the amplitude samples, whereby the exact value is not transmitted; instead we send a coded group of pulses indicating to the receiver in which subdivision the sampled amplitude lies. These subdivisions can be made as small as desired in order to transmit more and more detailed information. In place of the exact-amplitude measurement, it is only necessary to send the nearest whole number. It has been found that the ear is extremely tolerant to this type of distortion and that we can achieve good intelligibility using only four subdivisions or levels, good telephone quality with 32 levels, and broadcast quality for music with 128 levels.

The most usual way in which this signal is indicated to the receiver is by means of the binary system, although other methods are possible. As we have converted the speech into a type of telegraph signal, it is not unnatural that the system chosen is directly analogous to the 5-unit code used for machine telegraphy. If, for example, we have available five possible pulses in each sample time, then we can indicate any number from 0–31 by a combination of ON or OFF pulses, as shown in Fig. 3.

The first, or most significant digit, indicates whether the sample is in the upper or lower half; in other words, we say it is equivalent to plus or minus 8 levels. The second indicates which quarter is in use and has a value of plus or minus 4 levels, and so on. The fifth or last digit, therefore, tells the receiver which thirty-second is meant, and has a value of plus or minus one half level. Level +4, for example, would be indicated by the group ON, OFF, OFF, ON, ON, if we adopt the convention that the most significant digit is transmitted first. Apart from the theoretical aspect mentioned earlier, which shows that this system gives us the best rate of exchange of bandwidth against signal-to-noise ratio, it is obvious that we are making minimum demands on the transmission system if we only require it to distinguish between ON and OFF. We are not concerned with accurate discrimination of the amplitude, phase,

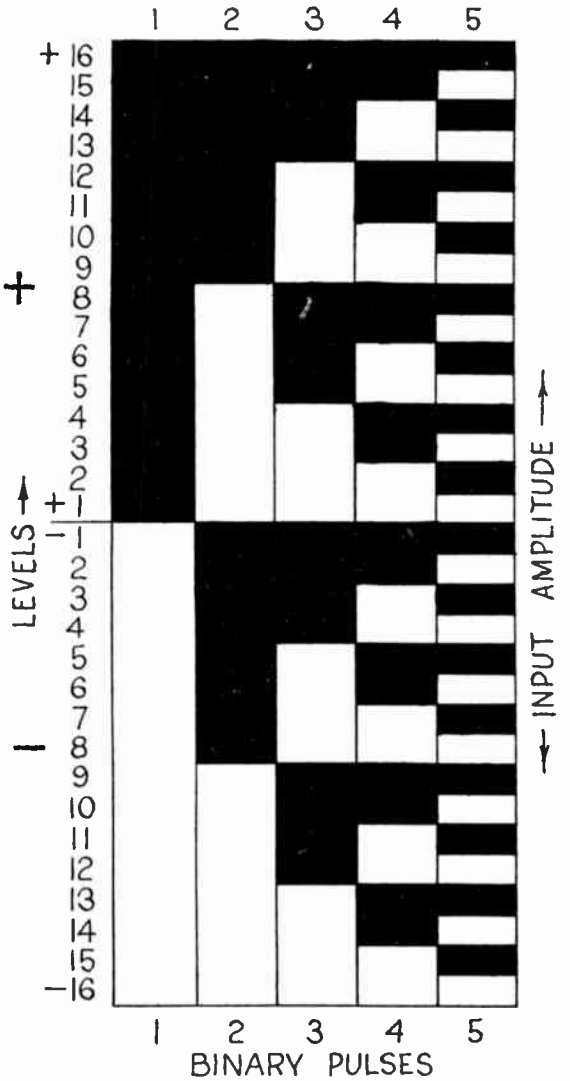

Fig. 3—Binary code.

length, or frequency of the pulses,—merely whether any pulse is intended to be present or not.

A further corollary is the ease with which multiple relays can be carried out without the noise or cross talk becoming cumulative. Fig. 4 illustrates how we can reproduce a slightly delayed but otherwise perfect version of the original pulse by taking both horizontal (voltage) and vertical (time) slices. In other words, we can, at intermediate points on a system, reconstitute or regenerate the pulses completely free from noise or interference.

One reason for delay in adopting such systems is the complexity which was involved in the earlier methods of obtaining and demodulating pulse-code modulation.

System 1

It is the aim of the present paper to indicate two methods of carrying out these functions; they involve little if any more complication than other methods of pulse modulation. They have both been tested and operated at speeds corresponding to a 5-digit, 12-channel speech system.

As mentioned earlier, time multiplexing is obtained for multichannel operation by collecting samples from the several channels in turn and then passing the combined video waveform through a common modulator. There is, therefore, no change in the PCM modulator for multichannel working apart from the increased speed of operation.

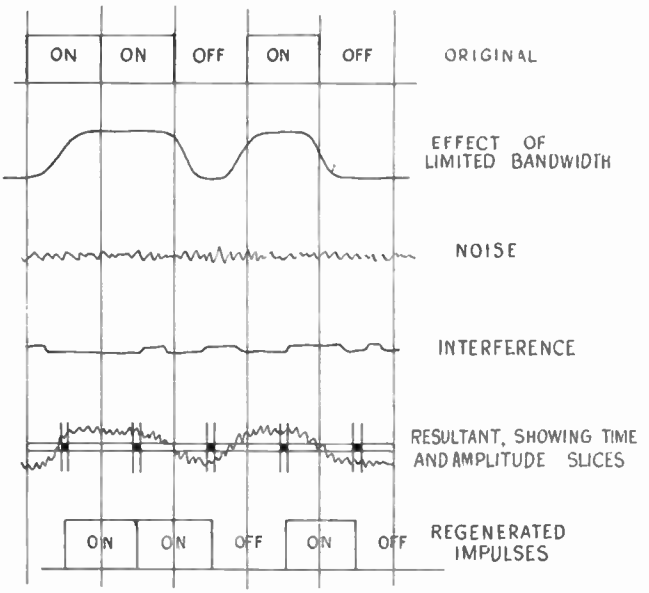

Fig. 4—Reconstitution process.

Modulator 1

The principles of operation of the two types of PCM modulator will, therefore, be described as for single-channel operation and simplified by replacing the various electronic switches by electromagnetic relays, as in Fig. 5 which illustrates the general principle of operation of the modulator for Method 1.

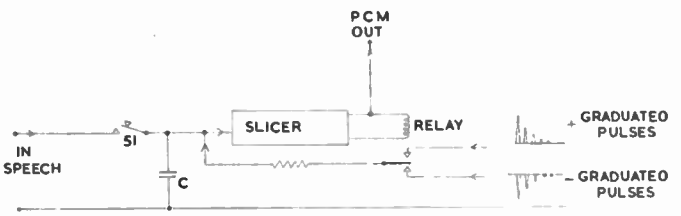

Fig. 5—Method 1. Modulator.

For illustration, we consider a system designed to transmit speech of telephone quality (300–3,000), namely 32 levels, or 5 digits. The speed of sampling is chosen as 6.66 kc, or just over twice the highest frequency to be transmitted.

The function of the modulator is to take periodic samples of the input-waveform at 150-μsec intervals and to decide which of the five pulses of a group, each 30-μsec long, should be transmitted.

The "slicer" shown in Fig. 5 may be regarded as a pulse-operated, high-gain amplifier normally biased to the short-center portion of its characteristic, so that a small change in voltage in either direction is sufficient to cause the relay at the output end to close on one side

or the other. The slicer is operated by the potential built up on the storage-condenser C. Two similar series of pulses one positive going and one negative going, are applied to the fixed-relay contacts. Each series of pulses contains five pulses, each one being spaced by its own length from the previous one, and each being one-half the amplitude of the previous one. These pulse trains are formed quite simply by impulsing a 33-kc tuned circuit and allowing it to ring with the appropriate decrement so that each positive half-cycle is one-half the amplitude of the previous one. This waveform is then rectified and applied to a cathode and anode follower to produce low-impedance, paraphased outputs. The first, or largest pulse, when selected by the relay, is integrated back into the condenser C and changes its potential by an amount equal to one-quarter of the maximum-peak to peak-input signal. Thus in a 5-digit 32-level system, these pulses correspond to plus or minus 8, 4, 2, 1, or $\frac{1}{2}$ levels, respectively. The slicer and relay circuit is so arranged that a positive-going signal on C at any instant causes a negative-going pulse to be selected from the five-pulse group, and vice versa.

Consider the operation of such a circuit designed to accept a 32-volt (plus or minus 16) peak-to-peak signal so that each level equals 1 volt. The sampling switch S_1 closes for 3 μsec at the start of the sampling time and charges C to the instantaneous value of the signal wave, which we will assume to be at say +11.85 volts (Fig. 6).

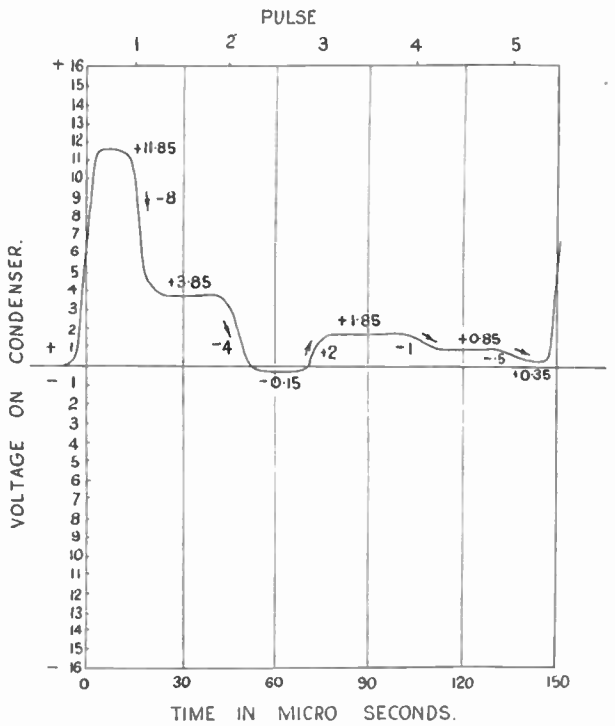

Fig. 6—Method 1. Modulator waveform.

This will operate the slicer positively and cause the relay to select the first and largest pulse in the negative direction, reducing the voltage on C by 8 volts, i.e., to +3.85 volts. As the slicer input is still positive, the second pulse selected will also be a negative-going one and will change the voltage on C by 4 volts to −0.15. The input now being negative, the third pulse will be selected as positive and add +2 volts to give +1.85 volts. The fourth pulse is therefore selected as −1 volt, changing the value to +0.85 volt, and finally the fifth pulse is selected as −0.5 volt, leaving a surplus voltage of +0.35 on the capacitor.

After the fifth pulse the circuit is ready to receive the next sample and start afresh, discarding the remainder in the process. The important point to note in this process is that the five pulses selected by the relay were −, −, +, −, −. Adopting the convention that a PCM pulse is sent when a *negative* pulse is selected by the relay, the group is sent as +, +, −, +, +. If the receiver then allocates to the five pulses their true significance, we get +8, +4, −2, +1, $+\frac{1}{2}$ = +11.5 volts, which is the nearest level to the original measurement of the signal input of +11.85 volts.

The examination process in the modulator is thus a reiterative process in which the original sample is examined in increasing detail and the PCM pulses are obtained as a by-product of this examination spaced at the correct intervals for transmission.

The method of operation is in fact that of a servomechanism which on receipt of a disturbing voltage tends to reset itself to zero in a series of predetermined steps of logarithmically decreasing amplitude. The waveform on the condenser C is plotted in Fig. 6, showing the operation of a few of the 32 possible combinations of pulses. It was mentioned above that the slicer was pulse-operated; this is necessary for the reason that having made a decision, positive or negative depending on the charge on C, the slicer must not change the relay position again until C has fully integrated the next graduated pulse and arrived at a new equilibrium level. The operating points for examination by the slicer are shown in Fig. 6, and they occur every 30 μsec.

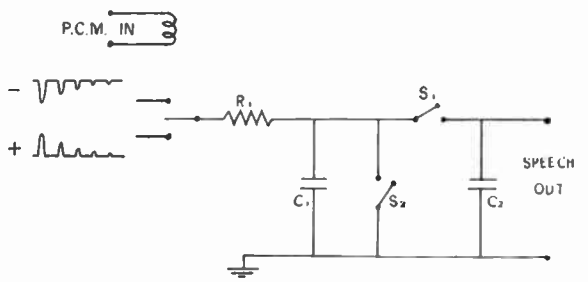

Fig. 7—Simple demodulator.

Demodulator 1

The simplified block diagram of the receiver is shown in Fig. 7. It will be seen that a pair of graduated-pulse trains similar to those employed in the transmitter are available from the receiver circuits. The receiver assigns to each incoming pulse its correct significance by switching an appropriately graduated pulse to the integration circuit R_1C_1 so that by the time all five pulses have arrived in either positive or negative sense C_1 has been charged to one of 32 different levels.

When successive samples follow different paths, the interesting picture shown in Fig. 8 can be observed on the screen of a cathode-ray tube. This pattern is visible

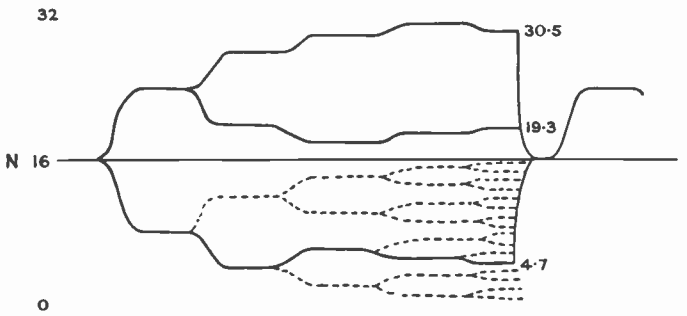

Fig. 8—Method 2. Demodulator waveform.

on the CRT in the equipment shown in Fig. 9, which is an experimental version of System 1 demonstrated at Radiolympia in 1949. Electronic switches S_1 and S_2 are provided in the receiver (a) to feed the final voltage obtained on the integrating condenser C_1 into a storage circuit C_2 and (b) to discharge C_1 to zero ready to build

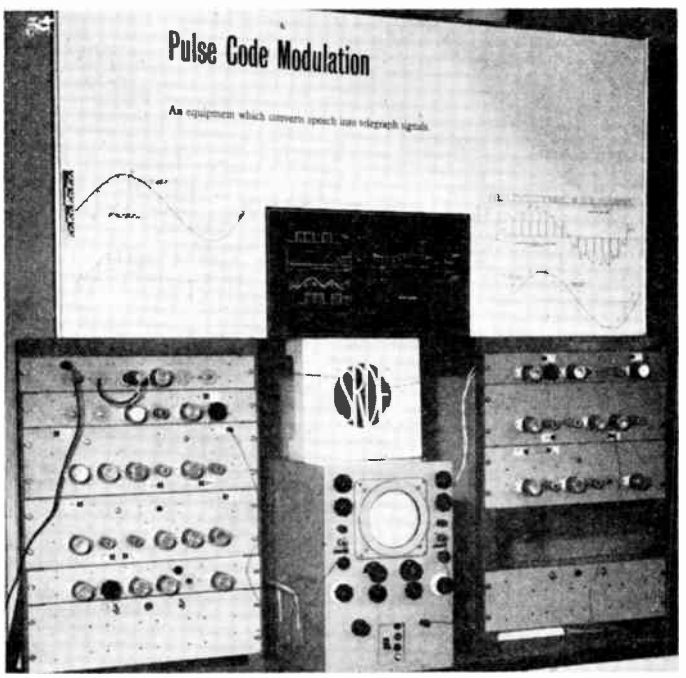

Fig. 9—Radiolympia, Sept. 28–Oct. 8, 1949. Pulse code modulation. S.R.D.E.

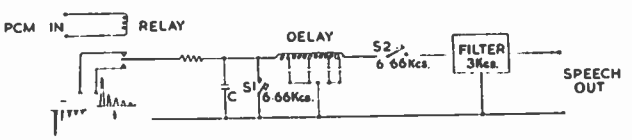

Fig. 10—Method 1. Demodulator.

up the next sample. It would normally be necessary to close S_1 immediately before S_2, but this difficulty is obviated as shown in Fig. 10 by putting the signal into temporary storage in a short-delay line while the two switches operate. The output from C_2 is then fed via a 3-kc low-pass filter into the audio-output circuits.

Logarithmic Levels

It is necessary to refer at this point to a refinement which, although simple to include, produces a considerable economy in available levels. The system described above quantizes the input signal in 32 equally-spaced levels whereas, in fact, in order to make the best use of a given number of levels it is desirable to cut them at logarithmic intervals from zero. This effect is achieved by passing the signal through a simple form of instantaneous-logarithmic compressor before modulating and the inverse process at the demodulating end before feeding it to the audio stage. This means that each step corresponds to a fixed number of decibels.

Synchronization

The transmission waveform produced by the apparatus described above is in the form of ON-OFF pulses, 30-μsec wide, 5 in a group, but with no dead time or spaces either between pulses or groups. At the demodulating end we are faced with the problem of deriving (a) a frequency of 33 kc corresponding to the pulse-repetition rate and (b) pulses at 6.66 kc corresponding to the group spacing, in order to indicate the beginning of each period so that the pulses can be assigned the correct value or significance and can be integrated correctly in groups of 5. There may or may not be a changeover of the pulse every 30 μsec, and we must derive enough information from those changeovers which are present to enable the receiver to fill in from memory those which are absent. This is a "spongy-lock" problem, often met in pulse-communication circuits, and can be solved so satisfactorily that the system can handle a gap of over 100-consecutive pulses without losing synchronism.

If the output from this locally generated 33-kc signal is counted in a divide-by-five circuit, we obtain a 6.66-kc signal which will produce the graduated-pulse chain required and operate the switches S_1 and S_2 (Fig. 7) once the phase has been correctly set. (There are 5 ambiguous positions, only one of which is correct.) It has been proved that such an arrangement is capable of running satisfactorily for many hours after having been phased correctly, but in order to provide an automatic-phasing signal we introduce a special pulse sequence into the transmission at frequent intervals, for example, several times per minute. This can be done without giving rise to any perceptible interference in the speech transmitted.

The special-pulse sequence chosen as the phase-synchronizing signal consists of two consequential groups of five pulses, all ON, i.e., 10 ON pulses in a row. Two precautions are involved: (a) This sequence must not be allowed to occur by accident and (b) these ten pulses must always start after an OFF pulse so that the tenth ON pulse is reached at the correct time.

Condition (a) is obtained by discarding level 32 which would normally be indicated by five ON pulses in a group. A circuit is included which inverts the last pulse when the modulator attempts to produce 5 ON in a group. (This circuit is known as the "spoiler.")

Condition (b) is obtained by allowing the circuit itself to select an appropriate instant to insert the synchronizing sequence. In other words, toward the end of the required interval between sequences, the circuit will begin to look for suitable groups in which the last digit is an OFF. When it finds one, it inserts, immediately following it, 2 groups of 5 ON pulses each, overriding the original signal. (This is referred to as the "inserter.") The spoiler must, of course, be prohibited from operating while the inserter is in action. The operation of the spoiler and inserter sounds rather complicated, but is in fact all carried out by a total of three double triodes.

It will be found that the modulator and spoiler cannot, in the ordinary way, produce a series of more than 8 ON pulses consecutively, so that it is a simple matter for the receiver to discriminate between this combination and the genuine 10 ON sequence in which the 10th ON pulse indicates the last of a group and so phases the receiver circuits.

System 2

It will be noticed that in the PCM modulator described above it is necessary, after each successive check on the polarity of the storage condenser Fig. 5, to add or subtract a charge of logarithmically decreasing amplitude. If, however, we could arrange for the residual charge to be amplified by a factor of two after each pulse, then we could add or subtract a fixed amount from it at each pulse. This would still further simplify the apparatus in that the networks to produce the graduated pulses could be eliminated.

Modulator 2

A block diagram of the alternative modulator is given in Fig. 11. The unit marked "A" is an in-phase linear amplifier provided with positive feedback from output to input through R_1 so that any charge impressed on C_1 by closure of the electronic switch 1 will thereafter "grow" exponentially according to the law

$$\frac{V_2}{V_1} = \exp \frac{(m-1)(t_2 - t_1)}{C_1 R_1}.$$

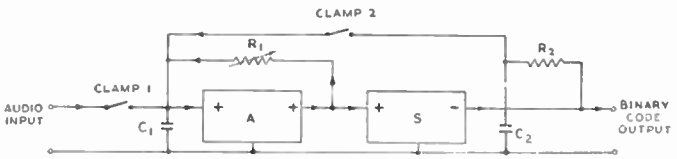

Fig. 11—Method 2. Modulator.

The unit marked "S" is a phase-reversing, nonlinear amplifier very similar to the slicer already mentioned for use in the original type of modulator. For example, it might be designed to produce at its output terminals 100 volts positive for any input below zero and 100 volts negative for any voltage above zero. Clamp 1 closes for a brief period at the start of each group and clamp 2 briefly between each pulse of the group.

A three-pulse system (8 levels) has been chosen to illustrate the operation of the circuit (Fig. 12). Suppose the input wave to be such that it successively runs through all 8 levels at the sampling times A–J, starting at the most positive level A.

Clamp 1 closes and impresses the sample A on C_1 and due to the feedback action this sample voltage proceeds to "grow" to a_1, Fig. 12. Meanwhile, the slicer output will be fully negative and building up a negative charge of fixed amplitude on C_2 thus producing an appropriate PCM output. At the end of the digit time, clamp 2 closes instantaneously and impresses on C_1 the negative charge from C_2, modifying the charge on C_1 to value a_2. This value is still positive and proceeds to grow again in this direction, still maintaining a negative charge on C_2. At the end of pulse 2, clamp 2 closes again and modifies the charge on C_1 from a_3 to a_4 which is still positive. This process is carried on until clamp 1 closes again at the end of the group time and sample B is

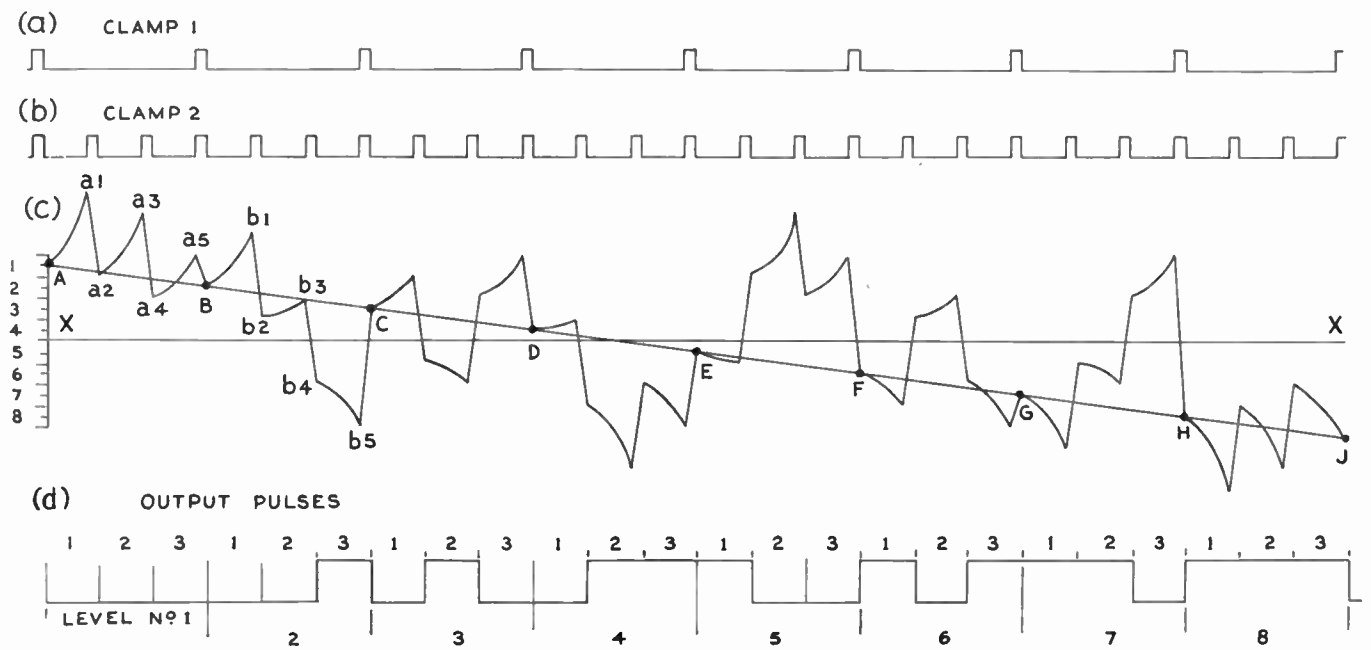

Fig. 12—Method 2. Waveforms.

examined in the same manner. In this case at point b_3, the charge carries resultant potential on C_1 negative with appropriate change in polarity of the last digit.

This system has been operated at 12-channel speed with the necessary type of electronic switches for clamps 1 and 2, but would also be particularly attractive for any lower speed application where mechanized switches or relays could be employed.

Demodulator 2

A similar "growing" technique is used in the receiver as shown in Fig. 13. Here clamp 2 operates at every pulse and clamps 1 and 3 close, one just before the other, at the end of each group of pulses.

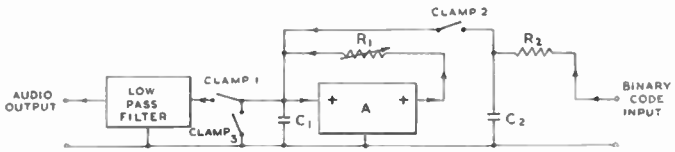

Fig. 13—Method 2. Demodulator.

The significant value of each pulse is inserted by this demodulator by allowing each pulse to remain in the growing circuit for an appropriate time so that by the end of the group period it has achieved its correct value. Here again the time constant of the circuit R_1C_1 is adjusted to give a 2 to 1 gain for each pulse period.

In both cases, receiver and transmitter, it has been found convenient to transmit the pulses in decreasing order of significance. However, this is merely a convention and can be varied to suit any special requirements.

Conclusions

The actual RF transmission may of course be carried out either by amplitude modulation or keying or by a carrier-shift method. In fact most of the techniques hitherto available for telegraph use may now be applied to the transmission of speech or music or any other high-speed waveforms. It has been suggested also that the application of PCM to various recording problems would result in increased signal to noise ratio in spite of deterioration of the recording medium.[7]

The two alternative systems have both been described because although the second system should permit still further simplification sufficient experience in its operation has not yet been obtained to decide which gives the optimum over-all performance.

Both the systems described depend for their economy in reducing all the decisions as to whether a pulse should be transmitted or not, to a check at a fixed voltage datum point, and in the use of a single circuit to carry out those checks. Although the functions may appear involved, they can be carried out with a small number of valves and they do not depend on adjustments which are too critical for easy setting up and maintenance.

[7] N. L. Yates-Fish and P. G. Forsyth, British Ministry of Supply Patent.

Bibliography

1. H. L. Kirke, "The application of pulse technique to broadcasting," *BBC. Quart.*, vol. 1, p. 139; 1946.
2. F. C. Williams, "Introduction to circuit techniques for radio-location," *Jour. IEE* (London), vol. 93, pt. IIIA, p. 289; 1946.
3. D. D. Grieg, "Pulse count modulation," *Elec. Commun.* (London), vol. 24; September, 1947.
4. W. R. Greer, "Pulse modulation systems," *Electronics*, vol. 19, p. 126; 1946.
5. M. M. Levy, "Pulse modulation and de-modulation theory," *Jour. Brit. I.R.E.*; March, 1947.
6. F. F. Roberts and J. C. Simmonds, "Multi-channel communication systems," *Wireless Eng.*; November, 1945.
7. B. M. Oliver, J. R. Pierce, and C. E. Shannon, "Philosophy of P.C.M.," Proc. I.R.E., vol. 36, p. 1324; November, 1948.
8. C. E. Shannon, "Communication in the presence of noise," Proc. I.R.E., vol. 37; January 10, 1949.

The Resistive-Wall Amplifier*

CHARLES K. BIRDSALL†, ASSOCIATE, IRE, GEORGE R. BREWER†, MEMBER, IRE, AND ANDREW V. HAEFF†, FELLOW, IRE

Summary—**Theory and experimental results are presented for a basically new type of electron-stream amplifier in which the stream flows near a resistive wall. The values of gain and bandwidth obtainable are found to be comparable to those of other microwave amplifiers, such as traveling-wave tubes. In contrast to such tubes, however, the gain is affected very little by appreciable changes in the circuit parameters or operating voltage; furthermore, self-oscillation is inherently absent because the input is effectively isolated from the output. Experiments are described that were performed mainly to verify the theory; the existence of the growing wave was demonstrated, and the measured gain was in good agreement with the theory.**

* Decimal classification: R132×R339.2. Original manuscript received by the Institute, January 13, 1953. Presented in part at the Conference on Electron Tube Research, June 16, 1952, Ottawa, Canada, and at the West Coast IRE Convention, Long Beach, Calif., August 28, 1952.

† Electron Tube Laboratory, Research and Development Laboratories, Hughes Aircraft Co., Culver City, Calif.

Introduction

IN ELECTRON-STREAM AMPLIFIERS, such as klystrons and traveling-wave tubes, it is desirable to have as little noise energy in the stream itself as possible in order to obtain satisfactory amplification of very weak signals. To accomplish this, one proposal has been that the stream, before entering the interaction circuit, be passed near a lossy circuit which presumably would absorb this unwanted energy. However, a theory due to L. J. Chu[1] suggested that just the opposite effect, amplification, could take place under these conditions. Similarly, a one-dimensional analysis by J. R. Pierce[2]

[1] L. J. Chu, "A-c kinetic energy in electron streams," private com.
[2] J. R. Pierce, "Waves in electron streams and circuits," *Bell Sys. Tech. Jour.*, vol. 30, pp. 626–651; July, 1951.

showed that if the circuit admittance has a dissipative component, there may be an increasing wave. We have found that the amplification obtainable with the combination of stream and resistive wall is of useful magnitude, and we have performed experiments that agree with this analysis.

In the "resistive-wall" amplifier (RWA) the gain is obtained through interaction between the stream charge and the wall charge which is induced by the stream. As contrasted to the traveling-wave type of interaction, there is essentially no interaction between the circuit wave (which is highly damped) and the stream. The wall charge acts on the stream so as to cause larger and larger bunches to be formed which result in exponential growth with distance of the original signal. Although some energy is dissipated in ohmicwall loss, there is a finite rate of growth for all stream currents. In an actual device the signal can be impressed on the stream by other circuitry and, after the stream flows near the resistive wall, the signal can be extracted similarly.

In Part I the analysis is carried out for a one-dimensional model of a stream flowing through a porous resistive medium; it is shown that two space-charge waves can exist, which are similar to the ordinary nongrowing klystron waves, except that the dielectric constant appearing in the plasma-wave number is now a complex number which results in a conjugate pair of propagation constants, representing a growing wave and a decaying wave.

In Part II, simple design data are obtained from an analysis of an elementary two-dimensional model of thin electron streams flowing between resistive sheets.

In Part III, the results of a field theory solution[3] are presented for an axially symmetric model of a stream encircled by a resistive tubing; here the gain is found to be substantially lower than that of the earlier models; this is due to the shunting capacitance of the space beyond the tubing. Practical methods of reducing or eliminating this capacitance are discussed.

In Part IV, experiments with the cylindrical model are described in which the growing wave was observed and the amplification measured, checking well with the theory. In one set of experiments, helices were used for modulating the stream, and in another experiment, cavities were used. In all tests the net gain of the resistive wall was obtained experimentally by a substitution method, thus avoiding the need for accurate knowledge of the helix and cavity parameters.

The RWA has several advantages. The gain and bandwidth are comparable to the helix-type traveling-wave tube. In contrast, the input is effectively isolated from the output by the lossy circuit so that oscillations due to internal feedback are inherently absent. Furthermore, there are no critical design or operating parameters; for example, substantial deviations from the optimum-wall resistance or stream velocity have but little effect on gain.

[3] C. K. Birdsall and J. R. Whinnery, "Waves in an electron stream with general admittance walls," *Jour. Appl. Phys.* vol. 24, pp. 314–323; March, 1953.

I. Theory of One-Dimensional Model of the Resistive-Wall Amplifier

For simplicity, consider first a model in which an electron stream flows through a medium that has conductivity σ as well as the usual dielectric properties (dielectric constant, $\epsilon_0\epsilon_2$). Let the medium be made porous in order to transmit the stream without interception. Fig. 1 shows a model of this stream and medium combination which will be called the resistive-medium amplifier (RMA). It will be assumed that the ac quantities (electric field, velocity, current, and charge densities) vary only in the z-direction. The treatment is for small signals, since products of the ac quantities are neglected.

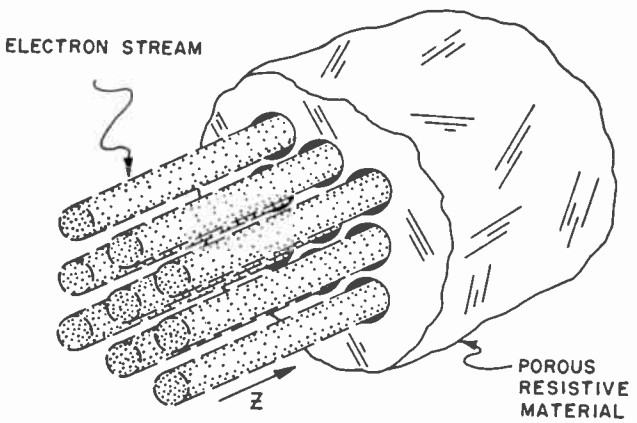

Fig. 1—Microscopic view of the cross section of a resistive-medium amplifier. An electron stream floods the pores of a lossy dielectric medium.

The propagation constants for the waves that may exist in this model are found in the usual manner, starting from the equations of Maxwell, of motion, and of continuity. These equations are linearized (small signals only) and are used for the case of nonrelativistic electron velocity, uniform field for a given cross section, and no motion normal to the z-direction. The ac quantities are assumed to vary in a wave-like manner as $\exp j(\omega t-\beta z)$.

The following additional symbolism is employed:

i, i_0 = ac, dc current densities, $i_0<0$.

v, u_0 = ac, dc velocities.

$\lambda_e=\lambda_0 u_0/c$ = stream wavelength; λ_0 = free-space wavelength.

V_0 = dc voltage with respect to the cathode; $u_0=(-2\eta V_0)^{1/2}$.

$\beta_e=\omega/u_0$, stream wave number.

$$\beta_p=\omega_p/u_0=\left[\frac{\eta i_0}{\epsilon_0 u_0^3}\right]^{1/2}$$ plasma wave number.

η = electron charge-to-mass ratio; $\eta=-1.76\times10^{11}$ coulomb/kg.

ϵ_0 = dielectric constant of vacuum; $\epsilon_0=(36\pi\times10^9)^{-1}$ farad/meter.

It is found that four waves can exist. (The derivation of the propagation constants is outlined in Appendix A.) Two of the waves are propagated at approximately the electron velocity and the other two, at the velocity that

a wave would have in the medium in the absence of the electron stream. The two pairs of waves are completely uncoupled; the latter pair, field waves, are decaying waves, important only in determining feedback in the direction opposite to that of the electron stream.

The two space-charge waves are closely related to the ordinary space-charge waves of empty space with which one is familiar from the work of Hahn[4] and Ramo.[5] For a one-dimensional model, the propagation constants of the empty-space waves are

$$\beta = \beta_e \pm \beta_p, \tag{1}$$

which represent two unattenuated waves. In the resistive-medium model the propagation constants are quite similar, differing only in that ϵ_0 in the expression for β_p is replaced (as is justified in Appendix A) by $\epsilon_0\epsilon_r$, which is a complex quantity accounting for the conductivity of the space shared by the stream and the medium. These waves are characterized by

$$\beta = \beta_e \pm \beta_p/\sqrt{\epsilon_r}, \tag{2}$$

where

$$\epsilon_r = \epsilon_2\left[1 - j\,\frac{\sigma}{\omega\epsilon_0\epsilon_2}\right]. \tag{3}$$

It is seen that the upper sign in (2) allows β to have (*i*) a positive imaginary part representing a wave growing in the $+z$-direction and (*ii*) a real part greater than β_e, indicating a phase velocity smaller than the average stream velocity. Both of these conditions are necessary in order to obtain amplification.[2] This growing wave may be excited to useful amplitude by ordinary means, as will be discussed later. The lower sign in (2) leads to a decaying wave with a velocity greater than u_0, so that this wave gives up energy to the stream.

In the limit, $\sigma = 0$, $\epsilon_2 = 1$, these waves revert to the ordinary unattenuated space-charge waves existing, for example, in a klystron amplifier. However, when loss is present ($\sigma > 0$), both gain and attenuation result because the propagation constants appear as a conjugate pair. For this reason, any scheme for attenuating a signal by a resistive wall (as for reducing noise energy) would necessarily also lead to a growing wave. To avoid exciting the growing wave, special initial conditions would be required, in general, not corresponding to noise space-charge waves as obtained from a thermionic cathode.

In expressing the gain and the phase velocity, it is convenient to introduce the dimensionless gain factor q and the phase factor p, defined by

$$\left[1 - i\,\frac{\sigma}{\omega\epsilon_0\epsilon_2}\right]^{-1/2} = p + jq, \tag{4}$$

so that

$$\beta = \beta_e \pm \beta_p\,\frac{(p + jq)}{\sqrt{\epsilon_2}}\,. \tag{5}$$

[4] W. C. Hahn, "Small signal theory of velocity-modulated electron beams," *Gen. Elec. Rev.*, vol. 42, pp. 258–270; June, 1939.

[5] S. Ramo, "The electronic wave theory of velocity modulation tubes," Proc. I.R.E., vol. 27, pp. 757–763; December, 1939.

The rate of exponential increase of the growing wave is then given by

$$8.69\beta_p\,\frac{q}{\sqrt{\epsilon_2}}\ \text{db/meter}, \tag{6}$$

and the phase velocity by

$$\frac{u_0}{1 + \dfrac{p}{\sqrt{\epsilon_2}}\,\dfrac{\omega_p}{\omega}}\ \text{meter/second}. \tag{7}$$

The factors p and q are plotted in Fig. 2 as functions of the $Q(=\omega\epsilon/\sigma)$ of the dielectric medium.

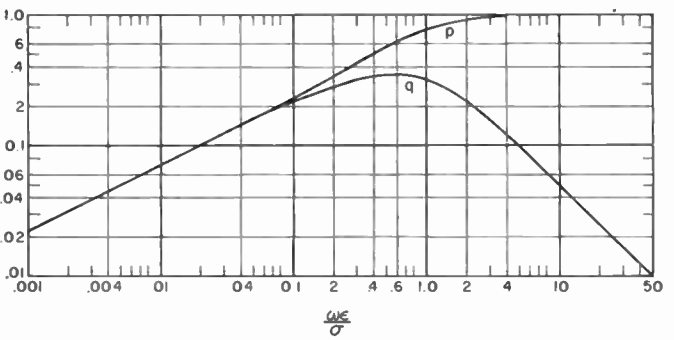

Fig. 2—Variation of gain factor q and phase factor p with $Q = \omega\epsilon/\sigma$ of the dielectric for the resistive-medium amplifier.

A. Rate of Gain and Over-all Gain

The over-all gain of a resistive-medium amplifier is the product of the gain due to the RMA section and that due to the coupling system employed. Such a coupling system is required in practice because of inherent weakness of the structure itself in exciting the space-charge waves. This weakness is due to the rapid decay with length of a signal applied directly to the circuit. It is felt necessary to use helices or cavities or grids in tandem with the resistive-medium section in order to modulate and demodulate efficiently.

The rate of gain, given by (6), reaches a maximum of

$$8.69\,\frac{\beta_p}{\sqrt{\epsilon_2}}\,\frac{1}{2\sqrt{2}} \cong \frac{3}{\sqrt{\epsilon_2}}\,\beta_p\ \text{db/meter}. \tag{8}$$

This value occurs for

$$Q = \frac{\omega\epsilon_0\epsilon_2}{\sigma} = \frac{1}{\sqrt{3}}\,. \tag{9}$$

This value of gain is the same as is available from an idealized double-stream amplifier[6] if one takes i_0 in the expression for β_p to be the sum of the current densities in both streams.

For an illustration of the available gain, we choose a representative current density of $-i_0 = 0.3$ amp/cm^2 and an electron velocity corresponding to a voltage of $V_0 = 400$ volts. In this case the gain of the growing wave computed from (8) is 5.8 db/cm or 14.7 db/inch at the optimum Q as given in (9) and with $\epsilon_2 = 1$.

[6] A. V. Haeff, "The electron wave tube—a novel method of generation and amplification of microwave energy," Proc. I.R.E., vol. 37, pp. 4–10; January, 1949.

It is seen that gain is affected by the electron velocity only through the plasma-wave number β_p. For constant perveance ($i_0/V_0^{3/2}$), the gain is essentially velocity independent, which is in great contrast to other stream-type amplifiers, particularly the traveling-wave tube.

As a step in estimating the over-all gain, it is necessary to know the behavior of an RMA section of any length for arbitrary excitation. The relative excitation of the two waves may be found by using the method of Appendix A and inserting the values of initial modulation. The ac current and velocity at a distance z from the plane of input current and velocity modulation, $i(0)$, $v(0)$, may be written as

$$\frac{i(z,t)}{i_0} = \left\{\frac{i(0)}{i_0}\cos\left[\frac{\beta_p z}{\sqrt{\epsilon_r}}\right] + j\frac{v(0)}{u_0}\frac{\omega\sqrt{\epsilon_r}}{\omega_p}\sin\left[\frac{\beta_p z}{\sqrt{\epsilon_r}}\right]\right\} e^{j(\omega t-\beta_e z)} \quad (10)$$

$$\frac{v(z,t)}{u_0} = \left\{\frac{v(0)}{u_0}\cos\left[\frac{\beta_p z}{\sqrt{\epsilon_r}}\right] + j\frac{i(0)}{i_0}\frac{\omega_p}{\omega\sqrt{\epsilon_r}}\sin\left[\frac{\beta_p z}{\sqrt{\epsilon_r}}\right]\right\} e^{j(\omega t-\beta_e z)}. \quad (11)$$

After a sufficient distance, ($\beta_p qz/\sqrt{\epsilon_2} > 2$ or 3), the growing wave predominates, leaving simply

$$\frac{i(z,t)}{i_0} = \frac{1}{2}\left\{\frac{i(0)}{i_0} - \frac{v(0)}{u_0}\frac{\omega\sqrt{\epsilon_r}}{\omega_p}\right\} \times \left\{\exp\left[\frac{\beta_p qz}{\sqrt{\epsilon_2}}\right]\right\} \times \left\{\exp\, j\left[\omega t - \left(\beta_e + \frac{\beta_p p}{\sqrt{\epsilon_2}}\right)z\right]\right\} \quad (12)$$

initial amplitude of the growing wave; growing term; phase term of unity magnitude

$$\frac{v(z,t)}{u_0} = \frac{1}{2}\left\{\frac{v(0)}{u_0} - \frac{i(0)}{i_0}\frac{\omega_p}{\omega\sqrt{\epsilon_r}}\right\} \times \left\{\exp\left[\frac{\beta_p qz}{\sqrt{\epsilon_2}}\right]\right\} \times \left\{\exp\, j\left[\omega t - \left(\beta_e + \frac{\beta_p p}{\sqrt{\epsilon_2}}\right)z\right]\right\}. \quad (13)$$

The gain in ac current (not necessarily ac energy) due to an RMA section of length L is given by

$$\text{current gain} = \frac{i(L)}{i(0)} = \frac{1}{2}\left[1 - \frac{v(0)/u_0}{i(0)/i_0}\frac{\omega\sqrt{\epsilon_r}}{\omega_p}\right]\exp\frac{(\beta_p qL)}{\sqrt{\epsilon_2}}\,\text{db}, \quad (14)$$

which is given in decibel form by

$$A_i + 8.69\frac{\beta_p qL}{\sqrt{\epsilon_2}}\,\text{db}, \quad (15)$$

where

$$A_i = -6 + 20\log_{10}\left[1 - \frac{v(0)/u_0}{i(0)/i_0}\frac{\omega\sqrt{\epsilon_r}}{\omega_p}\right]\text{db}, \quad (16)$$

is the apparent initial loss suffered in excitation.

The gain in ac velocity is, similarly,

$$\text{velocity gain} = \frac{v(L)}{u_0} = A_v + 8.69\frac{\beta_p qL}{\sqrt{\epsilon_2}}\,\text{db}, \quad (17)$$

where

$$A_v = -6 + 20\log_{10}\left[1 - \frac{i(0)/i_0}{v(0)/u_0}\frac{\omega_p}{\omega\sqrt{\epsilon_r}}\right]\text{db}. \quad (18)$$

For example, in a particular tube the stream might be velocity modulated by a short resonant gap preceding the resistive medium. At the exit from the medium, the stream would modulate a similar gap. Because of the division of the signal at the input, there is an apparent loss of 6 db; the power gain for the tube is

$$\text{power gain} = -6 + 8.69\frac{\beta_p qL}{\sqrt{\epsilon_2}}\,\text{db}, \quad (19)$$

over that when operated as a klystron. In the case of excitation by a growing wave, as at the exit from a helix, the initial loss A upon entering the RMA would be smaller and could be zero.

B. Frequency Bandwidth Available

The tremendous range of frequencies over which some gain is available is evident from Fig. 2. The slow-gain variation between half-power (3 db down) frequencies is also readily seen. For example, with a tube having 35-db gain and, for simplicity, no initial loss, these frequencies occur at roughly 50 and 170 per cent of the optimum-gain frequency, meaning 120 per cent bandwidth. Less gain would lead to more bandwidth. However, as is commonly found in practice with stream-type amplifiers, the bandwidth would probably be limited not by this figure but rather by the circuitry external to the tube.

C. Optimum Design Factors

The variation of gain with the material constant, ϵ/σ, is uncritical. Increasing σ by a factor of two over the optimum value reduces gain factor q by only 10 per cent. Since gain is proportional to $q/\sqrt{\epsilon_2}$, it is desirable to keep ϵ_2 as small as is practicable.

The medium itself may be characterized by the condition (9), which may be rewritten as $\sigma = (f\epsilon_2/9)$ mho/meter, effective conductivity, where f is in kilomegacycles. In the range 0.1 to 100 kmc, the optimum value of σ/ϵ_2 is roughly in the range 10^{-2} to 10; such conductivities for solids lie between those of good conductors (10^7) and good insulators (10^{-12}) and in the vicinity of some semiconductors.

The medium may be characterized in a somewhat different fashion in terms of the signal and dielectric relaxation frequencies. Recalling that in an isolated lossy

dielectric, an impressed-charge density ρ_0 decays with time as[7]

$$\rho = \rho_0 e^{-(\sigma/\epsilon)t}, \tag{20}$$

we define a fictitious relaxation frequency

$$\omega_r = \sigma/\epsilon_0\epsilon_2. \tag{21}$$

In this symbolism the abscissa in Fig. 2 becomes the ratio ω/ω_r and the frequency at optimum gain is $\omega = \omega_r/\sqrt{3}$. In a qualitative way we deduce that, for $\omega \ll \omega_r$, the wall charge decays too rapidly to influence the stream charge and, for $\omega \gg \omega_r$, the wall charge cannot reverse sign rapidly enough to aid in bunching; in both cases there can be but little gain. However, in the frequency region where the driving and the relaxation frequencies are about equal, $\omega \approx \omega_r$, we must look for a more exact relation between these charges in order to understand the mechanism of amplification.

The wall charge is found (in Appendix A) to be related to the stream charge in the following way:

$$\rho_m = -\rho_s(1 + j\omega/\omega_r)^{-1}. \tag{22}$$

This relation may be used to describe the mechanism of constructive interaction as follows. The out-of-phase component of ρ_m (this is the ordinary image charge) tends to reduce the debunching forces, thus allowing denser bunches to be formed. The quadrature component of ρ_m shifts the phase of the total field so as to put most of the electrons of a bunch in a retarding field. Thus, on the average, energy is given up by the stream to the growing wave and to ohmic losses in the medium.

D. Isolation of the Input from the Output

The field waves which can exist in the medium are highly attenuated. At the optimum-gain frequency the attenuation is

$$\alpha = 8.69 \cdot 2\pi \cdot \sqrt{\epsilon_2} \cdot 1/\sqrt{2} = 38.5 \cdot \sqrt{\epsilon_2}\ \text{db/free-space wavelength}. \tag{23}$$

At microwave frequencies the length of the RMA tubes would be of the order of one free-space wavelength. Thus, the attenuation would be ample for preventing self-oscillation, even in the case of complete reflection.

II. The Resistive Sheet Model

The use of a semiconductor full of small holes for the passage of electrons appears impractical. However, the results derived above for this idealized model serve as a rough guide in estimating the performance of more practical models. To obtain more useful design data without recourse to a complete-field solution, a more practical model will be analyzed.

Consider a sandwich of insulating sheets of dielectric constant $\epsilon = \epsilon_0\epsilon_2$, coated with a lossy material, and with sheet-electron streams flowing through the interspaces as shown in Fig. 3. Assume that the thicknesses involved are all small compared to a stream wavelength; that is, $s, g \ll \lambda_s$ and $d \ll g$. Upon inserting the effective conductivity and dielectric constant into (2) in terms of the actual σ and ϵ, we find that the propagation constants may be written as

$$\beta = \beta_e \pm \beta_p\left[1 + \frac{g}{s}\epsilon_2\right]^{-1/2}\left[1 - j\frac{2\sigma d}{\omega\epsilon_0(s + g\epsilon_2)}\right]^{-1/2}. \tag{24}$$

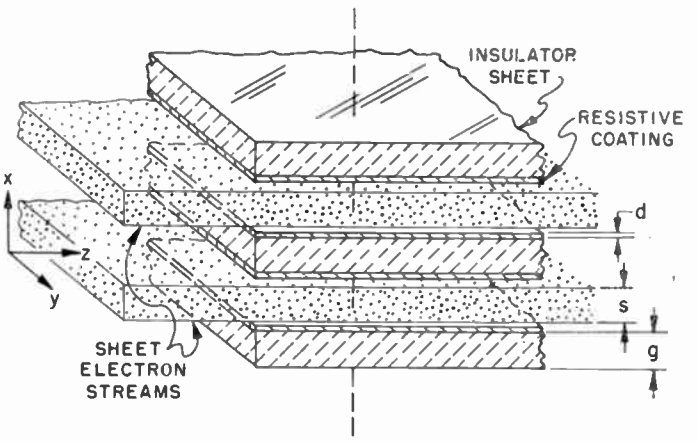

Fig. 3—Resistive-sheet model in which electron streams flow between resistive layers; this model is a practicable version of the resistive-medium amplifier of Fig. 1.

The gain and phase velocity for this model are given by (6) and (7) and Fig. 2, as in the previous case, but with an obvious interchange of functions. The optimum gain is obtained at

$$\frac{\omega\epsilon_0(s + g\epsilon_2)}{2\sigma d} = \frac{1}{\sqrt{3}}, \tag{25}$$

which may be written as

$$R_\square \omega C_z = 1/\sqrt{3}, \tag{26}$$

where $2R_\square$ is the resistance per square of one coating and C_z is the capacitance measured along z, per unit length and width of an elementary stratum of the model in Fig. 3.

One could actually use lumped elements at a low enough frequency (long enough stream wavelength) where it would be mechanically possible to employ a number of elements per quarter stream wavelength.

For example, at the frequency of 3 kmc, the order of magnitude of resistances and gain are, for very thin insulating sheet, $(g/s)\epsilon_2 \ll 1$, $R_\square = 3{,}500$ ohms/square, $q_{max} = 0.351$; and, for fairly thick insulating sheet, $(g/s)\epsilon_2 = 1$, $R_\square = 1{,}700$ ohms/square, $q_{max} = 0.248$.

The design data obtained from this model are applicable even for models for which s and g are not small compared to λ_s, and the number of sheets in the sandwich is small rather than infinite.

III. Field Theory and Design Data; the Resistive-Wall Amplifier, a Two-Dimensional Model

To obtain more accurate gain and phase information, a third model, Fig. 4, corresponding to a single pore of the resistive medium will be analyzed using a two-dimensional field theory. The stream flow is assumed to

[7] For example, S. Ramo and J. R. Whinnery, "Fields and Waves in Modern Radio," John Wiley and Sons, Inc., N. Y., p. 200; 1944.

be confined to the z-direction by a very strong magnetic field so that the electron motion is affected only by the z-component of the electric field. Also, the stream is assumed to have uniform dc velocity and current density, which implies either small charge density or complete neutralization by positive ions. However, in this small-signal solution the ac quantities do vary with r (though not with ϕ) as the Bessel functions $J_0(Tr)$ and $J_1(Tr)$.

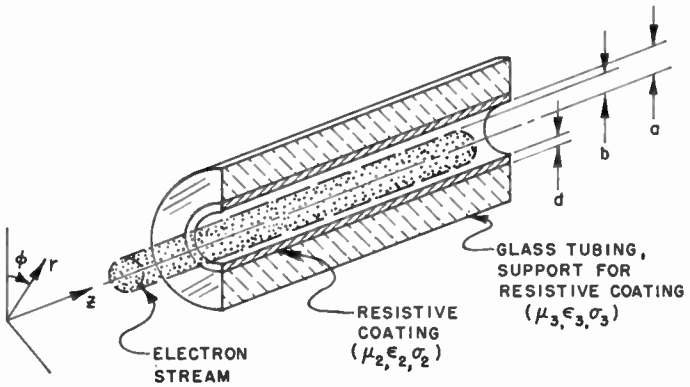

Fig. 4—Resistive-wall amplifier cross section of simplest design; this model represents a single-pore version of the resistive-medium amplifier of Fig. 1 and is the model actually used in the initial experiments.

The following restrictions are placed on the thickness of the resistive coating to insure that electrically it is very thin:

$$\sqrt{\omega\epsilon_2\sigma_2}\, d \ll 1, \quad \text{or} \quad d \ll \delta, \text{ the skin depth;}$$

$$\sqrt{\omega\epsilon_2\sigma_2} \ll \beta_e, \quad \text{or} \quad \delta \ll \lambda_s, \text{ the stream wavelength.}$$

The actual mechanics of the field solution are carried out elsewhere.[3] The particular result presented here is for the case of the stream filling the tube, $a=b$, the dielectric constant of the glass equal to that of free space ($\epsilon_3=\epsilon_0$), and $\mu_3=\mu_0$, $\omega\epsilon_3/\sigma_3 \gg 1$. These conditions may be approximated fairly closely, the second condition through use of very thin-walled glass.

The propagation constants of the space-charge waves in this case are given by (5), the rate of gain by (6) and the phase velocity by (7), all with $\epsilon_2=1$. However, p and q are numerically different from the previous values. Contours for constant p and q are shown in Fig. 5; the abscissa $\beta_e b$ is the ratio $2\pi b/\lambda_s$ of the stream circumference to the stream wavelength, and the ordinate is $2\omega R_z C_z$, where $R_z=R_\square/2\pi b$, the resistance per unit length, or ohms per square of the coating divided by the circumference, and $C_z=\pi b^2\epsilon_0$, the capacitance per unit length. For a given tube with $R_\square$ and u_0 fixed, the gain factor q varies with the frequency along a line of slope unity, since

$$2\omega R_z C_z = \beta_e b R_\square u_0 \epsilon_0. \tag{27}$$

For a given tube at fixed frequency, the gain varies with the stream velocity along a horizontal line. In designing a tube, given $\beta_e b$, the gain varies with $R_\square$ or R_z along a vertical line.

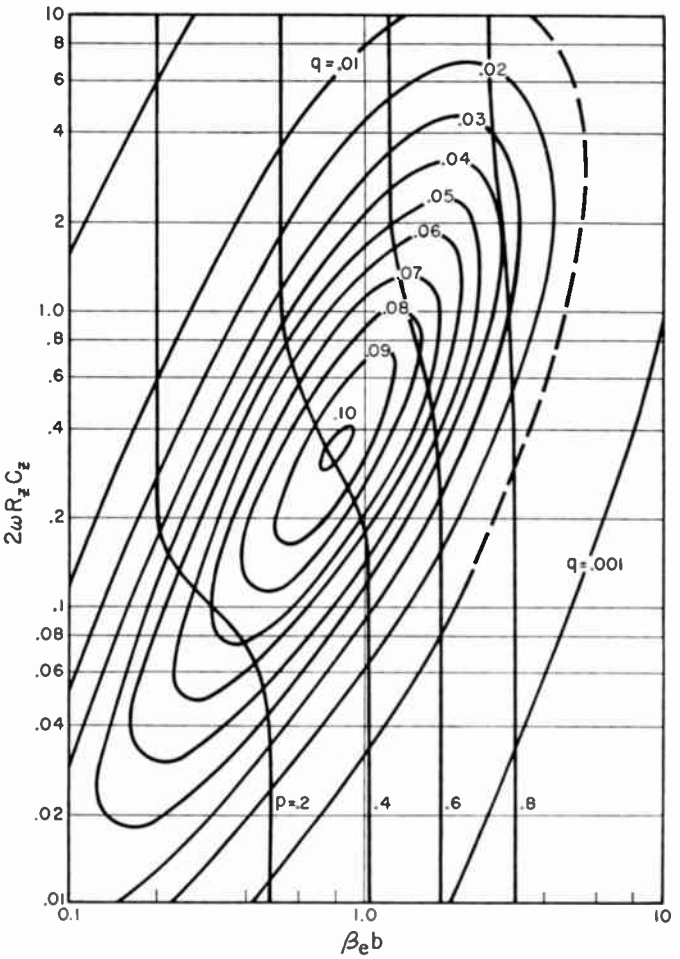

Fig. 5—Contours of constant gain factor q and phase factor p as functions of $\beta_e b=2\pi b/\lambda_s$ and $2\omega R_z C_z=\beta_e b R_\square u_0\epsilon_0$ for the resistive-wall amplifier model of Fig. 4.

In Table I the properties of this model and of the RMA are compared. Also, the values of attenuation of the return waves are found to be comparable.

TABLE I

Basis of Comparison	RMA	RWA
(a) Maximum of the gain factor q (all $\epsilon=\epsilon_0$).	0.351	0.10
(b) Bandwidth between half-power frequencies, assuming no initial loss, 35-db peak gain.	120 per cent	70 per cent
(c) Dependence of gain on resistive-wall potential at constant perveance.	None	Variation of ±50 per cent to go 3 db down from max. of 35 db.

Except for (a), it is seen that the useful properties of the RMA are fairly well retained in the RWA. However, the RWA gain is considerably lower and, in actual models, it unfortunately will be lower still, owing to higher dielectric constant of the glass tubing and looser coupling of the stream to the wall when the stream fills but a fraction of the hole cross section.

Fortunately, part of this "lost" gain may be retrieved through use of honeycomb structures as shown in Fig. 1. Also, mounting resistive coating on an inductive wall,[3] so as to cancel out part or all of the capacitance beyond resistive coating, gives higher gain.

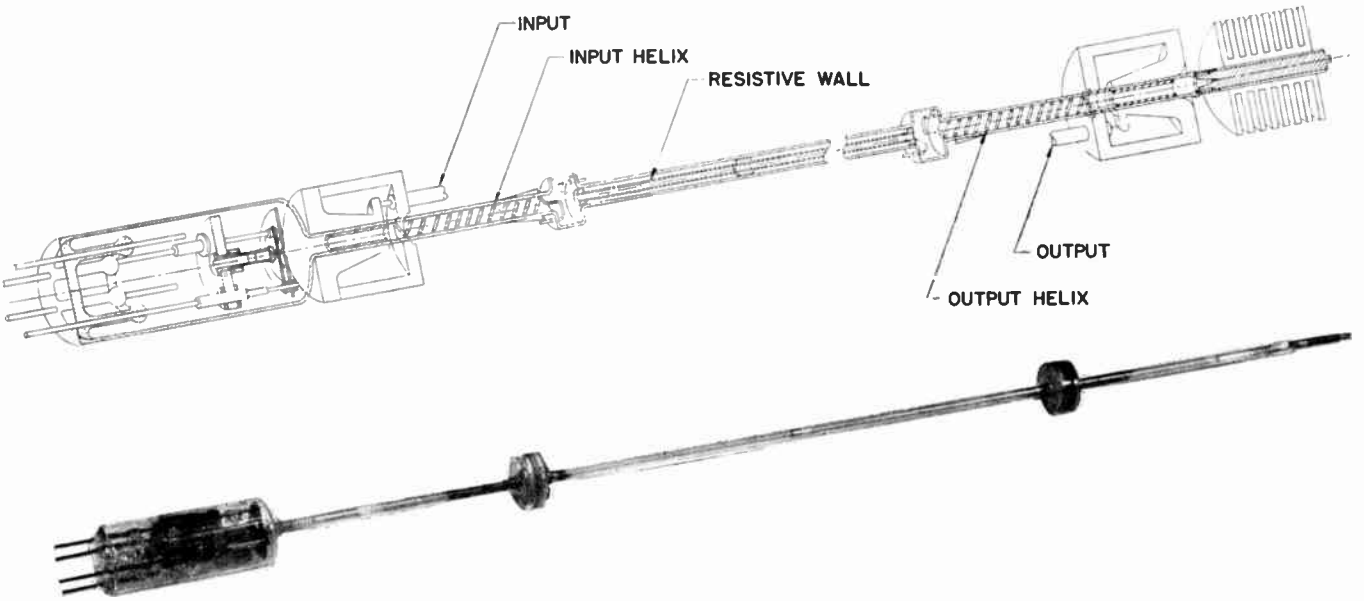

Fig. 6—A resistive-wall amplifier with helix coupling for use in the frequency range of 1 to 4 kmc. The drawing shows the details of construction of the actual tube.

IV. Description of the Experiments

The experiments on the resistive-wall amplifier were conducted primarily to demonstrate the existence of resistive-wall amplification and to determine some of the operating characteristics of this amplifier. In the initial experiments, the model consisted of a cylindrical-electron stream surrounded by a coaxial glass tube coated on the inside with a resistive material. This may be thought of as a single pore of the resistive medium. An auxiliary circuit in the form of a helix was added to each end of the resistive-wall section to modulate and demodulate the stream. Fig. 6 shows a drawing and photograph of a typical tube.

Because the helices are capable of amplification as in ordinary traveling-wave tubes, it is difficult to determine accurately the gain of the resistive-wall section of the tube from measurements on a single tube. Though some indication of the division of total gain can be obtained from calculations, there are uncertain parameters (stream diameter, helix impedance, and so forth) that reduce the accuracy of such calculations. Therefore the resistive-wall amplification was determined more directly by means of a substitution method. After measuring over-all gain with the resistive wall, the gain was remeasured with a metallic drift tube substituted for the resistive-wall section, all other parts remaining unchanged. In each case the gain was measured for a number of different stream currents. The difference between the two values of gain was substantial, indicating the existence of a growing space-charge wave in the resistive-wall section. Further evidence of the existence of such a growing wave was also found through observation of the interference between the growing and decaying waves at the end of the interaction region.

Four resistive-wall experiments have been performed, three with helix input and output circuits and one with resonant-cavity circuits. Three of these tests were made in a demountable vacuum system and one with a sealed-off tube. In the demountable system, Fig. 7, the various elements of the tube were individually supported in a large continuously evacuated bottle, allowing accurate alignment and ease in substitution, a method well adapted to this type of measurement.

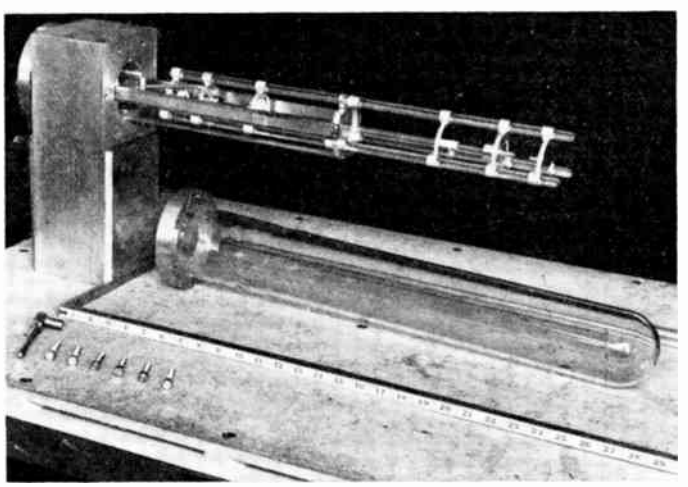

Fig. 7—The demountable vacuum system in which some of the initial RWA experiments were performed. The construction employed allowed easy interchange of the resistive wall for the metallic drift tube.

To obtain maximum gain, it would be desirable to use a self-supporting resistive material surrounding the electron stream as the resistive wall. Practically, it was found necessary to bond the existing usable resistive materials to a dielectric support, in this case, glass. As pointed out in Section C, Part I, the capacitive-shunting effect of the dielectric-support material reduces the gain available from the resistive wall. To minimize this effect, the glass tubing was etched to a thickness of about 0.005 inch. The resistive layer was a coating of tin oxide about 10^{-5} inch thick on the inner surface of the glass tube, obtained by deposition of tin oxide onto the hot glass from stannous chloride vapor. This

process can be controlled to yield any desired resistance value from the order of 10 ohms to hundreds of megohms per square. The coating is very tough mechanically, remaining stable under conditions of moderate electron bombardment and up to temperatures near the softening point of the glass.

In this work the resistive walls were coated to an rf resistance (measured at $\lambda_0 = 3$ and 10 cm) near 2,000 ohms/square, about half the dc value.

In the experimental tubes the coated tubing was 10 inches long and the helices placed at each end were 3 inches long. Each helix was terminated nearest the resistive wall by a layer of "Aquadag." The tube was operated in confined flow with a magnetic field of about 800 gauss.

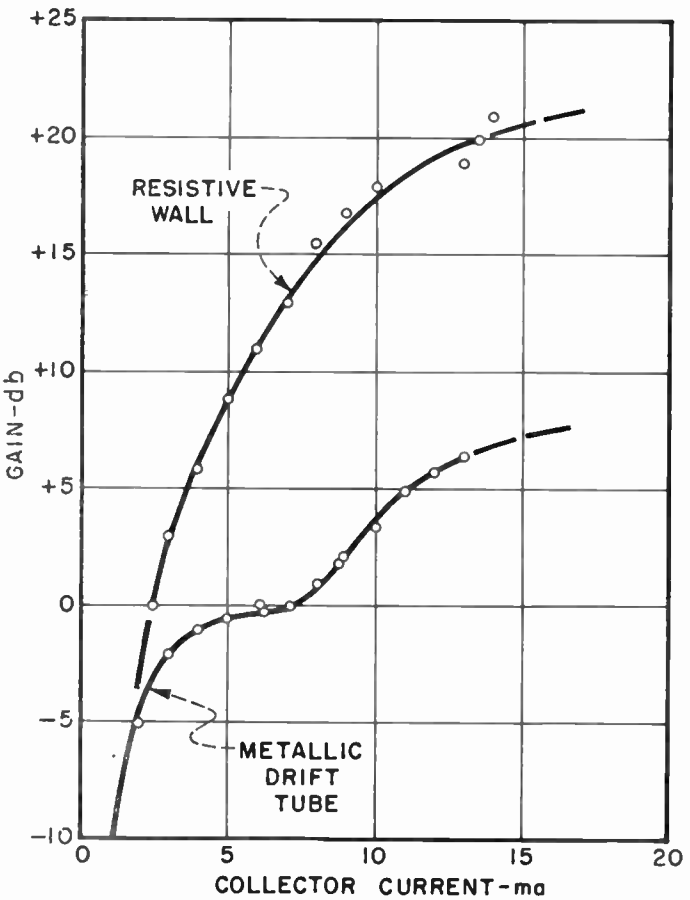

Fig. 8—Over-all gain of a helix-coupled tube as a function of the stream current for a resistive wall and a metallic drift tube, as measured near 3 kmc. The resistive coating measured about 3,000 ohms/square with dc. (Demountable system.)

Fig. 8 shows a plot of measured over-all gain as a function of collector current ($\approx$97 per cent of the cathode current) for both the resistive-wall and the metallic-drift tube. The gain observed in the case of the drift tube is, of course, due entirely to the helices. The difference in gains ($\approx$14 db at 10 ma) is interpreted as due to the growing wave in the resistive-wall section. From the knowledge of this net gain and the operating parameters, an experimental value of 0.035 was obtained for the gain factor q. From the theoretical curve of Fig. 5, $q = 0.073$. This value should be reduced by about 48 per cent because the stream did not fill the cross section ($b/a \approx 0.77$) and further reduced by 88 per cent to account for the capacitive effects of the glass; the final theoretical value for q is 0.031. In both calculations it is assumed that the stream has a uniform diameter and is concentric with the walls; experimentally the diameter is not uniform (the mean diameter can only be estimated) and the concentricity is doubtful. Thus, exact agreement between experiment and theory would be fortuitous.

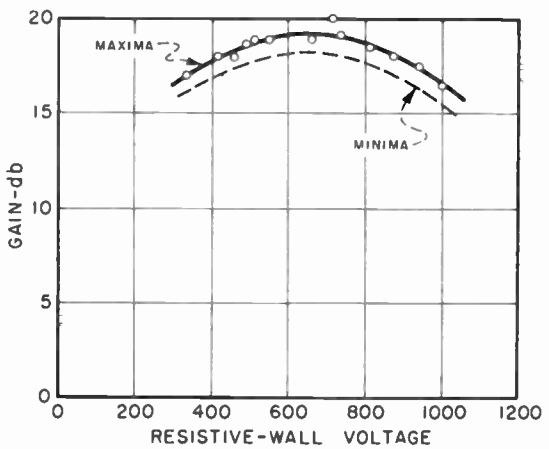

Fig. 9—Over-all gain as a function of resistive-wall potential for a helix-coupled tube. The points shown are the measured maxima and the dashed line indicates the loci of the minima. Stream currents and other potentials were held constant. (Demountable system.)

One of the distinguishing features of the resistive-wall amplifier, as mentioned previously, is its relative insensitivity to changes in stream voltage. Fig. 9 shows the measured gain as a function of resistive-wall voltage for constant-stream current and helix potentials. It is seen that the gain changes little for a voltage range from 300 to 1,000 volts. There are small variations due to constructive and destructive interference between the larger-growing and the smaller-decaying wave at the exit from the resistive wall, as well as to a small velocity jump at each end. In addition, when the potentials of the anode, helices, and the resistive wall were derived from a common supply, it was found that the gain also varied slowly with the supply voltage. The difference between potentials where gain was 3 db below the peak value was about 22 per cent of the potential at peak gain, as measured at several frequencies. This voltage "bandwidth" was delimited primarily by the short helices and could be increased by the use of even shorter helices. Although no special precautions were taken to maximize the insertion loss, the measured isolation between input and output terminals of the tube varied between 55 and 85 db over the frequency range 2,000 to 4,000 mc.

We also constructed a resistive-wall tube with resonant cavities as the coupling elements to the electron stream. To determine the net gain, the method of substitution of a drift tube for the resistive wall was used in this test also. The experimental data of gain versus

current, Fig. 10, show that a net gain in the resistive-wall section of about 12 db was obtained at 10 ma, meaning an experimental gain factor of $q=0.034$. (This test employed the same resistive wall as used with helices.) Upon substitution of the drift tube, the system behaved as a two-cavity klystron with a long-drift space. The gain of this klystron was estimated[8] for one value of current which is seen to be a little lower than the measured value.

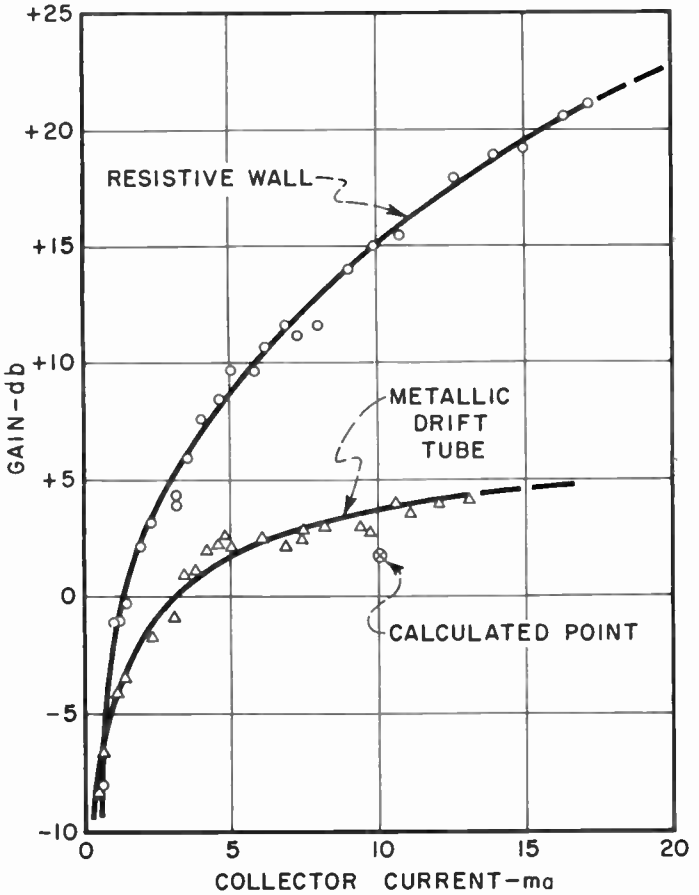

Fig. 10—Over-all gain of a resonant-cavity-coupled tube as a function of a stream current for a resistive wall and a metallic drift tube, as measured at 2,920 mc. (Demountable system.)

Fig. 11 shows the variation of gain with the potential of the resistive-wall section. Curves (a) and (b) are much like those obtained with helix circuits; in both cases the ac velocity and current of the decaying wave are small compared with those of the growing wave, and the interference is therefore small. However, the case of klystron operation, curve (c), is quite different, exhibiting interference between unattenuated waves that are essentially equal in amplitude. The input cavity excites two waves with equal ac velocities, but with opposing ac currents (initial net current ≈ zero). Because the waves have different phase velocities, the ac currents add and subtract as they travel. Thus the output of the second cavity, which is sensitive to current, fluctuates rapidly as the space-charge wavelength is varied by varying the wall potential.

[8] L. T. Zitelli, "Space charge effects in gridless klystrons," Stanford University, Microwave Laboratory Technical Report No. 149; October, 1951.

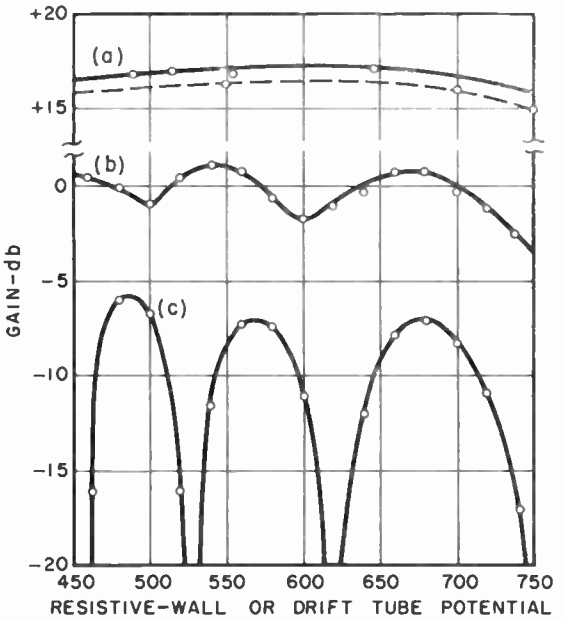

Fig. 11—Over-all gain as a function of resistive-wall potential for a cavity-coupled tube. Shown are curves for (a) resistive wall, high current, (b) resistive wall, low current, (c) metallic wall, low current. (Demountable system.)

A further check on the value of q is afforded by the measurement of G_c and G_d, the voltage gains at constructive and destructive interference. Assuming that the growing and decaying waves are equally excited by the velocity modulation and that $\beta_1 q$ varies slowly with resistive wall potential, we find

$$q = \frac{1}{2\beta_p L} \ln \frac{G_c + G_d}{G_c - G_d}, \tag{28}$$

where L is the length of the resistive-wall section. The value of q calculated this way from curve (b) of Fig. 11 is 0.032, as compared with the theoretical value, 0.031.

The interference patterns and the measured values of gain confirm beyond reasonable doubt that there are exponentially growing and decaying waves in the resistive-wall section.

Fig. 12 shows the variation of over-all gain with

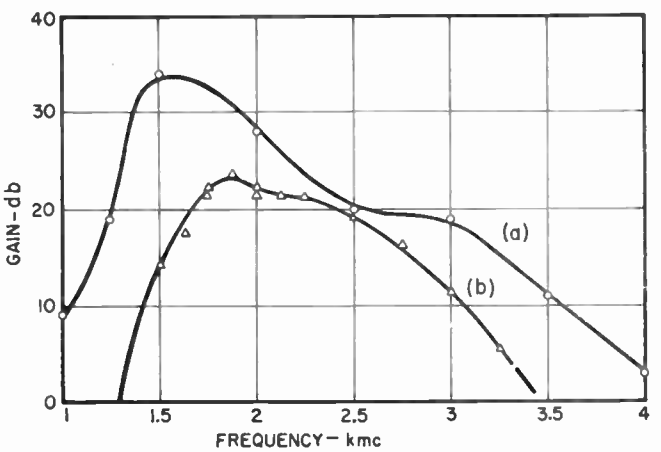

Fig. 12—Over-all gain as a function of frequency for a stream current of 15 ma: (a) all potentials adjusted for maximum gain at each frequency; (b) all potentials held constant. (Sealed-off tube.)

frequency for the helix-coupled sealed-off tube and coax-to-helix matches as shown in Fig. 6. The bandwidth is about 700 megacycles between half-power frequencies, or 33 per cent of the mid-band frequency with all potentials held constant (curve (a)). Of course, the bandwidth is limited by the helices and coupling units, as well as by the resistive wall.

Fig. 13 shows the saturation characteristics of the same tube for several stream currents at a frequency (3 kmc) above that for maximum gain. Although the efficiencies (3–4 per cent) are low compared to some types of tubes, they are comparable to those of low-power traveling-wave amplifiers; because efficiency (and gain) increase with stream current, higher efficiency could be obtained at higher-power levels.

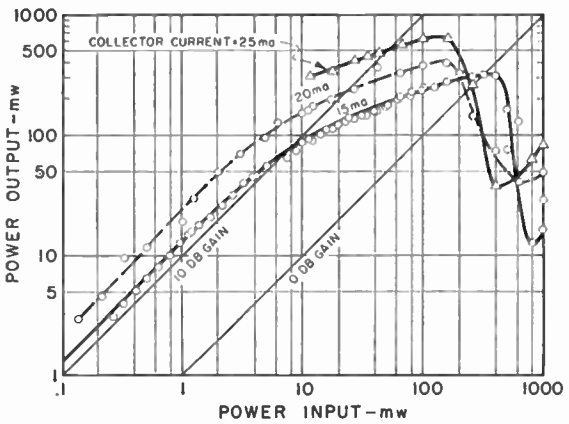

Fig. 13—Power output as a function of power input as measured at 3 kmc for all potentials about 650 volts. The electronic efficiency is seen to be about 3.1 per cent at 20 ma and 4.1 per cent at 25 ma.

Some spot measurements indicate the noise figure of this tube to be about 26 to 30 db at 15-ma stream current. No attempt was made to design the tube for a low-noise figure. One could expect the resistive-wall amplifier to exhibit the same value of noise figure as a traveling-wave tube (with the same helix and gun structure) because, if the input helix is long enough to insure predominance of the growing wave, then the noise figure is almost independent of what follows the first helix.

V. Other Possible Models and Applications

The initial experimental models were designed primarily to demonstrate the existence of resistive-wall amplification. It is believed that models with much higher gain can be constructed. The physical structure of such tubes would correspond more closely to either the resistive medium with a honeycomb support for the resistive coating and using, say, three or four holes, or to the sandwich model with a few more than two sheets. Two versions of such structures have been made as are shown in Fig. 14. One structure consists of four 0.006-inch walled glass tubes whose surfaces are to be coated with resistive material; in operation the open spaces would be flooded by an electron stream. The second structure (made by the Corning Glass Works using their Fotoform developing and etching technique) has slots of width 0.040-inch between glass fins of thickness 0.006 inch for passage of the stream. The fins are to be resistive coated. It is estimated that with such structures an effective value of gain factor q of about 0.2 or better could be obtained. This would result, for example, in a net resistive-wall gain of about 90 db for the same $\beta_p L$ as used in the tests described previously.

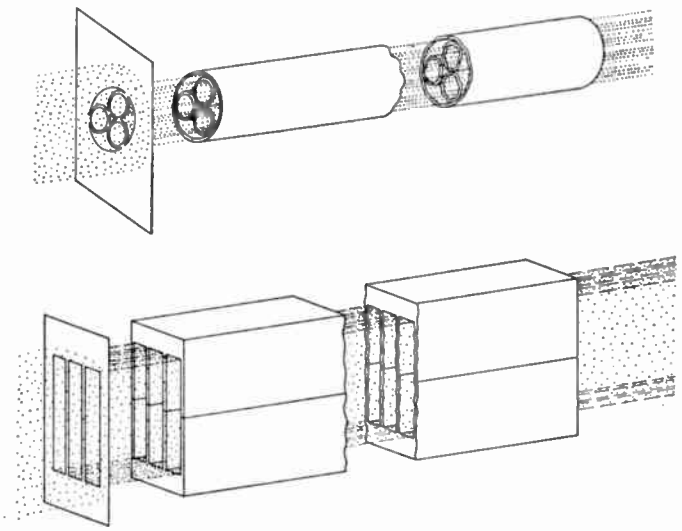

Fig. 14—Structures proposed for higher gain which are physically realizable approximations to the resistive-medium or sheet models.

The RWA, even in the form used, could fit into applications now filled or intended for the TWT. It would have most effective application where advantage is taken of its special properties such as the relative insensitivity of gain to variations in operating or design parameters and the high isolation between input and output.

Appendix A—Propagation Constants in the Resistive-Medium Amplifier

The propagation constants of the waves in the resistive-medium amplifier can be found as follows. We assume that the stream and the medium are intimately mixed (insofar as our macroscopic observation is able to discern) so that ϵ, μ, σ may be taken as continuous, being averaged values. It will be shown that in the conducting medium itself there are free charges of density ρ_m (usually taken as zero)[7] induced by the charge in the stream of density ρ_s.

The view shown in Fig. 1 is a microscopic picture. There we are observing only a small cross section (of diameter small compared to a stream wavelength) of a large structure that is operating in its fundamental mode. On this assumption, the stream may be regarded as drifting through a medium of arbitrary conductivity and dielectric constant.

The total charge density is ρ, the total convection current density is $i = i_s + \sigma E$, and the total dielectric flux density is $D = \epsilon E$.

To show that there exists a charge density in the medium, we employ the relations

$$\nabla \times H = i + \epsilon \frac{\partial E}{\partial t}, \tag{1a}$$

$$\nabla \cdot E = \rho/\epsilon. \tag{2a}$$

Taking the divergence of (1a) and using (2a), we see that i must be continuous. Because we already have assumed that the stream current is continuous, that is

$$\nabla \cdot i_s + \frac{\partial \rho_s}{\partial t} = 0, \tag{3a}$$

we find that the current in the medium also must be continuous, or

$$\nabla \cdot \sigma E + \frac{\partial(\rho - \rho_s)}{\partial t} = 0. \tag{4a}$$

It is seen that, for wave-like behavior of E, $(\rho - \rho_s)$ will have a value which is the charge density ρ_m in the medium. Assuming that the time dependence for all quantities is exp $(j\omega t)$ and combining (4a) with (2a), we obtain the relation

$$\rho_m = -\rho_s\left[1 + \frac{j\omega\epsilon}{\sigma}\right]^{-1}. \tag{5a}$$

For the waves in the medium, the inhomogeneous wave equation[9] is

$$\nabla^2 E - \mu\epsilon \frac{\partial^2 E}{\partial t^2} = \frac{1}{\epsilon}\nabla\rho + \mu \frac{\partial i}{\partial t}. \tag{6a}$$

When ρ_m in expressed terms of ρ_s, from (5a), and ρ_s and i_s in terms of E_s (assuming that the stream electrons have z-directed motion only), (6a) in cylindrical coordinates (r, ϕ, z) becomes

$$\nabla_{r,\phi}^2 E_s + T^2 E_s = 0, \tag{7a}$$

where

$$T^2 = (\beta^2 - \omega^2\mu\epsilon + j\omega\mu\sigma)\left[\frac{\beta_p^2}{(\beta - \beta_s)^2(\epsilon/\epsilon_0)\left[1 + \frac{\sigma}{j\omega\epsilon}\right]} - 1\right]. \tag{8a}$$

For the one-dimensional model (that is, no transverse variations, $\nabla_{r,\phi}^2 = 0$), in order for E_s to exist, T must be zero. Of course, this implies a cross section infinite in extent. However, even with a finite cross section, T can approach zero. One recognizes that (7a) is a Bessel equation with solutions for E_s of the form $J_n(Tr)e^{jn\phi}$. Suppose that the stream and the medium are encircled by a perfect conductor at the radius $r = b$; then $E_s(b) = 0$. For the case of no variations of E_s with ϕ $(n = 0)$, this requires that $J_0(Tb) = 0$, which means that $T = 2.405/b$ for the lowest order mode (smallest T). Hence, making b very large (essentially, one stream wavelength or more), we can approach the limit $T = 0$.

With $T = 0$, one obtains from (8a) two separate equations from which the four propagation constants are easily obtained. Those corresponding to the space-charge waves are the zeros of the second bracket as written out in (2).

ACKNOWLEDGMENT

The authors are grateful to J. R. Whinnery for his valuable contributions to all phases of this work and to S. Hansen for showing us how to apply a resistive coating to the inside surface of small-diameter glass tubing for use in our experimental amplifiers.

Thanks are also due to the many members of the Engineering Section of the Electron Tube Laboratory for their assistance in the construction of the experimental tubes.

[9] For example, J. A. Stratton, "Electromagnetic Theory," McGraw-Hill Book Co., Inc., New York, N. Y., p. 33; Eq. 71; 1941.

Some Aspects of Mixer Crystal Performance*

PETER D. STRUM†, ASSOCIATE, IRE

Summary—**A method for calculating the conversion loss and conductances of a crystal mixer is presented. The magnitude of the dependence of these characteristics on terminations at the image frequency and at the sum frequency is shown. Experimental verification of the calculations is shown by measurements and by reference to the literature. An investigation of crystal noise characteristics is reported, and it is shown that there is an optimum intermediate frequency for minimum noise figure. The design criteria for minimum receiver noise figure are shown.**

* Decimal classification: R357.41. Original manuscript received by the Institute, April 23, 1952; revised manuscript received January 15, 1953.

† Airborne Instruments Laboratory, Mineola, N. Y. A portion of the work described in this paper was supported by Contracts NOa(s)-8575 and NObsr-49148 with the Department of the Navy, Bureau of Ships.

I. INTRODUCTION

THE MINIMUM NOISE FIGURE attainable in a microwave receiver is limited by two characteristics—loss in the signal circuitry prior to amplification, and noise generated in the receiver components. Most microwave receivers presently use a crystal mixer as the first active network. In such receivers, most of the signal loss and excess noise are contributed by the crystal mixer. Therefore an improvement in mixer crystals, or in the manner in which they are operated, will allow the design of more sensitive receivers than is now possible.

This paper describes a theoretical and experimental investigation of the performance of microwave mixer

crystals. The purpose of the investigation was threefold: (1) to develop a simple mathematical method for numerically analyzing the performance of mixer crystals; (2) to obtain experimental data and data from the literature that substantiate the mathematical predictions and show noise temperature characteristics; and (3) to formulate from the results methods for predicting and improving the performance of standard crystals as mixers.

A mathematical method was developed that permits analysis of crystal characteristics. It was found that the conversion loss of a crystal depends on two characteristics of the crystal *E-I* curve. The fundamental characteristic is the slope $d\ (\log i)/d\ (\log e)$ for the high-conductance portion of the static *E-I* chacteristic. The symbol x is used hereafter to denote $d\ (\log i)/d\ (\log e)$. The other, and somewhat less important, characteristic is the relative back conductance.

The mathematical method was experimentally verified, and from noise temperature measurements it was found that there is an optimum mixer configuration and an optimum intermediate frequency for minimum over-all receiver noise figure.

II. Discussion

A number of authors[1-7] have given general analyses pertinent to crystal mixers based on linear-network theory. In each case the elements of the linear network were obtained from the Fourier analysis of the periodic crystal conductance pulses

$$g = g_a + \sum_{n=1}^{\infty} g_n \cos n\omega_0 t. \tag{1}$$

In (1), g is the instantaneous slope of the crystal *E-I* curve, g_n is the amplitude of the nth harmonic component of the periodic conductance, and g_a is the time average of g.

Several of the authors[2-5] have shown that a mixer using a nonlinear conductance of the form of (1) can be represented by an equivalent network of linear conductances in which frequency translations take place. (The purpose of this paper is not to derive an equivalent network, but to obtain numerical values of loss, conductance, and noise temperature. A brief discussion of the derivation is, however, included in the appendix for completeness.) Except for the frequency translations most of the usual laws of linear-network analysis apply.

The network conductances can be found from analysis of the current through g which results from the application of a small-signal voltage.

The resulting current is

$$\begin{aligned} i &= g e_r \cos \omega_r t, \\ &= \left(g_a + \sum_{n=1}^{\infty} g_n \cos n\omega_0 t\right) e_r \cos \omega_r t, \\ &= g_a e_r \cos \omega_r t + \sum_{n=1}^{\infty} g_{cn} e_r \cos (n\omega_0 + \omega_r) t \\ &\quad + \sum_{n=1}^{\infty} g_{cn} e_r \cos (n\omega_0 - \omega_r) t, \end{aligned} \tag{2}$$

where

$$g_{cn} = \frac{g_n}{2}. \tag{3}$$

It is seen that g_{cn} is a conversion conductance; i.e., g_{cn} is the ratio of the current flowing in g at the first upper or lower sideband of the nth harmonic of the conductance frequency to the signal voltage. For the usual case of fundamental mixing $n=1$.

The equivalent network of a mixer with appreciable impedance in series with g at each of the frequencies indicated in (2) would be an infinite-mesh network. In the usual crystal mixer the impedance at only a few of the indicated frequencies is of importance.

III. Equivalent Networks

In the least complex mixer possible there is impedance in series with the crystal at the signal frequency, ω_r, and at the intermediate frequency, $n\omega_0-\omega_r$. Frequently there also is impedance at the image frequency $2n\omega_0-\omega_r$, and perhaps at higher-frequency sidebands, such as the sum frequency, $n\omega_0+\omega_r$. It should be noted that in microwave receivers $\omega_0+\omega_r$ is almost equal to $2\omega_0$; and as a result, the effect of termination of this sideband is sometimes erroneously attributed to termination of the "second harmonic."

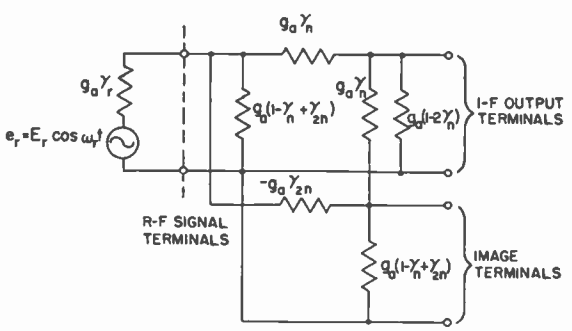

Fig. 1—Equivalent network for mixer calculations.

The equivalent network in Fig. 1 has been shown to be suitable for calculations when there is impedance at signal, image, and intermediate frequencies.[5] In the following analyses the various conductances are normalized with respect to g_a. The use of the normalized form

[1] M. J. O. Strutt, "Diode frequency changers," *Wireless Eng.*, vol. 13, pp. 73–80; February, 1936.
[2] E. Peterson and L. W. Hussey, "Equivalent modulator circuits," *Bell Sys. Tech. Jour.*, vol. 18, pp. 32–48; January, 1939.
[3] E. W. Herold and L. Malter, "Some aspects of radio reception at ultra-high frequencies," Proc. I.R.E., vol. 31, pp. 575–582; October, 1943.
[4] L. C. Peterson and F. B. Llewellyn, "The performance of mixers in terms of linear-network theory," Proc. I.R.E., vol. 33, pp. 458–476; July, 1945.
[5] E. W. Herold, R. R. Bush, and W. R. Ferris, "Conversion loss of diode mixers having image-frequency impedance," Proc. I.R.E., vol. 33, pp. 603–609; September, 1945.
[6] H. C. Torrey and C. A. Whitmer, "Crystal Rectifiers," vol. 15, Rad. Lab. series, pp. 111–178; McGraw-Hill Book Co. Inc.; 1948.
[7] A. B. Crawford, material included in G. C. Southworth, "Principles and Applications of Waveguide Transmission," D. Van Nostrand Co. Inc.; pp. 626–636; 1950.

simplifies the numerical calculations. An example is the normalized conversion conductance

$$\gamma_n = \frac{g_{cn}}{g_a}. \tag{4}$$

In Fig. 1 $g_a\gamma_r$ is the conductance presented to the point contact of the crystal at the signal frequency by the RF signal source. In a like manner the IF output terminals and image terminals indicate schematically the point contact of the crystal. The admittance reflected to the point contact at one of the frequencies is in effect connected to the corresponding pair of terminals.

Brief mention will be made of the case involving impedance at the sum frequency, $n\omega_0+\omega_r$, which is similar to the image in its effect. The effect of impedance at higher-order sidebands is considered negligible, and the following three particular cases of general interest will be analyzed:

Case 1: The mixer of Fig. 1 with the image terminals short-circuited.

Case 2. The mixer of Fig. 1 with an external conductance at the image terminals equal to the RF signal-source conductance; i.e., the so-called matched-image case.

Case 3: The mixer of Fig. 1 with the image terminals open-circuited.

In each of these cases the sum frequency, $n\omega_0+\omega_r$, can be substituted for the image, $2n\omega_0-\omega_r$, so far as the effect on conversion loss is concerned, provided the crystal susceptance is not appreciable at $n\omega_0+\omega_r$. This is usually not the case for crystals operating at rated frequency, but does apply when operation is at one-half rated frequency or less. For impedance considerations, the substitution can also be made provided the input and output terminals are reversed. Calculation of conversion loss at a single value of x will be made for a fourth case in which there is an open circuit at both the image-frequency and the sum-frequency terminals.

IV. Conversion Loss

Friis[8] has shown that, for a minimum noise figure, cascaded networks should each have maximum available gain. This concept is applicable to the crystal mixer. However, since it is customary, the term conversion loss will be used to describe the reciprocal of the available conversion gain. Conversion loss is therefore defined as the ratio of the power available from the RF signal source to the power available at the IF output terminals.

At this point it should be noted that a true power loss has little significance in the case of a crystal mixer designed for low noise figure. This is the case because there is little resistive loading at the input of a well-designed IF amplifier. Instead of an admittance-matching network at the junction of the IF amplifier and crystal mixer there should be a network to transform the mixer output admittance to the optimum admittance so as to minimize the noise figure of the IF amplifier.[9]

It was also pointed out by Friis that for maximum available gain the admittance of the generator feeding a network should be equal to the input image admittance of the network.[10] Therefore at the junction of the RF signal source and the crystal mixer there should be an admittance mismatch for minimum conversion loss. As will be shown later in the calculations, the optimum degree of mismatch is a function of the conversion loss.

The conversion loss for Case 1 will be a minimum, when the RF signal-source conductance, g_{r1}, is

$$g_{r1} = g_a\gamma_{i1}, \tag{5}$$

where γ_{i1} is the normalized signal-terminal image conductance for Case 1. From Fig. 1 it can be shown that

$$\gamma_{i1} = \sqrt{1-\gamma_n^2}. \tag{6}$$

When (5) is satisfied, the minimum conversion loss is

$$L_1^{(n)} = \left(\frac{1+\sqrt{1-\gamma_n^2}}{\gamma_n}\right)^2. \tag{7}$$

In a similar manner the minimum conversion loss for Case 2 can be shown to be

$$L_2^{(n)} = \left(1+\sqrt{\frac{1+\gamma_{2n}-2\gamma_n^2}{1+\gamma_{2n}}}\right)^2\left(\frac{1+\gamma_{2n}}{\gamma_n^2}\right), \tag{8}$$

when γ_r is made equal to

$$\gamma_{i2} = \sqrt{\frac{(1-\gamma_{2n})(1+\gamma_{2n}-2\gamma_n^2)}{1-\gamma_n^2}}. \tag{9}$$

For Case 3

$$L_3^{(n)} = \left[1+\sqrt{\frac{1+\gamma_{2n}-2\gamma_n^2}{(1-\gamma_n^2)(1+\gamma_{2n})}}\right]^2 \cdot\left[\frac{(1-\gamma_n^2)(1+\gamma_{2n})}{\gamma_n^2(1-\gamma_{2n})}\right], \tag{10}$$

when γ_r is made equal to

$$\gamma_{i3} = \gamma_{i2}\sqrt{1-\gamma_{2n}^2}. \tag{11}$$

In (7), (8), and (10) the notation for conversion loss is cumbersome, and in the following analysis the superscript will be omitted except for $n>1$. To obtain numerical values from (7), (8), and (10), it is necessary to find γ_n and γ_{2n}. A simple mathematical model has been found from which these parameters can be calculated.

[8] H. T. Friis, "Noise figures of radio receivers," Proc. I.R.E., vol. 32, pp. 419–422; July, 1944.

[9] G. E. Valley, Jr., and H. Wallman, "Vacuum Tube Amplifiers," vol. 18, Rad. Lab. Series, McGraw-Hill Book Co. Inc., 1948, pp. 636–641.

[10] In the following discussion the term *image admittance* is used in the network sense and should not be confused with the admittance connected to the image-frequency terminals.

V. Mathematical Model of Crystal

Inspection of the E-I curve of a crystal plotted on logarithmic co-ordinates as in Fig. 2 shows that the forward portion is a nearly straight line over a large part of the current range. Over most of the back voltage range the current is considerably smaller than it is for equal forward voltages. It is also a nearly linear function of the voltage. The E-I curve can be expressed

$$i_f = ke^x, \quad (e > 0), \tag{12}$$

and

$$i_b \cong g_b e, \quad (e < 0), \tag{13}$$

where i_f is instantaneous forward current; i_b is instantaneous back current; k is a proportionality constant similar to conductance; x is the nearly constant slope, $d(\log i)/d(\log e)$, of the forward portion of the E-I curve; and g_b is the nearly constant back conductance.

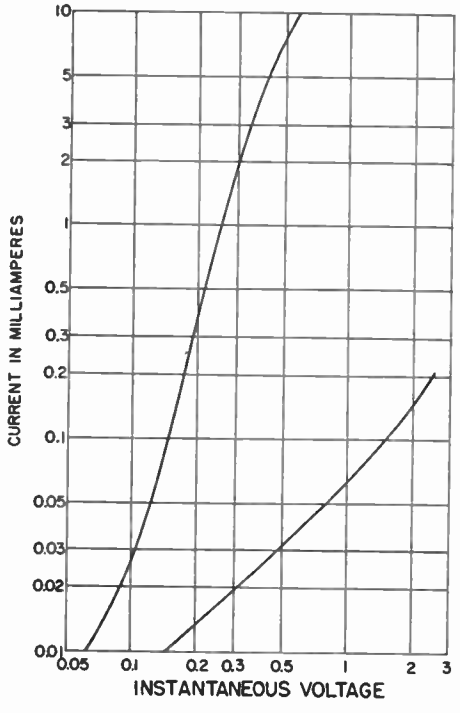

Fig. 2—$E-I$ curve of a typical mixer crystal.

Typical values of k and x for a 1N21B or 1N23B crystal are 0.05 and 3, respectively.

For mixing to occur, the crystal described by (12) and (13) must be excited by a local-oscillator voltage. In addition, sometimes a dc bias is used. The calculations will be carried out for a sinusoidal local-oscillator voltage, $e_0 = E_0 \cos \omega_0 t$, and zero bias. It will then be shown that the effect of bias is to change k, x and g_b; consequently, the results derived for zero bias will be directly applicable to various bias conditions.

From (12) the instantaneous small-signal conductance can be shown to be

$$g = \frac{di}{de} = kxe^{x-1}, \quad (e > 0)$$

$$\cong g_b, \quad (e < 0). \tag{14}$$

When local-oscillator voltage is applied

$$g = kxE_0^{x-1} \cos^{x-1} \omega_0 t, \quad \left(-\frac{\pi}{2} < \omega_0 t < \frac{\pi}{2}\right),$$

$$\cong g_b, \quad \left(-\pi < \omega_0 t < -\frac{\pi}{2} \text{ and } \frac{\pi}{2} < \omega_0 t < \pi\right). \tag{15}$$

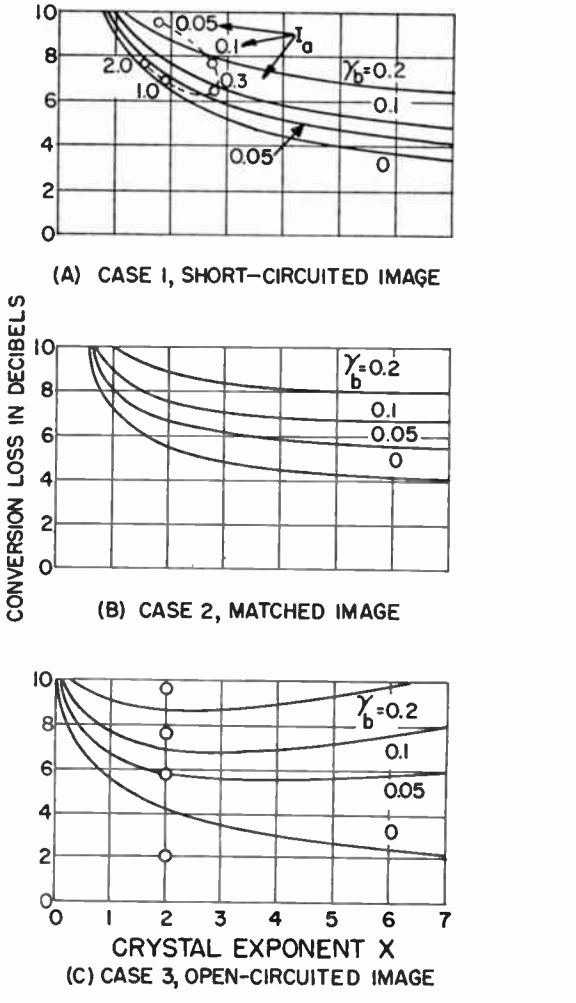

Fig. 3—Conversion loss for Cases 1, 2 and 3. (See text for a discussion of the interchange of the image and the sum-frequency $\omega_0+\omega_r$ and for a discussion of the single points for Case 3.)

Analysis based on (15) gives for the average small-signal conductance

$$g_a = \frac{kx}{2\pi} E_0^{x-1} \left[\frac{\sqrt{\pi}\, \frac{x-2}{2}\,!}{\frac{x-1}{2}\,!} \right] + g_b, \tag{16}$$

and for the normalized conversion conductance

$$\gamma_n = \frac{\left(\frac{x-1}{2}\,!\right)^2}{\left(\frac{x+n-1}{2}\,!\,\frac{x-n-1}{2}\,!\right) + \gamma_b}. \tag{17}$$

To find γ_{2n} it is necessary to substitute $2n$ for n in (17). Values of conversion loss can be calculated by substituting (17) into (7), (8), and (10). Fig. 3 shows calculated

values of the three fundamental conversion losses.

The conversion loss shown in Fig. 3(c) for Case 3 applies equally well to the case of the short-circuited image in combination with open-circuited, sum-frequency terminals. The case of open-circuited sum-frequency and image-frequency terminals, though not studied in detail, was considered to the extent of calculating the conversion loss for this condition at $x=2$. The calculated points are shown in Fig. 3(c). It is seen that in a low-loss mixer some care should be given to the termination of this sideband.

The dashed curve in Fig. 3(a) will be discussed under Section VII.

From Fig. 4 it is seen that, for $g_b=0$, the fundamental conversion losses for all three cases decrease with increasing x. The limiting values in each case are

$$\lim_{x\to\infty} L_1 = \lim_{x\to\infty} L_3 = 1, \tag{18}$$

and

$$\lim_{x\to\infty} L_2 = 2. \tag{19}$$

There is, therefore, a theoretical limit imposed by the type of mixer configuration regardless of crystal quality.

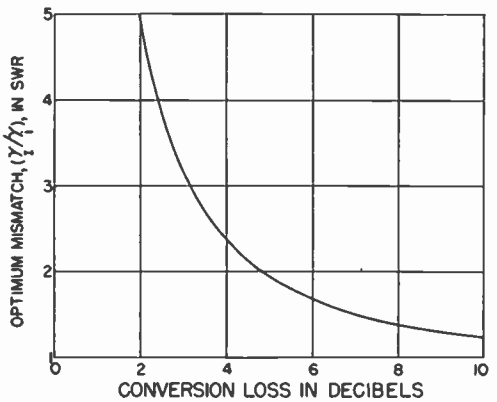

Fig. 4—Optimum mismatch.

The conversion loss for $n>1$ is known as harmonic conversion loss and can be easily calculated for Case 1. For $x>0$ and $n>2$, points of infinite loss occur at $x=n-1$, $n-3$, $n-5$, and so forth. Consequently care must be taken in operating a harmonic mixer to establish a value of x that is not near one of these points. Several methods for adjusting the value of x will be indicated in Section VII.

VI. Mixer Conductances

For the three conversion-loss cases the normalized, signal terminal image conductances can be calculated from (6), (9), and (11).

These calculated values differ from the input conductances of the mixer since no admittance match occurs at the output of the mixer. There will, therefore, be an optimum conductance mismatch at the mixer-input terminals for minimum conversion loss. This optimum mismatch will depend upon the conversion loss and the type of input network incorporated in the intermediate-frequency amplifier. The input networks can be placed into two categories, those with an admittance zero (impedance pole) at center frequency and those with an admittance pole (impedance zero) at center frequency. If it is assumed that the IF input network has an undamped admittance zero at center frequency, then the optimum center-frequency mismatch is given in Fig. 4 as a function of conversion loss. If the reciprocal IF input network is assumed, the reciprocal SWR pertains. If damping is present, the optimum SWR will be less than that in Fig. 4.

It is seen that, for a typical crystal with a 6-db conversion loss and negligible damping in the IF input network, an SWR of approximately 1.7 should exist at the input for minimum loss. The point was verified experimentally and will be discussed under Section IX.

When considering mixer tolerances the variation of conversion loss with changes in γ_r from optimum is of some interest. The relationship between conversion-loss increase and deviations of the ratio γ_r/γ_I from unity can be determined by conventional mismatch-loss calculations. Unity mismatch loss occurs at $\gamma_r/\gamma_I=1$ even though there is an SWR greater than unity in this case. If a design center were chosen such that the input SWR$=1$, which has been the case frequently in the past, the loss variations for a certain spread of SWR might be more than twice those for a design in which $\gamma_r/\gamma_I=1$. For instance, if $\gamma_r/\gamma_I=0.6$ and SWR$=1$ were design center values, conversion loss would vary 1 db for SWR variations from 0.6 to 1.7. But for the same relative SWR variations, conversion loss would vary only 1/4 db for $\gamma_r/\gamma_I=1$.

The normalized output conductances can be shown to be for Case 1,

$$\gamma_{op1} = \gamma_{I1}; \tag{20}$$

for Case 2,

$$\gamma_{op2} = \sqrt{\frac{1+\gamma_{2n}-2\gamma_n^2}{1+\gamma_{2n}}}, \tag{21}$$

and for Case 3,

$$\gamma_{op3} = \gamma_{op2}\sqrt{1-\gamma_n^2}. \tag{22}$$

Fig. 5 is a plot of (20), (21), and (22) with conversion loss as the independent variable. It is seen that the output conductance of a mixer can vary widely as a function of the image termination.

VII. The Significance and Control of x

There are several ways that x can be altered for a particular crystal.

1. The *E-I* curve of Fig. 2 shows that x increases for increasing peak currents up to about 1 ma, and decreases for higher peak currents. Hence the amplitude of the local-oscillator voltage, in the absence of bias, controls x.

2. An increase in x can be obtained with negative bias. This effect can be seen by replotting the E-I curve of Fig. 2 with co-ordinates translated to a new zero at the bias point.

3. The effective value of x can be increased by using a pulse-type local-oscillator voltage of low duty ratio. Ideally an infinitesimal duty ratio, corresponding to $x=\infty$, would give minimum conversion loss, provided $\gamma_b=0$. (One should note, however, that a square-wave local-oscillator voltage establishes $x=1$ giving a high conversion loss.)

4. Adjustment of the impedance in series with the crystal at local-oscillator frequency allows adjustment of x.

5. Control of the E-I curve by the manufacturing process can control both x and γ_b.

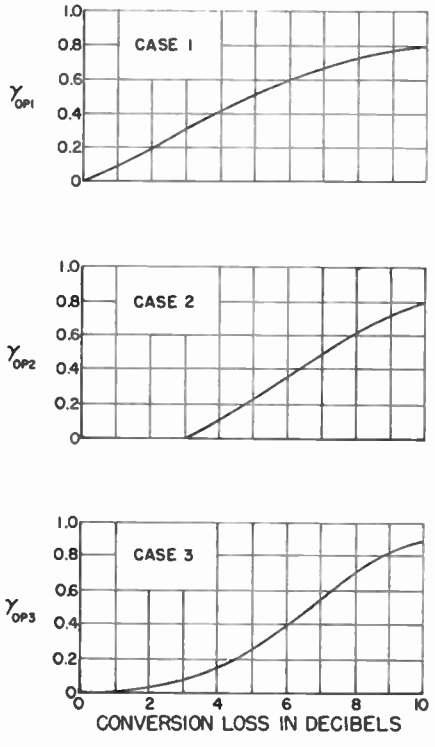

Fig. 5—Normalized IF output conductances.

The first is the usual method of establishing x. Experience has shown that, when there is little or no resistance in the dc return of the crystal, x is maximum when local-oscillator excitation is sufficient enough that a rectified current of approximately 0.2 to 0.7 ma flows. Hence mixers are usually operated with about 0.4 to 0.5 ma of rectified current. Examination of the E-I curve has shown that x is a maximum at about 0.2 ma of rectified current; but at such a low excitation level the back conductance, g_b, limits the minimum conversion loss. The dashed curve of Fig. 3(a) shows the effect on Case 1 conversion loss of the changes in x and γ_b which occur as a function of local-oscillator excitation. It is seen that the variations in x and γ_b counterbalance each other over a large range of rectified current corresponding to the optimum region determined from practice.

The second method is valid but should be used with caution since negative bias increases the excess noise generated in a crystal. For minimum noise figure the increase in x that is obtainable with bias must be balanced against an increase in crystal excess noise. The bias for minimum noise figure will depend on a number of factors, and will be discussed further in Section XIV.

The third method is hardly practical as such at microwaves. However, it does suggest the addition of local-oscillator power at the second harmonic to peak d the conductance pulses and hence increase the effective value of x.

In previous theoretical analyses no account has been taken of the fourth method listed for varying x. It can, nonetheless, be demonstrated that there can be a significant change in x, and hence conversion loss, caused by changes in impedance at local-oscillator frequency. Qualitatively, the effect is one of changing the shape of the current pulse, and consequently the conductance pulse, by changing the frequency response of the circuit in series with the crystal element.

The fifth method is beyond the scope of this paper. It can, however, be stated that on a linear plot the knee of the E-I curve for a hypothetical, improved crystal should be depressed below that for the ordinary crystal; and the high-current region for the improved crystal should rise more sharply than that for the ordinary crystal. A crystal checker based on this characteristic has been described elsewhere.[11]

VIII. Other Calculable Characteristics

There are several other characteristics of somewhat less interest that can be calculated. In particular, these include such large-signal characteristics as rectified current, absorbed power, and large-signal conductance. As used here large-signal conductance is the time-average conductance presented to a large-amplitude signal, such as that from a local oscillator. A signal of 0.1 v peak or larger will be considered of large amplitude.

When the local-oscillator voltage is sinusoidal the rectified current can be shown to be

$$I_a=\frac{k}{2\pi}E_0{}^x\left[\frac{\sqrt{\pi}\,\frac{x-1}{2}\,!}{\frac{x}{2}\,!}\right]. \tag{23}$$

Likewise the average power absorbed by the crystal from a large-amplitude signal can be shown to be

$$P_a=\frac{k}{2\pi}E_0{}^{x+1}\left[\frac{\sqrt{\pi}\,\frac{x}{2}\,!}{\frac{x+1}{2}\,!}\right]. \tag{24}$$

[11] P. D. Strum, "Mixer crystal checker," *Electronics*, vol. 23, pp. 94–97; December, 1950.

Similarly, large-signal conductance can be shown to be

$$G = \frac{i}{e},$$
$$= ke^{x-1}, \qquad (25)$$
$$= \frac{g}{x};$$

as distinguished from $g = di/de$, and

$$G_a = \frac{k}{2\pi} E_0^{x-1} \left(\frac{\sqrt{\pi}\, \frac{x-2}{2}!}{\frac{x-1}{2}!} \right). \qquad (26)$$

IX. Experimental Verification of Conversion Loss and Conductance Calculations

The experimental verification is in the form of data obtained both by measurements on actual high-frequency mixers and from the literature.

High-frequency verification has been obtained for (7), (8), (10), (16), (20), (21) and (22). The verification of (7), (8), and (10) is considered the measure of the usefulness of the proposed mathematical model of the crystal.

Conversion-loss data was obtained from another laboratory.[12] Measurements were made of L_1, L_2, L_3, and the E-I curve on a 1N23B crystal at 3 cm. They were made with constant available local-oscillator power at various average currents as established by control of the bias voltage. At each condition an optimum signal-frequency impedance transformation was established to yield a minimum loss.

To calculate the three losses at one power level is straightforward, but somewhat time consuming. Nevertheless an example will be shown.

The sequence of calculations is as follows:

1. From the measured E-I curve construct a family of curves assuming various values of bias. By geometrical measurement determine at each bias x and k for the crystal alone in the region of 1 ma. The slope in linear dimensions of the logarithmic plot is x, and the current intercept on the 1-v line is k.

2. By solution of (24) E_0 can be found, and I_a can be found from (23). These values should be marked on the curves.

3. If it is assumed that the crystal terminal admittances at signal and local-oscillator frequencies are equal, the local-oscillator source can be considered to be a conductance equal to g_{r2}. At each excitation point g_a should be found from (16) and g_{r2} from (9). The voltage I/g_{r2} should then be added to the E-I curves. The resulting curves are the composite E-I curves of the crystal and excitation generator. These curves govern the performance of the mixer.

4. Effective values of x and γ_b should next be determined from the resulting curves. The values of x measured at the 0.7 E_{pk} point is a good approximation to the effective values. The peak voltage, E_{pk}, is the sum $(E_0 + I_{pk}/g_{r2})$. Values of γ_b can be determined from the relation

$$\gamma_b = \left(\frac{i_b}{i_f}\right)_{pk} \left(\frac{2\sqrt{\pi}\, \frac{x-1}{2}!}{x\, \frac{x-2}{2}!} \right), \qquad (27)$$

where $(i_b/i_f)_{pk}$ is the peak back-to-front current ratio and x is an effective value. The values of effective x and γ_b obtained for 0.7 mw, 1.2 mw, and 2.0 mw are shown in Fig. 6. The families of calculated loss curves are shown in Fig. 7 with the experimental points.

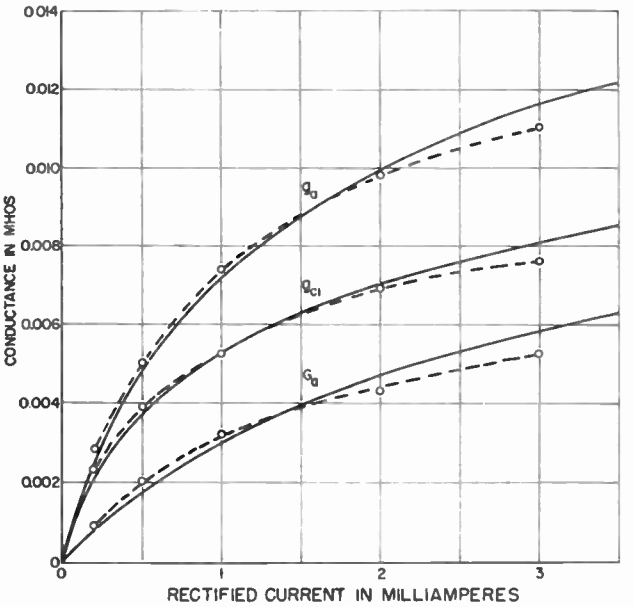

Fig. 6—Crystal conductances versus crystal current.

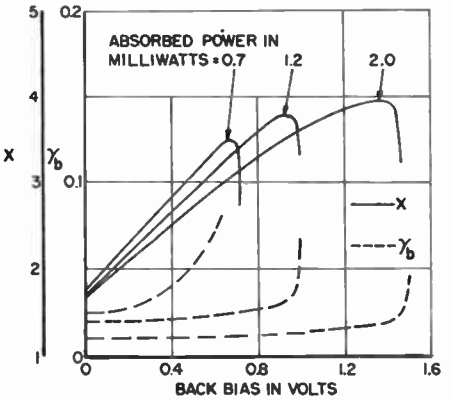

Fig. 7—Variation of x and γ_b with excitation.

It is seen that the agreement of theory and experiment is good, but the calculation lengthy. Good approximate results can usually be obtained by the following simplified procedure:

1. Find approximate x and γ_b at zero bias and at the bias for which $I = 0.1$ ma.
2. Fill in, by judgment based on Fig. 6, the variations of x and γ_b as a function of bias.
3. Read values of conversion loss from Fig. 3.

[12] Private communication from C. T. McCoy and B. Steinberg of the Philco Corporation, Philadelphia, Pa.

Qualitative verification of the magnitude and similarity of the effects of image-frequency and sum-frequency terminations on conversion-loss and IF-output conductance is to be found in the literature.[13] The variations of IF output (or conversion loss) and transformer tap position (or IF-output impedance) shown by Edwards[14] indicates the combined effect of impedance variations at both the image frequency and the sum frequency. In Fig. 15 of the same reference the effect of variations of image-frequency termination only is shown. The magnitudes of the variations are in approximate agreement with the results predicted in Fig. 3 and 5. Insufficient data on rectified crystal current and absolute conversion loss are available to determine the degree of agreement. It is probably true that, because of crystal barrier susceptance, the magnitude of the variations due to sum-frequency termination would have been less had the operating wavelength of the mixer been 3.2 cm, the rated crystal wavelength, rather than 7.2 cm. On the other hand, the effect of image-frequency termination would probably have been approximately the same as that found at 7.2 cm. The position of the sum-frequency, or second-harmonic, filter in the 7.2-cm mixer described may or may not have been in an optimum position. Its position should be such as to reflect an open circuit at the sum frequency at the point contact of the crystal. In this position the sum-frequency filter would minimize both the magnitude and the variation of the conversion loss as a function of sum-frequency reflections in the main waveguide. This result is from Fig. 3(c) and is predicated on the estimate that $\gamma_b = 0.05$ and $X = 2$ for an acceptable crystal. Crystals with $\gamma_b = 0.05$ and $x = 2$ would show little or no loss variation with position of the second-harmonic filter. If, however, $\gamma_b = 0.02$ and $x = 2$, a 1-db loss variation could be expected.

Indirect verification of the IF output conductances of (20), (21), and (22) was obtained from the literature. In table 7.1 of Torrey and Whitmer[15] values of IF resistance and conversion loss measured at 9,423 mc are shown for five random 1N23B crystals. In Table I are shown values of x and γ_b chosen to give a good fit for the measured values of L_1, L_2, and L_3. From Fig. 6 theoretical values of IF resistance were obtained for the five crystals using $g_a = 0.0068$ mho for 0.9 ma. The comparison of measured and calculated IF resistances is shown in the last three columns of Table I. The last column gives for each case the ratio of measured-to-calculated IF resistance. If this ratio were constant for the three cases the verification would be exact. The true value of g_a for each crystal can be found by dividing 0.0068 by the ratio R_M/R_C. It is seen that for crystals 2, 4, and 5 respectively, the ratios R_M/R_C are virtually constant for Cases 1, 2, and 3; and for crystals 1 and 3 the spread is not very large. Indirect verification of the IF output resistance is therefore obtained. It is interesting to note that the average value of g_a for the five crystals is only 3.5 per cent higher than that chosen from Fig. 6. It is also interesting to note that the spread in values of g_a is small although there was a considerable spread in IF output resistances.

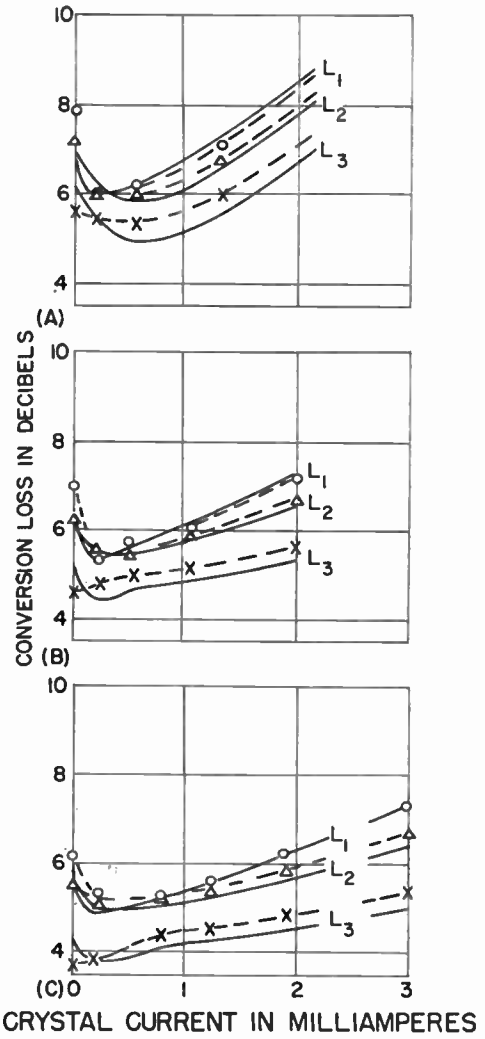

Fig. 8—Calculated and measured interrelationship of L_1 L_2, and L_3. (*A*), (*B*), and (*C*) respectively correspond to absorbed local-oscillator powers of 0.7, 1.2, and 2.0 mw.

Verification was obtained for the fact that a signal-frequency SWR other than unity is required for minimum conversion loss. On a microwave receiver using a high-Q T-R cavity, noise-figure measurements were made as a function of signal-frequency SWR.[16] On the average, for six 1N21B crystals that were used a minimum noise figure was obtained at a signal-frequency SWR of 1.3 at the cavity input. Because of cavity losses this SWR corresponds to a larger SWR at the crystal. For the particular cavity used, the shunt loss conductance was 0.17, giving an SWR at the crystal of $1/(1/1.3-0.17) = 1.7$. For each crystal the optimum signal-frequency SWR was greater than unity and of such phase that the signal-source conductance was higher than the mixer-input conductance. If one takes

[13] C. F. Edwards, "Microwave converters," PROC. I.R.E., vol. 35, pp. 1181–1191; November, 1947.
[14] *Ibid.*, Fig. 3.
[15] Torrey and Whitmer, "Crystal Rectifiers," *ibid.*, p. 233.
[16] This data was furnished by J. Lory and W. H. Spencer of Airborne Instruments Laboratory, Mineola, N. Y.

TABLE I

COMPARISON OF MEASURED AND CALCULATED IF RESISTANCES. MEASURED VALUES ARE FROM TABLE 7.1 OF FOOTNOTE REFERENCE 6. SIGNAL FREQUENCY = 9,423 MC. CRYSTAL TYPE IS 1N23B

Crystal Number	Case	X^*	$\gamma_b{}^*$	Measured IF Resistance, R_m	Calculated IF Resistance, R_C**	R_M/R_C
1	1	1.6	0.03	210	206	1.02
	2			330	355	0.93
	3			455	545	0.83
2	1	2.1	0.03	185	222	0.83
	2			325	405	0.80
	3			560	670	0.83
3	1	1.9	0.04	270	216	1.25
	2			415	385	1.08
	3			610	600	1.02
4	1	2.0	0.08	218	201	1.08
	2			325	323	1.01
	3			520	490	1.06
5	1	1.7	0.07	180	193	0.93
	2			282	320	0.88
				390	450	0.87

* X and γ_b are chosen for best fit of measured values of L_1, L_2, and L_3.
** $1/g_a = 147$ ohms (from Fig. 6 for rectified current of 0.9 ma).

an average Case 3 conversion loss of 6 db as representative, the theoretical SWR for optimum mismatch from Fig. 4 is approximately 1.7.

X. Excess Noise Study

In this section will be presented experimental results obtained from the literature and in the laboratory, concerning the excess noise generated in mixer crystals. It will be shown that, for minimum noise figure in a superheterodyne employing a crystal mixer there is an optimum intermediate frequency; and that the usual arbitrary use of conversion-loss, noise-temperature and resistance data can lead to erroneous conclusions concerning the design of such a receiver.

XI. Definition of Noise Temperature

The term *noise temperature*, which could more appropriately be called output noise ratio, is defined as

$$t = \frac{N_A}{N_T}, \tag{28}$$

where t is noise temperature; N_A is the noise power available from the crystal or mixer under consideration, and N_T is the available thermal noise power from a resistor at room temperatures. This available thermal noise power has been shown[17–19] to be

$$N_T = kTB, \tag{29}$$

where k is Boltzmann's constant, T is absolute temperature, and B is noise bandwidth. Noise bandwidth is defined by the expression $B = (1/A_0{}^2)\int_0^\infty A^2(f)df$, where $A^2(f)$ is the power gain versus frequency function and $A_0{}^2$ is the peak power gain.

The term noise temperature can be applied either to the crystal or to the complete crystal mixer. When applied to the crystal, the term can be used for either instantaneous values obtained with dc excitation or for average values obtained with ac excitation. When applied to the complete mixer, the term is used to indicate the noisiness of the output resistance of the mixer.

Since there is a contribution to the mixer output resistance from the resistance of the RF signal source, mixer noise temperature usually differs from crystal noise temperature. For mixer-noise-temperature considerations, the applicable crystal noise temperature is the average value resulting from the periodic excitation of the crystal by the local oscillator.

Noise generated by the local oscillator is sometimes found to increase the noise temperature of a mixer. However, since proper design can eliminate local-oscillator noise and since the mixer should not be charged with deficiency of the oscillator, this source of noise will not be considered in the discussion.

The theoretical noise temperature of the large-signal conductance G of a perfect crystal is unity. That is, the only noise present is thermal agitation noise. Any noise temperature in excess of unity must result from physical phenomena other than thermal agitation. This excess noise temperature $(t-1)$ will be called simply excess noise in the following discussion.

XII. Crystal Noise Temperature

A mixer crystal as a circuit element usually has a noise temperature, t_x, greater than unity, thus contributing to the excess noise of the receiver.

It has been considered in the past that the noise temperature of the mixer is identical to the noise temperature of the mixer crystal used. Such is not the case, as will be shown in the next section. However, a study of the noise characteristics of the crystal alone leads to certain important conclusions regarding mixer noise characteristics.

A study was made of the excess noise generated in a crystal as a function of steady direct current and as a function of the frequency at which the noise was measured. Others have made similar studies[20–23] and one of the results presented here is a compilation of their data into one integrated picture of excess crystal noise as a function of frequency.

Fig. 9 shows composite results of the compilation and the experiments. The sources of the data of Fig. 9 are listed in Table II.

[17] W. Shottky, "Spontaneous current fluctuations in various conductors," *Ann. Phys.*, vol. 57 ,pp. 541–567; December 20, 1918.
[18] J. B. Johnson, "Thermal agitation of electricity in conductors," *Phys. Rev.*, vol. 32, pp. 97–110; July, 1928.
[19] H. Nyquist, "Thermal agitation of electric charge in conductors," *Phys. Rev.*, vol. 32, pp. 110–113; July, 1928.
[20] P. H. Miller, Jr., "Noise spectrum of crystal rectifiers," PROC. I.R.E., vol. 35, pp. 252–256; March, 1947.
[21] J. F. Wilkerson, unpublished experimental data on a single 1N21B.
[22] R. V. Pound, "Microwave Mixers," vol. 16, Rad. Lab. Series, McGraw-Hill Book Co. Inc., 1948, p. 362.
[23] H. C. Torrey and C. A. Whitmer, "Crystal Rectifiers," vol. 15, Rad. Lab. Series, McGraw-Hill, 1948, p. 196.

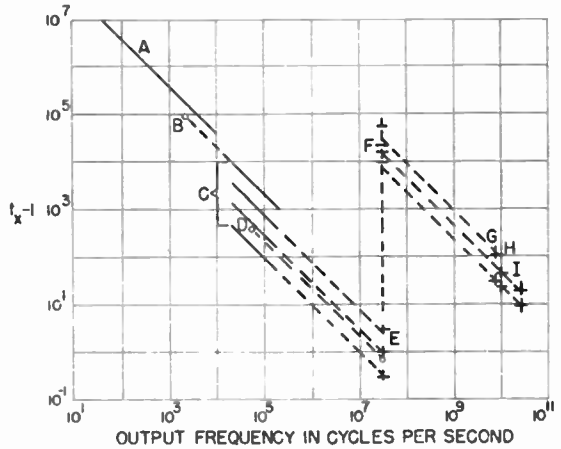

Fig. 9—Excess crystal noise versus output frequency.

TABLE II

SOURCES OF DATA IN FIG. 9

Identifying Letter	Source	Comments
A, B	P. H. Miller, Jr. "Noise spectrum of crystal rectifiers," PROC. I.R.E., vol. 35, pp. 252–256; March 1947.	Curve *A* is from Fig. 5, adjusted to 10,000 ohms a more probable resistance at −3 volts than 300 ohms and converted from (noise voltage)² to noise temperature. Point *B* is from Fig. 4, adjusted to 10,000 ohms and converted to noise temperature. The point is the three-crystal average for −20 μa.
C	J. F. Wilkerson, unpublished experimental data on a single 1N21B.	Curves obtained for dc excitation at 20 kc, 50 kc, 100 kc, and 200 kc. Upper curve is for −20 μa. Lower three curves in ascending order are for +1, +2, and +10 ma.
D	H. C. Torrey and C. A. Whitmer, "Crystal Rectifiers," vol. 15, Rad. Lab. Series, McGraw-Hill Book Co. Inc., 1948, pp. 192–193.	The quoted values of $t=400$ at 60 kc and $t=1.6$ at 30 mc are seen to be joinable by a line of slope f^{-1} on the $t-1$ plot.
E, F	Experimental data E obtained by the author on the crystal used by Wilkerson in C.	The data for *E* are shown, complete with the extrapolation to *F* in Fig. 10.
G	R. V. Pound, "Microwave Mixers," vol. 16, Rad. Lab. Series, McGraw-Hill Book Co. Inc., 1948, p. 362.	9,000 mc data quoted for −5 to −10 ma.
H, I	H. C. Torrey and C. A. Whitmer, "Crystal Rectifiers," vol. 15, Rad. Lab. Series, McGraw-Hill Book Co. Inc., 1948, p. 196.	10,000 and 24,000 mc data quoted for −3 to −4 ma.

As indicated in Table II, Miller's results had to be adjusted from their original form. Miller indicated the method for converting his (noise voltage)² to noise temperature; but his assumed resistance value of 300 ohms is apparently too low for the case of reverse dc excitation. A value of about 10,000 ohms more nearly fits existing *E-I* curve data; therefore, the noise temperatures obtained by Miller's method have been multiplied by 10,000/300.

The point *B*, from Miller's Fig. 4, at a back current of 20 μa, is seen to join quite accurately the extrapolation from the upper curve of group *C*, which was also measured at a back current of 20μa.

The four solid lines of group *C* were measured on a sample crystal in a separate investigation by Wilkerson[21] The sample crystal was made available for the present investigation. Measurements were made at 30 mc for the same range of dc excitation as used by Wilkerson. The 30-mc data are plotted as the solid curves in Fig. 10. In Fig. 9, the 30-mc data, group *E*, fall on extrapolations of the 20 kc to 200 kc data within experimental error.

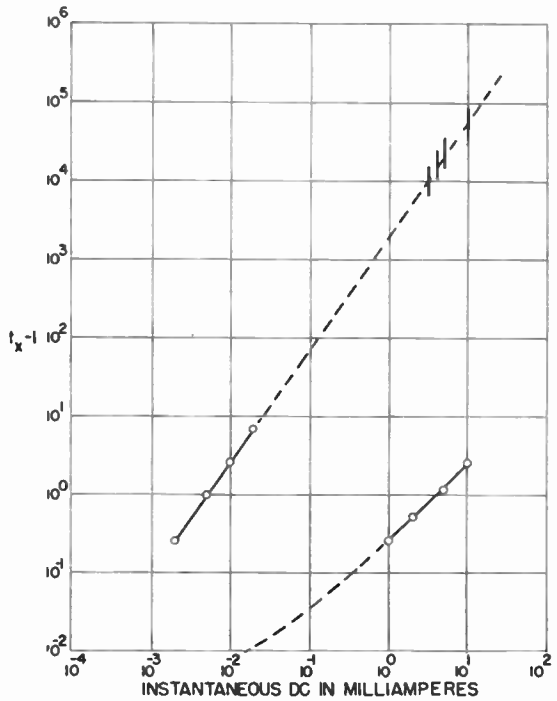

Fig. 10—Excess 30-mc crystal noise versus instantaneous direct current.

Data *D* apply to a crystal with 3-cm excitation. The three groups of data *G*, *H*, and *I* were reported as rather general results obtained by passing large back currents through crystals in crystal-noise-generator experiments. Among themselves, *G*, *H*, and *I* indicate an f^{-1} relationship between 9,000 and 24,000 mc.

The three groups of data *G*, *H*, and *I* may be joined to group *E* by two extrapolations. The back-current data of Fig. 10 are seen to lie on a straight line. Arbitrary extrapolation of this straight line upward to 10 ma should probably have at least an order of magnitude validity. Data group *F* of Fig. 9 corresponds in ascending order to the extrapolated values of $(t-1)$ for 3, 4, 5, and 10 ma respectively. It is seen that these values are well within an order of magnitude of corresponding values arbitrarily extrapolated by dashed lines of f^{-1} slope from 9,000, 10,000 and 24,000 mc. Although a certain amount of license is taken when extrapolations are made such as in Fig. 10, the agreement in this case is so good as to indicate that the f^{-1} dependency holds

from at least as low as 30 cps to at least as high as 24,000 mc. Unpublished results indicating that the f^{-1} proportionality extends to frequencies less than 1 cps were reported in discussions at the conference on Electron Devices at the University of New Hampshire in 1951.

In a later section the f^{-1} relationship of Fig. 9 will be shown to have an important bearing on the choice of intermediate frequency for a microwave receiver.

The instantaneous values of excess crystal noise shown in Fig. 10 can be averaged for ac excitation by the expression

$$(t_x - 1)_a = \frac{\int_{-\pi}^{\pi} g t_x d\theta}{\int_{-\pi}^{\pi} g d\theta} - 1, \qquad (30)$$

where g and t_x are periodic functions of θ with a period small compared with the period of the intermediate frequency. The first right-hand term of (30) is the ratio of the average mean-square noise current of the excited crystal to the mean-square thermal noise current from g.

The result for (30) for a particular crystal depends on the amount of ac excitation and dc bias used. From the data of Fig. 10 it can be shown that a forward bias of approximately 0.1 v is at the approximate minimum of the excess noise. Maximum curvature of the $E = I$ curve also occurs at approximately 0.1 v forward bias. Therefore, for mixing with small local-oscillator excitation, an optimum bias for minimum noise figure of approximately 0.1 v is predicted (an expression for noise figure is given in (32)).

At larger values of ac excitation the optimum bias for minimum noise figure depends largely on the relative magnitudes of the excess mixer noise and excess IF amplifier noise. It has been shown that large negative bias gives minimum coversion loss. Fig. 10 shows that large negative bias also gives large noise temperature.

Three sets of conditions can therefore be postulated, each requiring a different optimum bias for minimum noise figure.

1. Where the excess mixer noise is large compared with the excess IF amplifier noise the optimum bias is about 0.1 v forward bias, the minimum point of Fig. 10. This is coincident with the optimum bias for small local-oscillator excitation.

2. Where the excess mixer noise and excess IF amplifier noise are comparable, the optimum bias will usually lie in the vicinity of zero bias.

3. Where the excess mixer noise is negligibly small compared with the excess IF amplifier noise, either because of low-noise-temperature crystals or because of a high-noise-figure IF amplifier, the optimum bias is a back bias of about 1 v. The use of such a large back bias to minimize conversion loss requires the use of a local-oscillator voltage large enough to give a positive rectified current. One means of obtaining such a result is to obtain the bias from a self-biasing resistor of several thousand ohms resistance.

Another prediction which can be made from (30) is that pulse-type excitation for which no back current flows should reduce the average excess noise. The addition of second-harmonic power to provide such excitation was also suggested as a means of lowering conversion loss.

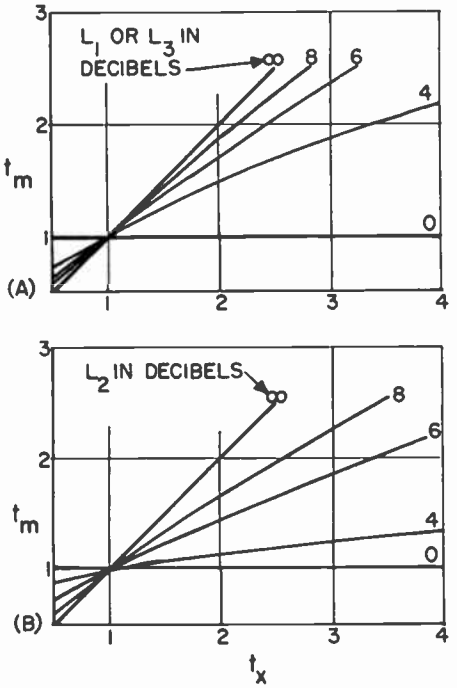

Fig. 11—Mixer-noise temperature versus crystal noise temperature and conversion loss.

XIII. Mixer Noise Temperature

From the equivalent networks of Fig. 1 it will be shown that mixer noise temperature depends upon the termination at signal and image frequencies. The noise temperature of the output conductances for Cases 1, 2, and 3 given in (20), (21), and (22) may be found by considering combinations of conductances of different noise temperatures. The effective noise temperature of a number of parallel conductances is

$$t_{eff} = \frac{g_1 t_1 + g_2 t_2 + \cdots + g_n t_n}{g_1 + g_2 + \cdots g_n}, \qquad (31)$$

which is seen to be an adaptation of (30) to the case of parallel conductances.

By application of (31) to the equivalent networks of Fig. 1, the curves of Fig. 11 were calculated. The two families of curves in Fig. 11 show mixer noise temperature versus crystal noise temperature with conversion loss as a parameter. The curves for Cases 1 and 3 are seen to be identical. This result would be expected from the considerations that in each the only external conductance is at the signal terminals and that the padding effect from the noise-free signal-source conductance through the noise mixer network depends only on the loss of the mixer network.

The noise temperature measured in standard test sets at 30 mc and quoted as a characteristic of the various crystal types is approximately the mixer noise temperature for Case 2. From this quoted characteristic, crystal noise temperature may be found from Fig. 11(b) for use in Fig. 11(a).

An approximate check of the variation of noise temperature with image termination as given in Fig. 11 can be made against data existing in the literature.[24] The approximate check will also further check the predictions of loss variations. Fig. 12 shows as solid curves the measured curves of Deringer as reported by Torrey and Whitmer. Beringer's curves were obtained at 3 cm, the rated wavelength of the 1N23B crystal used. The measurements were made for the conditions of matched signal terminals and image phase adjustable over one full cycle by a cavity with a reflection co-efficient of 75 per cent. The calculated points and estimated curves were obtained in the following manner:

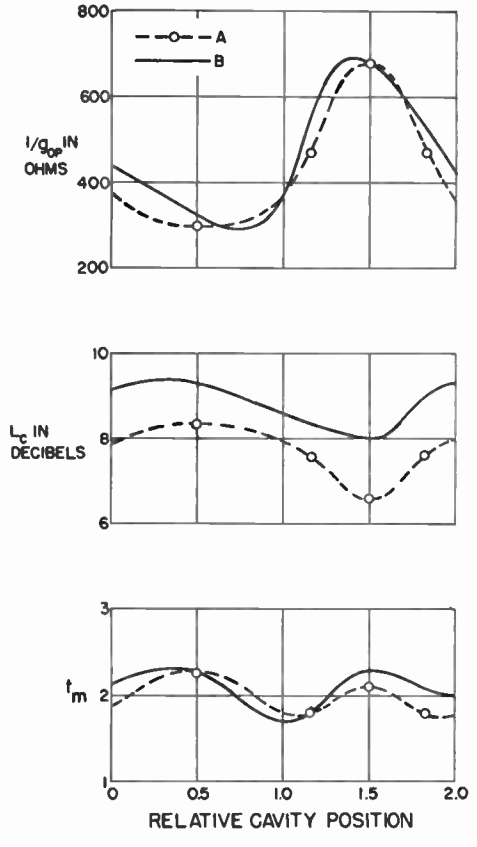

Fig. 12—IF resistance, conversion loss and mixer-noise temperature versus image-frequency termination.

1. Values of $x=1.5$ and $\gamma_b=0.07$ were chosen to give approximately the observed ratio of maximum to minimum output resistance.

2. A value of $1/g_a=230$ ohms was chosen to adjust the resistance variations approximately to the limits observed. It will be noted for comparison that a value of $1/g_a=210$ ohms was found at 0.5 ma of rectified current for the example crystal in Fig. 6.

3. The relative positions of 0.5 and 1.5 were estimated to be the minimum and maximum image impedance positions respectively.

4. It was found from a reflection-co-efficient chart that at a position approximately 1/6 wavelength from the minimum position a condition of approximate match of resistive impedance components is obtained. It was assumed that at this position the characteristics would be approximately comparable with those obtained at the condition of matched image.

5. It was assumed that the barrier shunting susceptance provided an effective short circuit at the sum-frequency terminals.

6. The calculated points were calculated for perfect short-circuit, open-circuit, and match conditions at the image-frequency terminals.

7. The dashed curves are estimated from the locations of the calculated points.

Although this type of data fitting is subject to several arbitrary choices, the agreement of the variation of the three characteristics with image phase tends to substantiate the theoretical predictions. It will be noted that the observed peaking of the loss and resistance curves around the point of high image impedance is predicted.

The two peaks observed in the noise temperature curve are also predicted. The asymmetries of the measured curves and the 1-db error in predicted conversion loss are not considered to be serious discrepancies. The observed asymmetries may have been due to reactive effects at signal- and image-frequency terminals and to incompleteness of the short-circuit assumed in assumption (5) above.

XIV. Optimum Receiver Design

The information of Figs. 9 and 11 can be applied, along with conversion loss information, to the design of minimum noise figure receivers. First, there is the choice of optimum mixer configuration; and, second, there is the choice of optimum intermediate frequency.

Over-all receiver noise figure can be expressed as

$$F = L_r L_c[(F_i - 1) + (t_m - 1) + 1], \qquad (32)$$

where F is over-all noise figure, L_r is RF circuitry loss, L_c is mixer conversion loss, F_i is noise figure of the intermediate frequency amplifier, and t_m is the mixer noise temperature. All units are power ratios. In this form the expression shows clearly that the term within the brackets is the sum of the excess noise of the intermediate frequency amplifier, the excess noise of the crystal mixer, and the theoretical thermal noise of unity.

For minimum noise figure each of the right-hand terms in (32) must be minimized; or, if there are interdependences, these must be determined and the product minimized.

[24] Torrey and Whitmer "Crystal Rectifiers," *ibid.*, p. 234.

Although theoretically independent, the RF circuitry loss, L_r, and the conversion loss, L_c, are somewhat dependent on each other as a result of the practical limitations on realizing loss-free microwave networks. For Cases 1 and 3 a high-Q RF circuit is required to permit a resistive impedance transformation at the signal frequency and a resistance-free short- or open-circuit termination at the image frequency. In radar receivers such a high-Q circuit is usually in the form of a T-R cavity with an insertion loss of approximately 1 to 1.5 db.

For Case 2 it is necessary that the RF circuitry be of relatively low Q. Low-Q T-R switches are available with an insertion loss of approximately 0.5 db. From these considerations it is seen that the product L_rL_c must be considered when choosing a mixer configuration for minimum noise figure of a radar receiver.

In (32), (F_i-1) and (t_m-1) are independent of each other; however, (t_m-1) is dependent upon L_c as shown in Fig. 11, and both (F_i-1) and (t_m-1) are dependent upon the intermediate frequency.

The excess noise of an intermediate-frequency amplifier using a particular tube type increases approximately directly with frequency.[25] The data in Fig. 9 shows that the excess noise of the mixer varies inversely with frequency. Fig. 13 shows a family of (t_m-1) curves and a typical (F_i-1) curve for the 6AK5 in a "cascode" circuit. The dashed curves showing total excess noise are seen to have a minimum at the frequency at which $(F_i-1)=(t_m-1)$. Fortunately, the sum $(F_i-1)+(t_m-1)$ does not vary rapidly in a broad region about the optimum intermediate frequency. Tube types other than the 6AK5 will give curves approximately parallel to the 6AK5 curve but displaced by an amount dependent upon input admittance, equivalent noise resistance, and so forth.

The use of Figs. 11 and 13 and the conductance and conversion loss calculations in determining optimum receiver design will be demonstrated by two examples.

First Example

Problem: Find the optimum mixer configuration and intermediate frequency for a 10,000 mc receiver of minimum noise figure. Determine optimum RF mismatch and IF output resistance, R_{if}, at 0.5 ma rectified current.

Data: The average measured value of L_2 for several hundred 1N23B crystals is 6.0 db. Average measured 30-mc noise temperature for the same crystals is 1.7. The IF tube type is to be the 6AK5 in a "cascode" circuit.

Solution: Solve (32) for Cases 1, 2, and 3. Assignment of values of x and γ_b is somewhat arbitrary, but $x=2$ and $\gamma_b=0.02$ are apparently reasonable choices to fit the loss data.

[25] G. E. Valley, Jr., and H. Wallman, "Vacuum Tube Amplifiers," vol. 18, Rad. Lab. Series, McGraw-Hill Book Co., Inc., 1948, pp. 641–643.

For Case 1:

$$t_m=2.2 \text{ (at 30 mc)},$$
$$IF_{opt}=53 \text{ mc},$$
$$F_i-1=t_m-1=0.65 \text{ (at 53 mc)},$$
$$L_c=6.6 \text{ db (from Fig. 3)}.$$

Let $L_r=1.25$ db;

$$F=1.33\times4.57\times2.3,$$
$$=14.0,$$
$$=11.5 \text{ db};$$
$$SWR_{opt}=1.5;$$
$$R_{if}=320 \text{ ohms}.$$

For Case 2:

$$t_m=1.7 \text{ (at 30 mc)},$$
$$IF_{opt}=40 \text{ mc},$$
$$F_i-1=t_m-1=0.49 \text{ (at 40 mc)},$$
$$L_c=6.0 \text{ db (from data)}.$$

Let $L_r=0.5$ db;

$$F=1.12\times3.98\times1.98,$$
$$=8.8,$$
$$=9.5 \text{ db};$$
$$SWR_{opt}=1.7;$$
$$R_{if}=580 \text{ ohms}.$$

For Case 3:

$$t_m=1.9 \text{ (at 30 mc)},$$
$$IF_{opt}=47 \text{ mc},$$
$$F_i-1=t_m-1=0.58 \text{ (at 47 mc)},$$
$$L_c=5.0 \text{ db (from Fig. 3)}.$$

Let $L_r=1.25$ db;

$$F=1.33\times3.16\times2.16,$$
$$=9.1,$$
$$=9.6 \text{ db};$$
$$SWR_{opt}=1.9;$$
$$R_{if}=800 \text{ ohms}.$$

It is seen that with the assumed values of L_r Cases 2 and 3 give similar results, leaving the choice of mixer configuration to be determined by requirements other than minimum noise figure. If L_r were equal in the two cases, Case 3 would be preferable by 0.7 db. It is also seen that, if the high-Q mixer is chosen, a total variation of approximately 2 db may be expected as a result of variations in image-frequency termination from open circuit to short circuit. The frequently used intermediate frequencies of 30 or 60 mc are seen to be about equally good choices for this example receiver.

Second Example

Problem: Find the optimum mixer configuration and intermediate frequency for a 3,000 mc receiver of minimum noise figure. Determine optimum RF mismatch and IF output resistance, R_{if}, at 0.5 ma rectified current.

Data: The average measured value of L_2 for a small number of 1N21C crystals is 5.0 db. Average measured 30 mc value of t is 1.2. The IF tube type is to be the 6AK5 in a "cascode" circuit.

Solution: The values $x=3.2$ and $\gamma_b=0.01$ are apparently reasonable choices to fit the loss data.

For Case 1:

$$t_m=1.4 \text{ (at 30 mc)},$$
$$IF_{opt}=32 \text{ mc},$$
$$F_i-1=t_m-1=0.40 \text{ (at 32 mc)},$$
$$L_c=5.2 \text{ db (from Fig. 3)}.$$

Let $L_r=1.25$ db;

$$F=1.33\times3.31\times1.80,$$
$$=7.9,$$
$$=9.0 \text{ db};$$
$$SWR_{opt}=1.8,$$
$$R_{if}=400 \text{ ohms}.$$

For Case 2:

$$t_m=1.2 \text{ (at 30 mc)},$$
$$IF_{opt}=22 \text{ mc},$$
$$F_i-1=t_m-1=0.26 \text{ (at 22 mc)},$$
$$L_c=5.0 \text{ db (from data)}.$$

Let $L_r=0.5$ db;

$$F=1.12\times3.16\times1.52,$$
$$=5.4,$$
$$=7.3 \text{ db};$$
$$SWR_{opt}=1.9;$$
$$R_{if}=900 \text{ ohms}.$$

For Case 3:

$$t_m=1.3 \text{ (at 30 mc)},$$
$$IF_{opt}=26 \text{ mc},$$
$$F_n-1=t_m-1=0.32 \text{ (at 26 mc)},$$
$$L_c=3.9 \text{ db (from Fig. 3)}.$$

Let $L_r=1.25$ db;

$$F=1.33\times2.45\times1.64,$$
$$=5.3,$$
$$=7.3 \text{ db};$$
$$SWR_{opt}=2.4;$$
$$R_{if}=1{,}400 \text{ ohms}.$$

Again it is seen that with the assumed values of L_r Cases 2 and 3 give virtually identical results, but the difference between Cases 1 and 3 is less than in the first example. The higher performance crystals obtainable at 3,000 mc allow noise figures approximately 2 db lower than for the 10,000 mc receiver of the first example. The corresponding optimum intermediate frequency is approximately half that of the 10,000 mc receiver.

It is interesting to note that the much-used value of 300 ohms for IF resistance of a mixer may be very much in error in a receiver of low conversion loss. As a consequence, if an IF amplifier designed to give minimum noise figure with a source resistance of 300 ohms were used for Case 3 in the second example, the error of 4.7 times in resistance would cause approximately a 1-db increase in over-all noise figure. If the same receiver were designed for unity RF SWR, there would be an additional 0.7-db increase in over-all noise figure. For a receiver with a higher intermediate frequency the over-all noise figure is more critically dependent on the magnitude of the IF resistance of the mixer than in the example receiver.

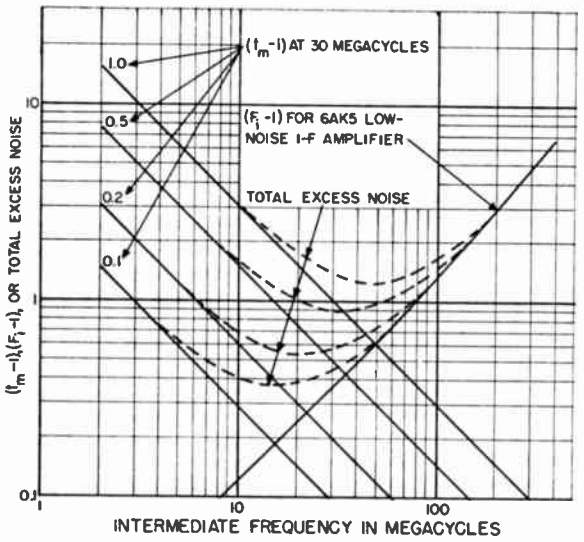

Fig. 13—Total excess noise versus intermediate frequency.

Experimental Verification of Optimum Receiver Design

Experimental data indicating the validity of Fig. 13 were obtained on two microwave receivers. These data are listed in Table III together with noise figures computed with the aid of Fig. 13.

TABLE III

Comparison of Computed and Measured Receiver Noise Figures*

	For 6-mc IF Amplifier			For 30-mc IF Amplifier		
	IF Amp. Noise Fig.	Comptd. Av. Noise Fig.	Meas. Av. Noise Fig.	IF Amp. Noise Fig.	Comptd. Av. Noise Fig.	Meas. Av. Noise Fig.
Rec. I†	1.0	12.9	13.2	1.7	9.9	10.6
Rec. II‡	0.7	8.5	9.5	1.7	7.7	8.3
Rec. III§	0.5	8.2	7.0	1.2	6.7	7.0

* All noise figures are in decibels.

† This receiver was an experimental receiver furnished by R. Weinberger of Martin Aircraft Company, Baltimore, Md.

‡ Experimental receiver furnished by L. Murdock of General Electric Company, Syracuse, N. Y.

§ This receiver was the same as Receiver II except for the improved IF noise figures.

Receiver I was a 10,000 mc receiver using 1N23B crystals in a balanced broadband waveguide mixer. Receiver II was a 3,000 mc receiver using 1N21C crystals in a balanced broadband waveguide mixer. For Receivers I and II the measured data check very well with the noise figures predicted with the aid of Fig. 13.

Receiver III was the 3,000 mc receiver with newer crystals and improved IF noise figures of 0.5 and 1.2 db. In this instance the average measured noise figures were 7 db at both frequencies. This result indicates that crystal noise temperatures were probably slightly less than

1.1, instead of 1.2 as used in the computations; and that the optimum intermediate frequency was approximately 14 mc.

Conclusions

It can be concluded that an accurate mathematical method for making mixer crystal calculations was demonstrated. With the aid of the mathematical method one can predict numerically the conversion loss and conductance behavior as a function of image-frequency or sum-frequency termination.

The fundamental aspects of the mathematical method have been verified experimentally. Certain experimental results given previously in the literature without theoretical explanation were explained by application of the present analysis.

On the basis of theoretical predictions given here, it should be possible to evaluate more accurately the conversion loss behavior in future mixer designs. Certain of the secondary aspects of predicted mixer behavior were not completely verified, such as the effect of admittance at local-oscillator frequency on conversion loss and the use of added second-harmonic power to reduce conversion loss.

It has been shown that the literature contains data indicating that the f^{-1} dependence of excess crystal noise extends from very low frequencies to at least as high as 24,000 mc. A means of using this information to help predict optimum mixer design and optimum intermediate frequency for minimum noise figure has been demonstrated with supporting data. A means of predicting the variation of noise temperature with image-frequency termination was shown to give approximate agreement with the published results of a previous experimental investigation. It was shown that, if one does not consider RF circuitry loss, over-all receiver noise figure will be a minimum with a mixer having open-circuited image terminals. For typical crystals, however, the difference between the noise figure in that case and the noise figure in the case of matched image is less than 1 db. This difference may be offset by the usual difference in RF circuitry loss for two cases. If such is the case, it can be concluded that low-Q mixers and high-Q mixers of good design should give approximately equal noise figures.

Acknowledgment

For their encouragement and helpful suggestions, the author wishes to thank F. C. Cahill and M. T. Lebenbaum of Airborne Instruments Laboratory, who supervised much of the work reported here. The author also wishes to thank Mr. Lebenbaum and C. A. Fowler for their help in preparing the illustrations, and W. L. Prichard of Raytheon Manufacturing Company for his helpful comments on the text.

Appendix

The equivalent network of Fig. 1 can be obtained from the admittance matrix form of (2). A brief qualitative discussion of the network follows.

The series arms of the network are conversion conductances, g_{ca}, obtainable from (2). The validity of these elements of the network can be shown by considering them as transfer admittances. Conversion conductance in a mixer is, by definition, a transfer conductance.

The algebraic sign of the conversion conductance is determined from consideration of the direction of rotation of the sideband vectors. If susceptances were to be considered, conjugate notation would be required in certain of the elements to properly account for the directions of vector rotation. This concept is dealt with in detail by Torrey and Whitmer.[6]

The shunt arms of the network must be of such magnitude that, with all other pairs of terminals short-circuited, the driving point conductance at each pair of terminals is the average small-signal conductance, g_a. Again, by definition, average small-signal conductance is the conductance of an excited crystal as a two-terminal small-signal circuit element. This value of the shunt conductance is obtained by subtracting algebraically from g_a the series conductances that connect the particular pair of terminals to all other pairs of terminals.

Standards on Electron Devices: Methods of Measuring Noise*

COMMITTEE PERSONNEL
STANDARDS COMMITTEE, 1952–1953

A. G. JENSEN, *Chairman*

M. W. BALDWIN, JR., *Vice Chairman* L. G. CUMMING, *Vice Chairman* E. WEBER, *Vice Chairman*

J. Avins	C. A. Cady	F. J. Gaffney	G. D. O'Neill	D. C. Ports	N. Smith
R. R. Batcher	P. S. Carter	W. D. Goodale, Jr.	C. H. Page	P. C. Sandretto	R. A. Sykes
J. G. Brainerd	A. G. Clavier	R. A. Hackbusch	W. M. Pease	R. Serrell	W. G. Tuller
M. R. Briggs	J. L. Dalke	J. G. Kreer, Jr.	W. J. Poch	R. F. Shea	J. P. Veatch
F. T. Budelman	A. W. Friend	E. A. Laport	A. F. Pomeroy	R. E. Shelby	R. J. Wise

Definitions Co-ordinating Subcommittee

M. W. BALDWIN, JR., *Chairman*

P. S. CARTER
P. J. HERBST
J. G. KREER, JR.
E. A. LAPORT

E. WEBER—*Measurements Co-ordinator*

Committee on Electron Devices, 1949–1952

G. D. O'NEILL, *Chairman*
L. S. NERGAARD, *Past Chairman*
R. M. RYDER, *Vice Chairman*

E. M. Boone	C. E. Fay	L. B. Headrick	R. B. Janes	R. L. McCreary	H. J. Reich
R. S. Burnap	W. R. Ferris	L. A. Hendricks	J. W. Kearney	J. A. Morton	A. C. Rockwood
J. W. Clark	M. S. Glass	T. J. Henry	G. Ross Kilgore	I. E. Mouromtseff	A. L. Samuel
W. Dodds	A. M. Glover	M. E. Hines	S. J. Koch	H. L. Owens	W. G. Shepherd
W. G. Dow	J. E. Gorham	E. C. Homer	H. Krauss	O. W. Pike	R. W. Slinkman
G. A. Espersen	J. W. Greer	S. B. Ingram	L. Malter	P. A. Redhead	H. L. Thorson

C. M. Wheeler

Subcommittee on Small High-Vacuum Tubes

T. J. HENRY, *Chairman*
G. D. O'NEILL, *Past Chairman*

E. M. Boone	E. C. Homer	R. M. Ryder
R. C. Hergenrother	E. H. Hurlburt	A. C. Rockwood
L. N. Heynick	E. D. McArthur	W. G. Shepherd
M. E. Hines	W. T. Millis	R. W. Slinkman

Task Group on Noise

R. M. RYDER, *Chairman*

J. J. Freeman	E. H. Hurlburt	D. O. North
W. A. Harris	N. T. Lavoo	E. K. Stodola

* Reprints of this Standard, 53 IRE 7 S1 may be purchased while available from the Institute of Radio Engineers, 1 East 79 Street, New York 21, N. Y., at $.75 per copy. A 20 per cent discount will be allowed for 100 or more copies mailed to one address.

10.0 NOISE MEASUREMENTS

SPURIOUS SIGNALS, which are undesired and often unrelated to the desired signals, are always present in signaling systems and their components. Such spurious signals are generally called *noise*. Since noise reduces the amount of information that can be transmitted with a specific signal power, and since it adds spurious information that impairs performance or causes annoyance, quantitative measures of noise are often indispensable to engineering evaluations of signaling systems.

Test measurements for noise might logically be expected to begin with some generally useful quantitative measure of information-handling capacity in the presence of noise, or of the amount of annoyance which it creates. Such tests can be made in specific instances, but encounter numerous difficulties. Often they are subjective and hard to evaluate accurately. Furthermore, the effects of noise vary enormously, depending on the system in question, and on the levels and characteristics of both signal and noise. It is useful, therefore, to measure noise in the engineering terms commonly used to describe signals. To give a description of noise measurement in these terms is the purpose of this section.

Measures in terms of power are particularly comprehensive for an important type of noise, called "Gaussian," which is rather thoroughly characterized by its power spectrum at all frequencies. Gaussian noise includes the important types of "thermal" noise arising from thermal aggitation of charge carriers in conductors, and usually includes "shot" noise from random electron transits in a vacuum tube, as well as contact noise and transistor noise. Any noise which is steady or stationary in character, and which consists of the linear superposition of a sufficiently large number of small independent events, almost always has a Gaussian amplitude distribution in time.

Other types of noise also exist which may not be Gaussian—for example, "impulse" noise from ignition systems, atmospheric noise, power-line hum, and crosstalk. Complete characterization of these types requires, in addition to their power spectrum, other information such as the waveform of a typical pulse or the phase of the interference. However, for practical purposes, treatment by the methods below is often adequate anyway; if not, special methods, not described here, may be necessary to deal with non-Gaussian noise.

For simplicity, the test methods assume linearity of system response. Since noise usually enters the system at a point where the signal level is low, linearity will generally exist in the sense that the principle of superposition applies; that is, signals and noise produce currents and voltages which are simply additive, without the complicated intermodulation effects between different frequency components which occur in nonlinear systems. When the noise arises from independent uncorrelated sources, the average power of such independent noises is also additive in a linear system. Heterodyne systems, incorporating frequency shifters, are linear in this sense when the signals are small.

IRE standard definitions of some of the terms used in this Standard are listed in the Appendix.

10.1 NOISE FACTOR MEASUREMENTS

10.1.1 Introduction

A useful measure of the effect of noise in a system is the *noise factor* or *noise figure*. On the assumption that all the noise under consideration is characterized by its power spectrum, transmission by a linear system can only alter its noise spectrum or superpose additional noise. Accordingly, the performance of the system is rated by comparing its actual noise-output power with that which would have existed had the noise input been transmitted in the same manner as a signal with no accretions from noise sources within the system. Since the actual noise input is not a property of the system, the noise-performance measure is constructed by adopting a standard noise input, namely the thermal noise at standard temperature of the normal-input termination for the system. This measure of noise performance is called the *noise factor*, because it is the factor by which the output noise exceeds the reference level that would ideally be developed at the output from the standard-thermal input acting alone. The measure is taken with the transmission bandwidth limited to a small value (in principle infinitesimal) by appropriate filters. To emphasize that the measure is a point function of frequency, the term *spot noise factor* may be used.

In any communication system the signal is distributed over some finite bandwidth over which both signal-and noise-time averages may vary with frequency. Theoretically, in treating the interfering effect of the noise, it would be necessary to consider the frequency distributions (spectra) of both noise and signal; but in practice many cases are sufficiently well approximated by considering only the total powers of signal and noise. When only the total noise power in the band need be considered, it also may be referred to the reference thermal level. The corresponding measure of noise performance is the *average noise factor*, or weighted average of the noise factor over the band in question, the weighting factor being the operating power gain as described below. The measure of average noise factor is taken with the transmission bandwidth of the system at its normal value, not limited by added filters.

Since the *average noise factor* measures the degradation of the ratio of signal to noise[1] in passing through the system, it is a figure of merit (more strictly, of demerit) measuring the performance of a system as a whole. Consequently the average noise factor has often been called the *noise figure*. However, usage in the literature has been rather varied. Consequently it is felt that, for

[1] In constructing the input signal-to-noise ratio, the input standard-thermal noise power is taken to be limited by the noise bandwidth of the system.

clarity, henceforth noise factor and noise figure must be considered synonymous, both referring to point functions of frequency, and both being carefully distinguished from the average noise factor (average noise figure), which is the weighted average over the band. These distinctions, as well as the technical definition for each term, should be carefully noted, for there are many published treatments of the subject that differ among themselves and that differ from these Standards with respect to both nomenclature and definition.

Either kind of noise factor is a numeric, basically a power ratio, which may be expressed in decibels by multiplying its common logarithm by 10. It is a function of the internal structure of the system and of the source impedance. However, the noise factor is not a function of output-termination impedance, nor is the average noise factor either, except insofar as the output-power mismatch varies with frequency, thus modifying the characteristic relating operating power gain and frequency. The noise factor of a complete system depends on the noise factors of each tandem section of the system; the composition formula will be found in (9).

The noise-factor concept is useful over the entire frequency range, from audio to microwaves. Since it compares the actual noise with the fundamental limit set by thermal agitation, the noise factor gives a broad and direct evaluation of the degree to which a system approaches the ideal. For calculation of the output signal-to-noise ratio, knowledge of the average noise factor is sufficient whenever the input signal, the input noise, and the noise bandwidth of the system are all specified.

In making measurements of noise factor, numerous precautions must be taken to avoid difficulties with spurious frequency responses in the network, nonlinearities, spurious noise contributions, and indicating devices that are not true power-reading instruments. Where it is desired to measure spot noise factors, suitable filters must be provided to restrict the passband to a small percentage of the passband actually used.

In order to evaluate the noise factor it is necessary to obtain a measure of the noise power that is actually delivered to the output. This measure is divided by a similar measure of the output noise that would have been present if the system were noise-free and merely transmitted the thermal noise of the input termination at standard temperature. The following general methods of measurement are recognized for performing the evaluation. In each method a measure of the output noise is taken directly, but the methods differ in the ways of determining the reference noise of the ideal noise-free system.

a. *CW-Signal Generator Method.* (See section 10.1.2.1.) In this method a power meter at the system output and a calibrated signal generator at the system input are used to determine the gain-frequency function for the system. From this function there is determined a *noise bandwidth* which has the same transmission over its entire width as the actual function has at a reference frequency f_0, and which would transmit from the standard thermal source the same power as would the actual passband. By use of this noise bandwidth, the portion of the output noise resulting from the input-termination noise can be determined. Dividing total output noise by this reference noise gives the average noise factor.

b. *Dispersed-Signal Source Method.* (See section 10.1.2.2.) In this method a signal generator having its output dispersed uniformly over the passband of the system, and calibrated in terms of power output per unit bandwidth, is used to determine that portion of the output-noise power which results from the input-termination noise. Suitable dispersed-signal generators are noise diodes, gas tubes such as fluorescent lamps, or an oscillator whose frequency is swept through the band at a uniform rate.

c. *Comparison Method.* (See section 10.1.2.3.) This method consists of direct comparison between the network being tested and a secondary standard in the form of a network of the same type for which the noise factor has been determined.

Of these three methods the first, involving the direct measurement of band shape, although somewhat cumbersome, is accurate when carefully done. The noise diode dispersed-signal method is frequently simpler, and may be used for production testing when noise levels and frequency are not too high. The gas-discharge-generator dispersed-signal method is especially useful for frequencies so high that the noise output of the diode may be affected by transit-time or lead effects. The swept-oscillator dispersed-signal method may have some application as a supplementary method, especially when the noise level and frequency are both high. Comparison methods are primarily of use in production testing.

Sometimes the noise factor of only a first section of a receiver is desired as, for instance, in rating a preamplifier designed for maximum sensitivity. The contributions of succeeding stages can then be eliminated by using the cascade formula with precautions discussed below.

The noise factor or noise figure (the terms may be used interchangeably) of a 4-pole is, in effect, the ratio of the noise power delivered to the output termination of the system to the noise power that would have been delivered if the network had not degraded the input signal-to-noise ratio.[2] The noise figure is basically a numerical-power ratio, and it may be expressed in decibels by multiplying the common logarithm of this ratio by 10. In all cases the ratios referred to in the following discussion will be the numerical-power ratios.

Since the noise factor of a network depends upon the impedance of the source from which it operates, measurements should be made with a generator having the impedance characteristics from which the network being tested is intended to operate. This does not mean the two circuits are to be "matched" but merely that a specific condition of "match" or "mismatch" is necessary.

[2] It is assumed that the noise from the input termination is thermal at standard temperature of 290°K. See definitions.

Heterodyne systems may have appreciable responses at frequencies outside the band specifically required for transmission of the desired signal. Such image-frequency responses can often be eliminated by appropriate filters. In usual practice, the noise factor is defined only for the principal frequency transformation of the system. When image responses are present, corrections may be made as described (See section 10.1.2.1, 10.1.2.2).

10.1.2 Measurement of Average Noise Factor

The general method whereby the average noise factor may be measured involves the use of a signal generator for driving and a power-measuring device for measuring the output of the network under consideration. Several variations of method are possible, as will appear, but the general arrangement of apparatus is shown in Fig. 1.

Fig. 1—Noise-factor test arrangement.

Certain requirements must be met by each of the three components of Fig. 1 if the noise-factor concept is to be applied and a measurement made:

a. The calibrated generator should have an output impedance identical with that of the source to which the network is ordinarily connected. Calibration for available output power should take account of any elements that have been added to the basic generator to simulate the impedance characteristics of the source from which the network is ordinarily excited.

b. The signal generator may deliver either cw power or power uniformly distributed through a frequency spectrum including all significant responses of the network. In either case the instrument must be accurately calibrated in terms of its available power output.

The available power of a signal generator may be considered in the following manner. If the signal generator is as represented by the circuit of Fig. 2(a) it

Fig. 2—(a) Signal generator (b) matched load.

will deliver its maximum or available power to a matching load as shown in Fig. 2(b). This power is $E^2/4R$ and is *available* regardless of whether or not the load is one, such as that of Fig. 2(b), which *absorbs* it. That is to say, the *available* power is a property of the signal generator only, and not of the manner in which it is loaded.

c. The network under test must be linear in the sense that its available output-power change for a given available input-power change is independent of the initial power level for all values used in testing. It may include linear elements or linear frequency shifters, but, particularly, simple envelope detectors must be excluded. For example, in testing a conventional heterodyne receiver, the power-measuring device must be connected ahead of the second detector (unless the latter is itself a suitable power meter; see next paragraph).

d. The power-measuring device must indicate quantitatively the relative values of (1), the noise power at the output of the system with no signal input and (2), the total power at the output when an input signal is applied. The measuring device may be either a true power-measuring device such as a bolometer or thermocouple, or some other type of instrument which has been calibrated to read power for the particular wave forms used in testing.

10.1.2.1 Signal Generator Method

The measurement of average noise factor with a cw sine-wave signal generator will now be described. The average noise factor to be determined may be written

$$\bar{F} = \frac{N_0}{kT_0BG_0} \tag{1}$$

where

N_0 = noise-power output in watts,
k = Boltzmann's constant, 1.38×10^{-23} joules per degree K,
T_0 = absolute reference temperature, 290°K,
B = noise bandwidth in cycles per second (cps), and
G_0 = network operating power gain (transducer gain) at the reference frequency f_0.

With the signal generator connected to the network, but with the generator output at zero except for its thermal noise, let the network-power output be Q_1. With the available signal power of the generator set at P_s, let the network-power output be Q_2. Then the operating-power gain is $G_0=(Q_2-Q_1)/P_s$. Also the noise-power output will correspond to the original reading Q_1, so that (1) becomes

$$\bar{F} = \frac{Q_1}{Q_2 - Q_1}\,\frac{P_s}{kT_0B}. \tag{2}$$

In making the measurement it is desirable to make Q_2 several times greater than Q_1 since accuracy is promoted in this manner. However, for convenience and to avoid saturation, it is common to make $Q_2=2Q_1$ in which case (2) becomes $F=P_s/kT_0B$, and P_s may be considered as a power equivalent to the noise output as referred to the input circuit.

The signal generator is set at the frequency f_0 selected within the passband, as described below. It will be noted that an absolute calibration of the power-output measuring meter is not necessary, that is, G_0 need not be determined.

10.1.2.1.1 Determination of Noise Bandwidth. The noise bandwidth B may be obtained by plotting on

linear scales the transmission characteristic, as shown in Fig. 3.

The object of this measurement is to find the width on the frequency axis of a rectangular-response curve that will have the same area and height at f_0 as the actual curve. The frequency f_0 is usually, but not always, the frequency of maximum response. The area to be considered is that above the noise contribution, since only the signal contribution is of interest here. The area under the response curve may be measured by a planimeter or by counting squares on graph paper, or calculated by suitable formulas such as Simpson's rule. If the

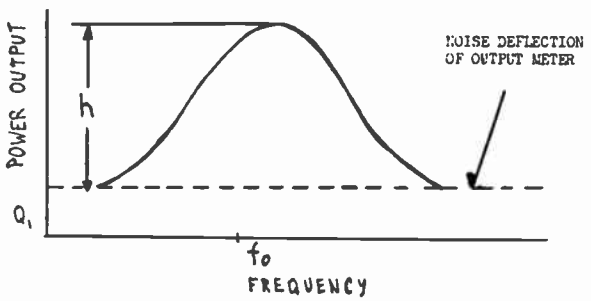

Fig. 3—Network relative power as a function of the frequency of a signal generator with fixed available power output to network.

area is M units of area, and the frequency scale is D cps per unit of length, and the height above noise h in Fig. 3 is in units of length, then the noise bandwidth referred to f_0 is $B = MD/h$. Since the noise factor refers only to the principal response of the system, spurious or image responses should be excluded from the selectivity curve.

If the characteristics of the network are such that signals large compared with the noise can be handled without saturation, the effect of noise can be ignored in determining the bandwidth B. That is Q_1 in Fig. 3 may become negligible. It may be possible to achieve this same effect by reducing the gain of the network to considerably less than its normal value, but it should be ascertained that this does not cause undesirable saturation effects and that bandwidth is not altered by reducing the gain, as may happen if regenerative effects exist.

10.1.2.2 Noise Measurement with Dispersed-Signal Source

Noise measurements may conveniently be made with a generator that delivers power uniformly over the response band of the network. To some extent this eliminates the need for a direct determination of the noise bandwidth as will appear below. Three examples of such generators are a noise diode, a gas-discharge tube such as fluorescent lamp, or a cw generator the frequency of which is continually swept at a uniform rate through the response band of the network. In any case, it is necessary that the output of the generator in watts per cps of bandwidth be accurately calibrated. If the system is connected as in Fig. 1, with the generator connected but with its output zero except for thermal noise, a reading Q_1 on the power-output meter will be obtained. If the generator is now made to have an available power of p watts per cps in addition to the initial thermal noise, the power output will be increased by pBG_0 and the new output meter reading will be Q_2 or, in terms of the same symbols as previously, $G_0 = (Q_2 - Q_1)/pB$. Also, as before $N_0 = Q_1$, or substituting in (1),

$$\overline{F} = \frac{p}{kT_0} \frac{Q_1}{Q_2 - Q_1}. \tag{3}$$

It should be noted that this measurement may involve spurious or image responses which will ordinarily give a noise factor that is deceptively good, i.e., too low, unless appropriate correction is made. In other words, if the dispersed signal covers passband responses not ordinarily used, such as images, which have appreciable gains compared to that of the passband ordinarily used, the test signal will produce an effect in the output circuit greater than would be produced if the dispersed-signal source were limited so as to include only the response ordinarily used. Hence, if important spurious responses exist, a bandwidth measurement must be made and the noise factor initially determined must be increased in the ratio of (1) the noise bandwidth including all spurious responses, to (2) the noise bandwidth when only the desired response is considered.

10.1.2.2.1 Noise-Diode Generators. A temperature-limited diode can be used as a noise generator when connected in a circuit such as Fig. 4(a). This circuit is typical, but many variations are of course possible. In

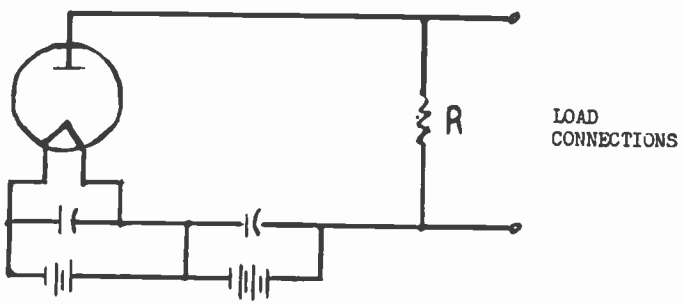

(A) TYPICAL DIODE NOISE-GENERATOR CIRCUIT

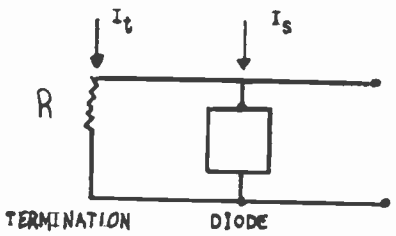

(B) EQUIVALENT CIRCUIT

Fig. 4—(a) Typical diode noise-generator circuit (b) equivalent circuit.

particular, R should be compensated so that together with the diode it simulates the actual input termination for which the system to be tested is designed. If the cathode temperature is adjusted to give a dc plate current of I_d amperes, then as a result of the diode shot noise there will be impressed across the resistor R of Fig. 4(b) a noise current I_s such that for each small in-

crement Δf of bandwidth

$$\overline{I_s^2} = 2eI_d\Delta f, \tag{4}$$

where e is the electronic charge, 1.60×10^{-19} coulomb, and $\overline{I_s^2}$ is the mean square noise current. In addition, from thermal noise in the resistor R will arise another current I_t, given by the relation

$$\overline{I_t^2} = 4kT\Delta f/R. \tag{5}$$

Looking back into the load connections of the circuit of Fig. 4(b) one sees a generator having an available-noise power per cps of bandwidth greater than thermal by the amount p watts per cps, where

$$p = eI_dR/2. \tag{6}$$

Inserting (6) into (3), one obtains the expression for average noise factor

$$\overline{F} = \frac{eI_dR}{2kT_0}\,\frac{Q_1}{Q_2 - Q_1}. \tag{7}$$

Since the numerical value of $kT_0/e = 0.0250$ volt,

$$\overline{F} = 20I_dR\,\frac{Q_1}{Q_2 - Q_1}, \tag{8}$$

where I_d is in amperes, R in ohms and Q_1 and Q_2 are relative noise-power outputs.

As before, it is desirable that Q_2 be considerably larger than Q_1 (preferably several times larger) so that the difference between Q_1 and Q_2 can be read with maximum accuracy in terms of Q_1. For convenience, Q_2 is often made equal to $2Q_1$. Sometimes a smaller value of Q_2 must be used because of limitations imposed on the diode dc plate current I_d. In such cases, additional care must be taken that Q_1 and Q_2 are stable, repeatable readings to assure reasonable accuracy in the result.

In the above discussions, no account has been taken of electron-transit time in the diode. If the transit time is an appreciable fraction of a cycle, the noise output of the diode will be lowered.[3]

10.1.2.3 Comparison Methods of Noise Measurement

The previously described methods may not be convenient or necessary for production testing. In such cases, noise factors can be checked approximately by carefully chosen comparisons with the performance of a master standard unit of known noise factor. When bandwidths of networks, both before and after detection, and also detector characteristics are maintained within close limits, then a measurement of signal-to-noise ratio after detection, with a fixed modulated-signal input, may be used for checking individual units.

10.1.3 Spot-Noise Factor

The noise figure discussed in 10.1.2 is the weighted average noise factor over the whole network passband. The spot noise factor, or factor at a particular frequency, can be determined by inclusion between the network and the power-measuring device of a very narrow filter at the desired frequency. When the spot frequency is near the center of the band, the factor so obtained may not be greatly different from the average.

10.1.4 Networks in Cascade

Frequently several networks are connected in cascade, and it is desirable to know how the noise factor of each affects the noise figure of the over-all system. This is necessary both in evaluating the effect of improvement in any part of the system and in measuring the noise factor of a single unit connected in a system.

For a number of networks in cascade, as shown in Fig. 5, the system spot-noise factor is given in terms of the component spot-noise factors by the formula:

Fig. 5—Networks in cascade.

$$F = F_1 + (F_2 - 1)/G_1 + (F_3 - 1)/G_1G_2 + \cdots \tag{9}$$

where G_1, G_2, and so forth, are the available power gains of the component networks.

An analogous formulation for average noise factor can be derived, but is more involved. When the frequency for spot noise factor is chosen near the center of the noise-transmission characteristic, then formula (9) for spot noise factor is often a satisfactory approximation for average noise figure also.

These formulas are also applicable to networks that attenuate rather than amplify, in which case the corresponding gains are fractional. It should be mentioned here that the spot noise factor of a passive attenuating network at standard temperature is the factor by which the available power is attenuated in passing through it. It should also be noted that, when the various networks each have substantial gains and the noise factor of the later stages is not excessive, then the over-all noise factor is largely determined by the noise figure of the first stage.

10.1.5 Precautions

Care should be taken that the apparatus which must be attached to the network to be measured does not materially affect the bandwidth of the system. For example, if regeneration is introduced that greatly narrows the bandwidth, the noise factor may be markedly altered. In any event, unwanted feedback usually makes the measurement much more difficult.

Careful shielding and filtering of input and output elements is essential, particularly when the difference in power level between output and input is large. If the measuring-signal generator has a temperature different from standard T_0, an appropriate correction must be applied.

[3] For transit-time correction, see D. B. Fraser, "Noise spectrum of temperature-limited diodes," *Wireless Eng.*, vol. 26, pp. 129–131; April, 1949.

Appendix

Noise Factor (Noise Figure). Of a linear system at a selected input frequency, the ratio of (1) the total noise power per unit bandwidth (at a corresponding output frequency) available at the output terminals, to (2) the portion thereof engendered at the input frequency by the input termination, whose noise temperature is standard (290°K) at all frequencies. (See Noise Temperature.)

Note 1—For heterodyne systems there will be, in principle, more than one output frequency corresponding to a single input frequency, and vice versa; for each pair of corresponding frequencies a noise factor is defined.

Note 2—The phrase, "available at the output terminals" may be replaced by "delivered by the system into an output termination," without changing the sense of the definition.

Noise Factor (Noise Figure), Average. Of a linear system, the ratio of (1) the total noise power delivered by the system into its output termination when the noise temperature of its input termination is standard (290°K) at all frequencies, to (2) the portion thereof engendered by the input termination. For heterodyne systems, portion (2) includes only that noise from the input termination which appears in the output via the principal frequency transformation of the system, and does not include spurious contributions such as those from image-frequency transformations.

Note 1—A quantitative relation between average noise factor, $\overline{F}$, and spot noise factor, $F(f)$ is

$$\overline{F} = \frac{\int_0^\infty F(f)G(f)df}{\int_0^\infty G(f)df},$$

where f is the input frequency, and $G(f)$ is the ratio of (a) the signal power delivered by the system into its output termination to (b) the corresponding signal power available from the input termination at the input frequency. For heterodyne systems, (a) comprises only power appearing in the output via the principal frequency transformation of the system; in other words, power via image-frequency transformations is excluded.

Noise Factor (Noise Figure), Spot. See Noise Factor. Used where it is desired to *emphasize* that the noise factor is a point function of input frequency.

Noise Temperature. At a pair of terminals and at a specific frequency, the temperature of a passive system having an available noise power per unit bandwidth equal to that of the actual terminals.

Noise Temperature, Standard. The standard reference temperature T_0 for noise measurements is taken as 290° Kelvin.

Note—$kT_0/e = 0.0250$ volt, where e is the electron charge and k is Boltzmann's constant.

A Direct-Reading Oscilloscope for 100-KV Pulses*

R. C. HERGENROTHER†, ASSOCIATE, IRE, AND H. G. RUDENBERG‡, MEMBER, IRE

Summary—**This paper describes the design, construction, and performance of an electrostatic oscilloscope tube suitable for direct operation on peak deflection voltages of 100 kv and pulse widths of a fraction of a microsecond. The deflection system comprises an electrostatic field divider between the deflection electrode and the electron beam, so that the high deflection voltage causes only normal beam deflection at the screen. The tube may be calibrated at a low anode voltage and operated at a high one during pulse measurement, reducing dc calibration voltage requirements fivefold or tenfold. Use of the tube avoids difficulties encountered with resistance-capacitance dividers in measuring radar modulator pulses.**

Introduction

A CATHODE-RAY TUBE with an electrostatic deflection system operated directly by high-voltage pulses would circumvent many of the problems encountered in the measurement and display of such pulses. The conventional techniques of measurement have not kept up with recent advances in the techniques of generation of high-voltage pulses. This difficulty of measurement seems to be particularly great in the radar field, where modern requirements demand shorter pulses of higher-peak powers than ever before. As radar transmitter powers have increased, the problems of measuring and timing modulator pulse shapes and amplitudes have become increasingly difficult.

Conventional techniques for the measurement of high-voltage pulses of short duration have severe disadvantages when they are applied to this problem and when the ultimate performance is required. The usual method of measuring such high-voltage pulses consists of using a voltage divider network so as to reduce the voltage to a level which can be applied to the deflection plates of a cathode-ray oscilloscope. This runs into serious limitations when voltages of the order of 100 kv and pulse widths of the order of fractions of a microsecond are to be measured. In an attempt to reduce the voltage stress on each high resistance, these are usually divided into sections. In a simple dividing network, it is possible to take into account the stray capacitances, and thus to

* Decimal classification: R371.5. Original manuscript received by the Institute, October 1, 1952; revised manuscript received January 21, 1953. Reprinted from TRANSACTIONS OF THE I.R.E. PROFESSIONAL GROUP ON ELECTRON DEVICES, PGED-1; November, 1952.

† Raytheon Mfg. Co., Waltham, Mass.

‡ Electronics Research and Development Corp., Melrose, Mass. Formerly with Raytheon Mfg. Co., Waltham, Mass.

compensate for their frequency characteristic. However, the actual magnitudes required for a divider to measure 100-kv pulses require a more complex network as the distributed capacitance is not lumped across each resistance section. Consequently, one has to use few resistor sections of relatively high dissipation, and the high-frequency error due to their stray capacitances can not be compensated completely. Other techniques, such as the use of networks resembling lumped transmission line sections,[1] suffer from the same limitations when applied to the problem of measuring 100-kv pulses.

A further method consists of rectifying the peak-pulse voltage with a diode rectifier and measuring the resultant direct voltage. This may also lead to difficulties, as diodes suitable for operation at such high voltages are not available with sufficiently small capacitances. When the construction of such diodes is contemplated especially for this purpose, then one might also consider the construction of an oscilloscope tube along the lines presented in this paper. As a diode can only give information on the peak voltage of the pulse whereas the oscilloscope tube displays the pulse shape as well, the latter alternative has much to offer.

These considerations have led to the belief that a cathode-ray tube having an electrostatic deflection system capable of being operated directly at the required voltage levels would have considerable utility. Although requiring considerable care to construct, its use avoids many of the difficulties encountered with resistance-capacitance dividers. The deflection system of the tube comprises a carefully designed electrostatic field divider between the deflection electrode and the electron beam, so that the high deflection voltage causes only normal deflection of the electron beam at the screen of the oscilloscope tube. Another advantage is that calibration can be simplified, as a low anode voltage can be used during calibration and a high one during pulse measurement, thus reducing the dc calibration voltage requirement by a factor of 5 or 10.

Design Requirements

The key problem in the design of an oscilloscope tube for this application is the electrostatic deflection system design. Foremost is the requirement that the system must withstand the high voltages to be applied directly to the tube. Thus, the deflection system must be designed so that high potential gradients, which might cause cold emission, are avoided. Also a substantial insulation surface length must separate the electrodes in the vacuum envelope as well as outside, so as to avoid insulation breakdown.

The other requirement is that deflection with 100-kv pulses will give a deflection that is comparable to that usual with lower voltage tubes. This means that the deflection factor in volts per radian of electron-beam deflection of this electrostatic deflection system should be about fifty times that of a conventional oscilloscope tube and also that this factor be essentially constant over the full deflection range. This can be achieved by reducing the coupling to the electron beam from the deflection system in one of several ways, so that the deflecting voltage may be sufficiently high. In fact, in the tube to be described the deflecting voltage exceeds the anode voltages of the oscilloscope tube.

Attempts to Use Conventional Deflection Plates

It might be thought possible to utilize modifications of conventional deflection systems by proper modification and shaping of the plates. The deflection factor in volts per inch deflection of conventional deflection plates can be increased by making the plates shorter and increasing their separation. If this is carried to extremes, the plates shrink to two parallel wires whose separation is large compared to their diameters. The deflection factors of such a deflection system has been analyzed[2] to be

$$\frac{E}{\theta} = \frac{2}{\pi} V \cosh^{-1}\left(\frac{d}{2r}\right),$$

where

r = radius of wires
d = center to center separation of wires
V = anode voltage
E = deflection voltage
θ = beam deflection angle in radians.

If it is required to get a deflection of 1 radian with a deflection voltage of 10^5 volts using an anode voltage of 10^4 volts, this equation gives

$$\cosh^{-1}\left(\frac{d}{2r}\right) = 5\pi$$

or

$$\frac{d}{2r} = 6 \times 10^6.$$

The lower limit of r is set by cold emission effects which require that potential gradients at the conductor surfaces should be less than 10^6 volts per cm.

These computations indicate that it is impossible to meet the deflection factor requirements by modification of a conventional deflection electrode system and that some other type of deflection system must be devised.

Attenuation of Deflection Fields

Let us, therefore, re-examine the factors governing the deflection of an electron beam. The deflection factor of an arbitrary deflecting system has been analyzed to give

$$\theta/E = c/2Vk_0,$$

[1] C. L. Dawes, C. H. Thomas, and A. B. Drought, "Impulse measurements by repeated structure networks," *Trans. AIEE*, vol. 69; 1950.

[2] H. G. Rudenberg, "Deflection sensitivity of parallel wire lines in cathode-ray oscillographs," *Jour. Appl. Phys.*, vol. 16, pp. 279–284; May, 1945.

where c is the capacitance per unit deflection plate width that couples directly with the electron beam and k_0 is the permittivity of free space. It can be seen that only the capacitance coupling the beam directly with the deflection electrodes enters into this equation, and not the total deflection system capacitance.

The method used for reducing the angular deflection sensitivity, therefore, consists of attenuating this coupling capacitance by attenuating the corresponding deflecting field of the electrodes through a shield. By this means one may reduce this coupling capacitance at will without great affect on other construction problems.

A possibility existed that electrodes external to the glass wall of the cathode-ray tube might be adapted. In practice, it is known that electrostatic charges on the insulating glass walls can build up and contribute to erratic deflection, as these charges depend on the secondary emission and leakage properties of the surfaces of the vacuum enclosure. Reports on an investigation of these effects[3] indicated that considerable errors might be expected from a conventional cathode-ray tube using external high-voltage electrodes and shields. The electrodes were designed to be within the high-vacuum enclosure of the cathode-ray tube, and shielded internally so as to reduce the coupling capacitance to the electron beam in the present tube.

By proper shaping of the electrodes and shield, this coupling capacitance and also the shape of the equipotentials and the field traversed by the electron beam may be designed to meet the requirements of this particular electrostatic deflection system. As the radar pulses considered for measurement were negative only, the particular deflection system used here was designed single-ended. It consists of one deflecting electrode to be connected directly to the high-voltage pulses, a grounded shield with a sufficiently large slot to give the proper deflection, and a grounded second deflection electrode. Deflection systems based on this principle of field attenuation were studied in detail, using an electrolytic trough for measuring the deflection field pattern.

Deflection Electrode and Shield

An electrostatic deflection system comprising coaxial cylinders and utilizing the leakage field around a slot in the outer cylinder was studied by means of the electrolytic trough. The pattern of equipotentials measured for this configuration is shown in Fig. 1. These data show that the slot width chosen produces too high a deflection factor and shows undesirable variation in field strength across the deflection space, which would result in a variation of deflection factor with deflection angle.

The electrode shapes were repeatedly modified and the resultant field shapes measured with the objective of obtaining the required deflection factor and producing a close approximation to a uniform field which will satisfy the requirement for constant deflection factor.

The electrode shape finally chosen with its measured

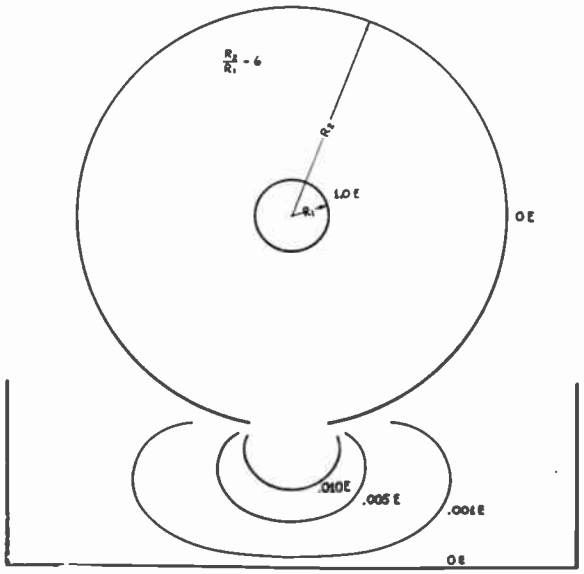

Fig. 1—Electric field of slotted coaxial shield.

potential configuration is shown in Fig. 2. The field region of interest, which will comprise the deflection space, is also shown. The deflection field is seen to be quite similar to the field between double-flared plates. It is quite uniform in the center of the deflection area and, in the region seen, encompasses 5 per cent of the total voltage applied to the system.

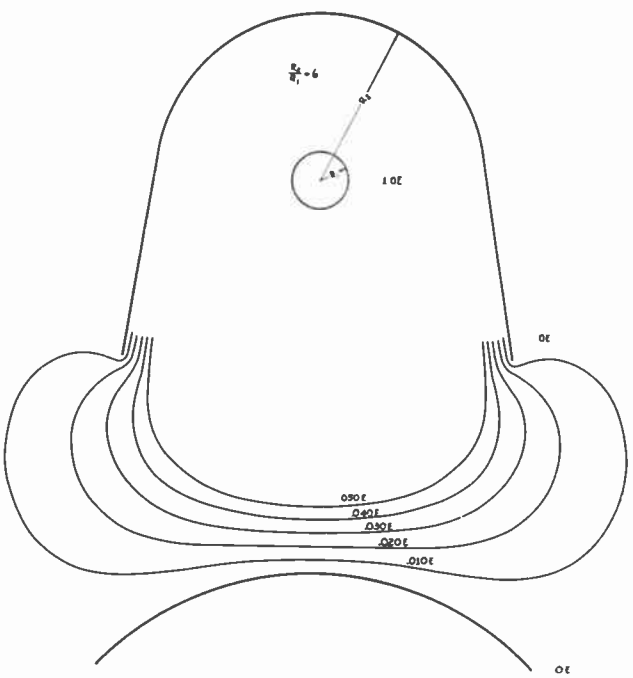

Fig. 2—Electric field of final electrode design. $R_1 = 0.062$ inch in the deflection-electrode structure used in the tube.

The dimensions to be chosen for this deflection system should be as small as possible for convenience in construction. A lower limit for the size will be set by the field intensity at the surface of the central electrode. The field intensity at the surface of the inner electrode of coaxial cylinders of radius R_1 and R_2 is given by[4]

[3] C. L. Dawes and K. Shen, private communication, Harvard University, Cambridge, Mass.

[4] C. V. Christie, "Electrical Engineering," pp. 18, 19, 20; 1938.

$$\mathcal{E} = \frac{E}{R_1 \ln \frac{R_2}{R_1}},$$

where

$\mathcal{E}$ = potential gradient in volts/cm
R_1 = radius of inner cylinder
R_2 = radius of outer cylinder
E = potential difference between cylinders in volts.

In order to avoid cold emission, voltage gradients should not exceed 10^6 volts per cm.

If a deflecting voltage of 0.25×10^6 volts is applied between coaxial cylinders having a diameter ratio of 6, which corresponds to the model, this equation shows that the voltage gradient will be 10^6 volts per cm when the inner cylinder radius is 0.14 cm. An inner cylinder radius of approximately twice this value was chosen for the design, giving a substantial factor of safety.

their positions accurately inside the bulb. The outer electrode is spot welded to the supporting wires.

The modulator output pulses to be measured are negative with respect to ground. The center electrode of the deflection system is used as the high-voltage electrode and the outer electrode is connected to the cathode-ray tube anode which is at ground potential. The deflection field will, therefore, bend the electron beam away from the center electrode. If the deflection system were aligned with the cathode-ray tube axis, only one half the fluorescent screen would be available for displaying the pulse. To make the whole diameter of the fluorescent screen available for displaying the pulse, the deflection system is displaced from the tube axis and the cathode-ray beam is given a fixed deflection by a magnetic field, causing the beam to pass through the deflection field area to one edge of the fluorescent screen as shown in Fig. 4. This bias deflection is produced by passing a direct current through one set of coils of a deflection yoke

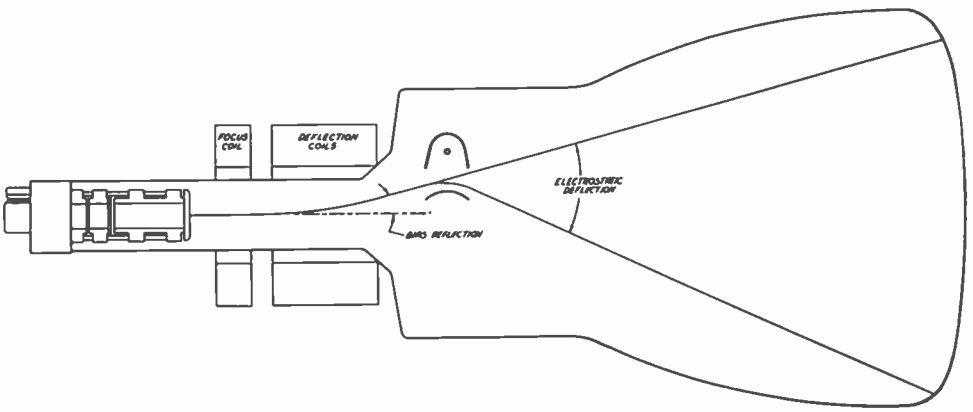

Fig. 4—Cross section of high-voltage pulse oscilloscope tube.

Constructional Features

The deflection electrode assembly which was constructed is shown in Fig. 3. The center electrode is supported from the ends of the conducting rods projecting into the tube. There is no supporting insulation in or near the deflection space. The deflection electrodes are assembled in the bulb by means of a jig which locates

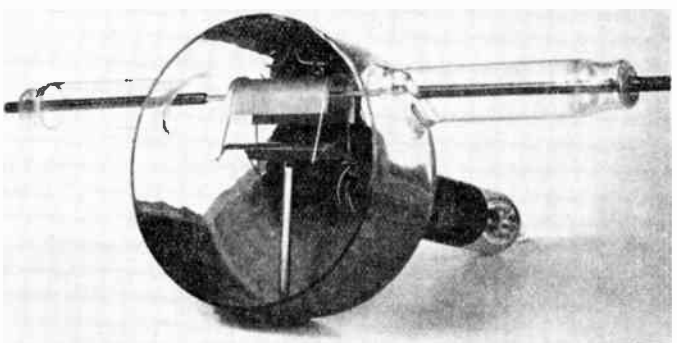

Fig. 3—Deflection-electrode structure. The deflection-electrode cross section has the same proportions as Fig. 2. The high-voltage electrode has a diameter of $\frac{1}{8}$ inch in the deflection region and the width of the other electrodes is 2 inches.

similar to those used for television. The other set of coils in the yoke is used for producing the time base deflection of the oscilloscope trace. These were especially designed for high sweep speeds.

Fig. 5 shows a photograph of the oscilloscope tube. When the tube is in use, spherical corona shields are placed on the ends of the arms. Tubes with electrostatic deflection for the time base and bias deflection present certain advantages for general-purpose measurements, and could also be used.

Calibration

The deflection factor of the tube is calibrated by using a measured anode voltage of several thousand volts and applying a measured dc deflection voltage to the deflection system. During pulse measurement a measured anode voltage of about 18,000 volts is used. The deflection factor during measurement is derived from the calibrated deflection factor by multiplying this figure by the ratio of the anode voltage used during measurement divided by the anode voltage used during calibration.

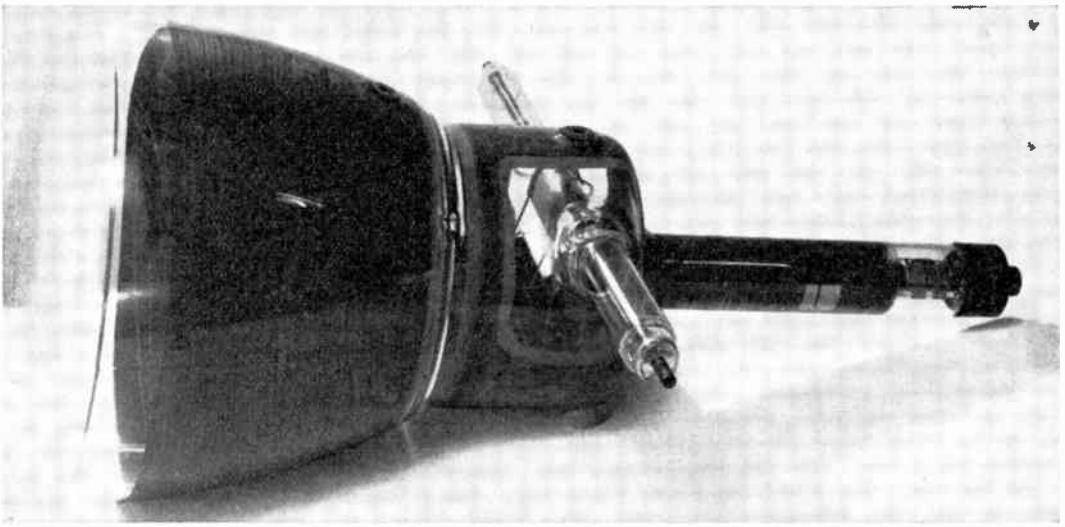

Fig. 5—High-voltage pulse oscilloscope tube with 8-inch diameter fluorescent screen.

A particular advantage of a deflection system, unlike resistance-capacitance dividers, is that direct calibration can be made at any frequency or with dc.

Oscilloscope Unit

A complete oscilloscope unit utilizing this oscilloscope tube is shown in Fig. 6. This unit was designed by Buckbee.[5] The unit contains the anode voltage and calibration-voltage power supplies. A sawtooth time base which is triggered by the same pulse used to trigger the modulator is included. The time base is adjustable in steps of $\frac{1}{2}$, 5, and 50 μsec per inch of deflection. During calibration of the deflection factor a measured dc voltage is applied to the deflection system and a 60-cycle ac voltage is applied to the time-base deflection coils to draw the spot out into a line, making the spot deflection measurement more accurate.

A photograph of a modulator voltage pulse applied to a magnetron is shown in Fig. 7. The voltage scale is in kilovolts.

Fig. 6—Complete high-voltage pulse oscilloscope unit.

[5] Mr. John Buckbee is Chief Circuit Engineer of the Raytheon Power Tube Division.

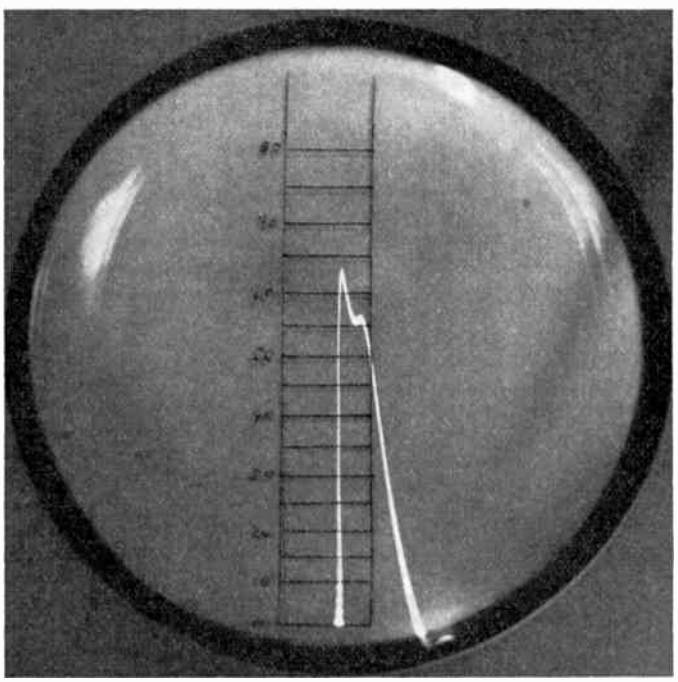

Fig. 7—Photograph of a 1 usec 63 kv modulator pulse as shown on oscilloscope screen.

Conclusion

The design, construction, and performance of an electrostatic deflection oscilloscope tube, suitable for direct operation on peak pulse deflection voltages of 100-kv and pulse widths of a fraction of a microsecond, has been described. This consists of a special deflection electrode shielded from the electron beam by a grounded electrode to provide proper attenuation of the deflecting field sealed into a normal cathode-ray tube. The unit is calibrated at a much lower anode voltage to simplify tests. These tubes have been very useful in adjusting and measuring high-power radar modulators. The tubes have given satisfactory operation and appear to have normal cathode-ray tube life.

Analysis of Control Systems Involving Digital Computers*

WILLIAM K. LINVILL†, MEMBER, IRE, AND JOHN M. SALZER‡, ASSOCIATE, IRE

Summary—**Digital computers have recently been used as elements in control systems employing otherwise conventional elements. The fact that data passing through the digital computer of the usual type must be sampled is an important property of such mixed systems. The description of the processes of sampling and desampling, as well as operations performed by the digital computer, in the frequency domain permits the extension of conventional servomechanisms analysis to mixed systems. The purpose of this article is an introduction to dealing with the unconventional parts of the system. Sampling is shown to be analogous to amplitude modulation by the continuous data of a carrier of unit impulses, while desampling is analogous to ripple filtering. Linear operations of the digital computer on sampled data are described by transfer functions. An illustrative example of computer program design in the frequency domain is given, and the applicability of these methods is indicated.**

I. Introduction

ALTHOUGH MOST digital-computer developments are directed toward the building of tools for the numerical solution of scientific and engineering problems, it is becoming increasingly more evident that digital computers will play an important role also in control applications. It is not impractical to think of using a digital computer for controlling an automatic process in a chemical manufacturing plant or for utilizing track-while-scan radar data in an aircraft control system. The digital computer becomes just one element in a closed-loop control system, in which its action can be compared with that of an analog computer or an analog filter. Just as an analog unit represents the solution of a differential equation, a digital unit can be thought of as representing the solution of a difference equation. The important requirement is that the computer be sufficiently fast for the application; that is, it should be able to operate in real time.

It is beyond the scope of this paper to deal with the merits or demerits of applying a digital computer for controlling. It suffices to state here that each application should be considered on an individual basis. Some, but by no means all, of the considerations will come to light in what follows. The question that can be asked is this: If it has already been decided to employ a digital computer in a control system, how can the resulting system be analyzed? In order to answer this question, one must understand the basic difference between a mixed system and a conventional all-analog system.

The present paper will concentrate on one particular aspect of mixed systems; namely, that the data must be sampled when passing through a digital computer. For whenever equipment is time-shared, it can handle any particular data only part of the time and some kind of sampling process is indicated. In a digital computer, as we think of it today, the arithmetic unit is used to perform operations in sequence, and furthermore, sequences of pulses are employed to execute each step of an operation.

Consider Fig. 1 which is the block diagram of a simple system employing a digital computer. This figure represents only one of a number of ways in which a computer may be incorporated in a control system, but the analysis of this specific system poses the same problems generally encountered. The sampling and coding

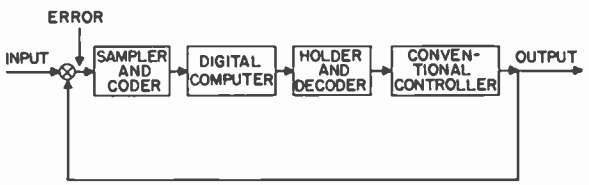

Fig. 1—A simple servo system employing a digital computer.

unit converts continuous and analog data into sampled (discrete in time) and numerical form for use by the digital computer. The digital computer performs a series of operations on the input data and supplies the result still in sampled and numerical form to the holding and decoding unit. The latter converts the data to continuous and analog form for use by conventional analog equipment.

Note that the system of Fig. 1 presents three new problems of analysis: the descriptions of (1) the sampling process at the input of the computer, (2) the operation on the input samples by the computer, and (3) the desampling (holding) process at the output of the

* Decimal classification: 621.375.2. Original manuscript received by the Institute, September 2, 1952; revised manuscript received February 6, 1953.

† Electrical Engineering Department, Massachusetts Institute of Technology, Cambridge, Mass.

‡ Research and Development Laboratories, Hughes Aircraft Co., Culver City, Calif.

computer. The rest of the system is conventional and operates on continuous data. In an actual case the conventional part may constitute the bulk of the system.

The analysis of such a mixed system is greatly facilitated by describing all of its portions in terms of the same language. The frequency domain has been chosen as one possible common ground of approach because: (1) frequency techniques have proved extremely effective in dealing with conventional control systems and much of a control system remains conventional even when a digital computer is used as a component, (2) the processes of sampling and desampling are very conveniently described in the frequency domain, and (3) the computer operations are often linear and consequently can be described in the frequency domain.

In short, the results of this paper are: (1) sampling is like amplitude modulation, (2) desampling is like ripple filtering in amplitude demodulation, and (3) linear digital computer programs can be described by transfer functions. A control system involving a digital computer is strikingly analogous to a familiar type of control system having one part wherein the signals are given directly and another part wherein the signals are given as modulation envelopes of suppressed-carrier amplitude-modulated waves. The direct-signal part corresponds to the conventional part of the system, the modulated-signal part to the digital computer.

The present paper will deal with the frequency analysis of only the unconventional parts of the control system. In a previous paper on sampled-data control systems the analysis of an over-all system having a sampled-data part, but no digital computer, has been described.[1] The analysis of an over-all system involving a digital computer follows readily once the computer is defined by a transfer function. The purpose of the present paper is to indicate in general terms how a digital computer is fitted into a conventional system. A more thorough treatment of digital computers and their properties in the frequency domain will be given by one of the authors in an ensuing paper.

II. Equivalent Representation

Consider Fig. 2 which shows the unconventional part of a mixed system. Since a direct description of the input and output samples in the frequency domain is not

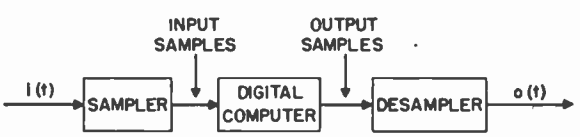

Fig. 2—A digital computer operating on a continuous input.

possible, the use of equivalent data is suggested. In particular, if each sample of Fig. 2 is replaced by an impulse of the same (area) value, the equivalent circuit shown in Fig. 3 results.

[1] W. K. Linvill, "Sampled-data control systems studied through comparison of sampling with amplitude modulation," *A.I.E.E. Trans.*, vol. 70, part II, pp. 1779–1788; 1951.

The equivalence between Figs. 2 and 3 can be established by showing that $o(t)$ is related to $i(t)$ equally in both cases. In the actual equipment, the signal, $i(t)$, is sampled at uniformly-spaced instants resulting in a sequence of samples, which may be coded as binary numbers for the computer. In the equivalent circuit, $i(t)$

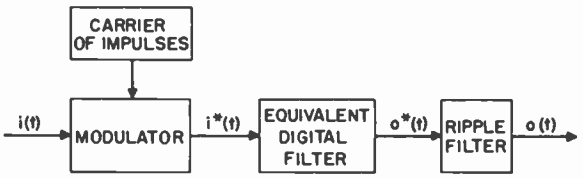

Fig. 3—Equivalent circuit of Fig. 2.

modulates a carrier of sharp unit-area pulses having a repetition frequency $1/T$, where T is the interval between sampling instants. There is a one-to-one correspondence between the areas of this sequence of impulses and the numerically-coded samples which are actually fed into the computer. The equivalent digital filter operates on the successive impulses in precisely the same way the computer operates on the successive numerical samples. It follows, therefore, that the areas of the output pulses of the equivalent-digital filter correspond to the output numbers of the actual computer in a one-to-one fashion. Finally, the demodulator of Fig. 3 has an impulse response exactly equal to the sample response (sometimes called the holding function) of the actual holding unit. The identity of the final outputs for both the actual and equivalent circuit follows in a trivial manner.

Having established the equivalence between the actual circuit and the equivalent circuit, we will now describe the latter in more specific terms. We will refer to Fig. 4, which shows the form of data at various points of the equivalent circuit for a particular example. The digital computer is used to differentiate the input function, and the effect of each step is illustrated in both the time domain and the frequency domain.

III. The Sampling Process

As already noted, the sampling of $i(t)$ is analogous to the modulation of an impulse chain by $i(t)$. A Fourier analysis of the carrier (the impulse chain) shows it to have a constant component, a fundamental of period T, and all harmonics of equal size. To state this mathematically, we call the carrier $u^*(t)$ and write

$$u^*(t) = \sum_{k=-\infty}^{\infty} u(t - kT) = \frac{1}{T} \sum_{k=-\infty}^{\infty} e^{-jk\Omega T} \qquad (1)$$

where $u(t)$ is the impulse function, T the time interval between impulses, $\Omega = 2\pi/T$ the radian sampling frequency, and e the Naperian base. Equation (1) shows that the amplitudes of all frequency components equal $1/T$. Fig. 4(a) shows the continuous input signal, $i(t)$, while Fig. 4(b) depicts the carrier, $u^*(t)$.

Modulating the pulse train is the same as simultaneously modulating each of its Fourier components and

adding together these modulated components. The component which is obtained from modulating the constant term in the Fourier series by the pure signal, $i(t)$, is $1/T$ times the pure signal itself. The components obtained from modulating the sinusoidal terms are like sidebands, but now there are an infinite number of sidebands corresponding to the carrier frequencies of Ω, 2Ω, 3Ω, and so forth, radians per second. Call the modulated sinus-

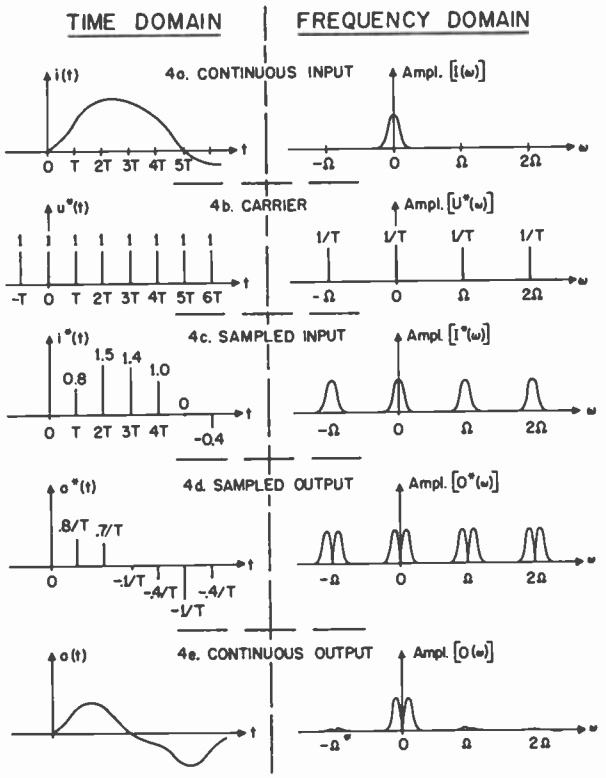

Fig. 4—Description of signals in the equivalent circuit of Fig. 3.

oids complementary signals. They are generated by the modulation process and appear at the output of the modulator in addition to the pure signal. Figure 4(c) indicates this result by showing the pure and the first few complementary components. The Laplace transform of the sampled signal, $i^*(t)$, is related to the transform of the continuous signal, $i(t)$, as follows

$$I^*(s) = \frac{1}{T} \sum_{k=-\infty}^{\infty} I(s + jk\Omega). \tag{2}$$

IV. The Desampling Process

The description of sampling in the frequency domain points out how desampling should be done. It behooves us, therefore, to discuss desampling at this point and postpone dealing with the operation of the computer. First we shall talk about how the original signal can be regained by following the sampling process by a desampling process immediately. Then, we shall indicate that the same considerations apply when the output of the computer is desampled. Finally, we shall discuss the effect of the digital computer on the sampled input. It is seen from Figs. 4(a) and 4(c), as well as from (2), that to recover a pure signal from its samples one merely filters out the complementary signals to leave only the pure signal. Thus sampling is like modulation; desampling is like ripple filtering in demodulation. Just as it is practically impossible to remove all ripple from a demodulator by low-pass filtering, it is also impossible to remove all complementary signals from the sampled signal by filtering. Recall that ripple filtering for demodulators becomes more difficult for wide-band signals because signal and ripple get closer together frequency-wise. This fact applies also for desampling. Whereas the pure signal spectrum in a sampled wave is centered around zero frequency, the complementary signals are centered around Ω, 2Ω, 3Ω, $\cdots$. The low-pass filter can pass the pure signal and reject the complementary signal only if there is enough frequency spread between the wanted and unwanted signals. As the bandwidth of the pure signal approaches $\Omega/2$ filtering becomes impossible because the wanted and the unwanted-signal spectra overlap. Even if pure and complementary signals do not overlap, one must make the usual choice between ripple discrimination and filter-phase lag. Good ripple rejection can be had only at the expense of considerable lag.

When the desampling unit is used at the output of the digital computer, its purpose is not to recover a continuous function which has existed previously. Rather it is to obtain a new continuous function, $o(t)$, from the sampled output, $o^*(t)$, of the computer, as illustrated in Figs. 4(d) and 4(e). Nevertheless, the basic requirement is still the same; namely, the desampler must have a low-pass filter characteristic to remove the complementary signals of $o^*(t)$.

V. The Operations of the Digital Computer

The insertion of the digital computer did not change the sampled nature of the data, but only the values of the samples. The essence of the advantage of the digital computer is that it can handle the individual samples in a very precise and, if need be, involved fashion. The computer operates on the input sequence, $i^*(t)$, in a very definite manner to obtain the output sequence, $o^*(t)$. The relation between the two sequences is the transfer characteristic of the computer, whose operation is determined by a set of instructions placed in its storage. This set of instructions is called the program of the digital computer. A linear computer program may be characterized by a transfer function, and a striking similarity can be noted between the design of programs and the design of networks.

Consider the example of Fig. 4. The task of the computer is to differentiate its input. Recall that one definition of differentiation is

$$\frac{d}{dt} i(t) = \lim_{T \to 0} \frac{i(t) - i(t - T)}{T}; \tag{3}$$

but since the digital computer operates on sampled data, it cannot obtain a derivative in the strictest sense of the

word. The sampling period, T, must remain finite or else we do not have a sampled-data system. The digital computer can perform the operations indicated on the right side of (3) without going to the limit. If so, the output of the computer is related to its input by

$$o^*(t) = \frac{i^*(t) - i^*(t - T)}{T}, \tag{4}$$

where $i(t)$ of (3) is replaced by $i^*(t)$ since at the sampling instants the area under $i^*(t)$ equals the ordinate of $i(t)$.

Equation (4) is analogous to a linear difference equation, which would normally be written in the following notation:

$$o_j = \frac{i_j - i_{j-1}}{\Delta t}. \tag{5}$$

The samples indicated in (5) are replaced by impulses of the same areas in (4) according to the equivalent circuit already discussed. If the impulsed functions $o^*(t)$ and $i^*(t)$ have the Laplace transforms $O^*(s)$ and $I^*(s)$ respectively, the transform of (4) becomes

$$O^*(s) = \frac{I^*(s) - I^*(s)e^{-sT}}{T} \tag{6}$$

where e^{-sT} corresponds to a delay operator. By definition, the transfer function, $W^*(s)$, of the computer program is the ratio of the output transform over the input transform. Thus, from (6)

$$W^*(s) = \frac{O^*(s)}{I^*(s)} = \frac{1 - e^{-sT}}{T}. \tag{7}$$

It is interesting to inquire about the accuracy of this approximate differentiation formula by comparing it with the exact derivative operator,

$$W(s) = s. \tag{8}$$

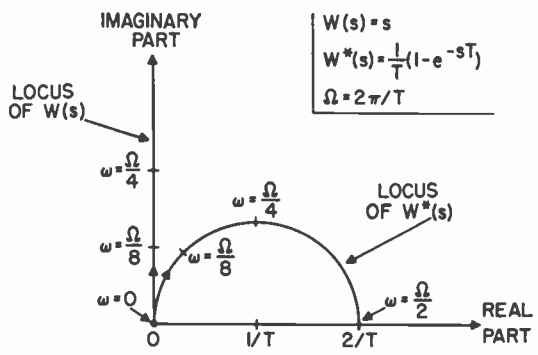

Fig. 5—Comparison of the loci of differentiation and first-difference formula.

The loci of both $W(s)$ and $W^*(s)$ are shown in Fig. 5, which confirms at a glance some well-known facts. The locus of $W(s)$ is the $j\omega$ axis itself, while the locus of $W^*(s)$ is the polar plot of $(1/T)(1-e^{-j\omega T})$, which is just a clockwise circle, as indicated in the figure for the range $\omega = O$ to $\omega = \pi/T = \Omega/2$. It is seen in Fig. 5 that as long as the frequency of the signal, $i(t)$, is low in comparison with the sampling frequency, the numerical formula is a good approximation to exact differentiation. For a zero frequency—that is, for a constant function—the divided-difference formula coincides with the precise derivative, as it should indeed. At any other frequency the computer program falls short of perfection in both amplitude and phase, but at any rate its effect can be precisely analyzed in the frequency domain. For instance, if the spectrum of the input is known, the root-mean-square error of the program can be determined.

It is illuminating to inquire how the limiting process indicated in (3) converts the locus of $W^*(s)$ into that of $W(s)$. Since both the center and the radius of the circular $W^*(s)$-locus of Fig. 5 go to infinity as $1/T$ when T approaches zero, it is seen that the circle goes into a straight line coinciding with the imaginary axis. Similarly, from (7) it follows that

$$\begin{aligned} \lim_{T\to 0} W^*(s) &= \lim_{T\to 0} \frac{1 - 1 + sT - 1/2(sT)^2 + \cdots}{T} \\ &= \lim_{T\to 0} \left(s - \frac{T}{2} s^2 + \cdots \right) \\ &= s = W(s), \end{aligned} \tag{9}$$

as required.

Figs. 4(c) and 4(d) illustrate the effect of the computer program. For instance, in the time-domain illustration the output-sample area at $4T$, $o^*(4T) = -0.4/T$, is obtained according to (4) as $(1/T)[i^*(4T) - i^*(3T)] = (1/T)(1.0 - 1.4) = -0.4/T$. In the frequency domain something like a differentiation is indicated as the output amplitude is obtained from the input amplitude by multiplication by $|W^*(j\omega)|$. Note that the computer program has identical effect on both the pure signal and on all the complementary signals. This is so because the program transfer function, $W^*(s)$, has the same periodicity, $j\Omega$, as the input transform, $I^*(s)$. The periodicity of $I^*(s)$ is manifested in (2), while that of $W^*(s)$ follows from (7) because

$$e^{-(s+jn\Omega)T} = e^{-jn\Omega T} e^{-sT} = e^{-sT} \tag{10}$$

recalling that $\Omega T = 2\pi$. We could have predicted this result from our knowledge that the output of the digital computer is just as sampled as its input and, therefore, must also have a periodic transform. But, if both $O^*(s)$ and $I^*(s)$ are periodic, and if

$$O^*(s) = W^*(s)I^*(s), \tag{11}$$

then $W^*(s)$ must turn out to be periodic, as it did.

VI. Recapitulation

It seems worth the while to summarize the highlights of our discussion before proceeding further. For the specific example chosen, we have described the equivalent circuit of Fig. 3 in the frequency domain. We have demonstrated that both the digital computer and the

desampling unit can be characterized by transfer functions in the linear case, and that the sampling unit acts like a modulator. The following two equations serve to connect the transforms of the input and output of the whole circuit:

$$I^*(s) = \frac{1}{T} \sum_{k=-\infty}^{\infty} I(s + jk\Omega) \tag{2}$$

and

$$O(s) = H(s)W^*(s)I^*(s) \tag{12}$$

where $H(s)$ is the transform function of the desampler, which is some kind of a low-pass filter. We have used an asterisk to indicate a periodicity of $j\Omega$ in a function of s.

As far as this simple example is concerned the picture is complete. If the circuit (or setup) of this example is placed in the closed loop of Fig. 1, the analysis of the complete system can be conducted along the lines indicated in Reference 1. The insertion of the digital computer poses no new problem of a basic nature because the computer is described by a transfer function just as a conventional analog unit is. It is true that the transfer function of the computer program obtained in (7) is not a rational function of s as it would be for linear-analog filters; nevertheless, $W^*(s)$ is a function of s and has a specific amplitude and phase at any real frequency $s = j\omega$. Its analysis is, therefore, straightforward.

What remains is to generalize the result of the example in regard to the digital computer. A systematic treatment of this generalization is left to an ensuing article, as already noted, but a heuristic illustration is recapitulated below because it might be of interest to the reader.

VII. Illustrative Design of Computer Program

Suppose that the approximation to the first derivative in the above example is not sufficiently good. How could we obtain a more satisfactory computer program? Of course, numerical analysis has produced swarms of differentiation formulae, and one could analyze these in the frequency domain until a satisfactory one is found. But let us rather attempt an approximation directly in the frequency domain based upon our scant knowledge acquired in the above example.

The geometric constructions of Fig. 6 illustrate our design procedure. In Fig. 6(a) the angle α represents the phase of the differentiation formula, $W^*(s)$, used in the above example at a particular frequency ω_1. This phase falls short of the ideal one, which is $\pi/2$, or 90° at all frequencies. If we could somehow find a transfer function having a phase $(\pi/2) - \alpha$, the multiplication of two transfer functions would produce one which has the desired phase. From plane geometry it is known that the a triangle inscribed in a circle and having one side along a diameter is a right triangle. It follows, therefore, that β of Fig. 6(a) is equal to $(\pi/2) - \alpha$.

Figure 6(b) shows the locus of

$$W_1^*(s) = k(1 + e^{+sT}) \tag{13}$$

which does have the phase β. Thus, $W^*(s)W_1^*(s)$ would have a phase of $(\pi/2)$ at all frequencies of interest. It can be shown,[2] however, that the resulting computer program could not be realized, for in calculating a present output it would make reference to future values of input data, inadmissible in a real-time application.

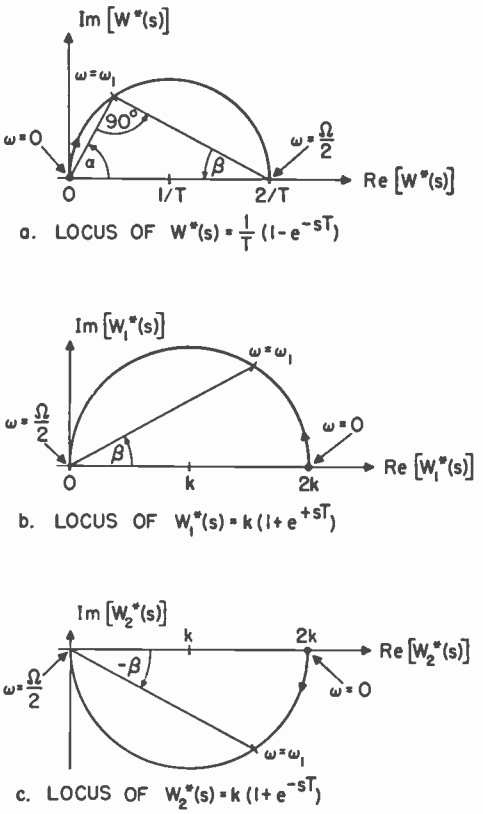

Fig. 6—Steps in obtaining ideal-phase derivative program.

The unrealizability of $W_1^*(s)$ is tied up with the positiveness of the exponent in e^{+sT}, the latter corresponding to a time-advance operator. However, if one attempts to use

$$W_2^*(s) = k(1 + e^{-sT}) \tag{14}$$

the resulting locus has the phase $-\beta$, rather than $+\beta$, as can be readily seen in Fig. 6(c). In order to obtain an over-all phase of $(\pi/2) = \alpha + \beta$, one now has to divide, not multiply, $W^*(s)$ by $W_2^*(s)$. This leads to

$$W_3^*(s) = \frac{W^*(s)}{W_2^*(s)} = \frac{2}{T} \cdot \frac{1 - e^{-sT}}{1 + e^{-sT}} \tag{15}$$

after k of (14) has been replaced by 1/2 to make $W_3^*(s)$ go to s as T approaches zero.

It is not difficult to verify that $W_3^*(s)$ has the ideal phase. By replacing s by $j\omega$, one obtains

[2] J. M. Salzer, "Treatment of Digital Control Systems and Numerical Processes in the Frequency Domain," thesis for Sc.D. degree, Massachusetts Institute of Technology, p. 148; 1951.

$$W_3^*(j\omega) = j\omega \cdot \left[\frac{\tan(\omega T/2)}{(\omega T/2)}\right] \tag{16}$$

which differs from the ideal derivative

$$W(j\omega) = j\omega \tag{17}$$

only by the factor shown in brackets in (16). This factor introduces an amplitude error, without affecting the phase.

It is not our purpose here to examine the suitability of the newly-gotten differentiator. Rather, we return to (15) and ask ourselves if and how the transfer function $W_3^*(s)$ could be realized as a digital-computer program. Noting that by definition $W_3^*(s) = O^*(s)/I^*(s)$, we derive by simple cross-multiplication

$$(1 + e^{-sT})O^*(s) = \frac{2}{T}(1 - e^{-sT})I^*(s) \tag{18}$$

and then by rearrangement

$$O^*(s) = \frac{2}{T}[I^*(s) - I^*(s)e^{-sT}] - O^*(s)e^{-sT}. \tag{19}$$

The inverse transform of the last equation yields

$$o^*(t) = \frac{2}{T}[i^*(t) - i^*(t - T)] - o^*(t - T) \tag{20}$$

which is a linear difference equation. It is realizable by a real-time program because the present output is computed by means of only present and past, but not future, samples of the input and output.

It turns out that a linear real-time program, which corresponds to a difference equation of the form of (20), always has a transfer function which is rational in e^{-sT}. This contrasts with analog filters whose transfer functions are rational in s. There is then an interesting parallel between digital and analog filter, or stated more rigorously, between sampled-data and continuous-data filters. The difference between the two types of filters is notable and poses new problems in dealing with digital filters.

One method of attack is by introducing a new complex variable $z = e^{-sT}$ and performing the analysis and synthesis in terms of z. One can translate the design requirements stated in terms of s, the complex frequency variable, into terms of z and vice-versa. If the digital filter is not inserted into an analog system, one can stay entirely in the z-plane (so to say) without any reference to the s-plane. This approach has been used in the past in the calculus of finite differences, both in the manner of operational calculus and also in the manner of complex-variable calculus.

If the digital filter is to be a part in an otherwise analog system, it is necessary to find a variable common to both the digital and the analog parts. Such variables are t (time) and s (complex frequency).[3] In the present paper the s-domain was chosen and illustrated for reasons stated earlier. What remains is to further develop the methods of analysis and synthesis of digital filters in terms of the frequency variable. It turns out that numerous results of network theory and various methods of servomechanism design can be applied or extended to the treatment of digital filters. Such terms, as the amplitude and phase characteristics, stability criteria and error spectra, the loci and logarithmic plots, the impulse responses and so on, of computer programs can all be given useful substance and meaning once the transfer function of a realizable digital program has been defined. But these topics will be the subject of a later article.

VIII. Acknowledgment

The authors are grateful for the co-operation and interest shown by the Digital Computer Laboratory of Massachusetts Institute of Technology, under whose auspices most of this work was done.

[3] Actually, z has also been used[4] as a common variable by assuming that the continuous-data portion also operates on sampled data. This is an approximation justifiable only if the signal bandwidth is much smaller than $\Omega/2$, half the sampling frequency.

[4] W. Hurewicz, "Filters and servo systems with pulsed data," Chapter 5, James, Nichols, and Phillips, "Theory of Servomechanisms," Radiation Lab. Series, Vol. 25, McGraw-Hill Book Co., Inc., New York, N. Y.; 1947.

Analog Computer for the Roots of Algebraic Equations*

LARS LÖFGREN†, MEMBER, IRE

Summary—An electronic analog machine for computing the roots of algebraic equations of degrees through the eighth is described. The coefficients of the equation may be complex. The roots are indicated as points in the complex number plane light points on the screen of a cathode-ray tube. Once per second the roots are displayed, and when some of the coefficients are varied the corresponding curves described by the roots are made visible by the persistence of light emission from the screen.

An accurate determination of the roots is obtained by means of a comparison-root which can be moved all over the number plane and thus be brought to coincide with a root. The comparison-root is displayed by a scanning system, which also controls the positions of the roots, and so it is possible to obtain an accurate reading not influenced by distortion in the cathode-ray tube.

By means of a normalizing device, the voltage level in the machine is kept high throughout the computation, and so all the roots are determined with about the same percental accuracy. The modulus of an error will normally be of the magnitude of 1 per cent of the corresponding root-modulus.

Introduction

NUMERICAL PROBLEMS derived from branches of applied science can often be reduced to computing the roots of a high-degree algebraic equation. Such an equation of degree n can be written as

$$\sum_{\nu=0}^{n} A_\nu z^\nu = 0. \tag{1}$$

Equation (1) implicitly defines the n-valued function

$$z = f(A_0, A_1, \cdots, A_n). \tag{2}$$

The key problem is to find this function f of the coefficients A_ν. In general, the function f can be written explicitly by means of known transcendental functions.[1] These solutions, however, are not very suitable for numerical determination of the roots. It is easier to reach a solution by employing numerical methods.[1]

Sometimes, however, these methods turn out to be too laborious, especially when investigating how the roots change with variation of one or several coefficients A_ν. Investigations of this type are sometimes required, for instance, in certain linear stability problems within servo technique. In the complex number plane, the positions of the roots of the characteristic equation of the problem determine the extent of stability.

With special regard to such stability problems, an analog computer for determination of the roots of high-degree equations has been developed and built at the Radio Department of the Swedish Research Institute of National Defense.[1]

Such stability problems can, of course, also be treated on a differential analyzer. However, the solution of the corresponding algebraic equation gives information on the stability in a form which is more suitable for further numerical treatment. Also, in stabilizing originally strongly unstable systems, the equation solver proves advantageous.

Many different types of equation solvers have been planned, but the underlying principles of all these types of computers can be shown to belong to one of three fundamental groups, according to a classification made by Murray.[2] These groups are based on

1. The principle of similitude,
2. Direct calculation,
3. Adjusters.

A survey of the history of equation solvers up to 1945 is given by Frame,[3] where examples of Principle No. 1, and especially of Principle No. 3, are to be found. The most typical example of the last principle is the isograph which has been described by Dietzold.[4] Among the equation solvers developed during the last few years the computers described by Borselino,[5] by Calvert, Johnston and Singer,[6] and by Marshall[7] are to be mentioned. All these computers operate in accordance with Principle No. 3, which seems to be especially suited for high-degree equation solvers, as it is rather easy to simulate each term in the left member of (1) with z as the independent variable. Then the function f can be obtained by inverting the left member of (1) either by hand, i.e. to adjust z until (1) is satisfied, or by an auxiliary calculating system according to Principle No. 3. This inversion of the left member in (1) is difficult, however, as f in (2) is a many-valued function.

The Root Selection Method

In the computer described below, a selecting method is used for obtaining the roots. This selecting method for the solution of equations in general can be formulated as follows:

* Decimal classification: 621.375.2. Original manuscript received by the Institute, May 23, 1952; revised manuscript received January 22, 1953.

† Research engineer, Swedish Research Institute of National Defense, Stockholm, Sweden.

[1] Löfgren, L., "Apparat, lösande algebraiska ekvationer," Ind.-Tg. Norden, vol. 76, p. 231; 1948 (in Swedish).

[2] Murray, F. J., "The Theory of Mathematical Machines," King's Crown Press, New York; 1948.

[3] Frame, J. S., "Machines for solving algebraic equations," Mathematical Tables and Other Aids to Computation, I, p. 337; 1945.

[4] Dietzold, R., "The isograph, a mechanical root finder," *Bell Labs. Record;* 1932.

[5] Borselino, A., "Un metodo elettrico par la determinazione approssimata delle radici reali o complesse di una equazione algebraica," *Il Nuovo Cimento*, p. 23; February, 1948.

[6] Calvert, Johnston, Singer, "Root-solver for tenth degree algebraic equations," *Proc. N.E.C.* (Chicago), p. 254; 1948.

[7] Marshall, B. O., Jr., "The electronic isograph for roots of polynomials," *Jour. Appl. Phys.*, p. 307; April, 1950.

Quantities corresponding to the roots to be found are varied automatically and periodically within a certain space. In an analog part, a function of the varying quantities is built up. In a selector controlled from the analog part, restrictions on the function are set up in a way sufficient for defining the desired roots. The selector then picks out those values of the varying quantities which meet with the restrictions. These values, the roots, are stored in a memory, with a storing time not shorter than the repetition period of the varying quantities.

As it is possible, in such a selector machine, to make the repetition period shorter than the reaction time of a human operator, the selector will give immediate solutions of problems, which is of special value when treating many-valued functions. The selection principle as applied to algebraic equation solving is illustrated in Fig. 1. There are here two varying quantities (r and ϕ).

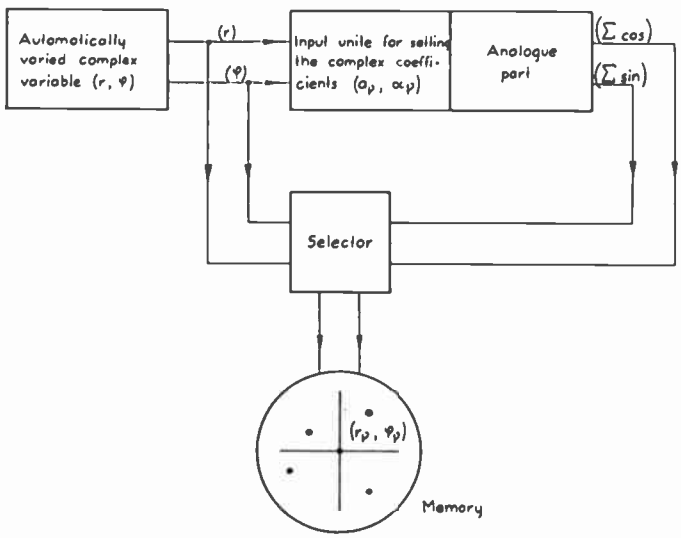

Fig. 1—Block diagram showing the principle of the equation solver. The input coefficients, in polar co-ordinates (a_ν, α_ν), are manually set on potentiometers and the solution (r_ν, ϕ_ν) is indicated and stored as points in the complex number plane (light points on the screen of a cathode-ray tube).

This permits a rather simple design of the memory device. The memory consists of a cathode-ray tube with a persistent screen, on which the two quantities are represented by the position of a point.

Outlines of the Computer

We start from (1), where z and A_ν, which may both be complex, are written in polar co-ordinates:

$$z = re^{i\phi}, \qquad A_\nu = a_\nu e^{i\alpha_\nu}.$$

Equation (1) is thereby transformed into the equation system

$$\left.\begin{aligned}(u\equiv)\sum_{\nu=0}^{n} a_\nu r^\nu \cos(\nu\phi + \alpha_\nu) &= 0\\ (v\equiv)\sum_{\nu=0}^{n} a_\nu r^\nu \sin(\nu\phi + \alpha_\nu) &= 0\end{aligned}\right\}, \qquad (3)$$

where r and ϕ are the varying quantities. The range of variation is at first chosen as the area between two bounding circles of radii 1 and $\frac{1}{2}$. The varying quantity ϕ, which is made directly proportional to time, is varied 1,000 times faster than r, which is varied with a period of 1 second. The point representing the quantity z therefore describes a tight spiral in the complex number plane. The tolerances of the selector circuit can thus be made sufficiently small to ensure good accuracy without the z-variation being incomplete. The time-dependence of r over its period is exponential: $r = e^{-kt}$.

The fundamentals of the analog part will now be described with reference to Fig. 2. Each term in (3) contains two characteristic functions of the varying quantities ϕ and r, a circular function and a power function. These terms are simulated as sinusoidal alternating voltages which are amplitude-modulated in accordance with the power functions.

The pure alternating voltages are obtained by filtering square waves of multiple frequencies $\nu\omega$, ($\phi = \omega t$). The eight multiple frequencies are generated in a frequency-divider chain. In this chain the division continues down to $\omega/1024$, which is the repetition frequency of the varying quantity r.

The eight multiple frequencies are fed to eight "term channels." The first stage of the νth term channel is a modulator, Mod$_\nu$, which amplitude-modulates the incoming square-wave $Sq(\nu\omega t)$ with the power function $r^\nu = e^{-k\nu t}$. These power functions are generated as voltages over RC circuits (parallel circuits) with time-constants: $1/k\nu$ respectively. Each circuit is charged once every second via an electronic switch to a voltage proportional to the modulus a_ν of the coefficient. This modulus is set in a normalizing device. The square-wave $Sq(\nu\omega t)$ is modulated with the voltage $a_\nu r^\nu$ in a second electronic switch, which connects $a_\nu r^\nu$ to the output of Mod$_\nu$ during the positive halves of $Sq(\nu\omega t)$. During the negative halves, the output is switched to zero. Thus the voltage $a_\nu r^\nu Sq(\nu\omega t)$ is generated in Mod$_\nu$.

The next stage in the term channel is a unit in which the argument α_ν of the coefficient is set. This unit operates only on the fundamental of the incoming square-wave. The harmonics are by-passed in the filter circuit terminating each channel. At the output, the voltage $a_\nu r^\nu \cos(\nu\omega t + \alpha_\nu)$ is obtained. The output voltages of the term channels are summed in two adders. One of these is a conventional adder,[2] i.e. an amplifier with feed-back through resistors; the other is an amplifier with feed-back through a capacitor and resistors to the inputs. The second adder thus produces the necessary phase-shift to convert the cosine-sum into a sine-sum. The remaining terms in the sums forming the left members of equation system (3), the two constants $a_0 \cos \alpha_0$ and $a_0 \sin \alpha_0$, are added separately.

The two sums are finally fed to the selector, which picks out those values of r and ϕ which make the sums equal zero at the same time. Basically, the selector consists of two zero-indicators, a gate, and a cathode-ray

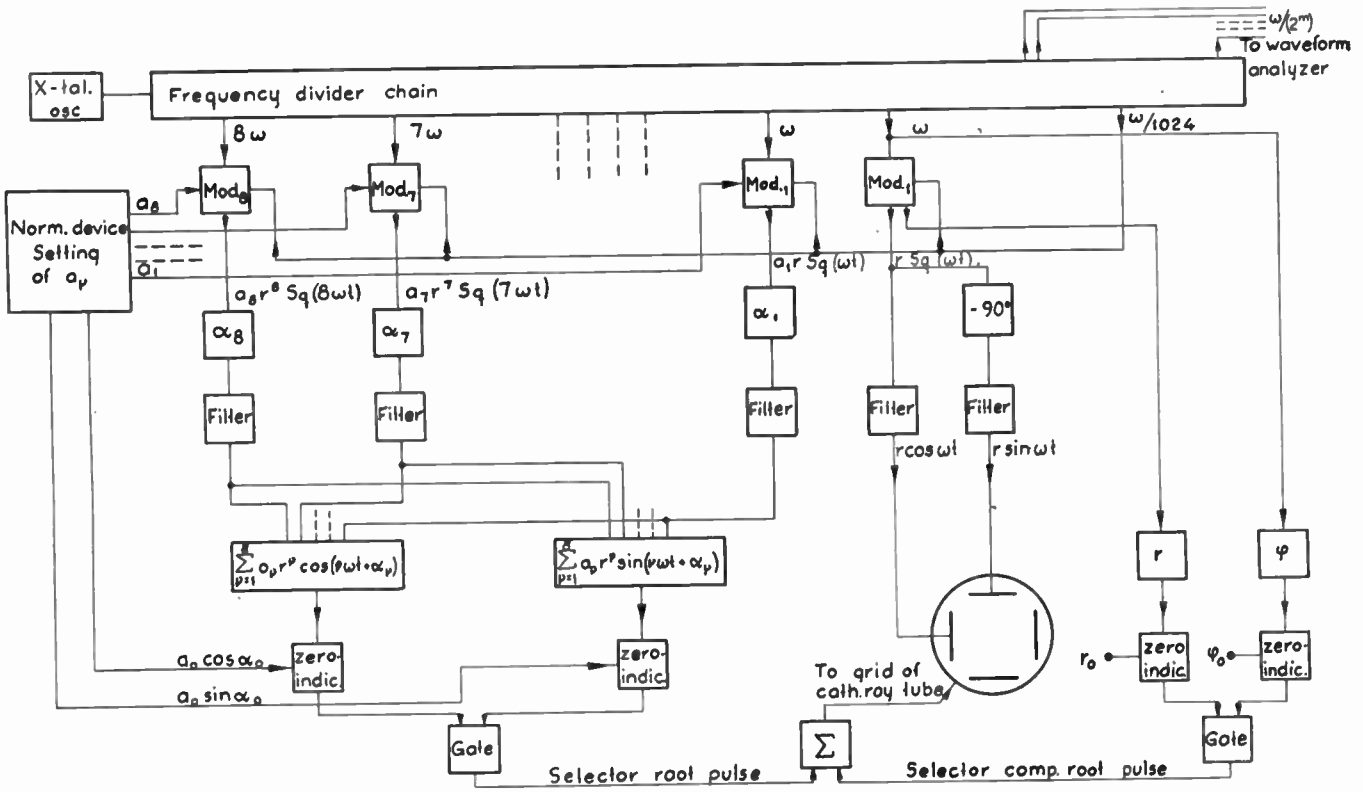

Fig. 2—Block diagram of the equation solver.

tube. Each zero-indicator generates a pulse when the corresponding sum is zero, and those pulses which appear simultaneously are selected by the gate. The output of this gate, the selector pulse, is fed to the intensity grid of the cathode-ray tube. The beam of the tube is normally suppressed, but is released when the selector-pulse appears at the grid. The varying quantities r and ϕ, transformed to the corresponding rectangular Cartesian co-ordinates $r\cos\phi$ and $r\sin\phi$, are applied to the deflection plates of the cathode-ray tube. Thus a visible spot on the screen, which represents the complex number plane, will always occupy a position corresponding to a z-value satisfying (1).

The co-ordinate voltages $r\cos\omega t$ and $r\sin\omega t$ are generated, as shown in Fig. 2, in a separate channel from which the modulated square-wave $rSq(\omega t)$ as well as the modulating voltage r are taken. From the square-wave, $r\cos\omega t$ and $r\sin\omega t$ are filtered out, the latter being obtained from the former by addition of the argument -90 degrees.

The modulating voltage r is also used in a comparison-root circuit (to the right in Fig. 2). This circuit generates a comparison root, which by means of two manually operated potentiometers can be moved over the number plane. The potentiometer dials are graduated in modulus and argument respectively. The comparison-root circuit consists mainly of two zero-indicators generating pulses when r and ϕ assume the arbitrarily chosen values r_0 and ϕ_0, which are set on the potentiometers. The pulses are then gated, yielding a selecting comparison-root-pulse which is applied to the intensity grid of the cathode-ray tube together with the selecting root-pulses. In this way, an accurate graduation is obtained of the whole number plane, notwithstanding distortion in the cathode-ray tube, since the comparison-root as well as roots to (1) are displayed by the same scanning system.

Selector

When using the selecting principle for inversion of polynomials, the selector has to be constructed with special care in order to obtain good accuracy. (In the following, the notations u and v will be used for the left members of the equation system (3).)

Behavior of the voltages u and v in the vicinity of a root

The left member of (1) can be written

$$w = u + iv = \prod_{\mu} (z - z_\mu)^{m_\mu}, \tag{4}$$

where z_μ are the roots and m_μ their multiplicity. Considering the manner in which z is varied, we can put $z = r_\mu e^{i\varphi}$, and study w, when $\phi = \phi_\mu + \epsilon$ is in the vicinity of ϕ_μ, i.e., when ϵ is small. It is now sufficient to study the factor $(z - z_\mu)^{m_\mu}$ in (4). The other factors in the product can be regarded as constants and will be written K. Thus

$$\begin{aligned} w(\epsilon) &= K {r_\mu}^{m_\mu} e^{i m_\mu \phi_\mu} (e^{i\epsilon} - 1)^{m_\mu} \\ &= K {r_\mu}^{m_\mu} e^{i m_\mu \phi_\mu} (i)^{m_\mu} \left(\epsilon^{m_\mu} + \frac{m_\mu}{2} i \epsilon^{m_\mu + 1} \right), \\ &= u(\epsilon) + iv(\epsilon). \end{aligned}$$

In considering a real root of multiplicity 1, and assuming real coefficients in (1) we get

$$u(\epsilon) = -K r_\mu \tfrac{1}{2}\epsilon^2,$$
$$v(\epsilon) = K r_\mu \epsilon,$$

where K is real. Thus the zero-passage of u will be slow, as $u(\epsilon)$ is a parabola in the vicinity of zero. $v(\epsilon)$ on the other hand is a straight line.

It is now clear that the conventional method of generating a pulse when a sweeping voltage passes a certain voltage level, i.e. by amplification around the level and subsequent derivation, is quite inappropriate. With such a method, the real roots cannot be indicated as the derivative of u is zero. This has also been verified experimentally.

If, however, the w-plane is treated as a static correspondence to the z-plane, there are possibilities of treating the problem as follows.

Structure of the zero range

The problem is to indicate when the polynomial w has a value within a small range containing the origin, the zero range.

There seems to be several ways of defining such a zero range with practical interpretations. The following have been analyzed and tried experimentally:

(a) $u^2+v^2 \leqq \delta$: the zero range is determined by a circle around the origin of the complex plane.

(b) $|u|+|v| \leqq \delta$: the zero range is a square (diamond) with its corners on the real and imaginary axes.

(c) $|u|_{(|v|\leqq\delta)} \leqq \delta$: the zero range is a square with its sides parallel to the axes. (Fig. 3(a)).

In these expressions, δ is a small quantity, determining the magnitude of the range.

In alternatives (a) and (b), the idea is to produce one voltage which contains u and v in such a way that the zero-value of this voltage cannot be obtained unless the voltage u as well as v is zero.

In alternative (c), which has been chosen as the most suitable one for the computer, the restriction that u and v have to be small at the same time has been more properly considered. The principle implies two identical zero indicators and a gate (Fig. 1).

The zero indicators correspond to the primary conditions $|u| \leqq \delta$ and $|v| \leqq \delta$ (Fig. 4). Each zero indicator produces a pulse of the same duration as the time during which the corresponding sine or cosine sum voltage lies within a strip limited by two narrow levels on each side of the zero level, at distances $\pm\delta$ from this level.

Fig. 3(a) shows that condition (c) is satisfied within a small square of side 2δ and which the origin at its center. With this square in the u, v-plane correspond certain areas, the root-"points," in the z-plane. These areas may have different shapes, depending on multiplicity of roots. These root-"points" can be studied from (4).

In case of a root of multiplicity 1, there is a conformal mapping of the u, v-square on a square in the z-plane (Fig. 3(b)). Such squares corresponding to simple roots may be rotated, and their scales may be different.

In case of a root z_k of multiplicity 2, the product expression (4) can be written as

$$(z - z_k)^2 = w \frac{1}{\Pi'}.$$

In the immediate vicinity of the root z_k, the remaining product Π' can be regarded as a constant. The transformation of the w-plane into the z-plane is now two-valued in the vicinity of the root. Thus the w-square is transformed into an octagon limited by hyperbolic segments (Fig. 3 (b)).

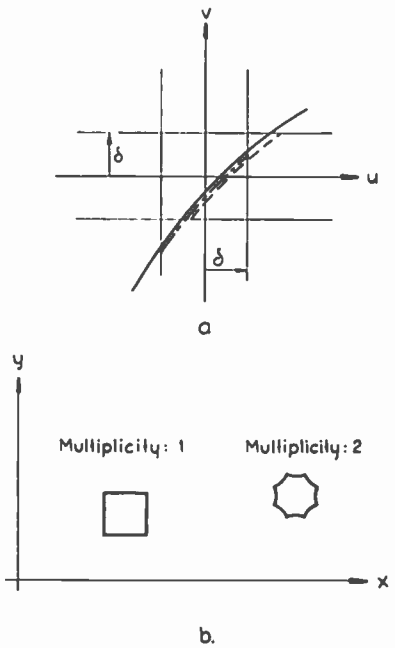

Fig. 3—(a) Scaled up zero-range in the w-plane. At the indicated zero-passage of the voltages (u, v), the pulse from the u-zero-indicator will appear in the —·—·—·— marked part and the pulse from the v-zero-indicator in the — — — — — marked part. Thus the gated selector pulse can only appear when (u, v) lies within the zero-range square with the side 2δ and the origin at its center. (b) Scaled up root-"points" in z-plane. "Point"-structure is shown for roots of multiplicity 1 and 2 respectively.

In the general case of multiplicity m, the root-"point" is limited by a contour having 4 m right angles.

So, the only possible place where a certain root-"point" can appear lies within a small area with approximately the same small dimension in all directions.

Zero-indicator

The principle of operation of the zero-indicator is shown in Fig. 4. It consists of two regenerative comparators with a small difference 2δ between their turnover levels, and of a switching circuit.

As comparators, use is made of cathode-coupled bistable multivibrators with compensation for the hysteresis-effect.[8] This compensation is achieved through the incorporation of a negative feed-back connection through a tube which acts as a delaying device. Each comparator delivers two output voltages which are complementary to each other, e_1 and e_1', e_2 and e_2', respectively.

[8] Löfgren, L., Swedish patent application No. 6147/51 of July 19, 1951; device for a bistable multivibrator.

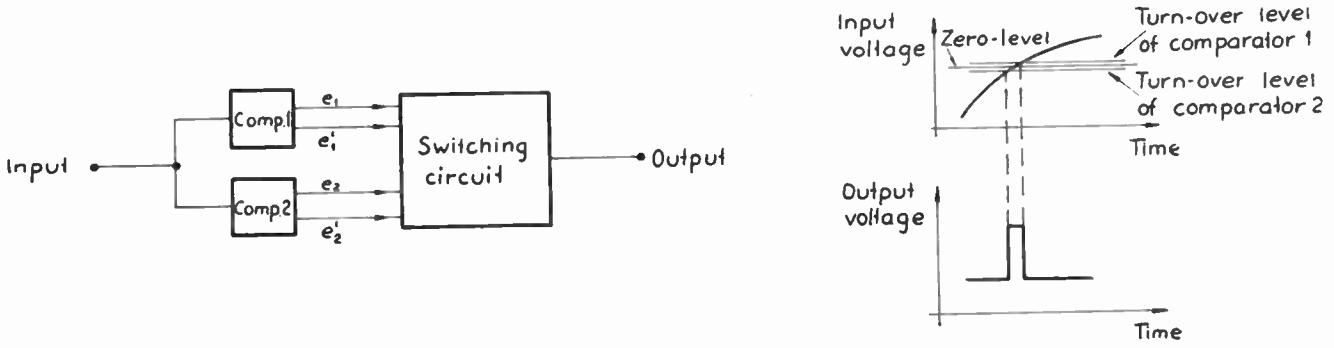

Fig. 4—Principle of zero-indicator.

The design of the switching circuit will now be discussed according to the theory of switching functions.[9] The switching circuit is to realize a switching function $f(e_1, e_2)$ of the two variables e_1 and e_2 from the comparators. e_1 and e_2 are themselves switching functions, i.e., the corresponding voltages have only two stable states: high, H, and low, L. There are four possible combinations of e_1 and e_2: H, H; H, L; L, H; and L, L. According to the above, it is desired that $f(e_1, e_2)$ shall be low (Fig. 4) when the input voltage to the zero indicator is entirely on one side of the indicating strip, i.e., when e_1, e_2 is H, H or L, L. Furthermore $f(e_1, e_2)$ shall be high when the input voltage lies within this strip, i.e., when e_1, e_2 is H, L or L, H. The following three switching functions thus meet these requirements:

e_1	e_2	f_1	f_2	f_3
H	H	L	L	L
H	L	H	L	H
L	H	L	H	H
L	L	L	L	L

Substituting 1 and 0 as H and L respectively, we get the normalized forms of the three functions

$$f_1 = e_1e_2', \qquad (e' = 1 - e)$$
$$f_2 = e_1'e_2,$$
$$f_3 = e_1'e_2 + e_1e_2'.$$

The switching function of a single triode and pentode is evidently $T(e_1) = 1 - e_1 = e_1'$ for the triode, and $P(e_1, e_2) = 1 - e_1e_2$ for the pentode, where e_1 and e_2 are applied to the control and suppressor grids, respectively. Combining two or more switching tubes in such a way that they share a common plate resistor yields a circuit with a switching function that is the product of the single tube functions.

From this the realization of f_1 and f_2 will be evident. They are both realized as two triodes sharing a common plate resistor. The inputs are then e_1', e_2 and e_1, e_2' respectively.

When realizing the function f_3, we transform it into a product. By ordinary rules of computation we obtain

$$f_3 = e_1'e_2 + e_1e_2' = 1 - e_1'e_2' - e_1e_2.$$

To this expression can be added the quantity $e_1'e_2'e_1e_2$, which is always zero. Thus

$$f_3 = 1 - e_1'e_2' - e_1e_2 + e_1'e_2'e_1e_2$$
$$= (1 - e_1'e_2')(1 - e_1e_2),$$

where each parenthesis represents a pentode function. Consequently f_3 can be realized as two pentodes sharing a common plate resistor.

The switching circuit that realizes f_3 has been chosen for the computer because this switching circuit is more convenient for a variation of the small difference 2δ between the turn-over levels of the two comparators.

Gate

The gate in which the two positive zero-indicator pulses produce a negative selector-root pulse is a single pentode. The sign of the selector-root pulse is changed in a summing amplifier which adds the comparison-root pulse. Thus the selector pulse is positive at the grid of the cathode-ray tube, and the corresponding values (r_ν, ϕ_ν) are picked out.

Normalization of the Equation

Prenormalization

The numerical quantities, which correspond to electric voltages in the computer, cannot be unlimited. Thus the roots and the coefficients of the equation have to be normalized, and the number 1 is chosen as an upper limit for their modulus.

For normalization of the quantity r, an upper limit for the modulus of the roots is needed. Such upper limits can for instance be obtained in the following manner:[1]

Equation (1) can be written as

$$w(z) \equiv z^n + A_{n-1}z^{n-1} + \cdots + A_0 = 0.$$

Let $|A_\nu|_{\max}$ be the highest modulus. Then

$$\left|\frac{w(z)}{z^n}\right| > 1 - |A_\nu|_{\max}[|z|^{-1} + |z|^{-2} + \cdots + |z|^{-n}]$$
$$= 1 - |A_\nu|_{\max} \cdot \frac{1 - |z|^{-n}}{|z| - 1}.$$

[9] "Synthesis of electronic computing and control circuits," The Staff of Computation Laboratory, Harvard University Press, Cambridge, Mass.; 1951.

If it is possible to find a value of $|z|$ which makes the right member positive, this member will be positive for all larger $|z|$-values. Thus this value has to be an upper limit for the modulus of the roots. In particular, the value

$$1 + |A_\nu|_{\max}, \tag{5}$$

which meets this condition, is an upper limit.

Very often an upper limit smaller than (5) can be found, if this formula is not applied to z itself, but to $z=\mu u$, where μ is a real constant, and u is a new variable, the upper limit of which is to be found. With this substitution, the equation becomes

$$u^n + \frac{A_{n-1}}{\mu} u^{n-1} + \cdots + \frac{A_0}{\mu^n} = 0,$$

where μ is chosen to be $\mu = \sqrt[\nu]{|A_{n-\nu}|}$ and ν is the value that gives the greatest μ. Thus none of the moduli of the coefficients of the above equation is greater than 1, and hence an upper limit of $|u|$ is 2. This corresponds to

$$2[\sqrt[\nu]{|A_{n-\nu}|}]_{\max} \tag{6}$$

as an upper limit of $|z|$.

In normalizing, the first thing to do, before the equations are set on the input table of the computer, is to choose the lower of the two limits (5) and (6). We denote this limit by M. We then substitute Mu for z and, if necessary, all the coefficients of the equation are divided by a common factor so that their moduli do not exceed 1.

Renormalization

When simulating the different terms of equation system (3) in the machine, each term is affected with a certain error of about 0.1 per cent of the maximum term value 1. To ensure high accuracy in determining the roots, it will thus be necessary to make the "term level" as high as possible. This is achieved by keeping the "root level" as well as the "coefficient level" high.

A high root level can be obtained by limiting the range of the variation quantity z. This is performed by introducing a lower bounding circle with the radius $R(<1)$, whereby only the roots with moduli between R and 1 are indicated. The equation is then renormalized by substituting Rz_1 for z. In this way also the roots z_1 are indicated in the high-level interval, R to 1, of the modulus. The renormalization is then repeated by substituting Rz_2 for z_1, and so forth. Thus the complete variation range of the roots of an equation is covered and the roots are determined with an accuracy which increases with increasing R. With regard to the highest degree of the equations to be treated in this computer, (eight), and to the magnitude of the term errors (0.1 per cent of unity) the value $\frac{1}{2}$ is chosen for R.

A high coefficient level is obtained by multiplying all the coefficients by a common factor 2^{k_s} at the sth step of substitution: $\frac{1}{2}z_s$ for z_{s-1}. This factor 2^{k_s} (k_s an integer) is determined in such a way that the highest coefficient modulus will lie in the high-level interval $\frac{1}{2}$ to 1.

These two operations are performed in a separate normalizing device where, at the sth step of renormalization, the νth coefficient modulus is multiplied by a number $2^{(k_s-\nu)}$.

Normalizing device

The purpose of the normalizing device is to give the renormalized moduli $a_\nu 2^{k-\nu}$, i.e., the device is also used for setting the moduli a_ν. Because of this a modulus is set in the form

$$a = (1 + \alpha)2^{-m},$$

where α is continuously variable within the limits $0<\alpha\leqq 1$, and m is an integer between 1 and 11. Each value of a between 1 and 1/2048 can thus be obtained by means of one, and only one, combination (m, α).

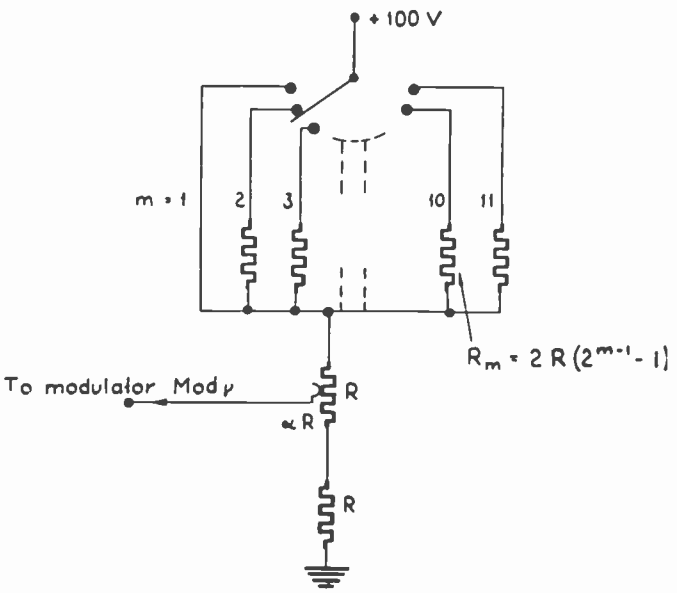

Fig. 5—Normalizing unit. The voltage fraction: $1+\alpha/2^m$ is obtained, where αR is the lower part of the potentiometer resistance R.

In Fig. 5 a normalizing element is shown. The mth position of a switch selects a voltage-divider consisting of three elements connected in series, a resistor R, a linear potentiometer having a total resistance of R, and a resistor of the value $2R(2^{m-1}-1)$. Thus a potentiometer setting α will give a voltage fraction of $(1+\alpha)2^{-m}$ (which is fed to the modulators).

When first setting a coefficient a the corresponding values (α, m) are taken from a table. α is set on the potentiometer and is left unchanged when the equation is renormalized. m is set on the switch. Renormalization is then performed by turning the νth switch ν steps. The step-numbers are marked on the dial of each switch. All the switches are then turned backwards a certain number of steps until one of them reaches the position of highest voltage level, where $m=1$.

The normalization device will ensure a rather good constancy of the percental accuracy of the roots. The normal error is of the magnitude of one per cent of the modulus of the root. However, when the roots are lying very near to each other, as for instance in the case of a root of high multiplicity, the error will be greater. Otherwise, when the roots are well separated, the error will be smaller than the indicated value of one per cent.

Conclusions

The ideas of this computer were first conceived in 1947. With some interruptions, development and design has been going on since 1948. The building of the first machine is now completed; the total number of tubes exceeds 200 slightly. The computer is rather spaciously built, but a more commercially designed computer could probably be made much smaller. In such a design, it will be of value to replace the normalizing switches with relays, whereby a complete renormalization can be performed merely by pressing a button.

In 1950 Glubrecht of Germany published a work on a computer designed for high-degree equations,[10] in which the same principle is used as has been presented previously.[1] His work, however, is based on two German patent applications of 1942 and 1943. Unfortunately, as he has recently informed me, his computer as well as the two patent applications were destroyed during World War II.

[10] H. Glubrecht, "Elektrisches Rechengerät für Gleichungen höheren Grades," *Zeits. für angewandte Phys.*, p. 1; January, 1950

Sketch for an Algebra of Switchable Networks*

JACOB SHEKEL†, ASSOCIATE, IRE

Summary—**A network containing switches is equivalent to a number of networks that differ in the values of their components, in the arrangement of the components, or in both respects. When analyzing or synthesizing such a network, one may treat each different network by itself, and then combine the results. This paper describes a method by which the different aspects of a switchable network may be treated simultaneously.**

The mathematics by which the network is treated is a combination of ordinary field algebra (complex numbers) and Boolean algebra. The mathematical foundation is first laid out, then interpreted in terms of switchable network elements. The paper is concluded with some examples of analysis and synthesis of switchable networks.

PROBLEMS IN NETWORK algebra (analysis and synthesis) are usually patterned as: "Given a certain configuration of network elements, what are its properties?" or, "To realize certain properties (subject to realization conditions), what is the required network configuration?" The numerical values of the network elements are a secondary consideration, that concerns only the final arithmetical stage of the computation. In this sense, network algebra deals with generalizations, treating different numerical values in one expression.

Is it sometimes desirable to go one step further in generalization, and treat networks of different *configurations* simultaneously? The answer depends on the degree of similarity between the different configurations. It is doubted if anyone will build a network that changes, by the flick of a switch, from an FM discriminator to a low-noise IF preamplifier; on the other hand, the change in bandwidth of a band-pass filter is more readily realized by switching one or two elements than by constructing two different filters. Similar considerations apply to the mathematical approach to analysis-synthesis. There is little use in simultaneous treatment of widely differing networks, but it is a waste of effort and time to treat networks separately when they share many features. However, there is no sharp line of demarcation between both categories; the examples cited are rather extreme ones.

This paper describes an algebra that may be applied to switchable networks. The term *switchable network* is used to describe a network that contains switches that are set to definite positions before applying power to the network, but are not switched over during operation. This algebra, therefore, does not treat transients that appear when switches are switched during the operation. A switchable network is equivalent to a number of networks, any one of which may be selected before operation by setting the switches. Each of these networks will be termed an *aspect* of the switchable network. We assume that if a number of networks are constructed as aspects of a switchable network, they deserve to be treated as such in analysis-synthesis processes.

The paper first describes the algebra, which is a combination of the algebra of fields (algebra of complex numbers, to represent the network elements) and Boolean algebra (to represent the switches).[1] To follow the presentation, it is not necessary that the reader be grounded in Boolean algebra, as the necessary rules are mentioned or developed in this paper wherever needed.

* Decimal classification: R143. Original manuscript received by the Institute, October 6, 1952; revised manuscript received February 13, 1953.

† 8 Ben Yehuda St., Haifa, Israel.

[1] Boolean algebra is treated in many textbooks on Higher Algebra, e.g., G. Birkhoff and S. MacLane, "A Survey of Modern Algebra," McMillan; 1941. A concise summary of the algebra, and its application to switching networks may be found in C. E. Shannon, "Synthesis of Two-Terminal Switching Networks," *Bell Sys. Tech. Jour.*, vol. 28, p. 59; January 1949.

In the second part of the paper the algebraic expressions are interpreted as combinations of network elements and switches, and in the third part some examples of analysis and synthesis are presented.

Mathematical Foundation

Qualification

Let A, B, C . . . be elements of an algebraic field (e.g., complex numbers), with the ordinary meaning for the operations of addition and multiplication. Let x, y . . . be elements of a Boolean algebra, with addition defined by

$$0 + 0 = 0; \quad 1 + 0 = 0 + 1 = 1 + 1 = 1, \tag{1}$$

and multiplication by

$$1.1 = 1; \quad 1.0 = 0.1 = 0.0 = 0. \tag{2}$$

A juxtaposition of a Boolean element and a field element, like xA, is defined as a complex number, having two *aspects* depending on x:

$$xA = \begin{cases} A, & \text{when} \quad x = 1 \\ 0, & \text{when} \quad x = 0. \end{cases} \tag{3}$$

The operation of x on A, as defined by (3), will be termed *qualification*[2]; x, the *qualifier*, qualifies A, and xA is a *qualified complex number*. Qualification, in this sense, enables simultaneous treatment of cases where the complex number A is present or absent. The value of the qualifier indicates whether A is "in" or "out."

The qualified numbers are equal if, and only if, the qualifiers and qualificands in both numbers are equal:

$$xA = yB \text{ if, and only if, } x = y \text{ and } A = B. \tag{4}$$

The equality of x to y is to be interpreted, of course, in the sense of Boolean algebra.

From (2) and (3) the following equalities are evident:

$$(xA)B = A(xB) = x(AB) = xAB \tag{5}$$

$$x(yA) = y(xA) = (xy)A = xyA \tag{6}$$

$$(xA)(yB) = (yA)(xB) = (xy)(AB) = xyAB \tag{7}$$

where the last expression in each equation is a short notation for all the other expressions in the same line. Qualification is associative and commutative with Boolean multiplication and complex multiplication.

By direct application of (3)

$$x(A + B) = xA + xB, \tag{8}$$

so that qualification is distributive over complex addition. On the other hand,

$$(x + y)A \neq xA + yA, \tag{9}$$

for, when $x=y=1$,

$$(x + y)A = A,$$

$$xA + yA = A + A = 2A.$$

Qualification is *not* distributive over Boolean addition.

If x and y are mutually exclusive, so that both will not have the value of 1 simultaneously, (9) may be an equality. Such an interdependence may be expressed by the relation $xy=0$, and examples of such mutually exclusive qualifiers are given in (11) and (19).

The Complement

In Boolean algebra, each element x has a complement x',

$$x + x' = 1 \tag{10}$$

$$xx' = 0 \tag{11}$$

so that when either x or x' is 1, the other is 0.

Applying this to qualification,

$$xA + x'A = A. \tag{12}$$

The combination $xA+x'B$ is a qualified number having two nonzero aspects,

$$xA + x'B = \begin{cases} A, & \text{when} \quad x = 1 \\ B, & \text{when} \quad x = 0. \end{cases} \tag{13}$$

Qualified Functions

Any function of complex numbers, in which some or all of the complex numbers are qualified, is a qualified function. The qualifiers are indicated in the functional notation, as in

$$f(x, y; A, B, C) = \frac{xA + y \sin x'B}{BC - \log (y'A - B)}. \tag{14}$$

Assigning values of 1 or 0 to the qualifiers selects one aspect of the function:

$$f(1, 0; A, B, C) = \frac{A}{BC - \log (A - B)}. \tag{15}$$

A function with n bi-valued qualifiers has 2^n aspects.

Any qualified function may be *expanded* about a qualifier, as

$$f(x, y, \cdots ; A \cdots) = xf(1, y, \cdots ; A \cdots) + x'f(0, y, \cdots ; A \cdots) \tag{16}$$

To prove this equality, compare both sides of the equation when $x=1$, and when $x=0$. In each case, the left-hand side becomes identical with one term on the right-hand side, while the other term reduces to zero.

Each of the qualified functions on the right-hand side of (16) may be expanded about y,

$$\begin{aligned} f(x, y, \cdots ; A \cdots) = {} & xyf(1, 1, \cdots ; A \cdots) \\ & + xy'f(1, 0, \cdots ; A \cdots) \\ & + x'yf(0, 1, \cdots ; A \cdots) \\ & + x'y'f(0, 0, \cdots ; A \cdots) \end{aligned} \tag{17}$$

and so on, so that any qualified function may be expanded into a sum of its 2^n aspects, each of them suitably qualified.

[2] In the same sense as a statement is qualified.

A simple application of (16) is the division by a qualified number,

$$\frac{1}{xA + x'B} = x\frac{1}{A} + x'\frac{1}{B}.$$

(Division by xA alone falls under the same restrictions as division by zero.)

Identities (8) and (12), when read from right to left, are further special cases of the general expansion (16).

Multivalued Qualification

Consider a set of n interdependent Boolean elements,

$$x_i \quad (i = 1, 2, \cdots n)$$

subject to the conditions

$$x_1 + x_2 + \cdots + x_n = 1, \tag{18}$$

$$x_i x_j = 0 \quad (i \neq j). \tag{19}$$

From (1) and (18), *at least* one of the x_i must be 1; from (2) and (19), *only* one x_i may be 1. This set then has the property that one, and only one, of its elements has the value 1, and all others are 0.

The qualified number

$$x_1A_1 + x_2A_2 + \cdots + x_nA_n \tag{20}$$

has n aspects, and is equal to A_i when $x_i = 1$.

A qualified function containing multivalued qualifiers may be expanded as follows:

$$\begin{aligned}(fx_1x_2 \cdots x_n; A \cdots) = {} & x_1f(1, 0, \cdots 0; A \cdots) \\ & + x_2f(0, 1, \cdots 0; A \cdots) \\ & + \cdots \\ & + x_nf(0, 0, \cdots 1; A \cdots).\end{aligned} \tag{21}$$

This equality is proved by putting each $x_i = 1$ in turn and comparing both sides of the equation in each of the n aspects.

Interpretation

A switchable network presents different aspects, depending on the positions of its switches. Each of the network functions (input and transfer impedances and admittances, transfer ratios, etc.) or properties (resonant frequencies, bandwidth, etc.) may be expressed as a qualified function, containing qualifiers that depend on the position of the switches. As the impedances and admittances (or, in short, immitances[3]) of the network elements are the building blocks for the network functions, the basic elements to form those qualified functions are the qualified immitances.

The general problem in analysis is then, "Given a network containing qualified immitances, find the qualified network functions"; and in synthesis, "Given a qualified network function, with each of its aspects passing tests for realizability, construct a network containing some qualified immitances that realizes function."

[3] H. W. Bode, "Network Analysis and Feedback Amplifier Design," p. 15, D. Van Nostrand Co., New York, N.Y.; 1945.

Qualified Admittance

The *series* combination of an admittor Y and a switch (Fig. 1) has an admittance Y or 0 according to the position of the switch. The admittance of the combination may therefore be expressed as a qualified number xY, with $x = 0$ corresponding to an open switch, and $x = 1$ to a closed one. The "$x = 0$" in the caption to Fig. 1 indicates the position of the switch as drawn in the figure. All illustrations in this paper will contain a similar indication as to which particular aspect of the network is illustrated.

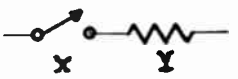

Fig. 1—Qualified admittance xY. ($x = 0$).

Y qualified by the series combination of two switches x and y is equivalent to x qualifying yY, or y qualifying xY. By (6), the combination has an admittance xyY (Fig. 2).

Y qualified by a parallel combination of x and y (Fig. 2) has the admittance Y when either x or y or both equal 1; the necessary qualifier, according to (1), is $x+y$.

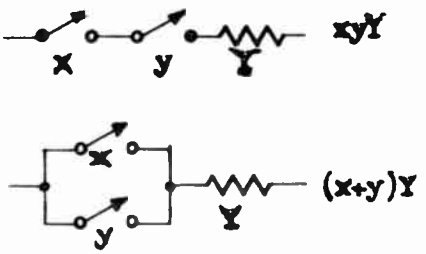

Fig. 2—Product and sum of admittance qualifiers. ($x = 0$).

The top part of Fig. 3 shows a parallel combination of two qualified admittors. The admittance of the combination is the sum of the separate qualified admittances. The second combination in Fig. 3 is similar to the first,

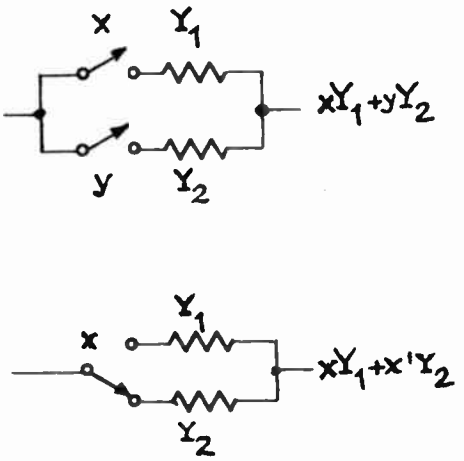

Fig. 3—The complement. ($x = 0$).

only the two qualifiers are interdependent, being parts of a change-over switch: when either x or y is 1, the other is 0. y is the complement of x.

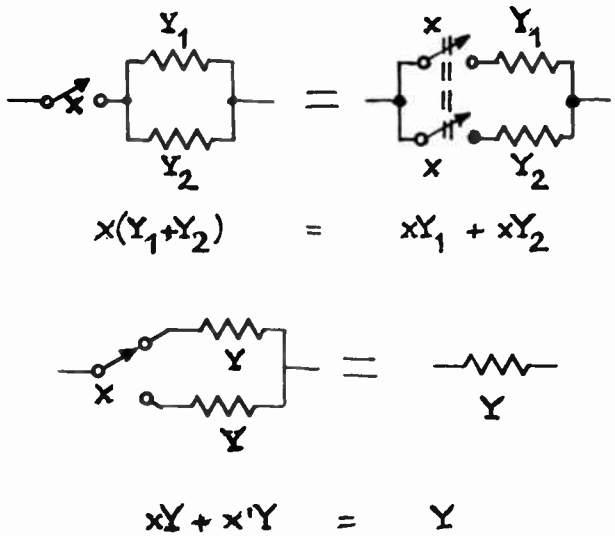

Fig. 4—Some identities of qualification. ($x=0$).

Fig. 4 illustrates identities (8) and (12) as interpreted by qualified admittances.

Qualified Impedance

The *parallel* combination of an impedor Z and a switch (Fig. 5) has an impedance Z or 0 when the switch is open or closed, respectively. The impedance of the combination is expressible by xZ, when $x=0$ corresponds to a closed switch and $x=1$ to an open one.

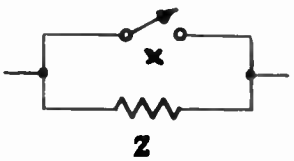

Fig. 5—Qualified impedance xZ. ($x=1$).

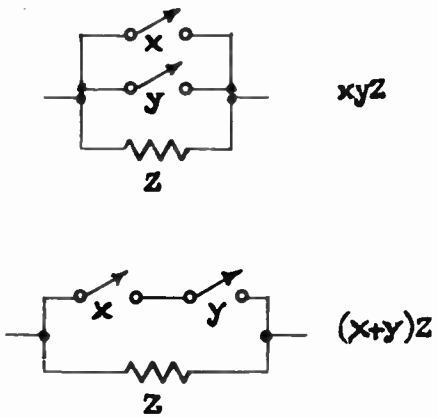

Fig. 6—Product and sum of impedance qualifiers. ($x=1$).

Z qualified by the parallel combination of the switches x and y has an impedance xyZ, being equivalent to qualifying yZ by x or xZ by y. Z in parallel with the series combination of x and y has an impedance of $(x+y)Z$, because the impedance is Z wherever x or y or both are open (Fig. 6).

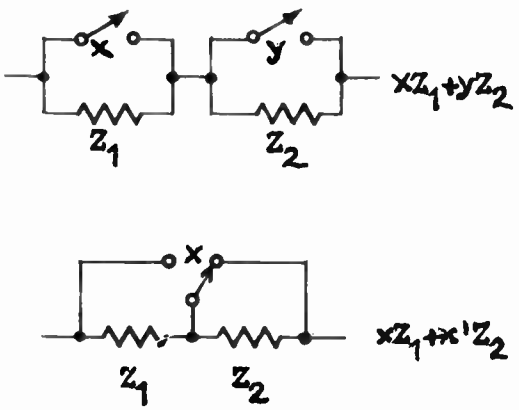

Fig. 7—The complement. ($x=1$).

Figs. 7 and 8 illustrate the same relations as in Figs. 3 and 4, interpreted by qualified impedances.

Duality

There is an evident duality in interpreting the qualified numbers by impedances or admittances, as summarized in the following table.

	Interpretation by *Admittances*	*Impedances*
xA is an element with a switch in	series	parallel
$x=1$ corresponds to a switch that is	closed	open
$x=0$ corresponds to a switch that is	open	closed
xy are two switches connected in	series	parallel
$x+y$ are two switches connected in	parallel	series

This duality is a direct result from the dualities of Boolean algebra[1] and of network algebra.[4] The usual duality relations of network algebra apply to switchable networks, with the addition of the duality between an open switch and a closed one. Figs. 1–4 show networks that are the duals of those in Figs. 5–8.[5]

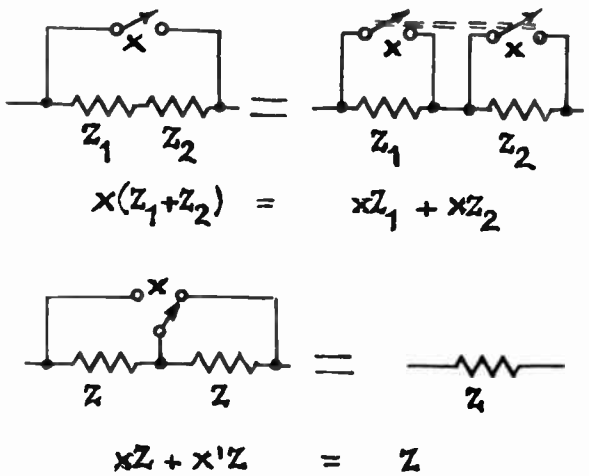

Fig. 8—Same identities as in fig. 4, interpreted by impedances. ($x=1$).

[4] E. A. Guillemin, "Communication Networks," vol. II, p. 246; John Wiley and Sons, New York, N. Y.; 1949.

[5] While figs 1–4 show the $x=0$ aspect, figs. 5–8 show the $x=1$ aspect. If all figures were showing the same aspect, duality would be complete, with an open switch in figs. 1–4 corresponding to a closed switch in figs. 5–8, and vice versa.

Multiposition Switches

Four admittors, A, B, C and D are shown in Fig. 9, qualified by five interdependent qualifiers that are parts of a five-position switch. At any position of the switch, one of the qualifiers is 1, and all the others are 0. The qualifiers may be members of a 5-set described by (18) and (19). Any n-position switch corresponds to such a set of n interdependent admittance qualifiers.

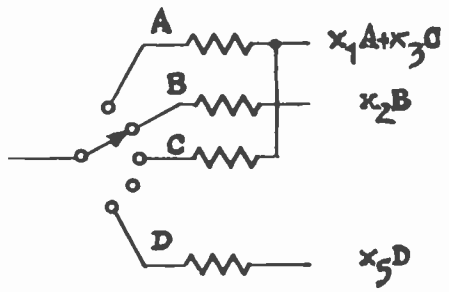

Fig. 9—Multivalued qualification. The qualified admittances indicated are the admittances between the switch pivot point and the corresponding terminals on the right. A, B, C, D are admittance values. ($x_i = 1$).

The dual set of impedance qualifiers would call for a switch where, at any setting, all contacts but one are closed. Such switches not being in general use, any network problem involving multiposition switches will be analyzed on an admittance basis.

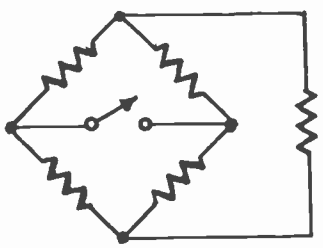

Fig. 10—A switch that does not qualify any immitance.

The Auxiliary Immitance

In some networks, a switch may span the branch between two nodes, without having any element in series or in parallel (Fig. 10). It may also happen that in a network analysed on the admittance basis, a switch is in parallel with an admittor; or a series switch appears in a network treated on the impedance basis. In all these cases, the difficulty may be by-passed by assuming an admittance (or impedance) whose value will finally tend to infinity, in series (parallel) with the switch. We will designate the value of this auxiliary impedance or admittance by S (for Switch). The impedance or admittance of the switch will be xS, with $x = 1$ corresponding to an open switch in the impedance case and to a closed switch in the admittance case.

S is then a number that, ***when unqualified***, tends to infinity, although xS is zero for $x = 0$. This number should be dealt with carefully, if paradoxes are to be avoided. The following examples show some "legitimate" uses:

$$\frac{1}{xA} = x\frac{1}{A} + x'S \tag{22}$$

$$\frac{1}{xS} = x'S. \tag{23}$$

The interpretation of qualified numbers could start from this xS representing a switch. The series combination of a switch and an admittor Y would then be computed to have the admittance

$$\frac{1}{\frac{1}{xS} + \frac{1}{Y}} = \frac{xSY}{xS + Y} = x\frac{SY}{S + Y} + x'0 = xY,$$

the last expression being the result of S tending to infinity. All other results enumerated in the interpretation sections might have been reached similarly in this roundabout formal method. The shorter method presented here, starting with qualified immitances, and using S in emergencies only, seems more practical and easier to apply. One can analyse a switchtable network by putting an "xS" for every switch, but the lumping of switches with other elements leads to shorter computations.

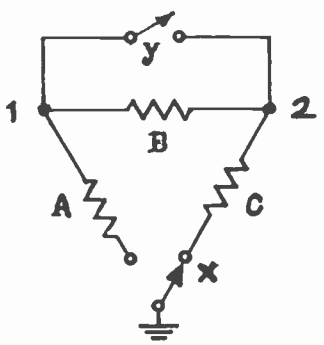

Fig. 11—Switchable network. A, B, C are admittance values. ($x = y = 0$).

Applications

Analysis

The first example is a very trivial one, chosen to illustrate the manipulation of qualified numbers.

A switchable network is shown in Fig. 11, and it is required to find the input admittance between node 1 and ground, and the voltage transfer ratio from a source at 1 to node 2 (both voltages referred to ground).

We will analyse the network on an admittance basis. A is qualified by x, C by x', and there is a switch yS in parallel with B. The admittance matrix of the network is

$$Y = \begin{Vmatrix} xA + B + yS & -B - yS \\ -B - yS & x'C + B + yS \end{Vmatrix} \tag{24}$$

and its determinant

$$\begin{aligned} |Y| &= (xA + B + yS)(x'C + B + yS) - (B + yS)^2 \\ &= (B + yS)(xA + x'C) \end{aligned} \tag{25}$$

where we have used the relation $xx' = 0$.

The input admittance at node 1 is computed as

$$Y_{in} = \frac{(B + yS)(xA + x'C)}{x'C + B + yS}. \tag{26}$$

The result may be left in this form, if it is needed for further computations; or it may be expanded as in (17), to present the four aspects explicitly:

$$\begin{aligned} Y_{in} &= xy\frac{(B+S)A}{B+S} + xy'\frac{BA}{B} \\ &\quad + x'y\frac{(B+S)C}{C+B+S} + x'y'\frac{BC}{B+C} \\ &= xyA + xy'A + x'yC + x'y'\frac{BC}{B+C}. \end{aligned} \tag{27}$$

The last line follows from the preceding one by letting S tend to infinity. In this simple example the results may be checked easily, by inspection, e.g., in the aspect shown in Fig. 11 ($x=y=0$), $Y_{in}=[BC/(B+C)]$.

The voltage transfer ratio may be written compactly

$$\frac{V_2}{V_1} = \frac{B + yS}{x'C + B + yS}, \tag{28}$$

or expanded

$$\begin{aligned} \frac{V_2}{V_1} &= xy\frac{B+S}{B+S} + xy'\frac{B}{B} + x'y\frac{B+S}{C+B+S} \\ &\quad + x'y'\frac{B}{C+B} \\ &= xy1 + xy'1 + x'y1 + x'y'\frac{B}{B+C}. \end{aligned} \tag{29}$$

Synthesis of Interconnections

This example is based on the circuit of a DC Crystal Checker,[6] with certain simplifications.

Problem: construct a network to test an unknown admittor X, so as to find its resistance by a simple ohmmeter measurement, and also to find the current through it under a voltage of 1 volt (X is assumed to be nonlinear). The measurement will proceed in four steps (Fig. 12):

1. A 1.5-volt dry cell is connected through a variable resistor to the meter M (1 mA full scale, 100 ohms internal resistance), and the reading set to full scale (zero ohms).

2. The unknown is inserted and its resistance read on the scale of ohms.

3. The network is arranged as in aspect $x_3=1$ of Fig. 12 and the meter reset to full scale.

4. The meter is interchanged with the 100 ohms resistor and the current through the unknown is read. Since the internal resistance of the meter is also 100 ohms, the voltage set in step 3 will not change.

[6] H. C. Torrey and C. A. Whitmer, "Crystal Rectifiers," p. 298, fig. 9.39; Radiation Laboratory Series, vol. 15, McGraw-Hill, New York, N.Y.; 1948.

It is required to build this network with a 4-position switch. Synthesis will follow general method of Kron.[7]

We first construct the "primitive" network, where all the elements are disconnected (Fig. 13). The final network will result from different interconnections of these elements. Some of the elements are not passive linear, but when analysing interconnections only we may substitute linear passive elements for the battery and series resistor, the meter and the nonlinear unknown. We use the letters B, M, X, D, E to designate the admittance values of those substitute admittors, as shown in Fig. 13.

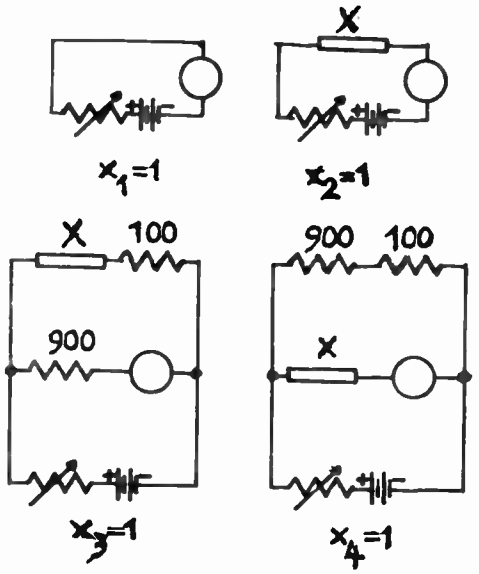

Fig. 12—Four aspects of a switchable network to be synthesized.

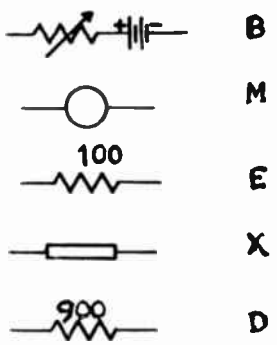

Fig. 13—The "primitive" network.

The admittance of the primitive network is the diagonal matrix

$$Y_0 = \begin{Vmatrix} B & 0 & 0 & 0 & 0 \\ 0 & M & 0 & 0 & 0 \\ 0 & 0 & E & 0 & 0 \\ 0 & 0 & 0 & X & 0 \\ 0 & 0 & 0 & 0 & D \end{Vmatrix}. \tag{30}$$

[7] G. Kron, "Tensor Analysis of Networks," John Wiley and Sons; 1939. See also, P. Le Corbeiller, "Matrix Analysis of Electric Networks," Chapter III; Harvard University Press; 1950. For the matrix manipulations, refer to any textbook on matrix algebra, e.g., E. A. Guillemin, "The Mathematics of Circuit Analysis," John Wiley and Sons; 1949. Equation (35) is a *congruent* transformation, treated on p. 136 of Guillemin's book.

The voltages across the five elements, V_B, V_M, $\cdots$ V_D after the interconnection are interdependent, and may be expressed as linear combinations of the independent voltages $\overline{V}_B$, $\overline{V}_M$ and $\overline{V}_E$. For example, in aspect 4 of Fig. 12,

$$\begin{aligned} V_B &= \overline{V}_B \\ V_M &= \overline{V}_M \\ V_E &= \overline{V}_E \\ V_X &= \overline{V}_B - \overline{V}_M \\ V_D &= \overline{V}_B - \overline{V}_E \end{aligned} \tag{31}$$

$$A = \begin{Vmatrix} 1 & 0 & 0 \\ x_1 & x_2 + x_3 + x_4 & 0 \\ 0 & 0 & 1 \\ x_2 + x_3 + x_4 & -(x_2 + x_4) & -x_3 \\ x_3 + x_4 & -x_3 & -x_4 \end{Vmatrix}. \tag{34}$$

The admittance of the network is obtained from the primitive admittance by

$$Y = \tilde{A} Y_0 A, \tag{35}$$

where $\tilde{A}$ is the transpose of A.

$$\begin{aligned} Y &= \begin{Vmatrix} 1 & x_1 & 0 & x_2 + x_3 + x_4 & x_3 + x_4 \\ 0 & x_2 + x_3 + x_4 & 0 & -(x_2 + x_4) & -x_3 \\ 0 & 0 & 1 & -x_3 & -x_4 \end{Vmatrix} \\ &\times \begin{Vmatrix} B & 0 & 0 & 0 & 0 \\ 0 & M & 0 & 0 & 0 \\ 0 & 0 & E & 0 & 0 \\ 0 & 0 & 0 & X & 0 \\ 0 & 0 & 0 & 0 & D \end{Vmatrix} \times \begin{Vmatrix} 1 & 0 & 0 \\ x_1 & x_2 + x_3 + x_4 & 0 \\ 0 & 0 & 1 \\ x_2 + x_3 + x_4 & -(x_2 + x_4) & -x_3 \\ x_3 + x_4 & -x_3 & -x_4 \end{Vmatrix} \\ &= \begin{Vmatrix} B + x_1 M + (x_2 + x_3 + x_4)X + (x_3 + x_4)E & -(x_2 + x_4)X - x_3 E & -x_3 X - x_4 E \\ -(x_2 + x_4)X - x_3 E & (x_2 + x_3 + x_4)M + (x_2 + x_4)X + x_3 E & 0 \\ -x_3 X - x_4 E & 0 & D + x_3 X + x_4 E \end{Vmatrix}. \end{aligned} \tag{36}$$

corresponding to a transformation matrix

$$A = \begin{Vmatrix} 1 & 0 & 0 \\ 0 & 1 & 0 \\ 0 & 0 & 1 \\ 1 & -1 & 0 \\ 1 & 0 & -1 \end{Vmatrix}. \tag{32}$$

Similar matrices may be written for the other aspects, resulting in a qualified transformation matrix:

$$\begin{aligned} A = x_1 &\begin{Vmatrix} 1 & 0 & 0 \\ 1 & 0 & 0 \\ 0 & 0 & 1 \\ 0 & 0 & 0 \\ 0 & 0 & 0 \end{Vmatrix} + x_2 \begin{Vmatrix} 1 & 0 & 0 \\ 0 & 1 & 0 \\ 0 & 0 & 1 \\ 1 & -1 & 0 \\ 0 & 0 & 0 \end{Vmatrix} \\ + x_3 &\begin{Vmatrix} 1 & 0 & 0 \\ 0 & 1 & 0 \\ 0 & 0 & 1 \\ 1 & 0 & -1 \\ 1 & -1 & 0 \end{Vmatrix} + x_4 \begin{Vmatrix} 1 & 0 & 0 \\ 0 & 1 & 0 \\ 0 & 0 & 1 \\ 1 & -1 & 0 \\ 1 & 0 & -1 \end{Vmatrix}. \end{aligned} \tag{33}$$

The last expression is the expansion of a single qualified matrix, that may be obtained by appropriately qualifying each element of each matrix in (33) and adding the matrices. The result is

Identities (6), (7) and (19) have been applied to derive the final result. (36) is the admittance matrix of the network shown in Fig. 14. When, B, M . . . etc. are translated back according to Fig. 13, and the qualifiers are represented by switches, the final result of the synthesis is as in Fig. 15.

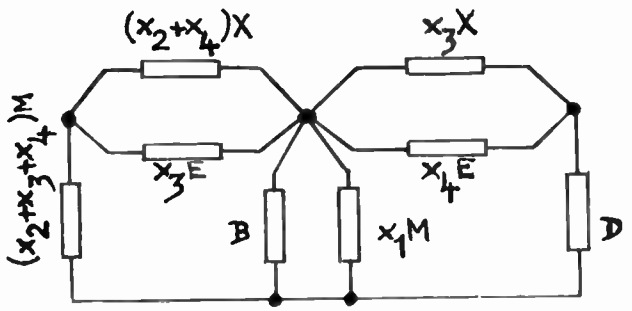

Fig. 14—Result of synthesis.

Synthesis of a Transfer Function

Our third example is based on a problem treated by Guillemin.[8] The paper describes the synthesis of an RC network, having[9]

[8] E. A. Guillemin, "A Note on the Ladder Development of RC Networks," PROC. I.R.E., vol. 40, p. 482; April 1952. For the derivation of the network constants see also, E. A. Guillemin, "Communication Networks," vol. II, pp. 211–216, John Wiley and Sons; 1948.

[9] We will designate impedances and admittance by capital Z's and Y's, respectively (instead of lower case z and y as in the original paper) so as not to confuse them with qualifiers. The lower case s appearing in the equations is the complex frequency.

$$Y_{22} = \frac{(s+1)(s+3)(s+5)}{(s+2)(s+4)(s+6)}, \tag{37}$$

$$Y_{12} = \frac{(s+2.5)^2(s+7)}{(s+2)(s+4)(s+6)}. \tag{38}$$

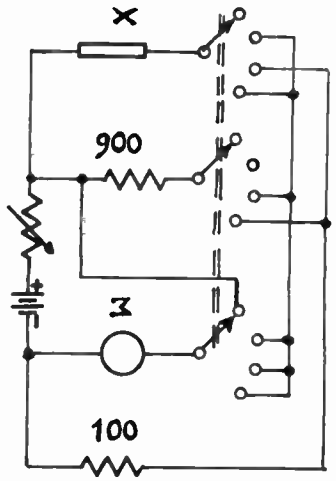

Fig. 15—Interpretation of fig. 14. ($x_1 = 1$).

We will modify the problem, by introducing a switch to shift the zero of Y_{12} from $s=-7$ to $s=-8$, without changing Y_{22}. (38) is then replaced by

$$Y_{12} = \frac{(s+2.5)^2(s+7+x1)}{(s+2)(s+4)(s+6)}. \tag{39}$$

The original network treated by Guillemin becomes the $x=0$ aspect of the required switchable network.

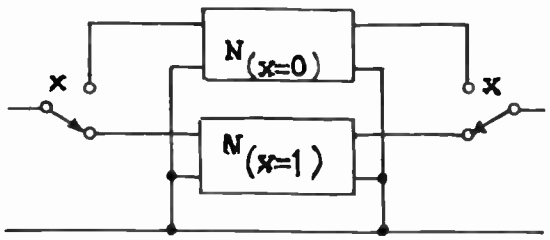

Fig. 16—Any 2-aspect network may always by synthesized in this way.

Any switchable network, all of whose aspects comply with the realizability conditions, may always be realized as in Fig. 16, realizing each aspect separately and combining them with switches. But as the two aspects of Y_{12} have so much in common, this trivial method is not economic, and we will proceed to realize both aspects simultaneously. The procedure follows Guillemin's paper, step by step, and the reader is advised to refer to Guillemin's paper while reading the details of the following example.

Guillemin develops Y_{22} as a ladder and provides a double zero of transmission at $s=-2.5$, leaving a remainder ((16) in his paper)

$$Z^{iv} = \frac{1.77(s+5.193)}{(s+4.25)}. \tag{40}$$

In this stage of the synthesis, the partly developed network has the form of Fig. 17. The next cycle should provide a transmission zero at $s=-7-x1$. This is the first time that the qualifier appears in the computation, so at this point we break away from the original paper, though still following its method.

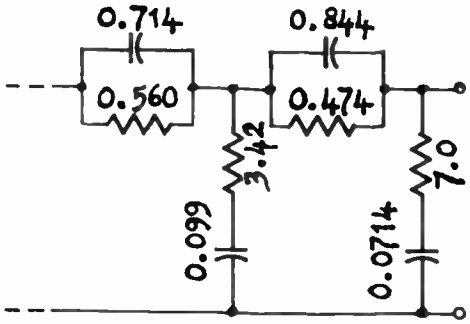

Fig. 17—Up to this point, the synthesis follows that in Guillemin's paper.

The value of Z^{iv} at the required zero is

$$Z^{iv} = \frac{1.77(-1.807 - x1)}{(-2.75 - x1)} = x1.325 + x'1.163$$
$$= 1.163 + x0.162. \tag{41}$$

In the last step we applied (8) and (12).

This value, in both of its aspects, is less than $Z^{iv}(\infty)$ so it may be removed as a series resistance

$$Z_5 = R_5 = 1.163 + x0.162, \tag{42}$$

leaving a remainder

$$Z^v = Z^{iv} - Z_5$$
$$= \frac{1.77(s+5.193)}{s+4.25} - (1.163 + x0.162)$$
$$= \frac{(0.607 - x0.162)s + (4.249 - x0.689)}{s+4.25}.$$

Expanding about x,

$$Z^v = \frac{x(0.445s + 3.560) + x'(0.607s + 4.249)}{s+4.25}$$
$$= \frac{x0.445(s+8) + x'0.607(s+7)}{s+4.25}$$
$$= \frac{(0.607 - x0.162)(s+7+x1)}{s+4.25} \tag{43}$$

$$Y^v = \frac{1}{Z^v} = \frac{s+4.25}{s+7+x1} \times \frac{1}{0.607 - x0.162}$$
$$= \frac{s+4.25}{s+7+x1}\left(x\frac{1}{0.445} + x'\frac{1}{0.607}\right)$$
$$= \frac{(1.648 + x0.599)s + (7.004 + x2.546)}{s+7+x1}. \tag{44}$$

A parallel conductance may be dropped off,

$$Y_7 = G_7 = \frac{7.004 + x2.546}{7 + x1}$$
$$= (7.004 + x2.546)(x\tfrac{1}{8} + x'\tfrac{1}{7})$$
$$= x1.194 + x'1.000$$
$$= 1.000 + x0.194, \quad (45)$$

and leave

$$Y_6 = Y^v - Y_7 = \frac{(0.648 + x0.405)s}{s + 7 + x1}. \quad (46)$$

Y_6 may be realized by expansion about x,

$$Y_6 = x\frac{1.053s}{s + 8} + x'\frac{0.648s}{s + 7}. \quad (47)$$

The final arrangement of Z_5, Y_6 and Y_7 is shown in Fig. 18. When Figs. 17 and 18 are joined at the broken lines, the final network will result.

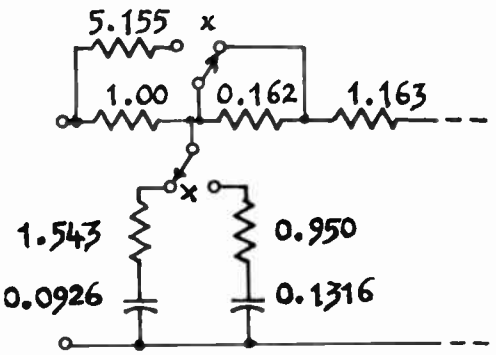

Fig. 18—Second part of synthesis, shown in $x=0$ aspect. The two switches are ganged.

Economy in switches is possible by combining the qualifiers of R_5 and G_7 into one change-over switch. The final arrangement requires a double-pole double-throw switch, which is not more than what was required by the trivial arrangement (Fig. 16) and there is an obvious economy in components.

An alternative realization of Y_6 is possible by finding the qualified R and C that result in (46).

$$R = \frac{1}{0.648 + x0.405} = x0.950 + x'1.543$$
$$= 0.950 + x'0.593 \quad (48)$$
$$C = \frac{0.648 + x0.405}{7 + x1} = x0.1316 + x'0.0926$$
$$= 0.0926 + x0.0390. \quad (49)$$

This alternative is shown in Fig. 19. Both switches have to be open simultaneously, and therefore cannot be combined into a change-over switch.

The solution of the synthesis problem is not unique; but this is true of any problem in network synthesis.

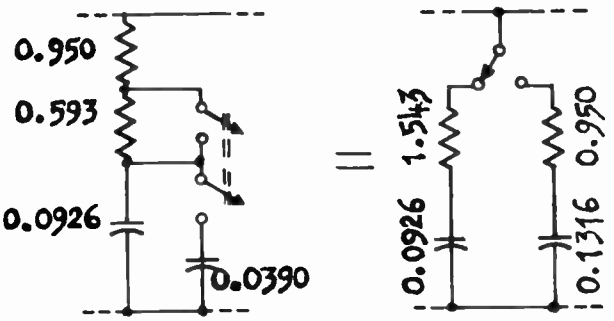

Fig. 19—Alternative realizations of Y_6. ($x=0$).

Conclusion

The algebra of qualified numbers may be applied to treat problems other than switchable networks. The following are some examples:

1. Networks switched by vacuum-tubes that are driven to cutoff. The vacuum-tube may be represented by a *qualified admittance matrix* xY, with $x=0$ corresponding to cutoff and $x=1$ to conduction biasing.

2. Small-signal operation of non-linear circuits. When a bias is used to shift the point of operation along the non-linear characteristic, and provided the bias takes only discrete values, the small-signal parameters may be expressed as multivalued qualified numbers, as in (20). Each value of the bias will then correspond to one aspect of the parameter.

3. In his discussion of feedback amplifiers, Bode[10] introduces the concept of *return difference*, which is the ratio of the circuit determinants for two different values of any given parameter. This may be expressed in terms of qualified numbers: In a network containing a qualified component, the determinant is expressed as a qualified function, expanded about the qualifier; the ratio of both aspects is the return difference.

In conclusion, we admit that the algebraic presentation of qualified number algebra in this paper is not mathematically rigorous, but hope that rigour has been sacrificed to simplicity of exposition. Also may we point out that the list of applications is illustrative rather than exhaustive, and the examples shown may not be the most striking ones; for, as its name implies, this paper is only a sketch of an algebra and its applications.

[10] H. W. Bode, *loc. cit.*, pp. 47–51.

The Transvar* Directional Coupler†

KIYO TOMIYASU‡, MEMBER, IRE, AND SEYMOUR B. COHN§, SENIOR MEMBER, IRE

Summary—**A new directional coupler capable of transferring variable amounts of power (0 to 100 per cent) from one waveguide to another is described and analyzed. The coupling element in this coupler is a long slot containing a grid of wires in the common narrow wall of the two waveguides. The coupler can carry nearly the full power of the waveguide and has been used for a variable high-power divider as well as in a variable high-power attenuator. The quantitative theory presented agrees closely with the experimental results.**

Introduction

DIRECTIONAL COUPLERS which can couple or transfer up to the total power from one guide to another have been previously described.[1,2] The coupling elements of these couplers are in the common *broad* wall of the two waveguides. A new total-power-transfer directional coupler which has a variable-length coupling element in the common *narrow* wall has been designed and tested. The coupling element consists of n closely spaced, identical apertures or, alternatively, $n-1$ grid wires as shown in Fig. 1. The

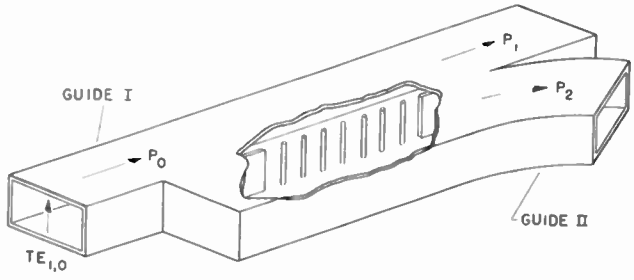

Fig. 1—Cutaway of the Transvar directional coupler.

sum of the two directive powers, P_1 and P_2 is equal to the input power P_0. By a suitable shutter arrangement to be described, the degree of coupling can be changed by varying the effective length of the coupling region. Because it is possible to transfer variable amounts of power, from 0 to 100 per cent, this coupler has been called the Transvar coupler. In the ensuing sections, a brief description and applications of the Transvar coupler are given. A quantitative theory for the coupler is presented in the Appendix.

Description of Transvar Coupler

The fundamental operation of the Transvar coupler can be described by the modes which satisfy the boundary conditions in the coupling region. In Fig. 2 a full-transfer Transvar coupler is shown. The power-flow density from one guide to the other is represented by the degree of shading as shown in Fig. 2 (a). The amplitude distributions of the electric field at three cross-sections in the coupling region are shown in Fig. 2(b). These boundary conditions can be essentially satisfied by the superposition of two propagating modes, one symmetrical and the other antisymmetrical relative to the common wall as Fig. 2 (c) shows. The two modes are approximately equal in amplitude, but differ in phase velocity. The antisymmetrical mode is unaffected by the grid wires or apertures, assuming small grid-wire diameter. The symmetrical mode on the other hand is inductively loaded by the grid wires, which results in a slower phase velocity.

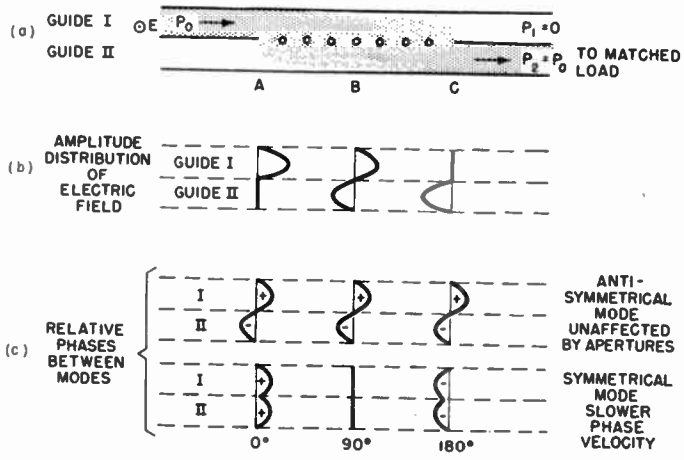

Fig. 2 (a) (b) (c)—Power distribution in a full-transfer coupler.

The superposition of two propagating modes in one waveguide has been considered previously. Kyhl[2] describes power transfer between two waveguides coupled through the common broad wall. In addition to the two propagating modes, Kyhl states that a third mode, a "ridge-guide" mode, which has a lower cut-off frequency, could exist, yielding spurious slot resonances if the coupling slot is asymmetrically located. Purcell and Dicke[3] discuss measurement difficulties when two

* Trade Mark of the Sperry Corp.

† Decimal classification: R310.4. Original manuscript received by the Institute, September 9, 1952; revised manuscript received, February 6, 1953. Presented at the 1951 IRE National Convention.

‡ Microwave Components Dept., Sperry Gyroscope Co., Great Neck, L. I., N. Y.

§ Head, Microwave Group, Stanford Research Institute, Stanford, Calif. Formerly Research Engr., Sperry Gyroscope Co., Great Neck, L. I., N. Y.

[1] H. J. Riblet and T. S. Saad, "A new type of waveguide directional coupler," PROC. I.R.E., vol. 36, no. 1, pp. 61–64; January, 1948.

[2] R. L. Kyhl, "Technique of Microwave Measurements," edited by C. G. Montgomery, M.I.T. Radiation Lab. Series, Vol. 11, Sec. 14.8, McGraw-Hill Book Co., Inc., New York; 1947.

[3] E. M. Purcell and R. H. Dicke, "Principles of Microwave Circuits," edited by Montgomery, Dicke and Purcell, M.I.T. Radiation Lab. Series, Vol. 8, Sec. 10.3, McGraw-Hill Book Co., Inc., New York; 1948.

propagating modes coexist. Krasnushkin and Khokhlov[4] describe spatial beating effects of two modes propagating in coupled semi-circular and elliptical waveguides.

Since the phase velocities and hence the guide wavelengths of the two propagating modes differ, a superposition of the two modes will yield an electric-field maximum where the two modes are in phase and a null where the two modes are in phase reversal. Mathematically, this phase reversal can be expressed in terms of two guide wavelengths as

$$\pi = (2\pi d/\lambda_{g^1}) - (2\pi d/\lambda_{g^2}) \tag{1}$$

where

λ_{g^1} = guide wavelength of the symmetrical mode
λ_{g^2} = guide wavelength of the antisymmetrical mode
d = distance between an electric-field maximum and an adjacent null in one guide.

Equation (1) can be rewritten as

$$d = 1/[(2/\lambda_{g^1}) - (2/\lambda_{g^2})] \tag{2}$$

Assuming that the amplitudes of the two modes are equal, the resultant electric field in guide I in the coupling region is expressed by

$$\begin{aligned} E_1 &= (E_0/2)(1 + \epsilon^{j\alpha}) \\ &= (E_0/2)(1 + \cos\alpha + j\sin\alpha) \end{aligned} \tag{3}$$

where

E_0 = input electric field
α = phase difference of the electric vectors of the two modes.

The amplitude is given by

$$|E_1/E_0| = \cos\alpha/2 = \cos(\pi l/2d) \tag{4}$$

where l is the length of the coupling region. Similarly for guide II,

$$E_2 = (E_0/2)(1 - \epsilon^{j\alpha}) \tag{5}$$

and

$$|E_2/E_0| = \sin(\pi l/2d). \tag{6}$$

If the length l of the coupling region is equal to d, then full transfer of power is effected. If l is less than d, the transfer will be partial as given by the equations

$$P_2/P_0 = \sin^2(\pi l/2d) \tag{7}$$

$$P_1/P_0 = \cos^2(\pi l/2d). \tag{8}$$

Similarly, full-power transfer can be obtained if l equals $3d$, $5d$, etc.

[4] P. E. Krasnushkin and R. V. Khokhlov, "Spatial beating in coupled waveguides," *Jour. Tech. Phys.* (Russia), vol. XIX, pp. 931–942; August, 1949.

The ratio of the resultant electric fields in the two guides is

$$E_1/E_2 = j\cot(\pi l/2d) \tag{9}$$

which indicates that the two fields are in phase quadrature independent of the degree of power transfer.

For some applications it is desirable to know the relative phase of E_1 as the effective coupler length is varied as shown in Fig. 3. If a reference phase is chosen to be

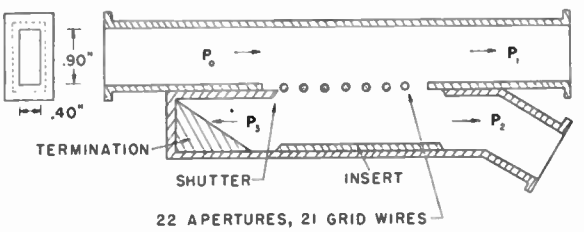

Fig. 3—Sectional view of variable Transvar coupler.

that phase of E_1 when the coupler length is zero, the phase of E_1 will lag the reference phase by $\pi l/2d$ radians as the coupler length is increased. Furthermore, from (9) the phase of E_2 at the same cross section will lag that of E_1 by 90 degrees. For example, if $l = d/2$, E_1 will lag 45 degrees and E_2 will lag 135 degrees relative to the reference phase. Experimental measurements have verified these phase differences.

It is important to note that the two modes mentioned, the antisymmetrical and symmetrical, are the lowest modes which can propagate in the coupling region of this type of coupler. Other higher order modes are necessary to satisfy exactly the boundary conditions but these evanescent modes have much smaller amplitudes and hence have a small net effect.

Bandwidth

Inasmuch as the phase velocities of both the antisymmetrical and symmetrical modes are functions of frequency, a particular coupler which transfers 100 per cent of the power at one frequency will be either too short or too long at other frequencies. Hence, the bandwidth of the Transvar coupler depends upon the tolerable decrease in power transfer. An approximate formula for the bandwidth can be obtained from the free-space-wavelength derivative of (2). This yields

$$BW \doteq (2/5\pi)(\sqrt{k}/gh) \tag{10}$$

where

k = tolerable percentage decrease in power transfer

$$g = \lambda_{g^2}/\lambda$$

$$h = \lambda_{g^1}/\lambda$$

For example, if $g = 1.42$, $h = 1.28$, and $k = 4$ per cent, (10) yields a BW of 14 per cent.

Experimental Measurements on the Transvar Coupler

A cross-sectional view of the first Transvar coupler constructed of 1 in. by $\frac{1}{2}$ in. OD waveguide illustrates the 22 rectangular apertures which are equivalent to 21 grid wires as Fig. 3 shows. The 0.040-inch diameter, 0.400-inch-long grid wires are spaced 0.375 inch between centers. One of the narrow walls in the secondary guide is opened to provide a shutter. Opposite this narrow wall, an insert is soldered to maintain the guide width constant. This insert is necessary if full-power transfer is desired. The lengths of the shutter and the insert as well as the total length of the 22 apertures, are $8\frac{1}{4}$ inches each. By changing the relative longitudinal position of the two waveguides, the number of exposed apertures and hence the effective coupling length can be changed. "C" clamps are used to provide the necessary electrical contact between the guides. Due to finite directivity in the secondary guide, a termination is used to absorb P_3.

Measurements made on this Transvar coupler are plotted in Fig. 4 with the power transfer and input

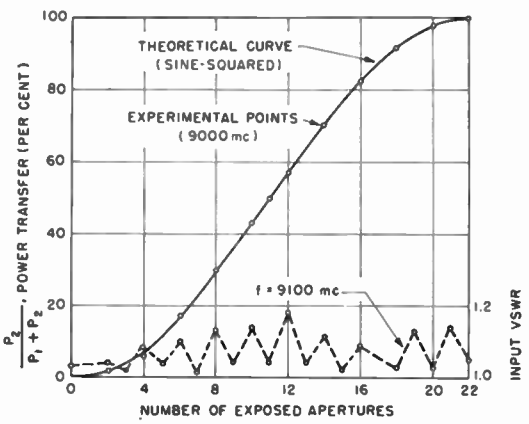

Fig. 4—Power transfer and input VSWR characteristic curves for an experimental directional coupler.

VSWR plotted as functions of the number of exposed apertures. The power transfer has been defined as $P_2/(P_1+P_2)$. The experimental points check exceptionally well with the theoretical sine-squared power transfer curve. The input VSWR is below 1.2 for all numbers of exposed apertures. The measurements indicated that the power P_3 which propagates in the backward direction is about 25 db below P_0 regardless of the number of exposed apertures; hence the directivity is highest when full transfer occurs. When the number of exposed apertures is two or more, there is directivity because the distance between adjacent apertures is approximately one quarter wavelength.

The measured frequency characteristics indicate that plotted in Fig. 5 the frequency at which maximum transfer occurs is about 9,000 mc. This frequency checks exceptionally well with the theoretical calculations obtained by the method outlined in the Appendix. The measured bandwidth agrees fairly closely with (10).

A second Transvar coupler was constructed which was identical to the first except that the grid wire diameter was 0.032 inch. The full-transfer frequency of this coupler was 10,000 mc, which also checked the theoretical calculations very closely.

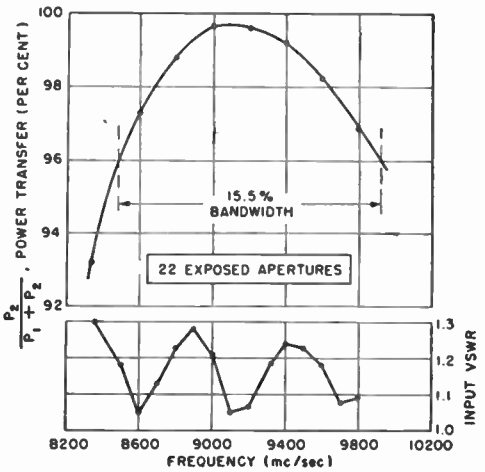

Fig. 5—Frequency characteristics (power transfer and input VSWR) for an experimental model coupler.

Applications

From an investigation of the boundary conditions, it is evident that the electric field strengths in the coupling region are no greater than those in the input guide. This means that the power-carrying capacity of the coupler is as great as that of the input guide, and that the coupler is particularly suited for high power applications. Hence, from the preceding discussion it can be seen that the Transvar coupler can be used as a variable power divider, for both high and low-power applications.

Another significant use of the coupler is in a variable high-power attenuator. Referring to Fig. 3, a conventional high power termination absorbs P_1, while P_2 is delivered to the load. The range in attenuation in *db* is from zero to infinity. The advantages of this type of attenuator are its low VSWR, large range in attenuation, high power capacity, and simplicity in design.

Conclusion

A new directional coupler which will permit up to full transfer of power from one guide to another has been designed and constructed. The theoretical approach, based on the superposition of symmetrical and antisymmetrical propagating modes, is applicable to many other problems involving directional couplers, coupled transmission lines, and other coupled circuits. The Transvar coupler may be used for almost any directional coupler requirements, but its specific properties discussed above make it particularly useful wherever heavy coupling, variable coupling, and high power-handling capacity are needed.

Appendix

Theory of the Transvar Coupler

The theoretical analysis of the coupler involves the determination of the guide wavelengths of the symmetrical and antisymmetrical propagating modes. Because the antisymmetrical mode is unaffected by the presence of the grid wires, this mode, which is the TE_{20} mode in the composite guide of the coupling region, has a guide wavelength equal to that of the TE_{10} mode in the single guide. Thus, in the following analysis, the guide wavelength of only the symmetrical mode will be considered.

The quantitative theory for the coupler is based upon an infinite, parallel-wire grid structure as shown in Fig. 6 (a). This structure can be shown to be equivalent to the coupler by the following reasoning. Assume that two waves E_1 and E_2, equal in amplitude and phase, are incident at equal angles on the grid. The transmitted and reflected waves will proceed in the directions parallel to those of the incident waves. The superposition of the incident, transmitted, and reflected waves will result in zero electric fields at planes parallel to the grid as Fig. 6 (b) shows. The nearest planes will be at a distance

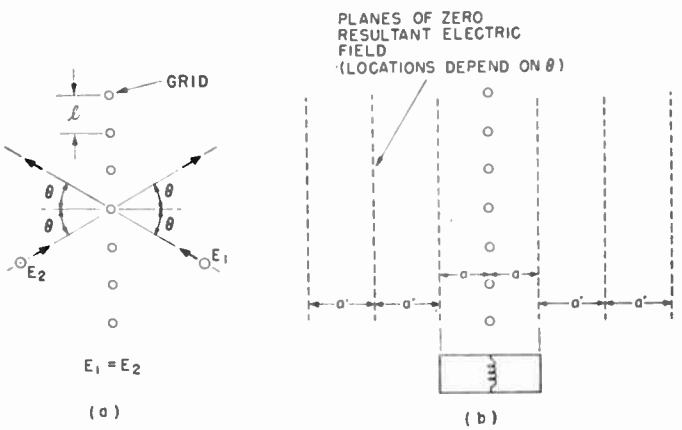

Fig. 6(a) (b)—Two equi-phase plane waves which are obliquely incident on an infinite parallel-wire grid.

a on either side of the grid. The other planes will be separated by a' from each other. The distances a and a' differ because of the inductive effect of the grid.

The locations of these planes will depend upon the angle of incidence of the waves. Strictly speaking, the surfaces at distance a will be slightly perturbed from a plane due to the effects of the higher order fields in the vicinity of the grid wires. Moreover, these surfaces will actually represent electric field minima although the magnitudes will be extremely small for the condition $l<a$ as stipulated in this problem.

Where the resultant electric fields are zero, it is possible to insert perfectly conducting metal walls without affecting the fields. Furthermore, since the configuration is uniform in the direction of the grid wires, it is possible to insert metal walls perpendicular to the grid wires without disturbing the fields. By connecting these four walls, a waveguide can be channeled which is in every way identical to the coupler. For the present problem the boundary condition requires the resultant electric field to be zero at distance a from the grid. This establishes a particular value for the angle of incidence from which the guide wavelength of the symmetrical mode can be obtained.

In simplifying the problem, one plane wave incident on the grid at an angle θ from the normal is considered having a free-space wavelength of λ_0 as shown in Fig. 7 (a). The phase wavelength of the component of the wave propagating perpendicular to the grid is $\lambda_x=\lambda_0 \sec\theta$. For obliquely incident waves, all impedances are referred to the component of the wave impedance of the incident plane wave which propagates normal to the grid. This "characteristic" impedance is $Z_0=120 \sec\theta$.[5] In order to satisfy the boundary conditions in the coupling region, the sum of the susceptances must be zero at the grid as shown in Fig. 7 (b). This is expressed by

$$(2/z_1) + (1/jx_1) = 0 \tag{11}$$

where

x_1 = normalized reactance of the parallel-wire grid
z_1 = normalized input impedance of the waveguide.

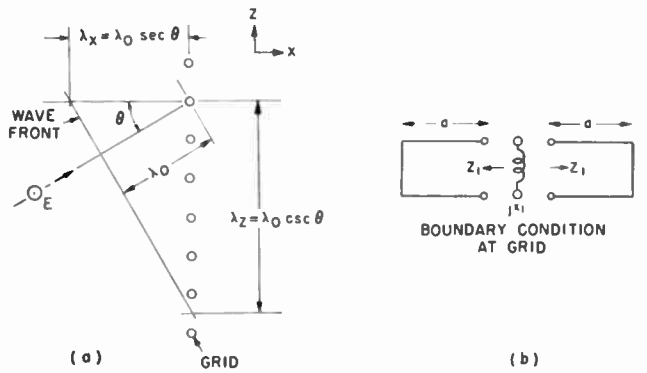

Fig. 7(a) (b)—Boundary conditions at the parallel-wire grid.

Substituting

$$z_1 = j \tan (2\pi a/\lambda_x) = j \tan [(2\pi a \cos\theta)/\lambda_0] \tag{12}$$

in (11) yields

$$\tan [(2\pi a \cos\theta)/\lambda_0] = -2x_1. \tag{13}$$

It is necessary to solve (13) for θ in order to compute the guide wavelength λ_z of the symmetrical mode in the coupling region, which is

$$\lambda_z = \lambda_0/\sin\theta. \tag{14}$$

The formula for the reactance of a parallel-wire grid is derived by Macfarlane.[6] With a change in notation, the reactance is

$$x_1 = [(l \cos\theta)/\lambda_0][\ln (l/2\pi r) + F(\theta, l/\lambda_0)] \tag{15}$$

where r is the radius of each wire ($\ll l$), and F is a correction term given graphically by Macfarlane as Fig. 8

[5] S. A. Schelkunoff, "Electromagnetic Waves," D. Van Nostrand Co., Inc., New York, p. 254; 1943.

[6] G. G. Macfarlane, "Surface impedance of an infinite parallel-wire grid at oblique angles of incidence," *Jour. Inst. Elec. Eng.*, vol. XCIII, pt. III A, no. 10, pp. 1523–1527; 1946.

shows. By substituting equation (15) in equation (13),

$$\tan\left[(2\pi a\cos\theta)/\lambda_0\right] = \left[(-2l\cos\theta)/\lambda_0\right]\left[\ln\left(l/2\pi r\right) + F(\theta, l/\lambda_0)\right] \quad (16)$$

or

$$(\tan p)/p = (-l/\pi a)\left[\ln\left(l/2\pi r\right) + F(\theta, l/\lambda_0)\right] \quad (17)$$

where

$$p = (2\pi a\cos\theta)/\lambda_0. \quad (18)$$

Although F is a function of θ, it is slowly varying when l/λ_0 is quite small. By solving (17) for p with the aid of tables[7] of $(\tan p)/p$, and then computing the angle of incidence θ from (18), the guide wavelength of the symmetrical mode can be calculated from (14).

[7] E. Jahnke and F. Emde, "Tables of Functions," Addenda, Table V, Dover Publications, New York; 1943.

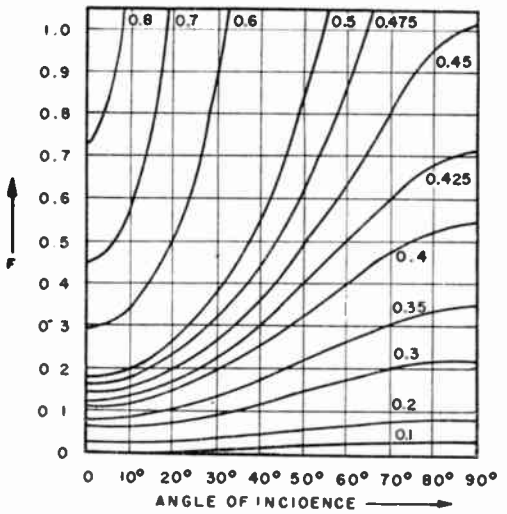

Fig. 8—Correction term $F(\theta, l/\lambda_0)$ as a function of an angle of incidence θ for parametric values of l/λ_0. Reproduced by special permission of the *Jour. Inst. Elec. Eng.*

Discussion on:

The Absorption Gain and Back-Scattering Cross Section of the Cylindrical Antenna*

S. H. DIKE AND D. D. KING

Ronold King:[1] The alleged difficulties which, in S. H. Dike's view, "have become apparent in the King-Middleton type of first-order solution of the Hallén integral equation" may, perhaps, be ascribed to 1) a lack of understanding of the fundamental principle of the method 2) the assignment of an exaggerated role to the expansion parameter as a factor in determining the accuracy of specific quantities appearing in, or derived from, the solution 3) a failure to recognize the limitations in generality and in accuracy of a particular *first-order* solution and 4) the implicit assumption that the experimental results reported by Dike and King are accurate. After the general background has been outlined under 1), the other three points are considered in turn.

1. The King-Middleton Procedure

The general procedure introduced by King and Middleton[2] for the approximate evaluation of Hallén's integral equation includes the following steps: a) the use of a function approximating the true distribution of current under the sign of integration b) the subsequent definition of one or more expansion parameters in terms of this function and c) the solution of the resulting integral equation or equations by iteration. Depending upon the nature of the particular quantities which are to be evaluated and of the ranges of length and radius over which they are desired, a relatively simple distribution function may prove adequate, or a more complicated one may be required if a large number of terms in the iteration is to be avoided.

In the analysis of the center-driven antenna a simple sinusoidal distribution function (corresponding to the leading term in the component of current in phase quadrature with the driving voltage) is adequate for determining the current and the impedance with considerable accuracy if at least second-order terms are included.[2,3] However, this is true only in a restricted sense as illustrated by the following exceptions.

If the electrical length of the antenna is very small ($\beta h \ll 1$), the component of current in phase with the driving voltage, the resistance, and the conductance are all extremely small, respectively, compared with the quadrature component of current, the reactance, and the susceptance. In order to determine the set of small quantities with an accuracy comparable with that achieved for the large ones, it is necessary to use a complex distribution function which represents the component of current in phase with the driving voltage as well as the quadrature component in the integral. By

* S. H. Dike and D. D. King, "The Absorption Gain and Back-scattering Cross Section of the Cylindrical Antenna," Proc. I.R.E., vol. 40, pp. 853–860; July, 1952.

[1] Cruft Laboratory, Harvard University, Cambridge, Mass.

[2] R. W. King and D. Middleton, "The cylindrical antenna: current and impedance," *Quart. Appl. Math.*, vol. 3, pp. 302–335; January, 1946; vol. 4, pp. 199–200; July, 1946.

[3] D. Middleton and R. W. King, "The thin cylindrical antenna: a comparison of theories," *Jour. Appl. Phys.*, vol. 17, pp. 273–284; April, 1946.

separating the resulting complex integral equation into its real and imaginary parts, two real integral equations are obtained which may be solved individually for the two components of current using an expansion parameter appropriate to each.[4,5] In this manner, accurate values of the resistance and conductance of very short antennas, as well as of the gain and the scattering cross section which depend upon the resistance, may be obtained.

If the antenna is very near resonance, the component of current in phase quadrature with the voltage becomes negligibly small compared with the component in phase with the voltage. In this case, a distribution function consisting only of an approximation of the quadrature current is not adequate if only a few terms in the iteration are available. Thus, even a second-order solution for R_0 may not be very accurate near resonance, whereas it is a good approximation for other lengths.

On the other hand, if a complex distribution function is introduced and two real integral equations obtained, and solved individually with appropriate expansion parameters, a much more accurate determination of the resistance of an antenna near resonance is achieved.[6] Incidentally, it is shown that the leading term in R_0 is of second order when $\beta h = \pi/2$, so that terms of third order must be retained if a first-correction term is to be included. Note that the leading term in X_0 is of zeroth order, the first-correction term of order one.

In the analysis of the center-loaded receiving antenna in a uniform linearly polarized field, similar situations are encountered, but with the added complication of odd, as well as even, currents when the antenna is not parallel to the field. For determining the even part of the current and the entire current in the load, a simple distribution function (consisting of the leading term for the current in phase quadrature with the field, a shifted cosine) is adequate[7,8,9] even for quite short antennas.[4,5] On the other hand, in order to determine the entire current in an antenna inclined with respect to the field, the current must be separated into its even and odd parts, separate symmetrical and antisymmetrical integral equations obtained, and each solved with an appropriate expansion parameter or parameters.[7]

For transmitting or receiving antennas that are long compared with the wavelength, the component of current in phase with the driving voltage or the incident field is always significant, and an accurate solution can not be expected in a few iterations in any general sense unless *both* components of the current are represented in the distribution function. This leads to two real integral equations the solution of which is under study. An alternative procedure for the long-receiving or scattering antenna is to resolve the integral equation into terms depending on the so-called free and forced currents, and to solve these independently using appropriate individual expansion parameters. It is readilv shown[7] that this procedure is equivalent to that of Van Vleck *et al.*[10]

In summary, the fundamental principle of the King-Middleton procedure is to so approximate the current under the sign of integration that, in a given range, the desired quantities are determined to the required accuracy with a relatively small number of iterations. For a very few quantities in limited ranges of antenna length and radius a *first-order* solution, obtained with simple-distribution functions representing only the quadrature component of current, is adequate. For most purposes involving antennas of moderate length, *second-order* solutions involving simple distribution functions are sufficiently accurate. However, for short, and very long antennas, and antennas near resonance, quantities (such as the conductance, resistance, gain, scattering cross section) that depend on the component of current in phase with the voltage or the field, such simple real distribution functions are not adequate and complex functions are required. In some instances quantitative accuracy requires complex distribution functions *and* a third-order solution.

2. The Role of the Expansion Parameter

Instead of improving the over-all accuracy of the solution either by introducing a superior-distribution-function or by carrying the iteration to higher orders, Dike has proposed an arbitrary redefinition of the expansion parameter. This is accomplished by so adjusting its value that the *first-order* gain obtained using the simple sinusoidal distribution function is exactly 1.5 in the limit as βh approaches zero. As has been shown in detail,[4] this procedure does not improve the over-all accuracy of the solution. Indeed, while artificially manipulating the *approximate first-order* formula for the gain to have no error, and thereby reducing the error in the first-order formula for the resistance, this procedure very greatly magnifies the error in the associated reactance. Since for the short antenna the reactance may be thousands of times greater than the very small resistance, the Dike procedure merely shifts

[4] R. W. King, "Theory of electrically short transmitting and receiving antennas," Tech. Rep. No. 141, Cruft Laboratory, Harvard University; March, 1952.

[5] R. W. King, "Theory of electrically short transmitting and receiving antennas," *Jour. Appl. Phys.*, vol. 23, pp. 1174–1187; October, 1952. (This paper is like the previous[4] but does not include the appendix dealing specifically with Dr. Dike's work.)

[6] R. W. King, "An alternative method of solving Hallén's integral equation and its application to antennas near resonance," Tech. Rep. No. 154, Cruft Laboratory Harvard University; September, 1952. Also *Jour. Appl. Phys.*; February, 1953.

[7] R. W. King, "Notes on Antennas," Ch. IV. Mimeographed at Cruft Laboratory, Harvard University; 1949. (A copy of this chapter was supplied to Dr. D. D. King for use by Dr. Dike in his research.) To be published under the title, "Theory of Linear Antennas," by Harvard University Press.

[8] R. W. King, "Graphical representation of the characteristics of cylindrical antennas," Tech. Rep. No. 10, Cruft Laboratory, Harvard University; October, 1947.

[9] R. W. King, "An improved theory of the receiving antenna," Proc. I.R.E., vol. 40, pp. 1113–1120; September, 1952.

[10] J. H. Van Vleck, F. Bloch, and M. Hammermesh, "Theory of radar reflection from wires or thin metallic strips," *Jour. Appl. Phys.*, vol. 18, pp. 274–294; March, 1947.

the large error from the small quantity to the large one where it is least desired.

As pointed out under 1) and in greater detail elsewhere,[4,5] the relatively great error (up to 15 per cent) in the *first-order* resistance, gain, and scattering cross section is a direct consequence of using an inadequate distribution function. Significantly, *all* quantities are improved in accuracy when this is corrected. It appears, therefore, that the Dike procedure has no mathematical foundation and accomplishes no practically useful purpose. It does not get to the root of the problem.

Dike's further suggestion[11] that something must be wrong with the King-Middleton procedure because the first-order solutions for the gain—obtained, on the one hand, by solving the receiving antenna using a real shifted-cosine distribution function and, on the other hand, by solving the transmitting antenna using a real sinusoidal distribution function—are not the same has been answered in detail elsewhere.[4] In brief, failure of two independent approximate formulas to agree *exactly* is not a shortcoming of the King-Middleton procedure, but is a characteristic of *all approximate* methods.

Consistency requires that the gains calculated from the two formulas should agree within the accuracies achieved by the two different first-order approximations, and no more. Dike's further attempt to establish that the expansion parameters for the simple transmitting and receiving cases must be equal by *equating* the two different first-order *approximations* of the gain also has been disproved.[4] The two expansion parameters must, in fact, be different if consistent results are to be obtained using *correct* values for all quantities involved.

3. Limitations of First-Order Solutions

The fact that Dike refers specifically to "difficulties in the King-Middleton type of *first-order* solution" (italics by the writer) is interesting. For the alleged difficulties are, indeed, characteristics of the first-order property and not of the King-Middleton procedure. It is not clear why Dike is surprised and distressed by the failure of a *first-order* solution using the simplest of distribution functions to give highly accurate results for all quantities over a wide range of lengths and radii.

In the very first presentation of the procedure[2] the limitations of a first-order solution were pointed out. Clearly, the fact that different expansion parameters yield different *first-order* scattering cross sections (Fig. 13 in Dike and King) is not a manifestation of a difficulty in the method of solution but, rather, a clear and positive indication that a first-order solution using these parameters is inadequate. Either more terms must be used in the iteration, or an expansion parameter must be determined in a solution using a more accurate distribution function.

[11] S. H. Dike, "Difficulties with present solutions of the Hallén integral equation," Tech. Rep. No. 14, Radiation Laboratory, Johns Hopkins University; June, 1951.

The inadequacy of the simple shifted-cosine distribution for long-receiving and scattering antennas also is shown by the work of Tai[12] using a variational rather than an iteration procedure. Since the Van Vleck formula, in effect, uses two different expansion parameters for the free and the forced parts of the current, it is not entirely surprising that it yields slightly better results for the longer and thicker antennas. Note that when $\beta h \leqq 4$ the Van Vleck formula is in good agreement with the first-order results from the King-Middleton formula using the shifted-cosine distribution function. This is shown graphically in Fig. 1. Over this range, and especially for the thinner antennas in which the in-phase component of the current is relatively smaller, the simple first-order formula yields surprisingly accurate results as is further verified under (4).

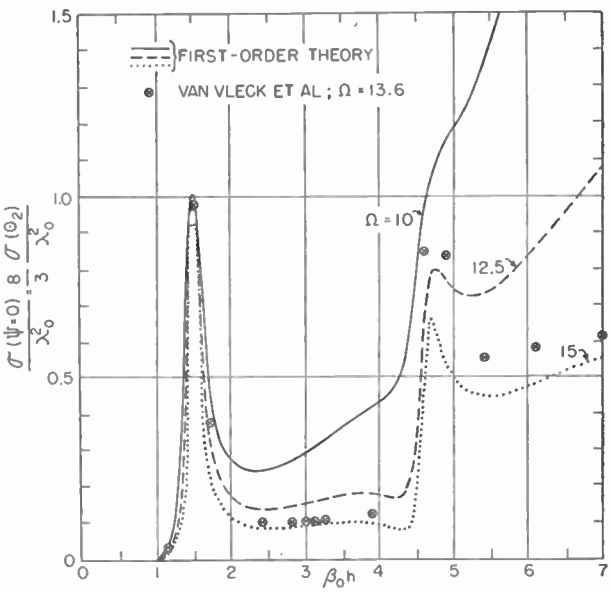

Fig. 1—Theoretical curves of the broadside back-scattering cross section of cylindrical antennas according to the formula of Van Vleck *et al.*, and the first-order formula of King and Middleton using a real sinusoidal distribution function: $\Omega = 2\ln(2h/a)$.

4. The Accuracy of the Experimental Results of Dike and King

A highly accurate set of data on back scattering from various obstacles including single antennas and simple arrays of antennas has been completed recently by Sevick.[13,14] Instead of using the time-consuming standing-wave-ratio method which requires the accurate measurement of a small change in a given signal, a more rapid and accurate procedure was developed. Its essential feature is the use of a coaxial hybrid junction to inject a signal into the circuit of the measuring probe

[12] C. T. Tai, "Radar response from thin wires," Tech. Rep. No. 18, S.R.I. Proj. No. 188, Stanford Research Institute; March, 1951

[13] J. Sevick, "An experimental method of measuring back-scattering cross sections of coupled antennas," Tech. Rep. No. 151, Cruft Laboratory, Harvard University; March, 1952.

[14] J. Sevick, "Experimental and theoretical results on the back-scattering cross section of coupled antennas," Tech. Rep. No. 150, Cruft Laboratory, Harvard University; March, 1952.

which cancels exactly the signal received from the transmitter *in the absence* of the scatterer. When the scattering antenna to be tested is placed in position, the new signal measured by the small, carefully calibrated probe is precisely that produced by the currents in the scattering antenna *alone*. Using a wavelength of 10 cm, a silvered scattering antenna erected on an outdoor-ground screen of sheet aluminum 36-ft square, and continuous monitoring, Sevick obtained the experimental data presented in Fig. 2. The ratio of the length of the

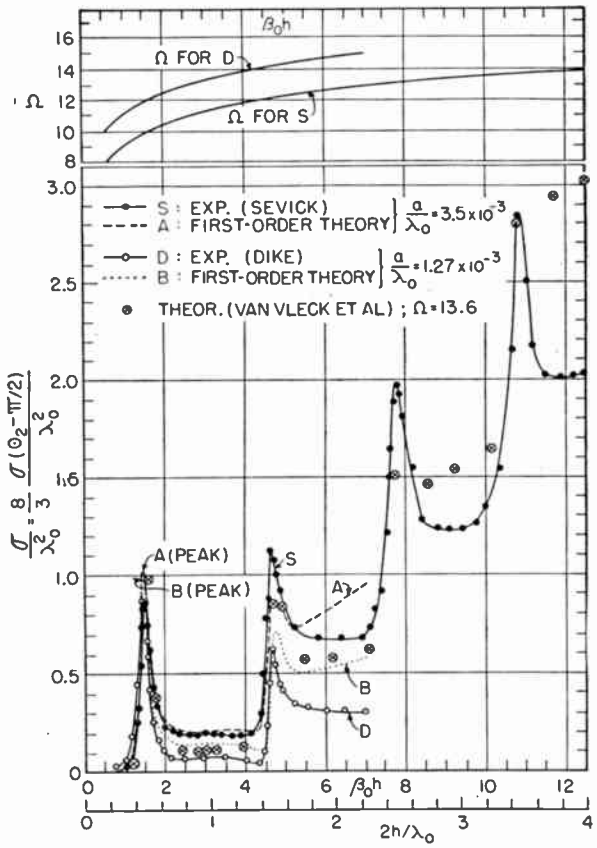

Fig. 2—Experimental and theoretical curves of the broadside back-scattering cross section of cylindrical antennas of constant radius.

small-measuring probe to the distance from the scatterer was only 0.008. The apparatus was checked using metal hemispheres of different sizes as standards.

Consistently excellent agreement was achieved, both with the well-known theoretical values of back-scattering cross section, and with the independently obtained experimental values of Aden[15] who used the same set of hemispheres and the standing-wave-ratio method. The accuracy of the apparatus was verified further by the close agreement between the measured back-scattering cross section of an array of two parallel antennas as a function of separation and orientation and a new theoretical treatment.[14,16] Since $\beta h = \pi/2$ and π in the measured and theoretical results, good and simple trial functions were available.

All evidence thus indicates that the great care exercised by Sevick in the design, operation, and standardization of his apparatus was rewarded by uniformly accurate results.

By interpolating between the curves of Fig. 1, the theoretical curve for the first-order King-Middleton formula was obtained for $a/\lambda = 3.5 \times 10^{-3}$ and plotted in Fig. 2. *Good agreement with Sevick's curve is evident* over the range of electrical length for which βh is less than $3\pi/2$, a range for which the simple-distribution function used in the first-order results in Fig. 1 may be expected to be satisfactory. The theoretical points calculated from Van Vleck's formula also are shown, but since they correspond to a fixed value of $\Omega = 2 \ln (2h/a) = 13.6$, they are not directly comparable with the experimental curve below $\beta h = 7$. However, since the Van Vleck formula is seen in Fig. 1 to agree well with the first-order King-Middleton formula over this range, it must, in fact, be in agreement with Sevick's experimental results. For longer antennas the Van Vleck formula evidently yields only the correct order of magnitude and does not correctly represent the details of the curve.

The measurements of broadside back-scattering made by Dike as reported by Dike and King[17,18] also are shown in Fig. 2, together with the corresponding first-order theoretical curve interpolated from Fig. 1 for the appropriate value of a/λ. Since Dike's measurements are relative, they have been normalized to agree with Sevick's experimental curve at the first resonance. With due regard for the differences in radii of the antennas, Dike's measurements evidently are not in good agreement with either Sevick's measured values or the theoretical curve. In fact, the scattering cross section determined by Dike lies well below *all* other values when βh exceeds $\pi/2$.

Dike also made his measurements at $\lambda = 10$ cm, but on an indoor-ground screen only 8×12 ft in size and, according to his photograph,[17] more or less surrounded by walls and furniture. He used large horns for both transmitter and receiver, the latter placed at right angles to the former. The ratio of maximum dimension of either horn to the distance from the scatterer was about 0.15, almost 20 times the same ratio in Sevick's measurements. There is no indication that the scattering antenna used by Dike was silvered. Since Sevick found that a very large ground screen completely removed from walls and other obstacles, silvered scatterers, and a very small receiving probe at a very large distance from the scattering antenna and from the transmitter are essential if accurate results are to be obtained, it

[15] A. L. Aden, "Electromagnetic scattering from spheres with sizes comparable to the wavelength," *Jour. Appl. Phys.*, vol. 22, pp. 601–605; May, 1951.

[16] J. Sevick, "Experimental and theoretical investigation of the back-scattering cross section of coupled antennas," Ph.D. dissertation, Harvard University; June, 1952.

[17] S. H. Dike and D. D. King, "The cylindrical dipole receiving antenna," Tech. Rep. No. 12, Radiation Laboratory, Johns Hopkins University; May, 1951.

[18] S. H. Dike and D. D. King, "The absorption gain and the back-scattering cross section of the cylindrical antenna," PROC. I.R.E., vol. 40, pp. 853–860; July, 1952.

seems legitimate to question the accuracy of Dike's measurements. Evidently, this applies as well to his measurements of broadside gain as of broadside back-scattering cross section.

Conclusion

The present discussion and the references upon which it is based suggest that Dike's theoretical arguments are not well founded and that his experimental measurements are not sufficiently accurate to permit their use as exclusive evidence in drawing definitive conclusions. He is, of course, correct in noting that first-order formulas derived using simple, real distribution functions do not yield highly accurate results for all quantities over an unlimited range of lengths and radii of the antennas. It is not clear why he should have expected anything else.

When properly applied and correctly interpreted, the King-Middleton type of solution leads to quantitatively useful and experimentally verifiable theoretical formulas for quantities and over ranges appropriate to the particular formulation. To date it has not been applied successfully to very long antennas primarily owing to the mathematical complications encountered in the use of adequate distribution functions and the evaluation of sufficient terms in the complicated integrals of higher-order iteration.

S. H. Dike:[19] Part 2 of R. W. King's discussion above does not apply directly to the paper under discussion, but to a paper appearing in another journal.[20] The statement that "Dike has proposed an arbitrary redefinition of the expansion parameter" is contrary to fact. Since the King-Middleton first-order solution for gain does not reduce to 1.5 in the limit of $\beta h = 0$, it was simply pointed out that it would do so if the expansion parameter had a particular value for very small βh. The calculation of gain using the integration of the Poynting vector for the total radiated power, yields the value 1.5 for $\beta h \rightarrow 0$ at constant Ω for any continuous even-current distribution, and in particular, for Hallén's solution—regardless of the choice of the expansion parameter.

This is simply the result of the fact that in the limit of zero length, only a dipole moment can exist. The statement is made in the paper[20] that this situation makes it appear "that an additional requirement should be imposed on the expansion parameter that has not previously been considered." As a result of this statement, an "improved" expansion parameter for very small βh is presented by R. W. King.[4] It is of interest to point out that the R. W. King "improved" parameter[4] gives errors in gain and back-scattering cross section for matched load, for $\beta h \rightarrow 0$, which are greater than those obtained using the original King-Middleton parameter. In the "improved" case, the error in the latter quantity is over 20 per cent! There are, incidentally, numerous errors in the appendix tables of the R. W. King paper[4] arising from an error in computing ψ in Eq. (41) of the paper.[20] For example, the "error" in effective length, using this value of ψ, is 1.46 per cent instead of 9.8 per cent.

As to the equality of expansion parameters for the receiving and driven case, the implication in R. W. King's discussion that the difficulty is restricted to low-order approximations is not so. The problem is the same for all orders of solution. One will always get two values for effective length unless the two parameters are the same. It is certainly desirable not to violate the principle of reciprocity even in approximate solutions.

There appears to be no reason to doubt the validity of Sevick's measurements. Nor is there any real reason to seriously doubt the accuracy of the measurements reported in the Proceedings paper.[18] These latter measurements were not made using a "time-consuming standing-wave-ratio method" as implied by R. W. King. The method used is basically the same as, but simpler than, that used by Sevick. By careful and precise positioning of the scattering receiver antenna, sufficient decoupling from the source field was obtained to obviate the need for the obvious magic-tee scheme for cancelling out this unwanted field. Several possible sources of error were thereby eliminated. As in Sevick's work, the field seen by the receiver was that due to the scatterer alone.

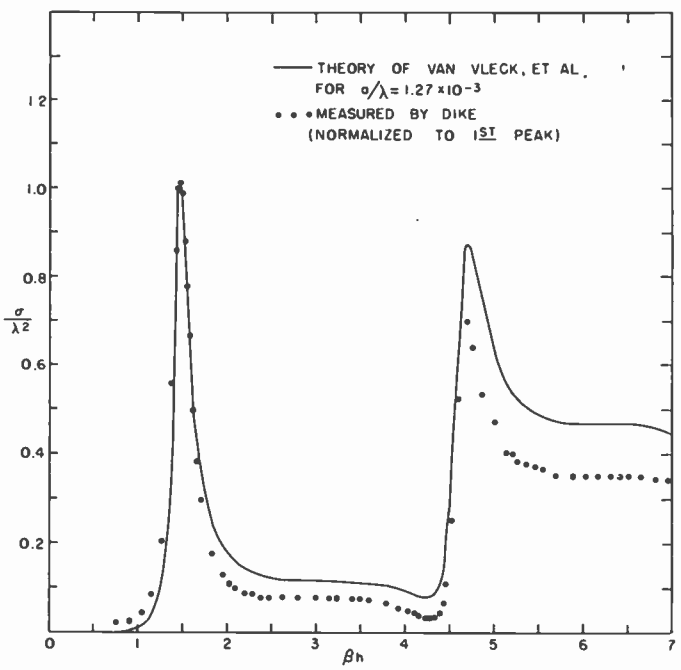

Fig. 3—Broadside back-scattering cross section of unloaded 0.010-inch diameter dipole ($a/\lambda = 1.27 \times 10^{-3}$)

The two sets of measurements are compared to Van Vleck's theory[10] in Figs. 3 and 4. Agreement is good in both cases, especially since, as R. W. King is careful to

[19] Sandia Corporation, Albuquerque, New Mexico.

[20] S. H. Dike, "Difficulties with present solutions of the Hallén integral equation," *Quart. of Appl. Math.*, vol. 10, pp. 225–241; October, 1952.

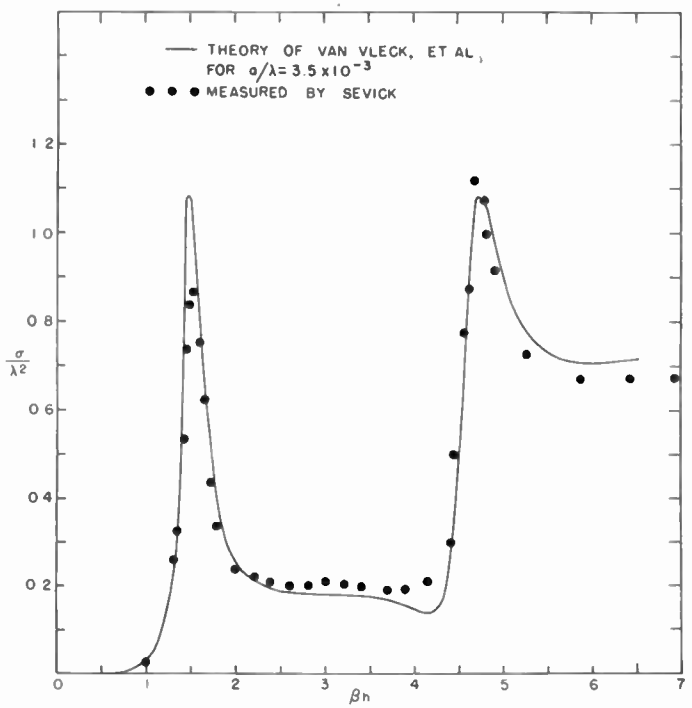

Fig. 4—Broadside back-scattering cross section of unloaded dipole ($a/\lambda = 3.5 \times 10^{-3}$).

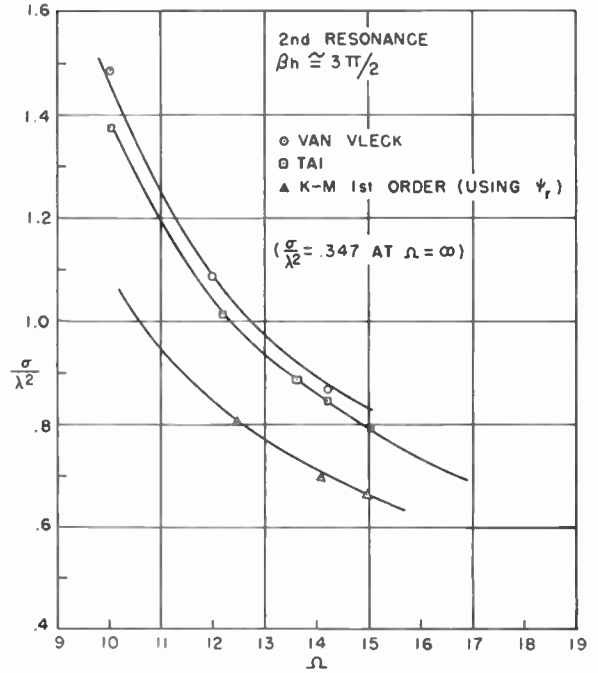

Fig. 6—Comparison of solutions for broadside back-scattering cross section of unloaded dipole at second-resonant length.

point out, the theory curves are only first-order approximations. Interpolation between the two sets of measurements presented as Figs. 9 and 10 in the paper under discussion yields points for $a/\lambda = 3.5 \times 10^{-3}$ which, when plotted on Fig. 4, agree with the theory equally as well as Sevick's points. The differences among the solutions of Van Vleck, King and Middleton, and Tai (using the trial function of Eq. (31) in the Tai paper[12]) are illustrated in Figs. 5, 6, and 7. The Tai solution is quite different from the other two at first resonance; otherwise Tai and

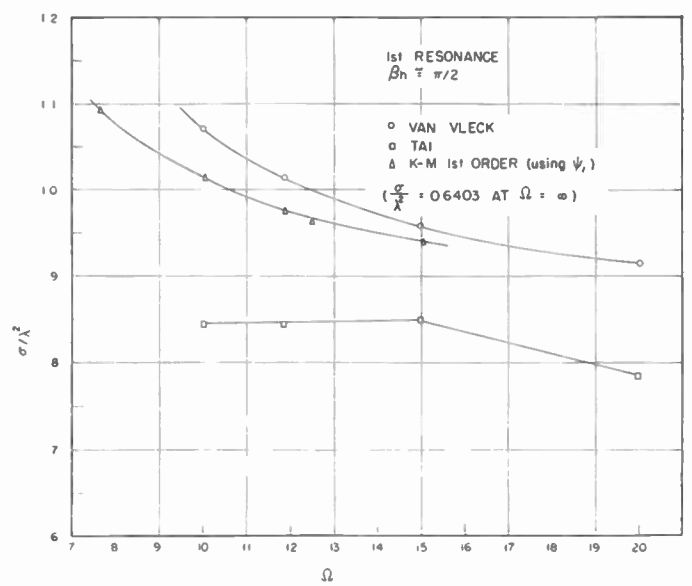

Fig. 5—Comparison of solutions for broadside back-scattering cross section of unloaded dipole at first-resonant length.

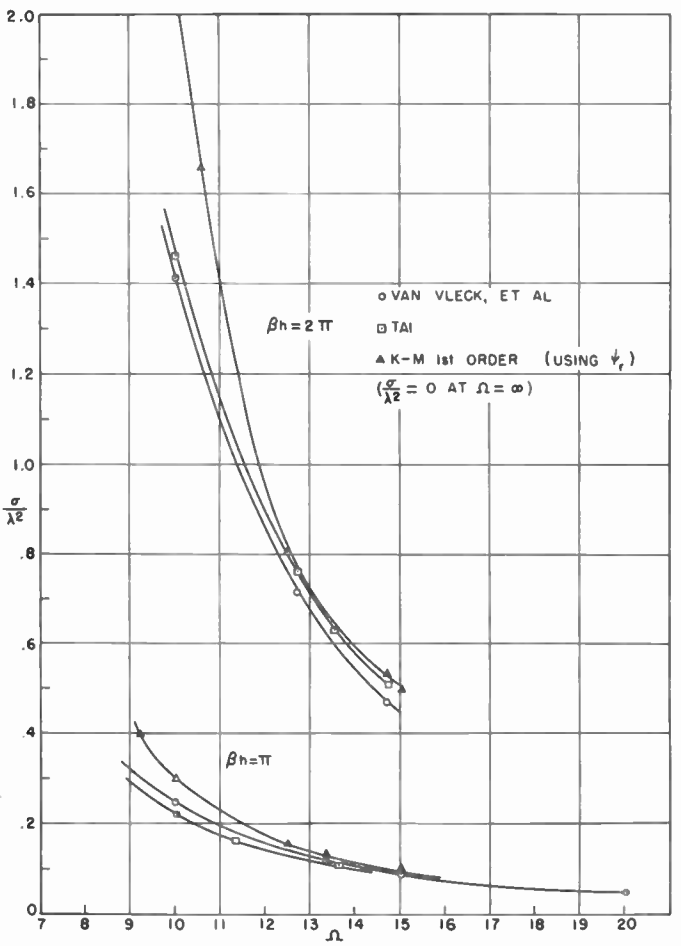

Fig. 7—Comparison of solutions for broadside back-scattering cross section of unloaded dipole at $\beta h = \pi$ and $\beta h = 2\pi$.

Van Vleck agree closely with each other but not particularly well with the solution of King and Middleton.

It is hard to understand why R. W. King so violently defends his particular method of choosing the expansion parameter when it is just as arbitrary as the method of Hallén or Miss Gray. At first sight the argument of King and Middleton sounds plausible, but one finds that it is invalidated when it leads to an expansion parameter which becomes infinite at some points and when it becomes necessary to make an arbitrary modification. The final choice is such that it yields curves such as Fig. 10 in paper[9] (or Fig. 7 in paper[4]) for absorption gain. It is likely that the indicated behavior near resonance in this figure is both contrary to reality and not obtained using other suggested expansion parameters.

A defense of any particular solution method of Hallén's integral equation is difficult to establish since as a mathematical problem this equation has no solutions.[21] A more precise statement is that, in the equation

$$\int_{-h}^{h} r^{-1}e^{-i\beta r}I(\xi)d\xi = C_1 \cos \beta z + C_2 \sin \beta |z| + C_3 \int_0^z I(\xi) \sin \beta(z-\xi)d\xi, \quad (1)$$

where

$$r = \sqrt{(z-\xi)^2 + a^2}, \quad (2)$$

and where C_1, C_3, $C_2 \neq 0$, $\beta \neq 0$, $a > 0$, and $h > 0$ are arbitrarily given constants, *there is no function $I(z)$ that is Lebesgue integrable on the interval $[-h, h]$, where $-h \leqq z \leqq h$, such that (1) holds on this interval*, it being understood that the integrals of (1) are considered as Lebesgue integrals.[22] The proof of this statement is elementary; it is independent of the conditions that $I(\pm h) = 0$ and $I(z) = I(-z)$, and it consists simply of showing that the terms involving integrals in (1) define continuous functions of z having continuous derivatives on $[-h, h]$, whereas the remaining terms define a continuous function which fails to have a derivative at $z = 0$.

The non-existence of a solution of (1) does not preclude the possibility that the actual physical problem is characterized by an integral equation whose individual terms are closely approximated by (1). Hence certain methods of approximation applied to (1) might give results "close" to the solution of the actual problem. Schelkunoff states that the Hallén-type of series solution for (1) must be divergent.[21]

[21] S. A. Schelkunoff, "Advanced Antenna Theory," John Wiley and Sons, Inc., New York, N. Y., p. 149; 1952.

[22] This fact was first pointed out to the writer by Dr. W. T. Reid of Northwestern University (after Refs. 18 and 20 were written).

Thus it would appear that it is to be expected that certain difficulties should exist with past solution attempts. Similarly it would seem, for example, that the words "true distribution" and "exact values" used in paper[4] can hardly be justified.

Ronold King: Since Dike's conclusions depended upon his other paper,[11,20] it was necessary to consider this in the discussion. Note also that the discussion was submitted to Dike for reply almost six months ago when his paper[20] had not appeared in print, and that the journal in which it is published does not accept discussions.

5. More About the Expansion Parameter

a. Dike's Parameter and the Improved King-Middleton Parameters

Dike has made no reply to the criticism of his modification of the expansion parameter, but he objects to have it called a redefinition. Does not the imposition of an additional requirement which produces an entirely different quantity constitute a redefinition?

In his comments regarding the improved King-Middleton expansion parameters, Dike has omitted pertinent facts. It is made very clear in the paper[4] that the new parameters are improved in the sense that they lead to better approximations of the *principal* quantities—the reactance in the case of transmission, the normalized current in the case of reception. Moreover, a major conclusion in the paper[4] is that the determination of the very small resistance of the short antenna (upon which the gain and scattering cross section depend) *can not be improved simultaneously* with the reactance simply by redefining the expansion parameter (as Dike has attempted to do!). It is precisely for this reason that another method is developed in paper[4] for determining accurate values, not only of the principal quantities, but of all relevant quantities including the gain and scattering cross section. This method is outlined briefly in Part I of the discussion.

As indicated by Dike an incorrect value of the modified expansion parameter introduced by Dike[11,20] was used inadvertently in the formulas for the normalized current and effective length in the appendix of paper.[4] The correct value of Ψ (Dike) is 9.74 instead of 7.375. This reduces the error in the Dike value for the effective length from 9.8 to 1.46 per cent as Dike has reported. However, he fails to indicate that it also *increases* the error in the normalized current from 1.7 to 10.1 per cent. Since the comparison of important quantities for the short transmitting and receiving antennas reported in the paper[4] has never been published and has several errors, and since Dike has brought them into this discussion, it is appropriate to tabulate them here in corrected form.

In Table I the resistance R_0 and reactance X_0 of the short transmitting antenna; the normalized current

u_0', the effective electrical length $\beta_0 h$, and the gain D of the short receiving antenna are given with numerical factors calculated for $\Omega = 2 \ln (2h/a) = 10$. The second column gives the accurate and completely consistent values obtained in the papers.[4,5] The third column lists the first-order values obtained from the King-Middleton formula when the single expansion parameter recommended by Dike is substituted arbitrarily. The fifth column gives the values obtained in the improved theory using the expansion parameter Ψ_{Dt} for the transmitting antenna and the different expansion parameter Ψ_{Dr} for the receiving antenna as derived in the papers.[4,5]

It is seen that for the principal quantities X_0 and u_0' the Dike values involve large errors, the King-Middleton values very small errors. On the other hand, the inverse is true of the very small resistance R_0 and the gain D which depends upon it.

In Tables II and III are the first-order reactance $[X_0]$, and the first-order normalized current $[u_0']$, (with convenient factors) as determined using several expansion parameters. Note that X_0 depends only on the transmitting parameter Ψ_t, u_0' only on the receiving parameter Ψ_r. In the formulations of Dike and Hallén the two parameters are the same.

Since for short antennas the expansion parameter defined by Dr. Dike differs little from the value of Ω (when $\Omega = 10$, Ψ (Dike) $= 9.74$) it can not differ greatly from Ω for longer antennas. However, since it is well known that the *first-order* formulas using Ω as the parameter are quantitatively inadequate in determining the impedance and effective length of antennas of all lengths, it follows that essentially the same situation must obtain if the Dike parameter is used.

TABLE I

$\Omega = 10$	*Exact* (References 4, 5)	First-order Dike: $\Psi = 9.74$ (References[4,11,20])	% Error	Improved King-Middleton-First-order: $\Psi_{Dt} = 6.61$ $\Psi_{Dr} = 7.0$ (References[4,5])	% Error
X_0	$\frac{-6.60 \times 60}{\beta_0 h}$	$\frac{-7.375 \times 60}{\beta_0 h}$	11.7	$\frac{-6.61 \times 60}{\beta_0 h}$	0.15
R_0	$18.3\beta_0^2 h^2$	$18.8\beta_0^2 h^2$	2.2	$20\beta_0^2 h^2$	9.3
u_0'	$\frac{\beta_0^2 h^2}{60 \times 6.90}$	$\frac{\beta_0^2 h^2}{60 \times 7.60}$	10.1	$\frac{\beta_0^2 h^2}{60 \times 7.0}$	1.4
$\beta_0 h_e$	$0.478\beta_0 h$	$0.485\beta_0 h$	1.46	$0.472\beta_0 h$	1.3
D	1.500	1.500*	0*	1.337	10.9

* Dike's expansion parameter ψ is chosen to make $D = 1.500$.

TABLE II

First-Order Reactance $[X_0]_1$

Ψ_t	$\frac{-\beta h [X_0]_1}{60}$ for $\Omega = 10$; $\beta_0 h \ll 1$	% Error
Exact (formula 17 in References[4,5])	6.60	
$\Psi_{Dt} = \Omega - 2 - \ln 4$ (Improved King-Middleton)	6.614	0.15
$\Psi_{K1} = \Omega - 2$ (King-Middleton)	6.819	3.3
$\Omega - 2 \ln 2$ (Gray)	6.991	5.9
ψ (Dike)	7.375	11.8
Ω (Hallén)*	7.470	13.2
Static Capacitance, $\Omega - 2.485$ (spheroid)	7.515	13.8

* It is to be noted that Hallén never recommended the use of *first-order* formulas using this parameter.

TABLE III

First-Order Normalized Current $[u_0^1]_1$ in Receiving Antenna

Ψ_r	$\frac{\beta_0^2 h^2}{60 [u_0^1]_1}$ for $\Omega = 10$; $\beta_0 h \ll 1$	% Error
Exact (formula 50 in References[4,5])	6.90	
$\Psi_{Dr} = \Omega - 3$ (improved K.M. for receiving antenna)	7.00	1.4
$\Psi_{Dt} = \Omega - 2 - \ln 4$ (improved K.M. for transmitting antenna)*	7.02	1.7
$\Psi_{K1} = \Omega - 2$ (K.M. for transmitting antenna)*	7.11	3.5
$\Psi_{U1} = \Omega - 1$ (K.M. for receiving antenna)	7.36	6.7
ψ (Dike)	7.60	10.1
Ω (Hallén)†	7.69	11.5

* These parameters are not obtained from an analysis of the receiving antenna. They are included to show how they compare if introduced arbitrarily.
† Hallén never recommended the use of *first-order* formulas using this parameter.

b. *Reciprocity and the Equality of Parameters*

If transmitting and receiving antennas are analyzed separately for mutually independent quantities, and the reciprocal theorem is applied in order to compare two independently determined expressions for the effective length, it is contradictory to assert that these results can be consistent only if the same expansion parameter is used. By definition two solutions are independent only if there are no conditions relating them.

It is shown in the paper[2] that the King-Middleton solution reduces exactly to that of Hallén with Ω as the expansion parameter if an infinite number of terms is used. Since in the analysis of Hallén the *same* expansion parameter occurs for both transmitting and receiving antennas, it is clear that Dike's own criterion for a single-valued effective length is satisfied. For a finite number of terms the King-Middleton solutions yield somewhat different effective lengths because both are approximate and independent.

It is shown in the paper[4] that by using *different* parameters for the short transmitting and receiving antennas the same and correct value of the effective length is obtained.

In general, it is not true that approximate solutions *must* be made to satisfy reciprocity exactly (rather than within the errors of the approximations) at the expense of large errors in principal quantities.

c. Defense of King-Middleton Parameters

Far from defending a particular method of choosing an expansion parameter, the discussion in Part 1 emphasizes that the method and the choice are best adapted to the particular quantity that is to be determined. The comparison in Tables II and III is illuminating in this respect. For the reasons advanced in Part 2 the only defense proposed is against arbitrary modifications such as the one made by Dike.

Dike's assertion that the expansion parameter of King and Middleton "becomes infinite at some points" is incorrect. Actually it is always less than the corresponding value of Ω which is finite for all non-zero radii. Dike's statement appears to be a free quotation from p. 146 of paper[21] where, however, it is not the constant expansion parameter Ψ that is under discussion, but the *variable function* $\Psi(z)$ which is used in the determination of Ψ. While it is true that $\Psi(z)$ becomes infinite for certain values of z along antennas that are sufficiently long *when a zeroth-order current* is used in its definition, these points are never chosen as the reference values in the definition of the expansion parameter. Moreover, in the original paper[2] (p. 315), King and Middleton are careful to show that when a better approximation of the current is used in the definition of $\Psi(z)$ *no* infinites occur along the antenna. Furthermore, the values of this function at the reference values which determine Ψ differ negligibly from those obtained using the zeroth-order current. It follows that the definition of the always finite expansion parameter Ψ is equivalent to one involving a likewise always finite function $\Psi(z)$.

6. Solution of the Integral Equation

The singularity at $z=0$ referred to and discussed by Dike in the last three paragraphs of his reply does not exist in the correct formulation of the integral equation of a cylindrical antenna driven from a *physically realizable* circuit such as a transmission line. This is discused in the paper.[23] Strictly, the integral equation for the current in an antenna driven, for example, from a two-wire line with spacing 2δ should not be written with the limits $-h$ to h in the integral but rather with the limits $-h$ to $-\delta$, δ to h. Moreover, it should be solved *simultaneously* with the corresponding equation for the current in the transmission line.

If the spacing 2δ of the line is sufficiently small, an approximate solution of the simultaneous integral equations may be obtained by solving each as if independent of the other, and providing an appropriate correction in the form of a lumped network at the junction to take account of the thus neglected coupling and end effects. In the physically unavailable limit of a transmission line consisting of two insulated conductors at near zero spacing ($\delta \doteq 0$), the line may be replaced by a fictitious, localized source of emf, *provided* this has, by definition, the essential properties of the closely spaced transmission line in maintaining the driving voltage. The solution of this problem does not involve any divergence.

The divergence discussed[21] is a consequence of the implicit assumption of a *physically impossible* driving mechanism concentrated at $z=0$. The solution for the current in the integral equation with limits $-h$ to h used as an approximation of the current in an actual antenna driven from a closely-spaced transmission line only insofar as it is unaffected by the divergence at $z=0$. Mathematical difficulties resulting from the divergence at $z=0$ are irrelevant to any physically meaningful problem since their origin lies in the arbitrary introduction of a boundary condition that has no counterpart in reality.

S. H. Dike: It appears necessary to point out again that paper[20] does not recommend any particular new expansion parameter. Statements implying otherwise in King's discussion should be disregarded.

The next-to-last statement in part (5b) above is misleading since it implies that paper[4] shows that the "same and correct value of the effective length" is obtained from either of the definitions of this quantity (Eqs. (30) and (36) in paper[20]) even though different expansion parameters are used in the solutions for the driven and receiving current distributions. This, paper[4] does *not* show, since effective length in this reference is nowhere calculated using the driven distribution alone. Neither do the various "exact" relations contain expansion parameters as such.

It is of interest to find that the calculation of broadside effective length from Eq. (30) of paper[20] (or from Eq. (13) in paper[18]) using for the current the "true distribution" of Eq. (35) in paper,[4] yields the value of 0.47942 βh instead of 0.47825 βh given in Eq. (53a), of the paper.[4]

Of course, the five-decimal-place-accuracy implication is ridiculous, but since the driven-current result involves an integration of the current, rather than a specific terminal value, it might be considered by King as a "more exact" value of effective length. This would then lead to a suitable revision of other quantities. The first-order value of effective length found from the driven current distribution using the "improved" parameter is 0.478 βh.

It is of further interest to note that the first-order value of Z_0 found with the "improved" parameter agrees exactly with that obtained by Tai[24] using a variational method; the value of X_0 agrees with the approximate relation in Schelkunoff and Friis.[25]

King's assertion that a "singularity at $z=0$" in Hallén's equation (Eq. (1) above) is "discussed by Dike" is incorrect. Actually the functions of (1) are always finite for all non-zero radii.

[23] R. W. King, "Antennas and open-wire lines, Part I," *Jour. Appl. Phys.*, vol. 20, pp. 832–850; September, 1949.

[24] C. T. Tai, "A variational solution to the problem of cylindrical Antennas," Tech. Rep. No. 12, SRI Project No. 188, Stanford Research Institute; 1950.

[25] S. A. Schelkunoff and H. T. Friis, "Antennas: Theory and Practice," John Wiley and Sons, Inc., New York, N. Y., p. 306 (eq. 11); 1952.

Correspondence

Note on "The Response of an LCR Circuit"*

I was very interested in reading the paper by Marique[1] on the response of an LCR circuit, especially as I have been recently somewhat concerned with the design of low-frequency spectrum analyzers.[2,3] A few additional notes to Mr. Marique's paper may be useful.

It is an interesting coincidence that still another writer, Hamilton,[4] was working on the problem at the same time as Hok,[5] and Barber and Ursell.[6] Hamilton's solution is quite different and involves the Fourier analysis of the input and output spectra.

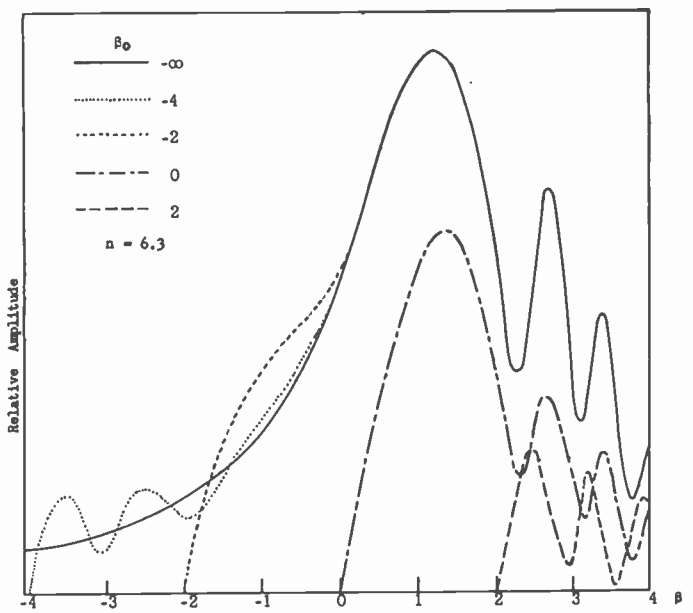

Fig. 1—Response of a resonant circuit to an applied signal varying linearly with frequency.

Marique neglects to mention the case where the initial applied frequency is less than the resonant frequency of the network (for $\epsilon > 0$), but still within its pass band. The response can be found by an extension of the Barber and Ursell work, and typical results are shown in Fig. 1. (β is a generalized and dimensionless time or frequency; n is a measure of the ratio of the rate of sweeping to the square of the bandwidth.) The "oscillations" near the beginning of the sweep have been observed experimentally and were the object of considerable interest and speculation before the theory was solved. The exponential decay at the beginning of a sweep due to nonzero initial conditions has also been observed.

These analyses have all been based on a simple LCR circuit, or more generally, a system which obeys a linear second-order differential equation. It might be possible to find a different network (not necessarily linear or passive) which has similar selective characteristics, but which has a dynamic response similar to the static response for larger values of n.

It might be mentioned that one form of selective circuit using a parallel-T inverse feedback amplifier[2] has a response exactly the same as a simple LCR circuit.

S. V. Soanes
Research Department
Ferranti Electric Ltd.
Toronto, Ont.

* Original manuscript received by the Institute August 21, 1952.

[1] J. Marique, "The response of RLC resonant circuits to EMF of sawtooth varying frequency," Proc. I.R.E., vol. 40, pp. 945–950; August, 1952.

[2] S. V. Soanes, "Some problems in audio frequency spectrum analysis—Part 1," *Electronic Eng.* (London), vol. 24, no. 292, pp. 268–270; June, 1952.

[3] S. V. Soanes, "Some problems in audio frequency spectrum analysis—Part 2," *Electronic Eng.* (London), vol. 24, no. 293, pp. 312–318; July, 1952.

[4] W. H. Hamilton, "The Response of a Tuned Amplifier to a Signal Varying Linearly in Frequency," Proc. NEC (Chicago), vol. 4, pp. 377–396; 1948.

[5] G. Hok, "Response of linear resonant systems to excitation of a frequency varying linearly with time," *Jour. Appl. Phys.*, vol. 19, pp. 242–250; March, 1948.

[6] N. F. Barber and F. Ursell, "The response of a resonant system to a gliding tone," *Phil. Mag.*, vol. 39, pp. 345–361; May, 1948.

Electronic Design for the Military*

Reference is made to the editorial "Electronic Design for the Military."[1] John D. Reid has certainly made a worthwhile point in the comparison between military and civilian electronic equipment reliability. It appears as though he has overlooked two significant points; the military design of terminal board mounting and rectangular wiring greatly simplifies the teaching of servicing techniques. This is a most important item in the present military personnel set-up; all extremely high-grade apparatus, such as good test equipment and telephone company equipment employs much of the same techniques as military construction.

The reference to plugs and sockets for interconnection is well made, and the weakness is recognized by the military. Inasmuch as some type of quick-disconnect devices are required, any design of better device would be acceptable if the requirements enforced by usage could be met. Unfortunately no basically different device is forthcoming.

It is believed that the government services are leading the way to more reliable equipment, rather than lagging. It was first under government sponsorship that the development of more reliable tubes was undertaken. Printed circuits, potted circuits, longer life and higher-rated components all were largely instituted under government cognizance. The environmental conditions for military equipment differ greatly from the requirements for civilian usage. I am sure that engineers working on military electronic equipment will readily adopt any ideas that will provide greater reliability, particularly where factors of human life and millions of dollars hang by a thread as slender as the grid wire in an electron tube.

Albert O. Behnke
Electronics Engineer, U.S.A.F.
A.D.C. Colorado Springs, Colo.

* Received by the Institute, February 16, 1953.

[1] J. D. Reid, "Electronic design for the military," Proc. I.R.E., vol. 41, p. 195; February, 1953.

Analysis of Twin-T Filters*

Through an oversight my recent paper on the parallel-T[1] did not include a reference to "Analysis of Twin-T-Filters" by Louis G. Gitzendanner, *Proc. NEC* (Chicago), pp. 121–128; vol. 6; 1950.

Gitzendanner circumvents a direct solution of the network equations and secures useful results by a study of the losses at low frequencies and at high frequencies. His discussion includes the equal arm-T operated between equal source and load impedances so as to give unequal low and high-frequency losses, and the design of unequal arm-T's between unequal source and load impedances so as to produce equal losses at the low and high frequencies.

Lawrence G. Cowles
The Superior Oil Company
Bellaire, Houston, Tex.

* Received by the Institute, February 13, 1953.

[1] L. G. Cowles, "The parallel-T resistance-capacitance network," Proc. I.R.E., vol. 40, pp. 1712–1717; December, 1952.

Correspondence

Russian Circuit Notations*

Notations of capacitances and resistances on Russian circuit diagrams are confusing to engineers seeing them the first time, since the units are generally omitted.

The following scheme is frequently used for indicating resistances: resistance values from 1 to 999 ohms are indicated by whole numbers without any symbol whatsoever; the numbers 1 to 99 followed by the letter "T" will represent thousands of ohms (the "T" stands for the Russian word "tysiatcha" meaning thousand); values of 100,000 ohms and greater are always given in megohms and are indicated by using a comma, which in Russian indicates the decimal point. Some examples follow:

R6	means	6	ohms
R60	means	60	ohms
R600	means	600	ohms
R6T	means	6000	ohms
R60T	means	60,000	ohms
R0,6	means	0.6	megohm
R6,0	means	6	megohms
R60,0	means	60	megohms

A similar scheme is followed for indicating capacitances: values from 1 to 999 $\mu\mu$f are indicated by the numbers alone, without any unit or symbol; numbers from 1 to 99 followed by the letter "T" indicate capacitances from 1,000 to 99,000 $\mu\mu$f; capacitances of 100,000 $\mu\mu$f and greater are always written with the comma (but without "T"), which means that the values are to be read as μf and not $\mu\mu$f. Some examples:

C6	means	6	$\mu\mu$f
C60	means	60	$\mu\mu$f
C600	means	600	$\mu\mu$f
C6T	means	6000	$\mu\mu$f
C60T	means	60,000	$\mu\mu$f
C0,6	means	0.6	μf
C6,0	means	6	μf
C60,0	means	60	μf

GEORGE F. SCHULTZ
Capehart-Farnsworth Corp.
Fort Wayne, Ind.

* Received by the Institute, January 5, 1953.

Electronic Design for the Military*

Mr. John Reid, in his editorial,[1] has apparently neglected several factors in his comparison between military and commercial design of electronic equipment.

First, it has been clearly shown as the result of carefully controlled vibration, shock and bounce tests, as well as from results obtained in the field, that the flimsy construction and point-to-point wiring techniques used in commercial practice simply do not stand up in military applications.

Secondly, a reasonable degree of neatness is required, but not for its own sake, or in ignorance, as Mr. Reid implies. The twin problems of servicing the tremendous variety of military electronic gear and the training of the ever-changing stream of personnel to do this job are vastly different from the servicing problems of the highly similar radio and television receivers that pass for the "competitive" commercial product of today. A neat layout and the use of terminal boards, for example, are essential to permit the use of a component identifying system, and together, greatly facilitate the servicing of complex military gear.

As for the statement "No reputable manufacturer sacrifices reliability for price consideration," I will allow it to pass since the booming television service industry is in a far better position to make comment

HERBERT BUTLER
Radio Engineer, Evans Signal Lab.
Fort Monmouth, N. J.

* Received by the Institute, February 17, 1953.
[1] J. D. Reid, "Electronic design for the military," PROC. I.R.E., vol. 41, p. 195; February, 1953.

More on the Sweep-Frequency Response of RG/6U Cable*

In a recent letter[1] Blackband commented on the data on sweep-frequency response of RG/6U cable which were published in an earlier paper[2] as an example of the sweep-frequency measurement method.

Blackband's letter and other correspondence received indicate that the wording in the original article, "The irregularity of the measurement trace shows clearly the frequency dependence and irregularity of the characteristic impedance of RG/6U cable, a common fault of all coaxial cables," can be misinterpreted and is in need of elaboration.

A perfectly manufactured cable terminated with a fixed impedance in value close to the asymptotic value of the characteristic impedance of the cable would exhibit an input resistance and reactance change with frequency characterized approximately by a smoothly decaying sinusoid (which Blackband refers to as "periodicity"). The "irregularity" referred to in the original paper was meant to apply to the marked deviation of the curves shown from a smoothly decaying sinusoid and not to the basic sinusoid as such. Cables of perfectly constant characteristic impedance from low to high frequency have yet to be realized in practice for reasons indicated by Blackband: thus, unless the cable is terminated in a perfect "artificial cable," even an ideally manufactured cable would exhibit "periodicity" because of mismatch of cable and termination.

In the curves published in the earlier paper the experimental error was negligibly small. The deviations from a smooth sinusoid were traceable almost entirely to diameter irregularities of the extruded polyethylene surrounding the inner conductor. Fig. 1 shows measurements of the polyethylene outer diameter for two different RG/6U cable samples. These data were furnished by W. J. King of Bell Telephone Laboratories.

The application of sweep vector impedance measurement to cables has proven very valuable in ascertaining the quality of cables before installation in critical applications. A rapid visual qualitative appraisal can be made of basic characteristic impedance by observing the general amplitude of the sinusoid and of the smoothness of the cable by observing the irregularities of the sinusoid. For instance, one might infer from the original publication that the cable involved had a basic asymptote of about 76 ohms, about 78- to 79-ohms characteristic impedance at 1 mc, and about 80 ohms at even lower frequencies, which coincides with Blackband's conclusions. A further significant observation is the increasing irregularity of the sinusoid with frequency. This reflects the increased electrical length of the cable in terms of wavelengths resulting in decreased dependence of the cable input impedance on the terminating impedance.

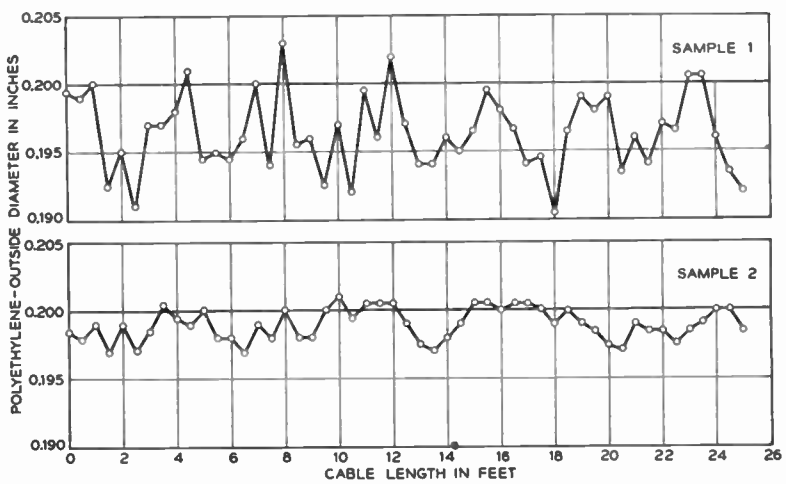

Fig. 1

D. A. ALSBERG
Bell Telephone Laboratories, Inc.
Murray Hill, N. J.

* Received by the Institute, October 20, 1952.
[1] W. T. Blackband, "The sweep-frequency response of RG-6/U," PROC. I.R.E., vol. 40, pp. 995–996; August, 1952.
[2] D. A. Alsberg, "A precise sweep-frequency method of vector impedance measurement," PROC. I.R.E., vol. 49, pp. 1393–1400; November, 1951.

Correspondence

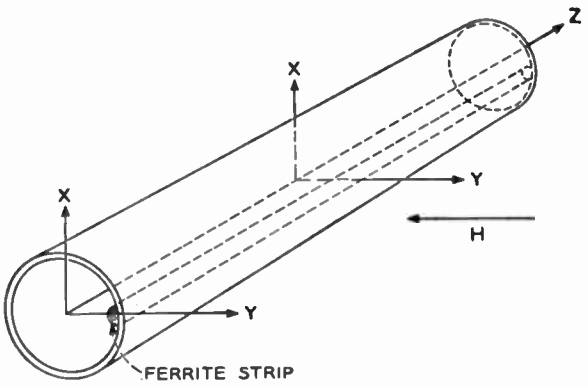

Fig. 1

A New Non-Reciprocal Waveguide Medium Using Ferrites*

A new non-reciprocal waveguide medium using ferrites has been constructed. A piece of ferrite placed on the sidewall of a waveguide and subjected to a transverse external magnetic field produces the effect. The non-reciprocal property is exhibited as a difference in phase constant for the two directions of transmission or, in general, as a non-reciprocal birefringence in round waveguide. This contrasts with the anti-reciprocal rotation obtained using a longitudinal field on an axially symmetric ferrite piece as in Hogan's scheme.[1]

In Fig. 1 we show the disposition of a strip of ferrite in dominant-mode circular guide: the ferrite is parallel to the guide axis and is at $X=0$, $Y=R$, where R is the guide radius. With no applied magnetic field, we can characterize propagation in this waveguide by means of an ellipse which we call the β-ellipse shown in Fig. 2a. This is analogous to a section of the indicial ellipsoid of optics. A wave whose principal electric vector is parallel to $X(Y)$ will have a phase constant $\beta_F(\beta_S)$. If now we apply a steady magnetic field in the $-Y$ direction we get the non-reciprocal birefringence mentioned earlier. For propagation in the $+Z$ direction the new β-ellipse is as shown in Fig. 2b; for propagation in the $-Z$ direction the new β-ellipse is as shown in Fig. 2c. Thus, for propagation in the two directions the axes of the β-ellipse are oriented differently, and this is what we mean by non-reciprocal birefringence. If the dimensions of the ferrite are such as to produce a 180-degree section $[(\beta_S-\beta_F)L=\pi]$, where L is the length of the section, then we have a non-reciprocal rotator of the plane of polarization. A wave which traverses the medium and is reflected back through it will be rotated by an amount twice the angle between the minor axes of the two β-ellipses. By selecting input polarization, any fraction of the total rotation may be taken in the $+Z$ direction.

We can obtain a qualitative explanation of the nature of the β-ellipses by examining the radio frequency magnetic field at the point $X=0$, $Y=R$, $Z=0$, in the absence of ferrite and as a function of time. If we have an input polarization such that the principal electric vector lies in the $X=Y$ plane and have propagation in the $+Z$ direction, then the RF magnetic field at $Z=0$, $Y=R$, $Z=0$ will lie in the $Y=R$ plane and as seen looking along A-Y direction is (in general) elliptically polarized with the magnetic vector rotating clockwise. For a polarization in the $X=-Y$ plane and propagation to $+Z$, the magnetic vector above rotates counterclockwise. The permeability is then greater for the second case if we put a piece of ferrite at the (0, R, 0) point and apply a steady magnetic field along the $-Y$ direction. Thus, the tendency is for the ellipse to be oriented as shown in Fig. 2b. A similar examination for propagation along $-Z$ indicates the orientation of the β-ellipse shown in Figure 2c.

A more complete theoretical explanation has been obtained and it is hoped this can be published soon.

E. H. Turner
Bell Telephone Laboratories
Holmdel, N. J.

* Received by the Institute April 8, 1953.

[1] C. L. Hogan, "The ferromagnetic faraday effect at microwave frequencies and its applications," Bell Sys. Tech. Jour., vol. XXXI, pp. 1–31; Jan. 1952.

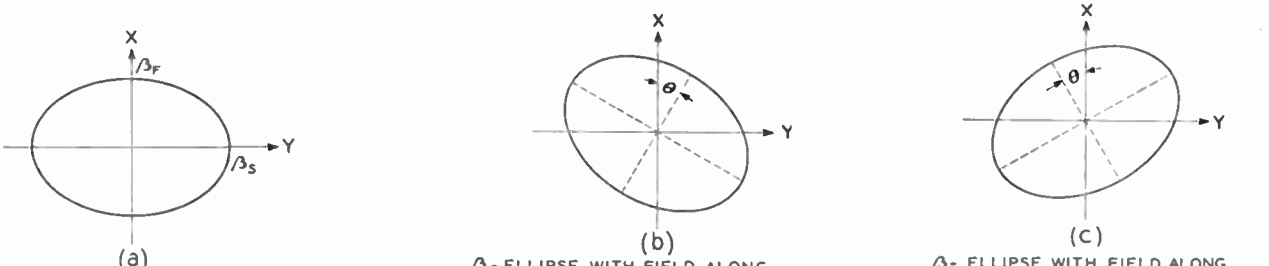

Fig. 2

Contributors to Proceedings of the I.R.E.

F. J. Bingley

Mr. Bingley (A'43–M'36–SM'43–F'50) was born in Bedford, England on November 13, 1906. He graduated from the University of London in 1926 and 1927, when he received the B.S. degrees in mathematics and physics, respectively. He has been continuously associated with television since his graduation from college, and was first employed by the Baird Television Company of London, in October, 1927. He was in charge of their New York laboratories for two years, and joined the Philco Corporation in 1931.

At Philco, Mr. Bingley has been associated with the development of transmitting and receiving equipment, as well as with television-systems engineering. He is presently engaged in an extensive program of color-television research. He is the author of a number of papers on the subject of color television and colorimetry.

Mr. Bingley is a member of the Franklin Institute, and has served on many industry committees concerned with the development of television standards.

❖

C. K. Birdsall

Charles K. Birdsall (S'47–A'51) was born in New York City on November 19, 1925. He received the B.S.E. and M.S.E. degrees in Electrical Engineering from the University of Michigan in 1946 and 1948, respectively, and the Ph.D. degree from Stanford University in 1951.

At Stanford, Dr. Birdsall was a Sylvania Fellow in 1949 and an RCA Fellow in Electronics from 1949 to 1951.

Contributors to Proceedings of the I.R.E.

Dr. Birdsall is a Member of the Technical Staff of the Hughes Research and Development Laboratories, and is engaged in microwave tube research in the Electron Tube Laboratory. He is a member of Sigma Xi and Tau Beta Pi.

❖

George R. Brewer (A'43–M'49) was born in New Albany, Indiana, on September 10, 1922. He received the B.E.E. degree in Electrical Engineering from the University of Louisville in 1943, the M.S.E. in Electrical Engineering in 1948, the M.S. degree in Physics in 1949, and the Ph.D. degree in Electrical Engineering in 1952 from the University of Michigan.

G. R. Brewer

Dr. Brewer has been engaged principally in research and development of electron tubes; from 1943 to 1944 at the Radiation Laboratory, M.I.T., from 1944 to 1947 at the Naval Research Laboratory, and from 1947 to 1951 at the Engineering Research Institute of the University of Michigan. He is now in the Electron Tube Laboratory of Hughes Research and Development Laboratories.

He is a member of the American Physical Society, Sigma Xi, and Phi Kappa Phi.

❖

For a photograph and biography of Dr. Seymour B. Cohn, see page 1126 of the September, 1952, issue of the Proceedings of the I.R.E.

❖

Robert Dressler (S'46–A'49) born in New York City on May 5, 1925, received the B.S. degree in 1946 and the M.S. degree in Electrical Engineering in 1948, both from the Columbia University.

Robert Dressler

Since 1946, Mr. Dressler has been in charge of various aspects of television research for Paramount Pictures Corp., including color television system and equipment development, UHF and VHF propagation studies, and the development of ammonium dihydrogen phosphate sound-on-film recording system.

Mr. Dressler has been Director of Research and Development in New York for Chromatic Television Laboratories, Inc., a Paramount subsidiary, since 1951.

❖

Andrew V. Haeff (A'34–M'40–SM'43–F'49) was born in Moscow, Russia, on December 30, 1904. In 1928, he received the degree of Electrical and Mechanical Engineer from the Russian Polytechnic Institute at Harbin, China. In 1928 he majored in electrical engineering at the California Institute of Technology, where he obtained the M.S. degree in 1929 and the Ph.D. degree in 1932.

Andrew V. Haeff

As a special Research Fellow at the California Institute of Technology in 1933, Dr. Haeff studied methods of generation of microwaves, and invented the deflection type traveling-wave tube. From 1934 to 1941 he was with the Research Laboratories of the Radio Corporation of America, where he contributed to the study of ultra-high-frequency phenomena and space-charge effects in electron tubes, and invented the inductive output tube and other ultra-high-frequency tubes and circuits.

In 1941, Dr. Haeff joined the staff of the Naval Research Laboratory as Consultant in Electronics, where he contributed to the early studies of radar systems, was responsible for the development of wide-band ultra-high-frequency signal generators, and took part in radar countermeasure activities. After the War, he organized the N.R.L. Vacuum Tube Research Branch, directed its work, and contributed by original inventions which included the memory tube and the electron wave amplifier.

In 1950, Dr. Haeff joined Hughes Research and Development Laboratories where he organized the Electron Tube Laboratory, which under his direction is presently engaged in research on microwave and storage tubes. Dr. Haeff is the first recipient of the Harry Diamond Memorial Award for "his contributions to the study of interaction of electrons and radiation, and for his contribution to the storage tube art."

❖

R. C. Hergenrother (A'37) was born on September 5, 1903 in Chemnitz, Germany. He received the A.B. degree from Cornell University in 1925. During 1925–1926 he was employed in vacuum-tube development work at Westinghouse Lamp Company, Bloomfield, N. J. He went to the Pennsylvania State College in 1927 as an instructor in physics, and there received the M.S. degree in 1928. He was awarded the Ph.D. degree from the California Institute of Technology in 1931.

R. Hergenrother

Dr. Hergenrother held a Rockefeller Foundation Research Fellowship in physics at Washington University, St. Louis, Mo., from 1932 to 1934. From 1934 to 1935 he was employed by the Farnsworth Television Laboratories in Philadelphia, Pa. From 1935 until 1945 he worked for the Hazeltine Corporation. Since 1945 Dr. Hergenrother has been employed by the Raytheon Manufacturing Company, of Waltham, Mass.

Dr. Hergenrother is a member of A.P.S., Sigma Xi, and Sigma Pi Sigma.

❖

William K. Linvill was born in Kansas City, Missouri on August 8, 1919. He received the A.B. degree from William Jewell College in 1941 and the B.S. and M.S. degrees in Electrical Engineering in 1945 and the Sc.D. degree in 1949 from Massachusetts Institute of Technology.

W. K. Linvill

During and since his graduate academic work Dr. Linvill has done teaching and research work at M.I.T. in the fields of network analysis, control systems, and computation. At present he is Assistant Professor of Electrical Engineering at M.I.T. He is a member of I.R.E., A.I.E.E., Eta Kappa Nu, Sigma Pi Sigma, Theta Chi Delta, and Sigma Xi.

❖

Lars Löfgren (M'52) was born on December 10, 1925 in Stockholm, Sweden. He graduated from the department of applied physics at the Royal Technical University in Stockholm in 1949.

Lars Löfgren

Mr. Löfgren has been employed by the Swedish Research Institute of National Defense, Radio Department, since 1947. He presently is research engineer in charge of the computing machinery section of the Institute.

Mr. Löfgren holds half a dozen patents within the electronic computation field. In 1952 he obtained a scholarship from the Foreign Student Summer Project at Massachusetts Institute of Technology, and then had the opportunity to work with transistors at the Research Laboratory of Electronics.

❖

Alan J. Oxford was born in London, England, on March 14, 1912, and received his B.S. degree from London University in 1933. He worked with the Gramophone Co., Ltd., until 1938 when he joined the War Office team working on Radar for the Army.

Alan J. Oxford

Mr. Oxford stayed with the Radar Research and Development Establishment at Malvern, England, until the end of the war; he was employed on the design of coast defense, gunlaying and searchlight control Radar equipment. During this period he also suggested and designed the time-multiplexing

Contributors to Proceedings of the I.R.E.

system for the Army Wireless Set No. 10, an eight channel pulse-width modulated system operating on uhf.

From 1945 to 1950, as a member of the Signals Research and Development Establishment at Christchurch, England, Mr. Oxford was involved in further work on speech transmission by pulse methods.

Since 1950 Mr. Oxford has been organizing the new Electronics Research Laboratory at Salisbury, South Australia, of which he is now Superintendent.

❖

H. G. Rudenberg (S'41–A'45–M'51) was born in Berlin, Germany on August 8, 1920. He received the B.S. degree in physics in 1941 and the MS degree in 1942, both from Harvard University. Until 1944 he was Teaching Fellow in Electronics at Harvard, and spent the next two years with the U. S. Army, Corps of Engineers, assigned to Los Alamos, N. M.

H. G. RUDENBERG

Dr. Rudenberg returned to Harvard University, from 1946 to 1948, for graduate work on distributed amplifiers and transformers, and received the Ph.D. degree in physics in 1952.

From 1948 to 1952 Dr. Rudenberg was a Research Staff Member of the newly formed Research Division of the Raytheon Manufacturing Company, Waltham, Mass., where he worked on microwave and semiconductor problems. Since 1952 he has been associated with the Electronics Research and Development Corporation, Melrose, Mass., as Director of Development, concerned with semiconductor devices.

Dr. Rudenberg is a member of A.P.S., Phi Beta Kappa, and Sigma Xi.

❖

John M. Salzer (S'46–A'51) was born in Vienna, Austria, on September 12, 1917. He received the B.S. and M.S. degrees in electrical engineering from Case Institute of Technology in 1947, 1948, and the Sc.D. degree in electrical engineering from Massachusetts Institute of Technology in 1951.

JOHN M. SALZER

From 1941 to 1945, he was with the U. S. Army doing technical work on anti-aircraft computers, instruments, radio and radar sets

In 1947 Dr. Salzer helped develop electronic controls for General Electric Co. in Schenectady, N. Y. He taught mechanics and electronics at Case (1947–48) and in 1950 circuits at M.I.T. He consulted for Commercial Television Corp., Cleveland, Ohio, on installation and servicing in 1948. From 1948 to 1951 he was Research Associate at the Digital Computer Laboratory of M.I.T. Since 1951 he has been with the Research and Development Laboratories of Hughes Aircraft Co., Culver City, Calif., in the analysis and development of digital-analog control systems. He is also Lecturer in Engineering at the University of California Los Angeles.

Dr. Salzer is a member of A.I.E.E., Association for Computing Machinery, Eta Kappa Nu, Tau Beta Pi, and Sigma Xi.

❖

David Sarnoff (A'12–M'14–F'17) born in Uzlian, Russia, on February 27, 1891 and brought to the United States at the age of nine.

DAVID SARNOFF

As shipboard wireless operator and ashore with the powerful Wanamaker station, he became successively Chief Inspector, Asst. Chief Engineer, Asst. Traffic Manager and, in 1917, Commercial Manager of the Marconi Co.

In 1919, when the Radio Corporation of America was formed, it acquired the American Marconi Co., and appointed him Commercial Manager. He advanced from Commercial Manager to General Manager, then Vice President, Executive Vice President and, in 1930, to President of RCA.

Mr. Sarnoff was elected to serve as Chairman of the Board as well as President in 1947, and in 1949 he resigned as President, continuing as Chairman of the Board and Chief Executive Officer of RCA, the position he holds today.

A Reserve Officer of the U. S. Army since 1924, he served in the Office of the Chief Signal Officer in Washington in 1941, and in 1944, as Special Consultant on Communications at SHAEF. During this period he was promoted to Brigadier General and received the War Department's Legion of Merit Medal.

Mr. Sarnoff is recipient of numerous awards including the Medal of Merit from President Truman. He was first recipient of the "One World Prize" awarded by the American Nobel Center in 1945. In 1944 the Television Broadcasters Association conferred on him the title of "The Father of American Television." In 1949, the United Nations presented him a citation for "his contribution in the field of Human Rights," and on his 45th anniversary in radio in 1951, the Princeton, N. J., laboratories of RCA were dedicated as the "David Sarnoff Research Center."

In June, 1952, the Radio-Television Manufacturers Association awarded him its Medal of Honor. In March, 1953, he received the Founders Award of the IRE, and in April, the National Association of Radio and Television Broadcasters presented him with its first Keynote Award.

For a photograph and biography of JACOB SHEKEL, see page 1611 of the November, 1952, issue of the PROCEEDINGS OF THE I.R.E.

❖

Peter D. Strum (A'45) was born in Brunswick County, Va., on April 25, 1922. He received the B.E.E. degree with honors from North Carolina State College in 1945 and the M.S. degree in electrical engineering from Stanford University in 1947.

P. D. STRUM

Mr. Strum was a temporary instructor in electrical engineering at North Caroline State College from August 1944 to February 1945, following the completion of his undergraduate studies.

In 1947 Mr. Strum joined the engineering staff of Airborne Instruments Laboratory in Mineola, N. Y., where he participated in receiver research and the development of receivers, beacons, automatic direction finders, and test equipments. In 1952 he was appointed Assistant Supervising Engineer of the newly-formed Applied Electronics Section of the Laboratory.

Mr. Strum is a member of Tau Beta Pi, Eta Kappa Nu, and Sigma Xi.

❖

Kiyo Tomiyasu (SM'52) was born in Las Vegas, Nev., on September 25, 1919. He received the B.S. degree in electrical engineering from the California Institute of Technology in 1940, and the M.S. degree in communication engineering from Columbia University in 1941. After further graduate study at Stanford University, and at Harvard University, he was awarded the Ph.D. degree in engineering science and applied physics from Harvard in 1948.

KIYO TOMIYASU

In 1947–1948, Dr. Tomiyasu was a research assistant at Harvard, under the ONR Contract N5-ori-76 T.O.1, supported jointly by the Navy Department, Office of Naval Research, and the Signal Corps of the U. S. Army. He was appointed a teaching fellow in 1946 and instructor in 1948 in the department of engineering sciences and applied physics, Harvard University, where he was engaged until September, 1949. Since then he has been at Sperry Gyroscope Company in the Microwave Components Department as engineering section head for microwave research.

Dr. Tomiyasu is a member of the American Physical Society and Sigma Xi.

Institute News and Radio Notes

Nominations—1954

At its May 6, 1953 meeting, the IRE Board of Directors received the recommendations of the Nominations Committee and the reports of the Regional Committees for officers and directors for 1954. They are:

President, 1954: William R. Hewlett
Vice President, 1954: Maurice J. H. Ponte
Director-at-Large, 1954–1956 (*two to be elected*): Lloyd V. Berkner, Axel G. Jensen, Arthur V. Loughren, Daniel E. Noble, George Rappaport (nominated by petition)
Regional Directors, 1954–1955 (*one to be elected in each Region*):
Region 1.—Lucius E. Packard
Region 3.—Lawrence R. Quarles, Harry W. Wells
Region 5.—Clyde L. Foster, Charles J. Marshall
Region 7.—C. Wesley Carnahan, Joseph M. Pettit

According to Article VI, Section 1, of the IRE Constitution, nominations by petition for any of the above offices may be made by letter to the Board of Directors, giving name of proposed candidate and office for which it is desired he be nominated. For acceptance, a letter of petition must reach the executive office before noon on August 14, 1953, and shall be signed by at least 100 voting members qualified to vote for the office of the candidate nominated.

Calendar of COMING EVENTS

National American Radio Relay League Convention, Shamrock Hotel, Houston, Texas, July 10–12
IRE-ONR-Univ. of Calif. Symposium on Statistical Methods in Communication Engineering, Berkeley, Calif., August 17–18
IRE Western Convention and Electronic Show, Civic Auditorium, San Francisco, Calif., August 19–21
International Sight and Sound Exposition and Audio Fair, Chicago, Ill., September 1–3
Conference on Nuclear Engineering, University of California, Berkeley, September 9–11
National Electronics Conference, Hotel Sherman, Chicago, Ill., September 28–30
1953 IRE-RTMA Radio Fall Meeting, King Edward Hotel, Toronto, Ont., October 26–28
Conference on Radio Meteorology, University of Texas, Austin, Texas, November 9–12
IRE Kansas City Section Annual Electronics Conference, Hotel President, Kansas City, Mo., November 13 and 14
1954 Sixth Southwestern IRE Conference and Electronics Show, Tulsa, Okla., February 4–6

Radio Pioneers Cite IRE Members

Citations to "outstanding living leaders in radio" were presented to several members of the IRE at the annual dinner of the Radio Pioneers held recently at the Hotel Statler in Los Angeles, Calif.

Those members of the IRE who received citations at the dinner included V. K. Zworykin, RCA Laboratories; E. F. W. Alexanderson, General Electric Co.; J. V. L. Hogan, Hogan Laboratories; and O. H. Caldwell, Caldwell-Clements Inc.

W. L. Everitt Named to Committee Studying Bureau of Standards

The Institute has nominated Dr. William L. Everitt, past president of the IRE and dean of the College of Engineering, University of Illinois, to serve on a committee of scientists formed at the request of Secretary of Commerce Sinclair Weeks to evaluate the present functions and operations of the National Bureau of Standards in relation to the present national needs.

The nomination came as a result of Secretary Weeks requesting each of the leading scientific and engineering societies to select one of their members to serve on the committee. Dr. M. J. Kelly, president of Bell Telephone Laboratories, will serve as chairman of the committee.

Other societies represented will be the American Institute of Electrical Engineers, American Institute of Mechanical Engineers, American Society of Civil Engineers, American Institute of Physics, American Chemical Society, and the American Institute of Mining and Metallurgical Engineers.

Dr. Everitt's nomination was made only after assurance had been received from Secretary Weeks that the committee will operate under the National Academy of Sciences, that it will not be concerned with personnel relationships between the National Bureau of Standards and the Department of Commerce, and that the report of the committee will be made public.

Dr. William L. Everitt has had a distinguished career as engineer, educator, consultant, and author of textbooks and scientific articles in the radio field. He has held teaching posts at Cornell University, the University of Michigan, and Ohio State University before joining the staff of the University of Illinois in 1945 as head of the department of electrical engineering. He was appointed dean of the College of Engineering in 1949.

In 1940 Dr. Everitt became a member of the communications section of the National Defense Research Committee, and during World War II served as director of operational research in the Office of the Chief Signal Officer. In 1950 he served on the Senate Advisory Committee on Color Television.

Dr. Everitt is a fellow, director, and past president of the Institute of Radio Engineers.

IRE Western Convention Set for August 19-21

Twenty-five sessions of broadly general as well as specialized interest are combined in the technical program of the Western Electronic Show and Convention. Sponsored jointly by IRE and the West Coast Electronic Manufacturers' Association, the meeting will be held at the Civic Auditorium, San Francisco, on August 19–21.

The program will be highlighted by two evening sessions. One on color television features W. R. G. Baker and D. G. Fink, chairman and vice-chairman respectively of the National Television System Committee; the second medical electronics, under the chairmanship of A. J. Morris, Office of Naval Research.

Sessions on specific topics are: two each on transistors, electron devices, computers, instrumentation, antennas, microwave techniques, servo systems, audio, circuits, and propagation; one each on nuclear electronics, color television, medical electronics, noise and signal spectra, and airborne electronics.

The convention will feature what has become the second largest annual trade and engineering show in the electronic field. The latest products of 278 companies will be on display. The convention program will be rounded out by an entertainment schedule of social events and field trips.

The importance of the meeting has led the IRE Board of Directors to cancel its regular September meeting, usually held at Institute headquarters in New York City, and to meet instead in San Francisco on August 18.

The transistor session includes coverage of a new hybrid emitter junction-collector type as well as papers on the measurement of transistor parameters, on basic semiconductor properties, broadcast-receiver, digital-device, vhf-fm transmitter, and carrier-telephony applications. In the electron devices sessions, papers will cover new developments in traveling-wave tubes, backward-wave oscillators, high-power klystrons, a new K-band amplifier tube with 60-db gain, and theoretical discussion relating to signal coherence. Computer sessions include papers on converters from series to parallel and analog to digital data and memory systems; and a panel discussion comparing the various memory techniques utilized.

Papers in the airborne electronics group will survey the Air Navigation Development Board program, communications systems, corona-interference reduction, magnetic amplifiers, and weather radar. Counter techniques and circuit innovations for wave clipping and triggering are included in the instrumentation sessions, while radiation measurements and the electronics of particle accelerators will be grouped in the nuclear electronics session.

The program, including a full listing of all papers and authors will appear in the August issue of PROCEEDINGS OF THE I.R.E.

Professional Group News

Airborne Electronics

The Dayton Chapter of the Professional Group on Airborne Electronics met recently at the Engineers' Club with Maurice Jacobs as Chairman. Mr. Golden, Sylvania Electric Products, spoke about "Transistors at High Altitudes." He reviewed the two schools of thought with regard to placing transistors on the market; one school feels that transistors should immediately be given to engineers for circuit development, the other that the market should be limited until transistors are perfected til they can be guaranteed. He predicted that it would be two years before adequately sealed, guaranteed transistors would be available in production lots. He felt it would be six months before Sylvania would be ready to "glass seal" transistors. He also discussed the high temperature and altitude characteristics of transistors.

Antennas and Propagation

The Chicago Chapter of the Professional Group on Antennas and Propagation met recently at the Western Society of Engineers Building with J. S. Brown as Chairman. S. M. Richie, deputy chief of the Facilities Division of the CAA Third Region, gave a paper entitled "Antenna Systems for Air Navigation." He covered the several different antenna requirements for aircraft navigation and landing, including ILS and GCA. The methods used by the CAA to meet these requirements and overcome the resulting problems were outlined and slides shown in conjunction with his talk. A discussion period followed his presentation.

Audio

The Chicago Chapter of the Professional Group on Audio recently held a joint meeting with the Chicago Audio Acoustical Group at the Civic Opera Building. Co-Chairmen of the meeting were R. Troxel of the IRE and Hale Sabine of the CAAG. Speaker of the evening was W. E. Kock, director of acoustics research, Bell Telephone. His paper was titled "Physics of Music and Hearing."

NEW CHAPTER IN SAN DIEGO

The Executive Committee of the Institute approved on May 5, 1953 the establishment of a San Diego Chapter of the Professional Group on Audio. F. X. Brynes is Acting Chairman.

Broadcast and Television Receivers

The Chicago Chapter of the Professional Group on Broadcast and Television Receivers met recently at the Western Society of Engineers Auditorium with Stephen Bushman as Chairman. Speaker was S. C. Kolanowski, chief engineer of Steward-Warner Electric Division. He demonstrated a technique new to the electronic industry of how components made to a tolerance of plus or minus five thousandths in length can be mounted between two printed circuit terminal boards so as to afford a great saving in space and in test, assembly, and replacement operation time and skill. Problems of component design and contact types were discussed. That contacts of a cupped shape have shown the best ability to overcome the difficulties of oxidation and foreign material in the contact was brought out by Mr. Kolanowski during his talk. Great interest was shown in the post-lecture display of sample mechanically-assembled units, typical of which was a television IF assembly.

SAN FRANCISCO CHAPTER ON ELECTRON DEVICES

The Executive Committee of the Institute approved on May 5, 1953 the establishment of a San Francisco Chapter of the Professional Group on Electron Devices.

Electronic Computers

The Washington D. C. Chapter of the Professional Group on Electronic Computers met recently at the Auditorium of the Potomac Electric Power Co. with C. V. L. Smith as Chairman. E. W. Veitch of the Research Division of Burroughs Adding Machine Co. described a graphical method of his in a paper called "Logical Design Methods as an Aid to the Minimization of Computer Equipment." The application of the algebra of logic to the design of digital computer switching circuits has been developed at the Harvard Computation Laboratory under the leadership of H. H. Aiken. The method developed there depends upon an explicit enumeration of all possible functions having the desired properties, and the optimum equipment-wise is found by inspection. Mr. Weitch has developed an ingenious graphical method of accomplishing this, leading to great saving in time and effort for the designer. He emphasized, however, that it cannot be demonstrated that any of the presently known methods yield a true minimum, and that the field is still wide open. He also pointed out that the "logical" methods only apply to the design of arithmetic and control organs, and that basic engineering decisions on the type of computer to be built naturally strongly influence the amount of equipment needed.

Engineering Management

The Washington Chapter of the Professional Group on Engineering Management recently held a joint meeting with the Society for the Advancement of Management at a round-table on scientific research at the Potomac Electric Power Co. Auditorium with Allen Schooley as Chairman. R. D. Bennett, technical director of the Naval Ordnance Laboratory spoke about "Human Elements in Research Management." A group discussion followed his presentation.

Industrial Electronics

The Chicago Chapter of the Professional Group on Industrial Electronics met recently at the Western Society of Engineers Building with A. Crossley as Chairman. R. J. Medkeff, project engineer with Askania Regulator Co. presented a paper on "Analog Computers." At a later meeting Julius Solomon, of Sciaky Brothers, Chicago, gave a paper entitled "Electronics in Welding Operations."

Information Theory

The New Mexico Chapter of the Professional Group on Information Theory has been holding meetings regularly twice a month during the winter at Mitchell Hall, University of New Mexico, Albuquerque. Yates M. Hill presided as Chairman at two meetings addressed by Lt. P. Clements of the U. S. Navy, who discussed "Optimum Linear Systems" at one and "Optimum Linear Systems Design" at another. At a meeting led by Vice Chairman E. G. Miller, Bennett Basore, Sandia Corporation, gave a paper entitled "Correlation vs. Linear Transforms." At two recent meetings led by Program Chairman Bennett Basore, Lt. Col. Y. Hill of the U. S. Air Force spoke on "The Realization of Filters which Separate Information from Noise."

Medical Electronics

At a recent meeting of the Buffalo-Niagara Chapter of the Professional Group on Medical Electronics with Wilson Greatbatch as Chairman, Dr. Karl Swartzel was the speaker. He showed three-dimensional color movies of 4 cancer operations: partial gasterectomy, arm amputation, radical mastectomy, and a groin dissection; and a heart operation, partial pericardectomy. The attendance at this meeting was quadruple that of the first meeting. The audience was impressed with the significance of the film as a visual aid in teaching. Plans for a fall symposium on electronic plethysmography are underway and Dr. Jan Nyboer of Dartmouth (author of the electronic plethysmography section of Glosser's "Medical Physics") will present a paper. It is hoped to have other papers by others prominent in the field, and to have working demonstrations of equipment.

Nuclear Science

The Chicago Chapter of the Professional Group on Nuclear Science met recently in the Western Society of Engineers Building with Bernard Schwartz as Chairman. Dr. Lindon Seed, director of the Radioisotope Laboratories of Augustana and Oak Park Hospitals and clinical associate professor of surgery at the University of Illinois was the speaker. He gave a paper entitled the "Clinical Use of Radioactive Material."

The Oak Ridge Chapter met recently at the ORINS Building with W. G. James as Chairman. Dana Coller of X-10 gave a paper titled a "Short Survey of Digital and Analog Electronic Computers."

Vehicular Communications

The Chicago Chapter of the Professional Group on Vehicular Communications has elected the following officers for the year 1953–54. Chairman: William J. Weisz; Vice-

(*continued next page*)

Chairman: Elmer Carlson; Secretary: James M. Clark. At a recent meeting at the Western Society of Engineers Building with R. V. Dondanville as Chairman, R. C. Romayne, senior engineer in the Radio Section of the Illinois Bell Telephone Co., talked about a "Three Frequency Mobile Telephone System."

The Washington Chapter met recently in the Burgundy Room of the Wardman Park Hotel with E. L. White as Chairman. Co-speakers were F. H. Menagh, superintendent of communications of the Erie Railroad, and W. J. Young, assistant superintendent, who discussed the subject of "Applications of VHF Radio to Trains, Base Stations, Switchers, Vehicles, and Harbor Tugs in Railroad Operational Service." At a later meeting at the Pepco Auditorium Henry Magnuski spoke about "Microwave Relay and its Relationship to VHF Vehicular Communication."

Technical Committee Notes

The **Standards** Committee convened on April 16. E. Weber took the chair in the absence of A. G. Jensen. Recommendations were made to the Executive Committee on IRE representation on other bodies for the term May 1, 1953 to April 30, 1954. Reports were submitted by committee chairmen on the status of work within their committees. Since these required no action and are essentially for information purposes, Dr. Weber directed that they be made a part of the minutes, to be circulated to all members of the Standards Committee. It was noted that not all chairmen had submitted approved or revised scopes along with their reports. The Technical Secretary is to distribute existing versions of all scopes with such changes as have been recommended to date. These will be reviewed by the Committee at an early date. Consideration of revisions to the Receivers Committee's scope was deferred at the request of J. Avins, pending general discussion on all scopes. Discussion on the list of Industrial Electronics terms was also deferred to enable J. L. Dalke to review comments with his committee. The remainder of the meeting was devoted to reviewing the proposed Standards on Antennas & Wave guides: Definitions of Terms.

Under the chairmanship of D. C. Ports the **Antennas and Wave Guides** Committee met on April 15. There was a discussion by the committee as to the definition of the term "Direction of Propagation." Action was taken on a number of Component definitions.

On April 17 the **Circuits** Committee convened under the chairmanship of C. H. Page. A number of terms defined in the past by Subcommittee 4.7 are servomechanism terms, rather than feedback terms. It was decided to delete these terms and to become disassociated from them in the master list now that there is a Servomechanism Committee. A number of feedback terms were modified. It was decided to send to the Standards Committee for action the proposed nonlinear definitions of 52 IRE 4. PS1 which have undergone the Grand Tour with the deletion of Bilateral Network, Gyrostatic Network and Unilateral Network.

The **Electronic Computers** Committee met with Chairman R. Serrell. A discussion took place about computer symbols. It has been suggested from time to time that these symbols should be standardized. Since computer symbols now differ widely from one group to another, it would be difficult to obtain common agreement at the present time. Nevertheless, it was thought that it would be useful to collect definitions of such computer symbols as are known to be in use. The Chairman asked M. Middleton, Jr., to prepare a list of all computer symbol definitions which he is able to obtain. It was felt that, since there probably is greater agreement concerning analog symbols than digital ones, this compilation could well start with analog symbols. N. Rochester presented a brief report on the activities of the Eastern Definition. He felt that good progress is being made; co-operation with the Western Subcommittee (8.5) is excellent. However, because of the magnitude of the work involved, the present task is not likely to be completed before 1954. C. V. L. Smith, reporting for W. H. Ware, also felt that definitions work is progressing satisfactorily and that some time will be required before present work can be completed. A discussion followed concerning the activities of the Subcommittee on Magnetic Recording for Computing Purposes headed by S. N. Alexander. D. R. Brown, speaking for J. A. Rajchman, described briefly the recent work of Subcommittee 8.3 on Static Storage Elements.

On April 27, the **Navigation Aids** Committee met under the chairmanship of P. C. Sandretto. The committee completed its work on the radar terms to be proposed as Standards. R. E. Gray and his committee will prepare the final draft for approval by the committee and presentation to the Definitions Co-ordinator.

The **Receivers** Committee convened on March 24 under the chairmanship of J. Avins. The first item discussed was the Revision of "Standards on Television: Methods of Testing Television Receivers, 1948." A general discussion of the problems involved in the proposed revision and assignment of specific tasks under the direction of W. O. Swinyard occupied a major portion of the meeting. R. F. Shea reported on the progress made by his Subcommittee 17.4. Oscillator Radiation measurement procedures have been standardized for UHF as well as VHF. Considerable progress has been made in the development of standard test procedures for measurement of interference from the deflection circuits of television receivers. A preliminary standard 53 IRE 17. PS1, "Methods of Measurement of Television Sweep Circuit Interference in the Range of 300–3000 kc" was completed. This standard is now being used by RTMA members to collect data which will be co-ordinated with field observations. When these tests are completed, the preliminary standard will be revised and submitted for adoption as an IRE standard. In the absence of L. C. Closson, Chairman of Subcommittee 17.9—Measurement of Ferrite Loop Receivers, Mr. Avins reported that Mr. Closson is in the process of organizing his subcommittee. The Chairman reported that the Standards Committee was in general agreement with the revised scope recommended by the Receivers Committee and reported in the Minutes 52 IRE 17. M2

On March 17 the **Sound Recording and Reproducing** Committee met under the chairmanship of A. W. Friend. L. Thompson, Chairman of Subcommittee on Mechanical Recording and Reproducing, reported that two drafts of material are in preparation and will be made available as soon as possible. A portion of this material relates to mechanical and optical means of calibration of standard test records. The Chairman announced that during the November 11, 1952 meeting of the Standards Committee, the "Tentative Standards on Sound Recording and Reproducing: Methods of Measurement of Noise in Sound Recording and Reproducing Systems" were approved essentially as revised. He also reported that the Standards Committee unanimously approved this standard and that they commended Committee 19 for its excellent work. This standard appeared in the April issue of the PROCEEDINGS. A. P. G. Peterson, Chairman of Subcommittee 19.1: Magnetic Recording and Reproducing submitted a report to be read in his absence and arranged for J. H. McGuigan, a member of the Sucbommittee to represent him.

The **Symbols** Committee convened on March 19 under the chairmanship of A. G. Clavier. C. D. Mitchell reported on the activities of his Subcommittee 21.2 on Semi-Conductor Devices. In the absence of A. C. Reynolds, Jr., Chairman of Subcommittee 21.3 on Functional Representation of Control, Computing and Switching Equipment, E. W. Olcott read Mr. Reynolds' report on the activities of the group. F. M. Bailey reported on the activities of his Subcommittee on Symbols and Abbreviations for Feedback Control Systems. M. P. Robinson reported on the progress of work in his Subcommittee on New Proposals and Special Assignments.

Confidential Symposium on Airborne Electronics

The IRE Professional Group on Airborne Electronics, together with the Research and Development Board and the University of California at Los Angeles, is jointly sponsoring a classified (Confidential) technical symposium to be held at UCLA on August 18.

The meeting is planned to be relatively short and informal, presenting papers of rather high technical content and perhaps of controversial interest. Those attending should arrange for security clearance through their proper service project office channels, and direct their security clearance to the Industrial Security Division, Hughes Aircraft Company, Culver City, Calif.

The attention of the engineers in the East is called to the fact that this symposium will be held prior to the IRE West Coast Convention, which is being held in San Francisco August 19th through August 21st. It is possible to obtain round-trip first-class tickets from the railroads or airlines which will permit you to travel by way of Los Angeles without extra cost.

IRE Members Become JTAC Officers

A. V. Loughren has been appointed Chairman of the Joint Technical Advisory Committee for the year July 1, 1953–June 30, 1954. L. V. Berkner will serve as Vice Chairman for the same period.

Community Activities of Wichita Subsection

The Wichita (Kansas) Subsection is currently sponsoring a unique educational series of radio programs and a TV problem committee designed to temper the initial impact of four new TV stations and their resultant problems on a city of 250,000 population.

The series of radio programs are designed to acquaint the *listening* public with the problems and limitations of TV, prior to the becoming a *viewing* public. Each program consists of a combination of short discourses built around question and answer sessions conducted by a panel of TV experts. The programs have been well received by the public, and the questions asked have demonstrated the need for such an educational program.

The Subsection is concurrently organizing a TV committee composed of power company, industrial, hams, and service dealers associations to cope with the initial problems of eliminating interference and handling TV complaints.

International Congress of Mathematicians 1954

The International Congress of Mathematicians 1954 will be held in Amsterdam, Holland from September 2–9 under the auspices of the Mathematical Society of the Netherlands.

The Organizing Committee has invited outstanding mathematicians to deliver one-hour addresses, so as to provide a survey of the recent developments in the whole field of mathematics. There will be sections on algebra and theory of numbers, analysis, geometry and topology, probability and statistics, mathematical physics and applied mathematics, logic and foundations, and philosophy, history and education. Half-hour addresses will be delivered by experts in each of these sections. Short 15-minute lectures will be given by members of the Congress who apply beforehand to the Organizing Committee. Depending upon the number of short lectures, the sections will be subdivided.

There will be two categories of membership in the Congress: *regular members* who will be entitled to participate in the scientific and social activities of the Congress and to receive the Proceedings of the Congress, and *associate members* who, accompanying regular members, do not participate in the scientific program nor receive the Proceedings, but will be entitled to many privileges.

The fees presumably will not exceed fifty guilders (about $14) for members and twenty guilders ($5) for associate members.

Those who wish to attend the Congress are requested to communicate their name (with degrees, qualifications, and so forth) and full address to the Secretariat, 2d Boerhaavestraat 49, Amsterdam, Holland.

Symposium on Statistical Methods in Communication

Under the joint sponsorship of the IRE Professional Group on Information Theory, the Office of Naval Research, and the University of California, a symposium on statistical methods in communication engineering will be held on the Berkeley, California, campus of the University of California, August 17 and 18, immediately preceding the Western IRE Convention.

IRE People

Philo T. Farnsworth (A'28–M'34–F'39), vice-president and director in charge of research and development laboratories of the Capehart-Farnsworth Corporation, was honored by the city of Green Bay, Wisconsin, on March 17, which was proclaimed "Philo T. Farnsworth Day." During festivities marking the opening of television station WBAY-TV in Green Bay, Mr. Farnsworth, who made the first satisfactory system of nonmechanical television, attended a dinner in his honor and was presented with the key to the city.

Mr. Farnsworth was born in Beaver, Utah, on August 6, 1906, and attended Brigham Young University from 1923–25. He began his career in television engineering with the Crocker Research Laboratory, San Francisco, as director of research in 1926. He continued in his position with their successors, Television Laboratories, San Francisco and Philadelphia, until 1930, when he became vice-president in charge of research.

Mr. Farnsworth remained in this position when this company in turn was succeeded by Farnsworth Television, Incorporated, in 1935. When the Pennsylvania Company of Farnsworth Television, Incorporated, was formed in 1936, he became its president. He has continued his association with this company as it expanded into being the Farnsworth Television and Radio Corporation, of Fort Wayne, Indiana, and finally merged into the Capehart-Farnsworth Corporation.

Other honors which have been bestowed upon Mr. Farnsworth include the Distinguished Alumnus Award from Brigham Young University in 1937 and in the same year honorable mention by Eta Kappa Nu as one of the outstanding young electrical engineers. Indiana Technical College, Fort Wayne, awarded him an honorary D.Sc. in 1951, and he received the Morris Liebman Memorial Prize in 1941.

Mr. Farnsworth has published numerous articles concerning his inventions. Among those for which he holds patents are an oscillator, television system, receiving system, light valve, synchronizing system, and dissector target.

Mr. Farnsworth has served on IRE television committees, is a Fellow of the Society of Motion Picture and Television Engineers, the American Association for the Advancement of Science, and a member of Sigma Xi.

❖

Max Skobel (SM'52), formerly chief engineer of the Aircraft Transformer Corporation, has been promoted to the position of director of engineering and research. He will co-ordinate expanding research and engineering activities on high temperature transformers and miniaturization.

Mr. Skobel was born in New York state on March 3, 1915. He received the B.S. degree in electrical engineering from the College of the City of New York in 1942 and the M.S. degree from Rutgers University in 1950.

From 1942 to 1947 Mr. Skobel was chief of the Transformer Section of the Signal Corps Engineering Laboratories at Fort Monmouth, N. J., where he was responsible for all research and development on transformers and similar components for the U. S. Army. From 1947 to 1951 he was chief of the Miscellaneous Section of the Armed Services Electro Standards Agency there, responsible for the preparation of MIL specifications on transformers, rf coils, batteries, dynamotors, rectifiers, tube sockets, and current regulating tubes.

Francis J. Gaffney (A'38–M'45–SM'46) formerly general manager of the Polytechnic Research and Development Company, Brooklyn, N. Y., has accepted the post of director of engineering for the Guided Missiles Division of the Fairchild Engine and Airplane Corp.

F. J. Gaffney

Mr. Gaffney was born on June 27, 1912 in Middleton, England. He received the B.S. degree in electrical engineering from Northeastern University in 1935. He did graduate study at Tufts College in 1939–40 and at the Massachusetts Institute of Technology.

From 1936–37 Mr. Gaffney was a radio engineer for the National Company, Malden, Mass.; he then became chief engineer of the Browning Laboratories, Winchester, Mass. He joined the staff of MIT Radiation Laboratories in 1941, and a year later was placed in charge of the measurement and test apparatus group. In 1945 he became associated with the Polytechnic Research and Development Company.

Mr. Gaffney is a member of Tau Beta Pi, the American Institute of Electrical Engineers, the American Physical Society, American Association for the Advancement of Science and is currently chairman of the U. S. Commission on Standards and Methods of Measurement of the URSI, and the IRE Committee on Measurements and Instrumentation. He also serves as a consultant to the Research and Development Board and is chairman of the Test Equipment Panel of the Committee on Electronics of the Department of Defense.

Sections*

Chairman		Secretary
R. M. Byrne 316 Melbourne Ave. Akron, Ohio	AKRON (4)	H. L. Flowers 2029—19 St. Cuyahoga Falls, Ohio
S. R. Smith 278-12 St. N.E. Apt. D8 Atlanta, Ga.	ATLANTA (6)	D. L. Finn School of Elec. Eng. Georgia Inst. of Tech. Atlanta, Ga.
C. E. McClellan 1306 Tarrant Rd. Glen Burnie, Md.	BALTIMORE (3)	C. D. Pierson, Jr. 1574 Waverly Way Baltimore, Md.
L. B. Cherry 1418 Central Dr. Beaumont, Tex.	BEAUMONT-PORT ARTHUR (6)	C. B. Trevey 2555 Pierce St. Beaumont, Tex.
J. H. Merchant 2 Cedar St. Binghamton, N. Y.	BINGHAMTON (4)	R. F. New 654 Chenango St. Binghamton, N. Y.
F. D. Lewis c/o General Radio Co. 275 Massachusetts Ave. Cambridge, Mass.	BOSTON (1)	A. J. Pote Harvard University Cyclotron Laboratory Cambridge, Mass.
Luis M. Malvarez Commandant Franco 390 Olivos—SCQBM Buenos Aires, Arg.	BUENOS AIRES	Alejandro Rojo Transradio International San Martin 379 Buenos Aires, Arg.
R. R. Thalner Sylvania Electric Prod. 254 Rano St. Buffalo, N. Y.	BUFFALO-NIAGARA (4)	D. P. Welch 859 Highland Ave. Buffalo 23, N. Y.
R. M. Mitchell 357 Garden Dr., S.E. Cedar Rapids, Iowa	CEDAR RAPIDS (5)	G. W. March 424 Liberty Dr. Cedar Rapids, Iowa
A. R. Beach Loueridge Circle E. Eau Gallie, Fla.	CENTRAL FLORIDA (6)	Hans Scharla-Nielsen Radiation Inc. P.O. Drawer Q Melbourne, Fla.
R. M. Krueger 5143 N. Neenah Ave. Chicago 31, Ill.	CHICAGO (5)	J. J. Gershon 2533 N. Ashland Ave. Chicago, Ill.
J. P. Quitter 509 Missouri Ave. Cincinnati, Ohio	CINCINNATI (5)	D. W. Martin Box 319-A, RR 1 Newtown, Ohio
J. L. Hunter 3901 E. Antisdale Rd. S. Euclid, Ohio	CLEVELAND (4)	H. R. Mull R.F.D. 3, Elyria, Ohio
J. H. Jaeger 361 Oakland Park Ave. Columbus, Ohio	COLUMBUS (4)	R. W. Masters 1633 Essex Rd. Columbus, Ohio
John Merrill 16 Granada Terr. New London, Conn.	CONNECTICUT VALLEY (1)	H. E. Rohloff The So. New Eng. Tel. Co. 227 Church St. New Haven, Conn.
R. A. Arnett 4073 Rochelle Dr. Dallas, Tex.	DALLAS-FORT WORTH (6)	J. A. Green 6815 Oriole Dr. Dallas, Tex.
A. H. Petit 444 E. Peach Orchard Ave. Dayton, Ohio	DAYTON (5)	M. A. McLennan 304 Schenck Ave. Dayton, Ohio
W. R. Bliss 2836 W. Archer Pl. Denver, Colo.	DENVER (5)	R. E. Swanson 1777 Kipling St. Denver, Colo.
W. L. Cassell Iowa State College Ames, Iowa	DES MOINES-AMES (5)	R. E. Price 1107 Lyon St. Des Moines, Iowa
F. W. Chapman 1756 Graefield Rd. Birmingham, Mich.	DETROIT (4)	N. D. Saigeon 1544 Grant Lincoln Park, Mich.
H. F. Dart 923 Farnham St. Elmira, N. Y.	ELMIRA-CORNING (2)	E. M. Guyer Corning Glass Works Cofning, N. Y.
Lt. Col. W. B. Sell A.F.F. Bd. No. 4 Fort Bliss, Tex.	EL PASO (7)	J. E. Hoefling Box 72 AA & GM Branch, Tas. Fort Bliss, Texas
R. E. Neuber 130 Willonwood Center Emporium, Pa.	EMPORIUM (4)	E. H. Boden Box 14 Emporium, Pa.
H. L. Thorson General Electric Co. Owensboro, Ky.	EVANSVILLE-OWENSBORO (5)	A. P. Haase 2230 St. James Ct. Owensboro, Ky.
L. F. Mayle The Magnavox Co. Fort Wayne, Ind.	FORT WAYNE (5)	Clifford Hardwick The Magnavox Co. Fort Wayne, Ind.
Arthur Ainlay RR 6, Mt. Hamilton Hamilton, Ont., Canada	HAMILTON (8)	John Lucyk 77 Park Row S. Hamilton, Ont.
F. L. Mason Electronics Office Naval Shipyard Pearl Harbor, Oahu, T H.	TERRITORY OF HAWAII (7)	J. W. Anderson 4035 Black Pt. Rd. Honolulu, T.H.
H. T. Wheeler 802 N. Avenue "A" Bellaire, Tex.	HOUSTON (6)	J. K. Hallenburg 1359 DuBarry Lane Houston, Tex.
H. R. Wolff 5135 E. North St. Indianapolis, Ind.	INDIANAPOLIS (5)	J. T. Watson 1304 N. Delaware St. Indianapolis, Ind.
R. E. Lee 205A Entwistel St. China Lake, Calif.	INYOKERN (7)	J. C. Keyes 704-A Kearsage China Lake, Calif.
D. G. Wilson 212 Elec. Eng. Lab. Univ. of Kansas Lawrence, Kan.	KANSAS CITY (5)	Mrs. G. L. Curtis Radio Industries, Inc. 1307 Central Ave. Kansas City, Kan.
W. F. Stewart 1219 Skyline Dr. N. Little Rock, Ark.	LITTLE ROCK (5)	J. E. Wylie 2701 N. Pierce Little Rock, Ark.
	LONDON, ONTARIO (8)	J. D. B. Moore 27 McClary Ave. London, Ont., Canada
Vincent Learned 2 Prescott St. Garden City, L. I., N. Y.	LONG ISLAND (2)	J. F. Bisby Airborne Instruments 160 Old Country Rd. Mineola, L. I., N. Y.
W. G. Hodson 10806 Smallwood Ave. Downey, Calif.	LOS ANGELES (7)	B. S. Angwin 238 N. Frederic St. Burbank, Calif.
M. C. Probst Rt. 7, Box 415 Louisville, Ky.	LOUISVILLE (5)	G. W. Yunk 2236 Kaelin Ave. Louisville 5, Ky.
Prof. F. B. Lucas 5340 Davis Rd., S.W. South Miami 43, Fla.	MIAMI (6)	C. E. Rogers 717 Santander Ave. Coral Gables 4, Fla.
D. E. Mereen 3260 N. 88 St. Milwaukee, Wis.	MILWAUKEE (5)	H. J. Zwarra 722 N. Broadway Rm. 1103 Milwaukee, Wis.
	MONTREAL, QUEBEC (8)	Sydney Bornneville 127 Valois Ave. Montreal, P. Q., Canada
C. W. Carnahan 3169-41 Pl., Sandia Base Albuquerque, N. M.	NEW MEXICO (7)	L. E. French 107 S. Washington Albuquerque, N. M.
H. T. Budenbom 82 Wellington Ave. W. Short Hills, N. J.	NEW YORK (2)	A. B. Giordano 85-99 Livingston St. Brooklyn, N. Y.
Prof. R. R. Wright Dept. Elec. Eng. Va. Polytechnic Inst. Blacksburg, Va.	NORTH CAROLINA-VIRGINIA (3)	B. C. Dickerson 1716 Broadfield Rd. Norfolk 3, Va.
C. E. Harp 524 E. Macy St. Norman, Okla.	OKLAHOMA CITY (6)	E, G. Crippen 3829 N.W. 23 St. Oklahoma City, Okla.
V. H. Wight 1411 Nemaha St. Lincoln 2, Neb.	OMAHA-LINCOLN (5)	M. L. McGowan 3521 N. 58 St. Omaha 4, Neb.
J. A. Loutit 674 Melbourne Ave. Ottawa, Ont., Canada	OTTAWA, ONTARIO (8)	D. V. Carroll Box 527 Ottawa, Ont., Canada
J. G. Brainerd Moore School Elec. Eng. Univ. of Penn. Philadelphia 4, Pa.	PHILADELPHIA (3)	C. R. Kraus 1835 Arch St. Philadelphia 3, Pa.
R. E. Samuelson 1401 E. San Juan Ave. Phoenix, Ariz.	PHOENIX (7)	Z. F. McFaul 4242 N. 2nd Dr. Phoenix, Ariz.
J. G. O'Shea 104 N. Fremont St. Pittsburgh, Pa.	PITTSBURGH (4)	J. H. Greenwood 530 Carlton House Pittsburgh, Pa.
M. J. Murdock 1533 S. E. 56 Ave. Portland, Ore.	PORTLAND (7)	J. M. Roberts 4325 N.E. 77 Portland, Ore.
J. S. Donal, Jr. RCA Labs. Princeton, N. J.	PRINCETON (3)	G. S. Sziklai Box 3 Princeton, N. J.
Garrard Mountjoy 100 Carlson Rd. Rochester, N. Y.	ROCHESTER (4)	R. N. Ferry 196 Lafayette Pkwy. Rochester, N. Y.
W. F. Koch 1340-33 St. Sacramento, Calif.	SACRAMENTO (7)	H. C. Slater 1945 Bidwell Way Sacramento, Calif.
H. J. Hicks 62 Whitehall Ct. Brentwood, Mo.	ST. LOUIS (5)	R. W. Benson 818 S. Kingshighway St. Louis, Mo.

* Numerals in parentheses following Section designate Region number.

Sections

Chairman		Secretary
Clayton Clark 710 N. First East St. Logan, Utah	SALT LAKE CITY (7)	J. S. Hooper 1936 Hubbard Ave. Salt Lake City 5, Utah
John Ohman 510 John Adams Dr. San Antonio, Tex.	SAN ANTONIO (6)	W. R. Schock 302 Freiling Dr. San Antonio, Tex.
C. R. Moe 4669 E. Talmadge Dr. San Diego, Calif.	SAN DIEGO (7)	F. X. Byrnes 1759 Beryl St. San Diego, Calif.
W. E. Noller 1229 Josephine St. Berkeley, Calif.	SAN FRANCISCO (7)	O. J. M. Smith Elec. Eng. Dept. Univ. of Calif. Berkeley, Calif.
D. E. Norgaard 1908 Townsend Rd. Schenectady, N. Y.	SCHENECTADY (2)	R. L. Smith Station WRGB Schenectady, N. Y.
L. A. Traub 2816—31 Ave., N. Seattle, Wash.	SEATTLE (7)	G. K. Barger 1229 9 Ave., W. Seattle, Wash.
Richard F. Shea 225 Twin Hills Drive Syracuse, N. Y.	SYRACUSE (4)	Major A. Johnson 162 Lincoln Ave. Syracuse, N. Y.
W. M. Stringfellow 136 Huron St. Toledo, Ohio	TOLEDO (4)	G. H. Eash 845 W. Woodruff Ave. Toledo, Ohio
J. R. Bain 169 Kipling Ave. S. P. O. 54 Toronto, Ont., Canada	TORONTO, ONTARIO (8)	E. L. Palin 2139 Bayview Ave. Toronto, Ont., Canada
C. E. Buffum Box 591 Tulsa, Okla.	TULSA (6)	W. J. Weldon 2530 E. 25 St. Tulsa, Okla.
O. A. Schott 4224 Elmer Ave. Minneapolis, Minn.	TWIN CITIES (5)	F. S. Hird 224 S. 5th St. Minneapolis, Minn.
A. H. Gregory 150 Robson St. Vancouver, B. C. Canada	VANCOUVER (8)	Miles Green 2226 W. 10th Ave. Vancouver, B. C. Canada
M. W. Swanson 1420 Mt. Vernon Memorial H'way Alexandria, Va.	WASHINGTON (3)	T. B. Jacocks 777 14 St., N.W. Washington, D. C.
R. C. Lepley R.D. 2 Williamsport, Pa.	WILLIAMSPORT (4)	W. . Bresee 818 Park Ave. Williamsport, Pa.

Subsections

Chairman		Secretary
R. F. Lee 2704-31 St. Lubbock, Tex.	AMARILLO-LUBBOCK (6) (Dallas-Ft. Worth)	C. M. McKinney 3102 Oakmont Austin, Tex.
Carl Volz 160 W. Hamilton Ave. State College, Pa.	CENTRE COUNTY (4) (Emporium)	R. L. Riddle Penn. State College State College, Pa.
F. G. McCoy Rt. 4, Box 452-J Charleston, S. C.	CHARLESTON (6) (Atlanta)	C. B. Lax Sergeant Jasper Apts. Charleston, S. C.
W. W. Salisbury 910 Mountain View Dr. Lafayette, Calif.	EAST BAY (7) (Los Angeles)	J. M. Rosenberg 1134 Norwood Ave. Oakland 10, Calif.
Allen Davidson 3422 Argyle Ave. Erie, Pa.	ERIE (4) (Buffalo-Niagara Subsection)	
S. L. Johnston 207 Edgewood Dr. Huntsville, Ala.	HUNTSVILLE (6) (Atlanta)	R. C. Haraway 603 College Hill Apts. Huntsville, Ala.
C. R. Burrows 116 Mitchell St. Ithaca, N. Y.	ITHACA (4) (Syracuse Subsection)	Benjamin Nichols Cornell University Ithaca, N. Y.
L. B. Headrick RCA Victor Div. Lancaster, Pa.	LANCASTER (3) (Philadelphia)	C. G. Landis Safe Harbor, Box 6 Conestoga, Pa.
D. M. Saling 2 Baker St. Poughkeepsie, N. Y.	MID-HUDSON (2) (New York)	E. A. Keller Red Oaks Mill Rd. R.D. 2 Poughkeepsie, N. Y.
S. D. Robertson Box 107 Red Bank, N. J.	MONMOUTH (2) (New York)	G. F. Senn 81 Garden Rd. Little Silver, N. J.
A. G. Richardson 180 Vreeland Ave. Boonton, N. J.	NORTHERN N. J. (2) (New York)	P. S. Christaldi 760 Bloomfield Ave. Clifton, N. J.
E. L. Michaels 1167 Casa Vista Dr. Pomona, Calif.	ORANGE BELT (7) (Los Angeles)	Eli Blutman 6814 Glacier Dr. Riverside, Calif.
O. G. Villard, Jr. 2050 Dartmouth St. Palo Alto, Calif.	PALO ALTO (7) (San Francisco)	J. V. Granger 772 Paul Ave. Palo Alto, Calif.
J. H. Vogelman 404 W. Cedar St. Rome, N. Y.	ROME (4) (Syracuse Subsection)	Fred Moskowitz 514 E. Bloomfield St. Rome, N. Y.
George Weiler 1429 E. Monroe South Bend, Ind.	SOUTH BEND (5) (Chicago)	A. R. O'Neil WSBT-WSBT-TV South Bend, Ind.
Capt. L. A. Yarbrough 3001 USAFIT Wright-Patterson Air Force Base, Ohio	USAFIT	Lt. Col. R. D. Sather Box 3344 USAFIT Wright-Patterson Air Force Base, Ohio
H. G. Swift Route 2 Derby, Kan.	WICHITA (Kansas City)	P. A. Bunyar 1328 N. Lorraine Wichita, Kan.
R. F. Tinkler 166 Portage Ave., E. Winnipeg, Canada	WINNIPEG (8) (Toronto)	H. R. Gissing 65 Rorie St. Winnipeg, Canada

Professional Groups

	Chairman
AIRBORNE ELECTRONICS	K. C. Black Polytechnics Res. and Devel. Co. Brooklyn, N. Y.
ANTENNAS AND PROPAGATION	P. S. Carter, RCA Labs Rocky Point, L. I., N. Y.
AUDIO	Narvin Camras Armour Research Foundation Chicago, Ill.
BROADCAST AND TELEVISION RECEIVERS	D. D. Israel 111 8 Ave., New York, N. Y.
BROADCAST TRANSMISSION SYSTEMS	Lewis Winner 52 Vanderbilt Ave., New York, N. Y.
CIRCUIT THEORY	R. L. Dietzold 34 W. 11 St., New York, N. Y.
COMMUNICATIONS SYSTEMS	Col. John Hessel Signal Corps Engineering Labs Fort Monmouth, N. J.
COMPONENT PARTS	Floyd A. Paul Northrop Aircraft, Inc. Hawthorne, Calif.
ELECTRONIC DEVICES	L. S. Nergaard, RCA Labs Princeton 5, N. J.
ELECTRONIC COMPUTERS	John H. Howard Burroughs Adding Machine Co. Philadelphia, Pa.
ENGINEERING MANAGEMENT	Gen. T. C. Rives General Electric Co.; Syracuse, N. Y.

	Chairman
INDUSTRIAL ELECTRONICS	Eugene Mittlemann 549 W. Washington Blvd., Chicago, Ill.
INFORMATION THEORY	Nathan Marchand Sylvania Electric Products Inc. Bayside, L. I., N. Y.
INSTRUMENTATION	I. G. Easton General Radio Co., Cambridge, Mass.
MEDICAL ELECTRONICS	L. H. Montgomery, Jr. Vanderbilt Univ., Nashville, Tenn.
MICROWAVE THEORY AND TECHNIQUES	Andre G. Clavier Federal Telecomm. Labs. Inc. Nutley, N. J.
NUCLEAR SCIENCE	L. R. Hafstad Atomic Energy Comm. Rm. 132, 1901 Constitution Ave., Wash., D. C.
QUALITY CONTROL	Leon Bass, General Elec. Co. Schenectady, N. Y.
RADIO TELEMETRY AND REMOTE CONTROL	M. V. Kiebert, Jr. Bendix Aviation Corp. Teterboro, N. J.
ULTRASONICS ENGINEERING	A. L. Lane, Naval Ordnance Labs White Oak, Md.
VEHICULAR COMMUNICATIONS	F. T. Budelman Budelman Radio Corp. Stamford, Conn.

Abstracts and References

Compiled by the Radio Research Organization of the Department of Scientific and Industrial Research, London, England, and Published by Arrangement with that Department and the *Wireless Engineer*, London, England

NOTE: The Institute of Radio Engineers does not have available copies of the publications mentioned in these pages, nor does it have reprints of the articles abstracted. Correspondence regarding these articles and requests for their procurement should be addressed to the individual publications, not to the IRE.

The number in heavy type at the upper left of each Abstract is its Universal Decimal Classification number and is not to be confused with the Decimal Classification used by the United States National Bureau of Standards. The number in heavy type at the top right is the serial number of the Abstract. DC numbers marked with a dagger (†) must be regarded as provisional.

The index to the Abstracts and References published in the PROC. I.R.E., from February, 1952 through January, 1953, is published by the *Wireless Engineer* and may be purchased for $0.68 (including postage; from the Institute of Radio Engineers, 1 East 79th St., New York 21, N. Y. As supplies are limited, the publishers ask us to stress the need for early application for copies. Included with the Index is a selected list of journals scanned for abstracting, with publishers' addresses.

ACOUSTICS AND AUDIO FREQUENCIES

016:534 1549

References to Contemporary Papers on Acoustics—R. T. Beyer. (*Jour. Acoust. Soc. Amer.*, vol. 25, pp. 164–168; Jan. 1953.) Continuation of 910 of April.

534.1+621.396.615:621.3.016.37 1550

Electrical and Acoustic Oscillation Build-Up Phenomena—Dänzer. (See 1626.)

534.231:532.517 1551

Acoustic Streaming due to Attenuated Plane Waves—W. L. Nyborg. (*Jour. Acoust. Soc. Amer.*, vol. 25, pp. 68–75; Jan. 1953.)

534.231:532.527 1552

The Theory of Steady Rotational Flow Generated by a Sound Field—P. J. Westervelt. (*Jour. Acoust. Soc. Amer.*, vol. 25, pp. 60–67; Jan. 1953.)

534.231.1:621.3.018.7 1553

Nonlinear Dissipative Distortion of Progressive Sound Waves at Moderate Amplitudes—J. S. Mendousse. (*Jour. Acoust. Soc. Amer.*, vol. 25, pp. 51–54. Jan. 1953.)

534.231.3 1554

The Physical Interpretation of the Expression for an Outgoing Wave in Cylindrical Coordinates—M. C. Junger. (*Jour. Acoust. Soc. Amer.*, vol. 25, pp. 40–47; Jan. 1953.) The sound field generated by a vibrating cylinder of infinite length is expressed in terms of acoustic impedance ratios. The effect of variation of wavelength on the propagation of the various possible modes is examined. Graphs of the impedance ratios corresponding to certain modes are presented.

534.232 1555

Effect of a Finiate Circular Baffle Board on Acoustic Radiation—T. Nimura & Y. Watanabe. (*Jour. Acoust. Soc. Amer.*, vol. 25, pp. 76–80; Jan. 1953.) The oblate-spheroidal wave function developed by Kotani and by Bouwkamp is used to calculate the effect of a circular baffle on the radiation field of a circular disk. Results are shown graphically.

534.232:534.321.9:538.652 1556

Critical Consideration of Ultrasonic-Wave Generators using Linear-Magnetostrictive Dumb-Bell-Type Oscillators—H. H. Rust & E. Bailitis. (*Akust. Beihefte*, no. 2, pp. 89–90; 1952.) In this type of generator the amplitude of the longitudinal oscillations suffers reduction as a result of the transverse effect. For Ni oscillators of usual dimensions, off-resonance amplitudes are less than half the values to be expected from the magnetostriction curve, taking account of the reduction of amplitude due to remanence. An arrangement is indicated in which the effect is compensated by using Ni laminations for the exciting bar and Fe-Ni laminations for the radiating pistons.

534.26 1557

Diffraction of Sound Waves by a Circular Aperture in a Rigid Screen—H. Severin & C. Starke. (*Akust. Beihefte*, no. 2, pp. 59–66; 1952.) Measurements were made of the sound pressure along the axis behind the aperture and in the plane of the screen, using apertures of radius 0.5 λ, λ, 1.5 λ, 2λ, 3λ and 4 λ. The results are compared with two approximate solutions calculated from Kirchhoff's theory. The observed distribution agrees best with theoretical values obtained by using a velocity potential derived on the assumption that the aperture area is covered with radiating dipoles. Corresponding work on e.m. waves is noted in 2412 of 1951 (Severin.)

534.321.9 1558

Interference of Ultrasonic Beams [incident on and] reflected by a Plane Wall. Conduction of Waves—F. Canac. (*Comp Rend. Acad. Sci.* (Paris), vol. 236, pp. 360–362; Jan. 26, 1953.) Shadow patterns obtained by a stroboscopic method show the wave formation for different angles of incidence. An analogy with waveguide propagation is illustrated using two parallel reflectors.

534.321.9 1559

Velocity of Ultrasonic Waves in Argon at Pressures up to 950 Atm—A. Lacam & J. Noury. (*Comp. Rend. Acad. Sci.* (Paris), vol. 236, pp. 362–364; Jan. 26, 1953.) Results of measurements by a light-diffraction method at about 900 kc show that the velocity increases nearly linearly with pressure over the range 250–650 atm.

534.321.9:532.528 1560

Methods for investigating Oscillation Cavitation in Liquids by means of Ultrasonics—T. Lange. (*Akust. Beihefte*, no. 2, pp. 75–82; 1952.)

534.321.9:534.614 1561

Ultrasonic Measurements—A. Giacomini. (*Ricerca Sci.*, vol. 23, pp. 75–80; Jan. 1953.) A pulse method for measuring the velocity of ultrasonic waves in solids is based on a comparison between the unknown velocity and the velocity in water.

534.321.9:534.833.4 1562

Investigations of Ultrasonic Absorption in Animal Tissues and in Plastics—R. Esche. (*Akust. Beihefte*, No. 2, pp. 71–74; 1952.) A method is described for measurements in the range 300–600 kc. The absorption coefficient is found to increase linearly with frequency, as at higher frequencies.

534.321.9–14 1563

The Behaviour of Ultrasonics in Liquids—J. Lamb. (*Research* (London), vol. 5, pp. 553–560; Dec., 1952.) The results of recent research are reviewed, with particular reference to the measurement and physical interpretation of relaxation effects in pure liquids, electrolytes and polymer liquids. About 50 references.

534.414 1564

The Effects of Viscous Dissipation in the Spherical Acoustic Resonator—H. G. Ferris. (*Jour. Acoust. Soc. Amer.*, vol. 25, pp. 47–50; Jan. 1953.) Analysis shows that the effect of viscosity is to decrease slightly the natural frequencies and to cause decay of the free vibrations. The attenuation of the purely radial modes of vibration is much less than that for modes with tangential velocity components.

534.613:534.37 1565

Radiation Pressure and Dispersion—E. J. Post. (*Jour. Acoust. Soc. Amer.*, vol. 25, pp. 55–60; Jan. 1953.) Discussion of basic theories relative to propagation in a dispersive medium, with particular reference to boundary conditions and the essential difference between acoustic and electromagnetic radiation pressure. An extensive annotated bibliography, dating back to 1870, is given.

534.614 1566

Precision Measurement of the Velocity of Sound in Air—P. W. Smith, Jr. (*Jour. Acoust. Soc. Amer.*, vol. 25, pp. 81–86; Jan. 1953.) A method is described in which the driving-point impedance of a loudspeaker connected to a closed tube of adjustable length serves as the frequency-controlling element of a bridge-stabilized oscillator. Results of measurements at 1 kc in air, corrected to standard conditions, give a velocity of 331.45 ± 0.05 m/s.

534.62 1567

Investigations for improving the Linings of Acoustically Damped Rooms—G. Kurtze. (*Akust. Beihefte*, no. 2, pp. 104–107; 1952.) By arranging Helmholtz-type resonators be-

hind absorbing wedges, the same amount of absorption is achieved with a reduction of one-third in the thickness of the lining and without raising the lower frequency limit.

534.78:681.613 1568

The Phonetic Type-sonograph or Phonetograph—J. Dreyfus-Graf. (*Tech. Mitt. schweiz. Telegr.-Teleph. Verw.*, vol. 30, pp. 363–379; Dec. 1, 1952. In French.) Developments of the steno-sonograph (271 and 1330 of 1950) are described. The present models give a phonetic transcript of speech in the form of known alphabetic symbols by means of an electric typewriter. The speech is transformed into groups of nine pulses which are compared two-by-two in an electrical computer operating on the trinary system (0+−). A system of lamps associated with the computer enables conversation to be followed by the deaf. The width of the frequency channel necessary for transmitting phonetograms is 270 cps according to Fourier theory, i.e., 135 cps in practice.

534.833 1569

Wide-Band Absorbers for Liquid-Borne Sound—E. Meyer & K. Tamm. (*Akust. Beihefte*, no. 2, pp. 91–104; 1952.) Description, with theory and performance figures, of absorbers for the frequency range 5–50 kc, suitable for lining measuring tanks. Porous elastic-rubber materials are used and the devices have ribs arranged to form parallel ducts whose walls are sloped for impedance matching.

534.844/.845 1570

Comparative Absorption-Coefficient Measurements 1950—A. Eisenberg. (*Akust. Beihefte*, no. 2, pp. 108–114; 1952.) Measurements previously reported by Meyer & Schoch (2412 of 1939) did not agree sufficiently well to serve as a basis for a test specification. Further measurements are now reported and a tentative test specification is presented for the determination of absorption coefficients by the reverberation-chamber method.

534.844.1 1571

The Accuracy of Reverberation-Time Measurements with Warble Tones and White Noise—W. Furrer & A. Lauber. (*Jour. Acoust. Soc. Amer.*, vol. 25, pp. 90–91; Jan. 1953.) Investigations in three rooms of very different volumes show that the probable error of reverberation-time measurements is less with warble tones than with white noise at 200 cps. the reverse being the case at 800 and 3200 cps.

534.846.4 1572

Improvement of Audibility in a Theatre by means of a Sound-Delaying "Quiet-Speaker" System—G. R. Schodder, F. K. Schröder & R. Thiele. (*Akust. Beihefte*, no. 2, pp. 115–116; 1952.) Account of experiments made inside a hall at Recklinghausen; the technique was similar to that used by Parkin & Scholes (1294 of 1951) in their investigations of an open-air theatre.

534.862:534.874.1 1573

Acoustic Problems at the "Waldbühne" Open-Air Sound Theater in Berlin—H. Simon. (*Jour. Soc. Mot. Pict. Telev Engrs.*, vol. 59, no. 6, pp. 512–516; Dec. 1952.) General arrangements for vision-sound synchronization for film reproduction are discussed, Uniform sound volume for an audience of 25,000 is achieved by careful adjustment of the beam direction of loudspeaker units at each side of the screen, each unit comprising two groups of three loudspeakers with different frequency characteristics. The calculated amplifier power required to give the required audibility over a wide frequency range is about 129 W, the acoustic power being 8–10 W.

534.874.1:621.395.61 1574

Methods of Directional Sound Reception—H. Grosskopf. (*Tech. Hausmitt. NordwDtsch. Rdfunks*, vol. 4, pp. 209–218; Nov./Dec. 1952.) Various methods for the directional reception of speech and music are reviewed, including those using (*a*) gradient microphones of the first, second or higher order, either singly or in groups, (*b*) microphones utilizing the interference of sound waves, some using reflectors, others groups of receivers, as in the tubular and line microphones of Mason & Marshall (1518 of 1939) and Olson (3600 of 1939). Figure 2 in the article should be rotated through 180°.

621.395.625.3 1575

The Field of Harmonically Magnetized Recording Tape. Playback under Open-Circuit Conditions with Ideal and with Very-Wide-Gap Head—O. Schmidbauer. (*Frequenz*, vol. 6, pp. 281–290 & 319–324; Oct. & Nov. 1952.)

621.395.625.3 1576

Performance of High-Output Magnetic Tape—L. B. Lueck & W. W. Wetzel. (*Electronics*, vol. 26, pp. 131–133; March 1953.) Performance figures are given for a new recording tape, to be known as Scotch Brand No. 120, which will give a 6-db greater output than the standard Scotch Brand No. 111 without rise of noise level. Remanence is increased by a factor of 2.2 compared with No. 111 tape, and the new tape has considerably lower distortion, so that greater signal voltages can be used without the distortion exceeding permissible limits.

621.395.625.3+534.852]:061.3 1577

U.E.R. [Union Européenne de Radiodiffusion] Conference on Magnetic Sound Recording, Hamburg, 18th–22nd November 1952—K. E. Gondesen. (*Tech. Hausmitt. NordwDtsch. Rdfunks*, vol. 4, p. 230; Nov./Dec. 1952.)

ANTENNAS AND TRANSMISSION LINES

621.315.212 1578

Investigations on Broadcast-Programme Line Using Star-Quad Cable without Coil Loading—E. A. Pavel & H. v. Schau. (*Fernmeldetech. Z.*, vol. 5, pp. 551–562; Dec. 1952.) Extensive measurements at frequencies up to 15 kc are reported on the "high-quality" cable running from Hamburg to Frankfort and back, a total distance of 1072 km, and incorporating 33 line amplifiers. A difference between input and output quality could be detected only after a repetition process corresponding to transmission over a cable length of about 5000 km.

621.392 1579

The Input Impedance of a Line, and the Location of Nonuniformities—R. Monelli. (*Alta Frequenza*, vol. 21, pp. 260–287; Dec. 1952.) Formulas are derived for the input resistance and reactance of a very long line with purely resistive characteristic and terminating impedances. A special function is introduced expressing the relation between attenuation and terminating-impedance mismatch. The information obtainable from RF-bridge impedance measurements is discussed.

621.392.09 1580

Theory of the Single-Wire Transmission Line—T. E. Roberts, Jr. (*Jour. Appl. Phys.*, vol. 24, pp. 57–67; Jan. 1953.) Equations are derived for the current induced in an infinitely long straight wire of finite surface impedance, connected to a flanged coaxial line. Radiation patterns are computed and the input conductance is determined. The current comprises two components, one of which is a modal current. Graphs are given for computing the efficiency of excitation of this component. A second system comprising a single wire between perfectly conducting parallel plates is investigated as a boundary-value problem; the solution is used in the discussion of the physical properties of a finite-length single-wire transmission line. Usual transmission-line concepts are applicable under certain restricting conditions.

621.392.22:517.9 1581

Applications of the Theory of Systems of Differential Equations to Multiple Nonuniform Transmission Lines—R. L. Sternberg & H. Kaufman. (*Jour. Math. Phys.*, vol. 31, pp. 244–252; Jan. 1953.)

621.392.26 1582

Theory of Propagation in Waveguides—E. Ledinegg & P. Urban. (*Acta Phys. Austriaca*, vol. 5, pp. 1–11; Nov. 1951.) See 2433 of 1952.

621.392.26 1583

An Exact Formulation of the Problem of Diffraction by Diaphragms with Slits in Waveguides with Rectangular Cross-Section—R. Müller. (*Z. Angew. Phys.*, vol. 4, pp. 424–433; Nov. 1952.) From results previously reported (625 of March) for waveguides of arbitrary cross-section, formulas are derived for the case of a diaphragm, with a symmetrically placed slit, in a rectangular waveguide. The original two-dimensional problem turns into a series of one-dimensional problems. In the absence of an incident wave a field can exist in the waveguide only for some particular values of wave number. Conditions for the existence of various modes are investigated and the singular behavior of H_{0n} waves is discussed. Analysis is given for the case of an incident H_{10} or H_{01} wave at a frequency such that it is the only homogeneous wave of its type of symmetry. For the H_{10} wave the solution is given by a symmetrical Fredholm integral equation of the first kind, for the H_{01} wave by a pair of such equations.

621.392.26 1584

Waveguide Attenuation and its Correlation with Surface Roughness—F. A. Benson. (*Proc. IEE* (London) part III, vol. 100, pp. 85–90; March, 1953.) The attenuation of 9.375-kmc waves in samples of standard commercial waveguide was determined by a method involving examination of the standing-wave pattern near a voltage minimum. Detailed studies were made of the roughness of the internal surfaces of the waveguides. Discrepancies between measured and calculated values of attenuation are attributed to surface roughness, though in some cases very high values of measured attenuation are attributable to high resistivity of the waveguide material. One particular sample of "copper" waveguide, with a dc resistivity nearly three times that of pure Cu, was analyzed and found to be made from deoxidized arsenical copper. Effects of small changes in waveguide dimensions on the attenuation are estimated and a modification of Kuhn's attenuation formula (1328 of 1947) is given which takes account of surface roughness.

621.392.26 1585

Low-Loss Waveguide Transmission—S. E. Miller & A. C. Beck. (Proc. I.R.E., vol. 41, pp. 348–358; March, 1953.) Report of experiments on long-distance transmission, using frequencies around 9 kmc with circular waveguide of diameter about 5 in. and propagating the TE_{01} mode, the theoretical loss being 2 db/mile. 0.1-μs pulses were transmitted over a distance of 40 miles. Observed losses averaged about 50% more than the theoretical values, as a result of surface roughness and mode conversion. Compared with dominant-mode transmission, this multimode system has the advantages of increased bandwidth, reduced delay distortion and reduced size, and the disadvantage of reduced mechanical tolerances. Mode filtering devices are discussed. See also 2992 of 1952 (King).

621.392.26:538.221 1586

Modes in Waveguides containing Ferrites—M. L. Kales. (*Trans. I.R.E.*, pp. 104–105; Dec., 1952.) Analysis shows that in a cylindrical waveguide filled with a homogeneous ferrite material subjected to a constant axial magnetic field no TE, TM or TEM modes are possible.

621.396.67 1587

Radiation from a Horizontal Dipole in a

Semi-infinite Dissipative Medium—R. H. Lien. (*Jour. Appl. Phys.*, vol. 24, pp. 1–4; Jan., 1953.) Formulas are derived for the radiation field. Solutions are obtained in the form of complex integrals which can be evaluated in closed form for low frequencies.

621.396.67 1588

The Radiation Resistance of a Straight Wire in Free Space—R. Müller. (*Arch. Elect. Übertragung*, vol. 7, pp. 56–57; Jan., 1953.) The function expressing the dependence of the radiation resistance on the ratio of wire length to wavelength is shown to have a periodic component superimposed on the monotonically increasing term.

621.396.67:621.397.6 1589

Multiple Television and Frequency-Modulation Transmitting Antenna Installation on the Empire State Building—J. B. Dearing, H. E. Gihring, R. F. Guy & F. G. Kear. (PROC. I.R.E., vol. 41, pp. 324–337; March, 1953.) Account of the development and performance of the installation, which comprises a steel tower supporting six aerial systems, radiating altogether five picture carriers, five sound carriers and three FM carriers. See also 1568 of 1951 (Kear & Hanson).

621.396.67:621.397.62 1590

Television Aerials—G. W. Luscombe. (*Wireless Eng.*, vol. 30, pp. 82–90; April, 1953.) An investigation of receiving antennas. The most important characteristics determining performance are the gain, the radiation pattern and the impedance. Methods of measuring these properties are described, the precautions necessary to ensure good accuracy being indicated. Results obtained with nine outdoor aerials of British manufacture are presented; measurements were made at vision-carrier and sound-carrier frequencies.

621.396.67.013.24 1591

Impulse Electromagnetic Fields—J. A. Feyer. (*Trans. S. Afr. Inst. Elec. Eng.*, vol. 43, part 10, p. 291; Oct., 1952.) An error in Kitai's paper (38 of January) is pointed out. At distances $>\lambda/2\pi$ the radiation field predominates over the induction field in respect of both intensity and the spectrum function at a given frequency.

621.396.677 1592

Further Effects of Manufacturing Tolerances on the Performance of Linear Shunt Slot Arrays—H. F. O'Neill & L. L. Bailin. (*Trans. I.R.E.* no. PGAP-4, pp. 93–102; Dec., 1952.) Calculations are made of the increase of side-lobe level due to specified deviations from the optimum array parameters, thus providing data of service in fixing manufacturing tolerances. Curves are given to facilitate the design of Dolph-Tchebycheff-type arrays with 12, 24 or 48 elements. See also 1241 of May (Bailin & Ehrlich).

621.396.677 1593

A Helical Beam [aerial] for Citizens' Radio—E. F. Harris. (*Electronics*, vol. 26, pp. 134–135; March, 1953.) Description, with radiation diagrams, of a 6-turn helical antenna of $\frac{3}{8}$-in. Cu braid embedded in fiberglas moulding of length 29 in. and diameter 6.5 in. With a 16×16-in. Al ground plate, good directivity is obtained from 390 to 600 mc. With 4 such elements on a common ground plate at each end of a radio link, the gain is increased by 12 db compared with the use of single units. See also 3511 of 1948 (Lurie) and back references.

621.396.677 1594

Optimum Design of Linear Arrays in the Presence of Random Errors—D. Ashmead. (*Trans. I.R.E.* no. PGAP-4, pp. 81–92; Dec., 1952.) Assuming the maximum error in the current at any radiator element is a constant fraction of the designed current, a method is given for finding the mean side-lobe suppression that can be obtained for any Tchebycheff distribution. Over-correction in the design may result in less suppression and lower gain. A method is also given for finding the aperture efficiency of a Tchebycheff distribution without calculating the individual currents. See also 1241 of May (Bailin & Ehrlich).

621.396.677 1595

Lattice Lenses for Centimeter Waves—J. Moussiegt. (*Onde élect.*, vol. 32, pp. 515–518; Dec., 1952.) See 3004 and 3355 of 1952.

621.396.677.029.6 1596

On Spherically Symmetric Lenses—J. E. Eaton. (*Trans. I.R.E.*, no. PGAP-4, pp. 66–71; Dec., 1952.) Generalization of Luneberg's spherical lens, with a solution of the integral equation for the ray paths.

621.396.677.029.6 1597

Astigmatic Diffraction Effects in Microwave Lenses—A. S. Dunbar. (*Trans. I.R.E.*, no. PGAP-4, pp. 72–80; Dec. 1952.) Discussion of the effects of astigmatism on the diffraction pattern and gain of a lens antenna.

CIRCUITS AND CIRCUIT ELEMENTS

621.314.22.015.7 1598

Design of Series Peaking Transformers—A. C. Sim. (*Wireless Eng.*, vol. 30, pp. 90–93; April, 1953.) Essential features of this type of transformer are (*a*) the load current is arranged to be negligible compared with the magnetizing current, and (*b*) the magnetizing current is allowed to reach a value much greater than that required to saturate the core. An easy and accurate design method is presented which does not require an analytical representation of the B/H characteristic. The example of a transformer to produce a voltage pulse of about 100 V for triggering a thyratron is worked out numerically. The voltage and duration of the pulse can be predicted to within about 20% of the measured values.

621.314.222 1599

Investigations on Voltage Transformers—H. Kafka. (*Elektrotech. u. Maschinenb.*, vol. 69, pp. 523–532; Dec. 1, 1952.) A conductance diagram is developed to show directly the variation of secondary voltage and phase angle as a function of the load. Its application in transformer design is illustrated.

621.314.5:537.525.92 1600

D.C./A.C. Convertor utilizing the Space-Charge Capacitance of a Valve—H. Wechsung. (*Frequenz*, vol. 6, pp. 336–337; Nov., 1952.) Two circuits are described for converting feeble dc to ac prior to amplification for measurement purposes. Both make use of the variation of grid-cathode capacitance with the voltage applied to the grid, the first circuit using a bridge balanced for a certain value of the grid-cathode capacitance, so that any variation produces a proportionate deflection of a meter. The second circuit uses a balanced arrangement of two valves with a differential transformer. Zero stability is good in both cases.

621.314.7(083.3) 1601

Transistor Equations—F. R. Stansel. (*Electronics*, vol. 26, pp. 156, 158; March, 1953.) Formulas giving circuit voltage and current gain, and impedance characteristics, in terms of transistor parameters are tabulated for grounded-base, grounded-emitter, and grounded-collector transistor amplifier circuits.

621.318.57 1602

Static-Dynamic Design of Flip-Flop Circuits—C. L. Wanlass. (*Trans. I.R.E.*, no. PGEC-1, pp. 6–18; Dec., 1952.) Discussion of the design of flip-flop circuits for operation from a relatively low supply voltage, a desirable feature for computer elements. The circuit adopted uses negative-pulse triggering and a diode input circuit, the minimum trigger voltage being adjustable by means of two variable resistors. Stability is determined by use of Routh's criteria. General directions for the design of flip-flop circuits for low-voltage operation are summarized.

621.392.5 1603

Design of Low-Frequency Constant-Time-Delay Lines—C. M. Wallis. (*Elec. Eng.*, (N. Y.), vol. 71, p. 1123; Dec., 1952.) Digest only. Analysis is presented for ladder-type low-frequency delay lines consisting of Pierce asymmetrical T sections, each section having two unequal coils in series, wound on a common core to give a coupling coefficient near unity, a capacitor being connected from the junction of the coils to earth. When properly terminated, such delay lines give delays constant to within ±1% over 60% of the pass band. Where many sections must be used, they have the decided advantage of requiring only two components per section, a double-winding inductor and a capacitor.

621.392.5 1604

Transfer Matrix of a Four-Terminal Passive Network in terms of its Image Parameters—H. P. Biggar. (*Electronic Eng.*, vol. 25, pp. 152–153; April, 1953.) The constants in the fundamental simultaneous equations relating the input and output voltages and currents for a linear passive quadripole have a particular significance and can be used to derive the transfer matrix of any passive network in terms of the image impedances. This is demonstrated for the L type of network.

621.392.5 1605

The Measurement of "A" Matrix Elements of Passive Networks—W. R. Hinton. (*Electronic Eng.*, vol. 25, pp. 151–152; April, 1953.) The general method of using the "A" matrix has previously been described (840 of 1950). A method is here described for determining the matrix elements from measurements of the impedance looking in at the sending end of a network, the receiving and end being first open-circuited and then short-circuited. The elements so found apply only for the measurement frequency. The analysis shows that networks are electrically equivalent at a given frequency when their "A" matrices are equal at that frequency.

621.392.5 1606

The Maximum Gain of an RC Network—A. D. Fialkow & I. Gerst. (PROC. I.R.E., vol. 41, pp. 392–395; March, 1953.) Analysis is presented indicating that any desired voltage gain can be achieved at a given real frequency by using networks of sufficient complexity as represented by the degree of the corresponding formulas. Transfer-function theory developed previously (3369 of 1952) is used. The relation between the maximum possible gain and the degree of the transfer function is determined. The results are illustrated by examples.

621.392.5 1607

Note on a Network Theorem—L. Storch. (*Wireless Eng.*, vol. 30, no. 4, pp. 77–81; April, 1953.) The formulation adopted by Zepler (1535 of 1952) is criticized, and it is shown that his results can be obtained more simply by using the conventional impedance concept rather than his unconventional power concept.

621.392.5.018.7 1608

Waveform Computations by the Time-Services Method—N. W. Lewis. (*Proc. IEE* (London), part III, vol. 100, pp. 109–110; March, 1953.) Discussion on paper abstracted in 55 of January.

621.392.5.018.75 1609

The Synthesis of a Network to have a Sine-Squared Impulse Response—W. E. Thomson. (*Proc. IEE* (London), part III, vol. 100, p. 110; March, 1953.) Discussion on paper abstracted in 348 of February.

621.392.5.029.64:538.221 1610
Reduction of the Loss in Ferrite Materials in the Microwave Region—H. N. Chait, N. G. Sakiotis & R. E. Martin. (*Jour. Appl. Phys.*, vol. 24, pp. 109–110; Jan., 1953.) The loss in microwave gyrators, of the type comprising a ferrite rod inside a circular waveguide surrounded by a solenoid producing an axial magnetic field, has in certain cases been reduced by application of an auxiliary transverse static magnetic field.

621.392.52 1611
Filter Transfer Function Synthesis—G. L. Matthaei. (Proc. I.R.E., vol. 41, pp. 377–382; March, 1953.) Theory is developed for circuits in which approximately constant attenuation is achieved over one or more frequency bands. An electrostatic-potential-analogue method is used [see 2750 of 1949 (Klinkhamer)]. The method is applied to some examples of low-pass filters.

621.392.52 1612
A Systematic Procedure for the Design of Filters—K. H. Haase. (*Frequenz.*, vol. 6, pp. 363–368; Dec., 1952. & vol. 7, pp. 8–14; Jan., 1953.) Continuing previous work on the formulation of the characteristic functions of filters (3377 of 1952), tables are developed which facilitate the determination of the circuit elements of coupling-free filters of various types.

621.392.52 1613
Multistage Band-Pass Filter with Optimum Approximation to the Ideal Rectangular Shape of the Response Curve—G. Drexler & H. H. Voss. (*Frequenz*, vol. 6, pp. 337–342; Nov., 1952.)

621.392.52 1614
The Design of Linear-Phase Low-Phase Filters—C. F. Floyd, R. L. Corke & H. Lewis. (*Proc. IEE* (London), part IIIA, vol. 99, no. 20, pp. 777–787. Discussion, pp. 860–866; 1952.) General design principles are outlined and a method applicable to certain low-pass filters required in television equipment is described. Adequate phase linearity of response can be obtained over the whole pass band only by limiting the discrimination required in the attenuation region of the insertion-loss characteristic. Practical examples include (*a*) a set of low-pass filters with linear phase characteristics from zero nearly to their cut-off frequencies, which range from 1.5 to 4 mc, (*b*) an asymmetric-sideband filter with a cut-off frequency of 6.12 mc and phase linearity from 3 to 7 mc, with 30-db discrimination above 7 mc.

621.392.52:538.652 1615
How to Use Mechanical I. F. Filters—M. L. Doelz & J. C. Hathaway. (*Electronics*, vol. 26, pp. 138–142; March, 1953.) Discussion of the construction and performance of electromechanical filters using magnetostrictive Ni wires as coupling units between metal-disk resonators. A typical 6-disk filter has a 6-db bandwidth of 3.1 kc centered on 455 kc, with a transmission loss <26 db and an operating temperature from $-30°$ to $+80°$C. The size of the complete assembly is only $2\frac{13}{16}\times 1\times\frac{15}{16}$ in.

621.392.6 1616
Fundamental Results and Outstanding Problems of Network Synthesis—V. Belevitch. (*Tijdschr. ned. Radiogenoot.*, vol. 18, pp. 33–51; Jan., 1953. In English.) See also 1547 of 1952.

621.392.6 1617
Synthesis of n-Terminal-Pair Networks—M. Bayard. (*Ann. Télécommun.*, vol. 7, pp. 517–524; Dec., 1952.) Dissipative networks only are considered. Generalization of the Gewertz reduced-matrix method and three methods involving auxiliary reactive networks are outlined and critically reviewed. The first auxiliary reactive network method considered was developed independently by Oono (65 of 1951) and Leroy (1616 of 1950 and 64 of 1951), the second was due to Bayard (593 of 1951) and the third to Belevitch (1547 of 1952).

621.396.6:061.4 1618
R.E.C.M.F. Exhibition Preview—(*Electronic Eng.*, vol. 25, pp. 168–171; April, 1953.) Short descriptions of selected exhibits at the exhibition arranged by the Radio and Electronics Component Manufacturer's Federation, London, April, 1953.

621.396.611.21 1619
Piezo-electric Oscillations of Quartz Plates at Even and Half-Odd Harmonics—S. Parthasarathy, M. Pancholy & A. F. Chhapgar. (*Nature* (London), vol. 171, pp. 216–217; Jan. 31, 1953.) A number of quartz plates of different dimensions were plated with Ag, Al or Cu by various methods and tested in the same circuit. Results show that a quartz plate has preferred modes of oscillation at the odd and even harmonics and at frequencies midway between these, though the amplitude of the odd harmonics is very much the greater.

621.396.611.33 1620
The Double Resonance in the Secondary of a System of Two Circuits with Inductive Coupling—R. Cazenave. (*Rev. gén. Élec.*, vol. 61, pp. 586–595; Dec., 1952.) The resonance condition is defined in terms of the primary and secondary impedances and the mutual inductance. The variation of secondary current with the coupling, frequency, and series capacitance is determined. In the case of a variable frequency with fixed coupling a graphical method is used to derive "equal-current" curves. By means of these a region can be defined within which two resonance peaks occur.

621.396.611.4 1621
Some Exactly Integrable Cases of Electromagnetic Oscillations in Two Coupled Cavity Resonators—L. Breitenhuber. (*Acta Phys. Austriaca*, vol. 5, pp. 45–68; Nov., 1951.) Calculations of resonance frequencies are made for cavity configurations whose boundaries coincide with coordinate surfaces of an elliptical-cylindrical coordinate system. The expressions obtained are developed explicitly for the case of weak coupling, and are compared with known approximations.

621.396.611.4 1622
Theory of Forced Oscillations in Electrodynamic Systems—E. Ledinegg & P. Urban. (*Acta Phys. Austriaca*, vol. 5, pp. 510–528; June, 1952.) The method of analysis using vector series progressing according to the eigenfunctions of the wave equation is applied to a system comprising cylindrical resonator and coaxial line. The theoretical assumptions underlying the method are examined and the Green tensor appropriate to linear electrodynamic processes is formulated.

621.396.611.4 1623
The Complete System of Natural Electromagnetic Oscillations of Uniaxal Anisotropic Cavity Resonators—E. Hafner. (*Arch. elekt. Übertragung*, vol. 7, pp. 47–56; Jan., 1953.) Analysis of the field inside an arbitrary cylinder completely or partially filled by a uniaxal crystal. The special cases of the circular-section cylinder and the parallelepiped are treated explicitly. See also 1315 of May.

621.396.615 1624
Perturbations of Filtered Oscillators: Part 2—G. Cahen (*Comp. Rend. Acad. Sci.* (Paris), vol. 236, pp. 356–358; Jan. 26, 1953.) Results previously obtained (1279 of May) regarding the stability, synchronization and frequency pulling of a nonlinear oscillator subjected to excitation by an external source are generalized by considering the dependence of amplifier gain on the rate of phase change.

621.396.615:621.3.016.35 1625
Nonlinear Oscillators and the Nyquist Diagram—A. Blaquière. (*Jour. Phys. Radium*, vol. 13, pp. 527–540; Nov., 1952.) Two types of nonlinear oscillators having amplitude limiting are considered. Their equations become linear when a particular value is chosen for the parameter involving the amplitude. A single curve can then be drawn for this particular value on the same principle as the ordinary Nyquist curve. Other values of the parameter yield a family of curves showing the stages in the evolution of oscillations. Conditions for stable and unstable oscillations are derived, and the results extended to cover response to a small perturbation, frequency stability and synchronization limits. A brief account of part of the work was given in 335, 1867 and 2735 of 1952.

621.396.615+534.1]:621.3.016.37 1626
Electrical and Acoustic Oscillation Build-Up Phenomena—H. Dänzer. (*Ann. Phys., Lpz.*, vol. 10, pp. 395–412; June 15, 1952.) Mathematical treatment of build-up phenomena such as those investigated experimentally by Trendelenburg et al. (1939 of 1938) for organ-pipe sounds.

621.396.615:621.396.611.34/.35 1627
Multimesh *RC* Networks for Phase-Shift Oscillators—R. Krastel. (*Funk u. Ton.*, vol. 6, pp. 649–653; Dec., 1952.) The required phase-shift for each mesh is calculated for a terminated 3-mesh network. The values, which total 180°, differ considerably from 60°.

621.396.615.029.53/.55:621.384.612 1628
A Wide-Range Oscillator of High Stability—D. E. Caro & L. U. Hibbard. (*Jour. Sci. Instr.*, vol. 29, pp. 403–408; Dec., 1952.) Description of a beat-frequency oscillator for the RF system of the Birmingham University proton synchrotron [700 of 1951 (Hibbard)]. The two similar oscillators used are tuned by $\lambda/4$ coaxial resonators on rubber shock mounts in a constant-temperature enclosure, the fixed-frequency oscillator operating at about 33 mc. A capacitor using a single-plate rotor with a stepped profile serves for varying the tuning of the other oscillator via a servomechanism. The beat frequency as a function of rotor setting is reproducible to within 0.03% throughout the range 0.25–10 mc.

621.396.615.17:621.314.25.015.7 1629
A Phase-Shifting Pulse Generator for Thyratron Control—J. C. West & D. K. Partington. (*Electronic Eng.*, vol. 25, pp. 120–121; March, 1953.) Description, with detailed circuit diagram, of equipment producing positive pulses with repetition frequency that of the mains (50 cps), but with phase variable with respect to that of the supply voltage. The phase lag is controlled by application of a small direct voltage to the grid of a high-vaccuum tube.

621.396.615.17:621.317.755 1630
Pulse-Operated Time-Bases—H. A. Dell. (*Electronic Eng.*, vol. 25, pp. 94–97; March, 1953.) Discussion of the basic principles and description of a practical timebase circuit of the single-sweep type, triggered by a delayed pulse developed from the transient or transmitter pulse to be examined.

621.396.615.17:621.397.621.2 1631
Timebase Circuits—H. Bähring. (*Tech. Hausmitt. NordwDtsch. Rdfunks*, vol. 4, pp. 219–227; Nov./Dec., 1952.) Discussion of the principles of operation of various types of timebase, including an anastigmatic system, and of HV generation by the fly-back method.

621.396.645 1632
The Three Possible Types of Valve Amplifier Circuit and Applications in Television Receivers—W. Taeger. (*Frequenz.*, vol. 6, pp. 330–335; Nov., 1952.) Analysis and comparison of grounded-cathode, grounded-grid and grounded-anode amplifier circuits.

621.396.645:621.317.3 1633
A Selective Detector Amplifier for 10–10,000

c/s—G. H. Rayner. (*Jour. Sci. Instr.*, vol., 30, pp. 17–20; Jan., 1953.) An amplifier is described for use as a detector in bridge or other measurements where a null indication is required. Tuning is accomplished by means of parallel-T feedback networks including only resistors and capacitors. Noise is equivalent to an input signal of 0.2 μV across 10$^4\Omega$.

621.396.645.015.7:621.396.822 1634

Background Noise in Ionization-Chamber Pulse Amplifiers—G. Valladas & A. Leveque. (*Jour. Phys., Radium*, vol. 13, pp. 521–526; Nov., 1952.) Two methods of particle-energy measurement are considered. For the charge-collection method Milatz & Keller (1750 of 1945) have calculated the absolute limit to measurement accuracy for the amplifier circuit used. For the pulse-slope method initiated by Sherr & Peterson (*Rev. Sci. Instr.*, vol. 18, p. 567; 1947) a slightly different limit is found. Circuits giving optimum signal/noise ratios are proposed in each case.

621.396.645.029.3 1635

Constant-Current Audio Power Amplifiers—H. T. Sterling & A. Sobel. (*Electronics*, vol. 26, pp. 122–125; March, 1953.) The design features are discussed of a push-pull amplifier using a pair of Type-5881 tubes in the output stage to feed a General Radio Type-942A toroidal output transformer. Constant-current operation of the output stage, with 1-kΩ resistors in the cathode leads for dc degeneration, minimizes variations due to valve aging or replacement. Full circuit details of the amplifier and its simple power-supply unit are given.

621.396.645.029.4 1636

Comments on the Performance of Pentode Output Stages—B. G. Dammers. (*Philips Tech. Commun.* (Australia), pp. 3–13; 1952.) Excerpt from Book V of the Philips series of books on electronic tubes (2765 of 1952).

621.396.645.36 1637

The Differential Amplifier—V. S. E. Lewis: B. F. Davies. (*Electronic Eng.*, vol. 25, pp. 82–83; Feb. 19, 1953.) Comment on 3392 of 1952 and author's reply.

621.396.645.37+621.396.615.11 1638

Electrically Tuned RC Oscillator or Amplifier—O. G. Villard, Jr., & F. S. Holman. (PROC. I.R.E., vol. 41, pp. 368–372; March, 1953.) Two variants are described of a feedback circuit including two all-pass phase-shifting networks. Tuning is performed by adding a variable amount of the output of the one phase shifter to the output of the other, the variation being controlled electronically by means of a modulator circuit. Theoretically the tuning range is from zero to infinite frequency; in practice the frequency ratio obtainable without appreciable change in gain is about 4:1.

621.397.645.029.62 1639

Fundamental Problems of H.F. and I.F. Amplifiers for TV Reception: Part 1—Gain and Bandwidth—A. G. W. Uitjens. (*Electronic Appl. Bull.*, vol. 11, pp. 205–228; Nov., 1950. Errata, *ibid.*, vol. 12, p. 17; Jan., 1951.) The gain-bandwidth product GB is shown to depend exclusively on the ratio of tube mutual conductance to the sum of input and output capacitances. Factors affecting G and B are discussed. Amplifier response curves are considered and the total bandwidth is deduced for amplifiers with synchronous circuits. Staggered tuning is discussed in detail. The unit-function response curves for double- and vestigial-sideband systems are treated and the distortion in the latter system is analyzed. The gain and bandwidth of quadripole coupling networks, particularly the Π network and the double-tuned band-pass filter, are discussed and characteristic data, including GB values, are tabulated for nine commonly used pentode circuits. Data for unit-function response curves when several identical groups are connected in cascade, and bandwidth factors for double-tuned coupling circuits, are also tabulated.

621.397.645.029.62:621.397.822 1640

Fundamental Problems of H.F. and I.F. Amplifiers for TV Reception: Part 2—Noise—A. G. W. Uitjens. (*Electronic Appl. Bull.*, vol. 12, pp. 2–17; Jan., 1951., Correction, *ibid.*, vol. 12, p. 64; March, 1951.) Noise factors of amplifiers operating under various specified conditions are calculated and tube noise is discussed. Formulas are derived for the noise factor at meter wavelengths for four special simplified cases, a general formula being given in an appendix. The concept of noise reference frequency f_n, the frequency at which the equivalent noise resistance of a tube is equal to the input resistance, is discussed and formulas are tabulated for both triode and pentode circuits with predominating partition noise. Graphs of noise factor for various cases show that above the frequency f_n the noise factor increases rapidly. The signal/noise ratio is calculated from the noise factor. It appears that the weakest signal that can be received reasonably well depends on the frequency, on the antenna noise, and particularly on the noise reference frequency of the first tube of the receiver.

GENERAL PHYSICS

535.13:517.941.9 1641

The First Boundary-Value Problem of Maxwell's Equations—E. Ledinegg & P. Urban. (*Ann. Phyz., Lpz.*, vol. 10, pp. 349–360; June 15, 1952.) Mathematical analysis of the generation of oscillations in an EM system by an external source, such as excitation of a cavity resonator by means of a waveguide feeder.

535.325-1 1642

Refractive Index of Dipolar Gas Mixtures at Decimeter Wavelengths—R.Schachenmeier & F. Weller. (*Naturwissenschaften*, vol. 40, pp. 17–18; Jan., 1953.) The refractive index of mixtures of air and water vapor was measured at frequencies from 600 to 1700 mc over a range of pressures, using a cavity-resonator method. Results are shown in curves. Discrepancies between the observations and values predicted from theory are attributed to the fact that the relaxation time of the water molecules is not negligible at low pressures.

535.37 1643

Capture and Recapture of Electrons in Phosphorescence—D. Curie. (*Ann. Phys.* (Paris), vol. 7, pp. 749–801; Nov./Dec. 1952.) The relative importance of these phenomena is discussed. and the mechanisms with which they are associated in phosphorescence decay are analyzed.

535.37:537.52 1644

The Luminescence of Phosphors in Strong Electric Fields—A Herwelly. (*Acta Phys. Austriaca*, vol. 5, pp. 30–44; Nov., 1951.) The account of the phenomenon of electroluminescence given by Destriau (see e.g. 110 of 1949) is critically discussed. Cells used for demonstrating the phenomenon always take the form of a stratified capacitor including a layer of gas and a layer of solid dielectric of much greater breakdown strength, the gas being occluded either in the electrodes or in or between the phosphor grains. With such an arrangement a glow discharge occurs in the gas layer for voltages above a certain threshold and below sparking voltage. It is concluded that this is the true explanation of the observed phenomenon.

537.1:530.12 1645

Circulation in the Flow of Electricity: Dirac's New Variables—O. Buneman. (*Proc. Roy. Soc. A.*, vol. 215, pp. 346–352; Dec. 5, 1952.) "Kelvin's circulation theorems are shown to be applicable to the generalized momentum vector in the relativistic flow of electricity. Vortex filaments become "vortex ribbons" in space-time, and Dirac's variables ξ and η are identified as the parameters which characterize the family of vortex ribbons."

537.213 1646

The Electric Potential in an Electrically Shielded Space—G. Piccardi & R. Cini. (*Ricerca Sci.*, vol. 23, pp. 113–114; Jan., 1953.) Experiments confirm the previously observed variation of potential inside a metallic enclosure; the phenomenon is attributed to the production of space charge by ionization due to spontaneous radiation from the enclosure walls.

537.336 1647

The Frequency Dependence of the Dielectric Properties of Dipolar Substances—J. J. O'Dwyer and R. A. Sack. (*Aust. Jour. Sci. Res., Ser. A*, vol. 5, pp. 647–660; Dec., 1952.) Inconsistencies in previous theories of dipolar interaction are pointed out. A new theory presented is based on Debye's theory of molecular relaxation and on an application of Onsager's method for treating ES interaction.

537.291+538.691 1648

The Solution of the Schrödinger Equation for Finite Systems, with special reference to the Motion of Electrons in Coulomb Electric Fields and Uniform Magnetic Fields—R. B. Dingle. (*Proc. Camb. Phil. Soc.*, vol. 49, part 1, pp. 103–114; Jan., 1953.)

537.291 1649

Motion of Gaseous Ions in Strong Electric Fields—G. H. Wannier. (*Bell Sys. Tech. Jour.*, vol. 32, pp. 170–254; Jan. 1953.) Amplified and extended version of papers noted in 97 of 1952 and 376 of February.

537.3 1650

Current Flow in Cylinders—W. R. Smythe. (*Jour. Appl. Phys.*, vol. 24, pp. 70–73; Jan., 1953.) The mixed-boundary-value problem of the flow of current into a right circular cylinder through a perfectly conducting coaxial disk electrode at one end is solved approximately.

537.315.6 1651

Numerical Calculation of the Potential and Field due to a Uniformly Charged Disk—M. Laudet. (*Jour. Phys. Radium*, vol. 13, pp. 549–553; Nov., 1952.) Various methods of calculating the potential at any point are discussed, the particular advantages of the relaxation method in the most general case being pointed out.

537.52:538.639 1652

New Types of Discharges in Magnetic Fields—K. Siebertz. (*Acta Phys. Austriaca*, vol. 5, pp. 134–142; Nov., 1951.) Discharge phenomena described by Ehrenhaft et al. (*Acta Phys. Austriaca*, vol. 4, no. 1, p. 129; 1950) are explained in terms of known concepts and laws of gas-discharge physics.

537.52:538.639 1653

Investigations of Discharges in Magnetic Fields. A Note on Righi's Magnetic Rays—W. H. Borgmann. (*Acta Phys. Austriaca*, vol. 5, pp. 425–428; June, 1952.)

537.525:538.566 1654

The Microwave Admittance of a Mercury-Vapour Discharge—H. A. Prime. (*Aust. Jour. Sci. Res., Ser A*, vol. 5, pp. 607–617; Dec., 1952).

537.525:538.63 1655

Theory of the Discharge Potential for Coaxial Cylindrical Electrodes in a Transverse Magnetic Field—G. Valle. (*Nuovo Cim.*, vol. 9, pp. 145–168; Feb. 1, 1952.)

537.527:538.566 1656

The Absorption and Reflection of Microwave Radiation by a Mercury-Vapour Discharge—H. A. Prime. (*Aust. Jour. Sci. Res., Ser. A*, vol. 5, pp. 592–606; Dec., 1952.) Results of measurements at 3-cm λ show that with increasing discharge current the real component

of the complex conductivity of the discharge increases almost linearly, the imaginary component, which is negative, increasing nonlinearly and less rapidly.

537.533:[537.29+538.63 1657
The Imaging Properties of Electron Beams in Arbitrary Static Electromagnetic Fields—P. A. Sturrock. (*Phil. Trans.*, vol. 245, pp. 155–187; Aug. 19, 1952.) Detailed theory of the aberrations of electron-optical systems with curved axes, with application to calculation of the imaging properties of a helical beam moving in the field of a pair of coaxial cylindrical electrodes.

537.533.8:[546.56-1+546.57-1]:539.234 1658
The Secondary Emission from Copper and Silver Films obtained with Primary-Electron Energies below 10 eV—H. P. Myers. (*Proc. Roy. Soc. A*, vol. 215, pp. 329–345; Dec. 5, 1952.) Values obtained for the secondary-emission ratio are lower than those hitherto recorded, both Ag and Cu having a ratio <0.1 in the primary-energy range 1–5 eV. The difference is attributed to the improved vacuum conditions used. Measurements of the energy distribution of the secondary electrons for primary energies <5 eV show that the secondary electrons are in fact elastically reflected primary electrons.

537.562 1659
Electromagnetic Properties of Plasmas—M. Bayet. (*Jour. Phys. Radium*, vol. 13, pp. 579–586; Nov., 1952.) Conditions for the propagation of longitudinal and transverse EM waves are considered, taking account of the effect of collisions on electron velocities and assuming no applied magnetic field. The mobility coefficient relating the electric field to the mean velocity imparted by it to the electrons, and dispersion formulae linking wavelength and frequency of the propagated disturbance, are derived.

537.562:538.56 1660
Studies in Magneto-hydrodynamics—S. Lundquist. (*Ark. Fys.*, vol. 5, part 4, pp. 297–347; Aug. 26, 1952.) A systematic treatment of the subject, designed to bring out the underlying physical principles. Basic equations for EM phenomena in a conducting liquid and their conditions of validity are discussed. These are applied in specific static, kinematic and dynamic problems. Experimental work is briefly summarized.

537.562:538.566:532.51 1661
A New Type of Propagation—C. H. Papas & W. W. Salisbury. (*Trans. I.R.E.*, pp. 47–52; Dec., 1952.) Discussion of the properties of magneto-hydrodynamic waves in various types of conducting fluids. See also 3469 of 1945 (Alfvén).

538.221 1662
Overlapping Energy Bands and the Theory of Collective Electron Ferromagnetism—A. B. Lidiard. (*Proc. Camb. Phil. Soc.*, vol. 49, part 1, pp. 115–129; Jan., 1953.)

538.221:538.65 1663
Motions of Material Particles in the Field of an Electromagnet—F. Stockinger. (*Acta Phys. Austriaca*, vol. 5, pp. 440–448; June, 1952.) Description and discussion of two different effects observed when ferromagnetic particles of order of magnitude 10^{-4}–10^{-2} cm are exposed to fields of strength up to 30,000 oersted in the air-gap of a magnet.

538.221:538.65 1664
The Behaviour of Ferromagnetic Particles in a Rotating Magnetic Field—K. V. Desoyer. (*Acta Phys. Austriaca*, vol. 5, pp. 429–434; June, 1952.) Account of an experimental investigation of the motion of ferromagnetic particles of order of magnitude 10^{-4}–10^{-2} cm, suspended in gas at pressures between 2 and 20 mm Hg, and subjected to illumination and to a magnetic field rotating at 50 cps.

538.566:535.42 1665
Theory of Diffraction by a Cylinder, taking account of the Surface Wave—W. Franz & K. Deppermann. (*Ann. Phys., Lpz.*, vol. 10, pp. 361–373; June 15, 1952.) Maxima and minima observed by A. Limbach in diffraction of centimeter EM waves by metal cylinders are found to be due to interference between the waves geometrically reflected from the cylinder surface and the surface wave creeping round to the back of the cylinder. Quantitative calculations based on the integral equations of the diffraction theory of Maue (*Z. Phys.*, vol. 126, p. 606; 1949) give results in good agreement with experiment.

538.566:535.42 1666
Diffraction Patterns in Circular Apertures less than One Wavelength in Diameter—H. L. Robinson. (*Jour. Appl. Phys.*, vol. 24, pp. 35–38; Jan., 1953.) Measurements were made of the field intensity at points along the aperture diameters parallel respectively to the electric and magnetic vectors, using normally incident radiation of wavelengths 16 cm and 32 cm. The results disagree with values calculated from Young's theory in two respects, viz., (*a*) the observations indicate a sharp increase at the ends of the diameter parallel to the electric vector; (*b*) along the diameter parallel to the magnetic vector the observed central peak for apertures of diameter near $\lambda/2$ was 50% greater than the calculated value, the high intensity being attributed to multiple reflections from the edges.

538.566:538.42 1667
The Electromagnetic Field in the Plane of a Circular Aperture due to Incident Spherical Waves—D. C. Hogg. (*Jour. Appl. Phys.*, vol. 24, pp. 110–111; Jan., 1953.) Measurements were made of the field in an aperture of diameter 50 cm illuminated with radiation of wavelength 1.25 cm from small radiators at various distances. Results are shown graphically; the curves obtained can be represented approximately by a modified form of Andrews' equation (3141 of 1950).

538.566.2:512.831 1668
Application of Matrices to the Problem of Transmission through a Multi-Layered Dielectric Wall—R. A. Henschke. (*Trans. I.R.E.*, pp. 117–134; Dec., 1952.) The matrix methods described by Watson (1329 of 1947) are applied to the determination of design formulae for dielectric walls of the symmetrical sandwich type.

GEOPHYSICAL AND EXTRATERRESTRIAL PHENOMENA

523.846:[523.77+53 1669
The Physical Conditions in Sunspots, deduced from their Spectra—R. Michard. (*Comp. Rend. Acad. Sci.* (Paris), vol. 236, pp. 182–184; Jan. 12, 1953.) Discussion of the theoretical consequences resulting from the sunspot model recently proposed (1324 of May). The vertical gradient of the magnetic field is found to be about 1.5 gauss/km.

551.510.52 1670
Nomograms for the Computation of Tropospheric Refractive Index—D. M. Swingle. (PROC. I.R.E., vol. 41, pp. 385–391; March, 1953.) Charts for calculating refractive index, refractive-index discontinuities, and vertical gradient are presented in a form convenient for use with standard radiosonde data. They are valid for wavelengths >1.5 cm.

551.510.52/.53:551.571.7(422) 1671
Humidity of the Upper Troposphere and Lower Stratosphere over Southern England—J. K Bannon, R. Frith & H. C. Shellard. (*Geophys. Mem.* (London), vol. 11, 36 pp.; 1952.) Detailed report of observations made on 130 flights during 1943–1946 at altitudes up to about 40,000 ft. For a summarized account, see *Nature* (London), vol. 171, pp. 381–382; Feb. 28, 1953.

551.510.535 1672
Abnormalities in the Ionosphere at High Latitudes—W. R. Piggott. (*Nature* (London), vol. 171, pp. 124–125; Jan. 17, 1953.) Study of the variations, with respect to time and location, of the frequency of occurrence of storm types E and D shows that the polar region may be divided into three zones, the polar zone, the storm belt and the polar quiet zone. Within the storm belt, the most dense forms of storm-E ionization are practically confined to an area centered near Canada, while the existence can be demonstrated of two centers of activity in the D region, spaced 180° apart, which rotate once around the earth every 48 hours.

551.510.535 1673
Geo-morphology of F_2-Region Ionospheric Storms—D. F. Martyn. (*Nature* (London), vol. 171, pp. 14–16; Jan. 3, 1953.) F_2-region ionospheric storms may be regarded as manifestations of a single world-wide phenomenon, viz., the es field of the solar diurnal current system, whose local effects depend markedly on local time and season. The theoretical (Chapman) characteristics of the F_2 region are normally perturbed by solar tidal electric fields (1053 of 1949). During magnetic storms the phase of the additional electric field present is such as to increase these perturbations at high latitudes and to reduce them at low latitudes, though the effect may be masked by local time variations of ionization density. In contradistinction to Appleton & Piggott (891 of 1950), no evidence is found that any magnetic storm affects the northern and southern hemispheres differently, when due allowance is made for the seasonal effect.

551.510.535:[523:521.396.822 1674
Study of the Ionosphere by Extraterrestrial Radio Waves—A. P. Mitra. (*Indian Jour. Phys.*, vol. 26, pp. 495–511; Oct., 1952.) A paper surveying experimental work on the use of galactic RF radiation for investigating ionospheric refraction, absorption, irregularities and the effects of sudden ionospheric disturbances. Results are compared with theory, and further lines of investigation are suggested.

551.510.535:523.78 1675
E Region during the Solar Eclipse of February 25, 1952—C. M. Minnis. (*Nature* (London), vol. 170, p. 453; Sept. 13, 1952.) Analysis of observations of E-layer critical frequencies at Khartoum during the eclipse indicates that the ionizing radiation from the solar disk is not uniformly distributed, as is also the case for the optical radiation. Part of the nonuniform component of the ionizing radiation appears to be divided about equally between the east and west limbs of the sun. This is consistent with observations made at Meudon of the distribution over the sun's disk of the intensity of the green coronal line. The main discrepancy between the values of the parameter J (proportional to the radiation flux) calculated from the coronal data and from the E-region measurements appears abruptly just after totality and suggests the existence of an intense source of ionizing radiation near the west limb of the sun which cannot be explained in terms of solar data available at present.

551.510.535:551.55 1676
A Study of Ionospheric Winds and Turbulence utilizing Long Radio Waves—G. H. Millman. (*Ann. Géophys.*, vol. 8, pp. 365–384; Oct./Dec., 1952. In English.) An experimental investigation of winds in the E layer was made during the period July 1951–March 1952, using vertical-incidence pulse technique, with waves of frequency 150 kc. The time variations of the reflected amplitudes are analyzed statistically and compared with results to be expected from

theory. Fades of duration 0.5–6.5 min are most prevalent. Diurnal and seasonal effects are observed. See also 720 of March.

551.510.535:621.3.087.4 1677

A High-Precision Ionospheric Sounding Equipment—B. M. Banerjee & R. Roy. (*Indian Jour. Phys.*, vol. 26, pp. 473–494; Oct., 1952.) Description, with circuit diagrams and oscillograms, of high-resolution equipment which provides pulses variable from 6 to 30 μs in duration and from 10 to 50 kW in peak power. The delta antennas are of the type considered by Cones (1567 of 1951), alternative terminations giving improved signal strength at frequencies <2.5 mc. During conditions of severe interference a horizontal receiving dipole is used. Interchangeable receivers covering a bandwidth of 50–200 kc are provided. The timebase circuit previously described (2477 of 1952) is modified to give a 12-line raster, each line corresponding to 50-km height. The evaluation of resolution is discussed in an appendix.

551.510.535:621.396.11 1678

Effect of the Geomagnetic Field on the Absorption of Short Waves in the Ionosphere (Vertical Incidence)—É. Argence, K. Rawer & K. Suchy. (*Comp. Rend. Acad. Sci.* (Paris), vol. 236, pp. 190–192; Jan. 12, 1953.) An approximate formula for the index of refraction is used to calculate the coefficient of absorption for five frequencies around 3 mc. The results are sensibly the same as those obtained by use of the rigorous Appleton-Hartree formula; those previously given by Argence, Mayot & Rawer (1300 of 1952) are about 3% higher.

551.510.535:621.396.11 1679

The Reflection and Absorption of Radio Waves in the Ionosphere—W. R. Piggott. (*Proc. IEE* (London), part III, vol. 100, pp. 61–72; March, 1953.) Investigations of the absorption of RE waves made in Britain since 1935 are reviewed and the theory of ionospheric absorption is outlined. The effects of double refraction, polariaztion, spatial attenuation, dispersion, ionospheric inhomogeneities and partial reflection, which modify the apparent attenuation of radio waves reflected in the ionosphere, are discussed and methods used to minimize absorption-measurement errors due to these factors are given, the experimental techniques used in routine absorption measurements being described fully. Detailed results of measurements of ionospheric absorption made in South-East England in the period 1935–1948 are being published separately.

551.510.535:621.396.812 1680

The Investigation of Ionospheric Absorption by a New Automatic Method: Part 1—Measurements on Vertical-Incidence Pulse Signals—J. B. Jenkins & G. Ratcliff. (*Electronic Eng.*, vol. 25, pp. 140–145; April, 1953.) Equipment is described which automatically measures echo pulse amplitude and produces records, at minute intervals, of the integral of all echo pulse amplitudes received during each minute. The output of a modified communications receiver, blanked so as not to respond to the transmitter pulse, is fed to two gated amplifiers, one of which selects the echo signal and associated noise, while the other deals with noise only. After integration for 1 min, the difference of the output voltages of the integrators is applied to a pen recorder, the integrators at the same time being reset to zero. Under good conditions, with little rapid fading, the results obtained are in good agreement with results noted by a skilled observer from a CRO display of the transmitted and echo pulses. Wide differences are found under poor conditions, with rapid fading, and the results furnished by the automatic equipment are considered the more reliable.

551.594 1681

Measurement of the Electric Field of the Atmosphere by means of Radioactive Probes—H. Wichmann. (*Arch. Met. A, Wien*, vol. 5, pp. 86–99; April 28, 1952.)

551.594.21 1682

Boys-Camera Study of the 'Air Discharge' and the 'Flash to Ground with Horizontal Top'—M. Sourdillon. (*Ann. Géophys.*, vol. 8, pp. 349–364; Oct./Dec., 1952.)

551.594.21 1683

Air Discharges and the Positive Charge at the Bottom of a Thundercloud—D. J. Malan. (*Ann. Géophys.*, vol. 8, pp. 385–401; Oct./Dec., 1952.)

LOCATION AND AIDS TO NAVIGATION

621.396.9 1684

Omnidirectional Reflectors for Microwaves—L. Grifone. (*Ricerca Sci.*, vol. 22, pp. 2307–2313; Dec., 1952.) Measurements at 3.2-cm wavelength of the reflecting power of a corner reflector relative to that of a plane reflector were made by rotating the reflector about a vertical axis through a total angle of about 90°. The results are shown graphically for angles of tilt of the reflector up to 40°. A reflector system with satisfactory omnidirectional characteristics, consisting of two staggered groups of four, one above the other, should be detectable at a distance of over 3 sea miles under adverse conditions, using radar equipment with peak pulse power of 35 kW.

621.396.9:627.3 1685

Shore-Based Radar for Harbor Surveillance—E. J. Isbister & W. R. Griswold. (*Elect. Eng.* (N. Y.), vol. 71, pp. 1072–1077; Dec., 1952.) General descriptions are given of the installations at the ports of Boston, Long Beach, New York and Liverpool.

MATERIALS AND SUBSIDIARY TECHNIQUES

533.5 1686

An Assessment of some Working Fluids for Diffusion Pumps—D. Latham, B. D. Power & N. T. M. Dennis. (*Vacuum*, vol. 2, pp. 33–49; Jan., 1952.) Choice of working fluid is largely determined by the particular pump to be used and conditions of use. Silicones are outstanding for general purposes and tubeless pumping to really low pressures, Apiezon-C is considered the best for lowest possible pressures in a fractionating pump, while Aroclor-1245 is good for applications where very low pressures are not required.

535.215:546.482.21 1687

Photoconductivity of Cadmium-Sulphide Crystals at Relatively High Temperatures—R. Caspary & H. Müser. (*Z. Phys.*, vol. 134, pp. 101–105; Dec. 17, 1952.) A variation of the method described by Frerichs (450 of 1948) resulted in the production of crystals up to 2 in. long. Curves are given showing the response to light of wavelength in the range 425–610 mμ for temperatures from 18° to 148°C. Maximum sensitivity occurs at wavelengths a little above 500 mμ; it decreases with increasing temperature and is displaced slightly towards longer wavelengths.

535.215:546.482.21:548.55 1688

Growth and Decay of the Photoconductivity of CdS Single Crystals—J. Fassbender & B. Seraphin. (*Ann. Phys., Lpz.*, vol. 10, pp. 374–394; June 15, 1952.)

535.215.1:[546.22.36+546.22.35 1689

Photoemission from Cesium and Rubidium Tellurides—E. Taft & L. Apker. (*Jour. Opt. Soc. Amer.*, vol. 43, pp. 81–83; Feb., 1953.) These materials are similar to Cs_3Sb (see 1690 below) except that their forbidden energy bands are almost twice as wide. Consistent with this, the energy distributions of the emitted photoelectrons show no evidence for electron-electron scattering up to $h\nu=6.7$ eV. These materials are of interest for ultraviolet photometry.

535.215.1:546.86.36 1690

Electron Scattering and the Photoemission from Cesium Antimonide—L. Apker, E. Taft & J. Dickey. (*Jour. Opt. Soc. Amer.*, vol. 43, pp. 78–80; Feb., 1953.) Measurements of the energy distribution of photoelectrons emitted from Cs_3Sb are reported. At values of $h\nu>4$ eV only a small proportion of the photoelectrons have energies >2 eV; this is attributed to scattering of excited electrons by valence electrons. The results give support to the energy-band structure proposed by Burton (*Phys. Rev.*, vol. 72, p. 531A; 1947.)

535.37+535.215:546.482.21:548.55 1691

Luminescence and Photoconductivity in Cadmium Sulfide at the Absorption Edge—C. C. Klick. (*Phys. Rev.*, vol. 89, pp. 274–277; Jan. 1, 1953.) Measurements on single crystals of CdS at 77°K and 4°K suggest that emission at the edge of the absorption band may occur at special centers and not be characteristic of the pure lattice.

537.226.2/.3 1692

Study of Dielectrics; Dielectric Constant, Losses and Breakdown—M. Bouix. (*Ann. Télécommun.*, vol. 7, nos. 11 & 12, pp. 466–479 & 497–512; Nov. & Dec., 1952.) A review of modern theories relating to calculation of the dielectric constant of and losses in nonpolar, polar and dipolar materials, and concerning dielectric breakdown.

537.226.2:539.22 1693

The Dielectric Constants of Heterogeneous Mixtures of Isotropic and Anisotropic Materials—W. Niesel. (*Ann. Phys., Lpz.*, vol. 10. pp. 336–348; June 15, 1952.) A general theory applicable to the calculation of the dielectric constants of mixtures is developed. The individual particles of the mixtures are assumed to be ellipsoidal. For the particular cases of aggregates of spherical or laminar particles the general formulae reduce to those given by Bruggemann (1284 and 2424 of 1936 and 1087 of 1937). Measurements on multicrystal $BaTiO_3$ aggregates are discussed in relation to the theory.

537.228.1:546.431.824–31 1694

Measurements on Barium Titanate—H. Schmidt. (*Akust. Beihefte*, no. 2, pp. 83–88; 1952.) Formulas are given for calculating the mechanical constants of piezoelectric disks from electrical measurements. Results of observations of the temperature dependence of electric and elastic parameters of $BaTiO_3$ and the mixed ceramic $BaTiO_3$-$PbTiO_3$ are shown in graphs, and values of the parameters for $BaTiO_3$ are tabulated.

537.311.33 1695

Modulation of the Conductance of a Semiconductor by an Electric Field—P. Aigrain, J. Lagrenaudie & G. Liandrat. (*Jour. Phys. Radium*, vol. 13, pp. 587–588; Nov., 1952.) An ac field is applied normally to the surface of an evaporated Te film through which ac of the same frequency is passed. The modulation of the conductance by the normally applied field gives rise to a dc component in the current through the specimen; from measurements of this component the conductance variations are deduced. Very small changes can be estimated by this method.

537.311.33:546.27.03 1696

Electrical and Optical Properties of Boron—J. Lagrenaudie. (*Jour. Phys. Radium*, vol. 13, pp. 554–557; Nov., 1952.) Measurements on three differently prepared samples are reported. The shape of the conductivity/temperature curves over a low-temperature range indicates the existence of several impurity energy levels. The material is a p-type semiconductor. Photoconductivity measurements indicate an intrinsic energy of about 1.2 eV.

537.311.33:546.289 1697

The Question of Thermally Produced Lat-

tice Defects in Germanium—K. Seiler, D. Geist, K. Keller & K. Blank. (*Naturwissenschaften*, vol. 40, p. 56; Jan., 1953.) Experiments are described which confirm that the specific resistance of pure Ge is not altered by heat treatment followed by rapid cooling; a change of resistance in these conditions indicates the presence of impurities, possibly only on the surface. Ca, Mg, Fe and Cu are likely impurities, Si is improbable. These results leave it undecided whether lattice defects can be produced in Ge by heat treatment.

537.311.33:546.289 1698

Surface Properties of Germanium—W. H. Brattain & J. Bardeen. (*Bell Sys. Tech. Jour.*, vol. 32, pp. 1–41; Jan., 1953.) Measurements are reported of contact potential (cp) and change of cp with illumination, using a Pt reference electrode. The influence of the ambient medium is investigated; the cp varies over a range of about 0.5 V between the value corresponding to the largest surface dipole, obtained in ozone or peroxide vapors, and that corresponding to the smallest surface dipole, obtained in vapors with OH radicals. For chemically prepared surfaces, the value of the surface recombination velocity is 50–70 cmc for *n*-type and 180–200 cmc for *p*-type Ge and is independent of cp. A theoretidal explanation is given in terms of surface traps. The experimental results afford direct evidence for the existence of a space-charge layer at the free surface of a semiconductor.

537.311.33:546.289 1699

Electronic Structure of the Germanium Crystal—F. Herman & J. Callaway. (*Phys. Rev.*, vol. 89, pp. 518–519; Jan. 15, 1953.) Study of the energy-band structure of the Ge crystal by the method of orthogonalized plane waves. Preliminary note only.

537.311.33:546.47-31 1700

New Method of Studying Lattice Defects in the Semiconductor ZnO by Radio-Frequency Spectroscopy—M. Freymann & R. Freymann. (*Jour. Phys. Radium*, vol. 13, pp. 589–590; Nov., 1952.) ZnO specimens were examined at frequencies from 1 kc to 1 mc and temperatures from 100° to 293°K. Two components of Debye absorption were found, the respective intensity and position of which vary according to specimen preparation, temperature and frequency. Energy levels for diffusion of the lattice defects are deduced, and the results compared with those of other workers.

537.311.33:546.561-31 1701

The Semiconducting Properties of Cuprous Oxide—J. S. Anderson & N. N. Greenwood. (*Proc. roy. Soc. A*, vol. 215, pp. 353–370; Dec. 5, 1952.) A procedure is described for preparing reproducible specimens of Cu_2O at the oxygen-poor limit of its composition range. Measurements of the electrical conductivity and thermoelectric power of such specimens are reported for the temperature range 20–1030°C. The curves for both properties consist of two sections, the discontinuity occurring at 355°C in both cases. Below this temperature the thermoelectric power has a constant value; at higher temperatures it decreases and remains characteristic of a positive-hole conductor up to the highest temperatures used. The effect of added oxygen was investigated; the theoretical implications of the results obtained are discussed.

537.311.33(083.72) 1702

Technical Vocabulary relating to Semiconductors—(*Onde élect.*, vol. 33, pp. 62–63; Jan., 1953.) Definitions (in French) are given of terms included in the Vocabulaire Electrotechnique International Électronique. The definitions were adopted by a sub-committee at Brussels, August 1952, but have still to be approved by national committees.

537.311.33.001.8 1703

Physical Properties of Semiconductors and Application in Radio Technique—P. Aigrain & C. Dugas. (*Onde élect.*, vol. 33, pp. 5–14; Jan., 1953.)

538.221 1704

Effects on the Magnetization Characteristic of Ferromagnetic Materials carrying Current—S. Krapf. (*Elektrotech. Z., Edn A*, vol. 73, pp. 745–746; Dec. 1, 1952.) A short account of changes produced in the magnetization curves of ferromagnetic wires by passing auxiliary current through them or subjecting them to mechanical stress. These effects find application particularly in measurement technique.

538.221 1705

The Complex Permeability of a High-Permeability Ferrite Core—R. Feldtkeller & O. Kolb. (*Z. angew. Phys.*, vol. 4, pp. 448–451; Dec., 1952.) Analysis of the locus-diagram representation of the variation of complex permeability with frequency in Ni-Zn ferrite. The shape of the curve is decided primarily by the main relaxation effect of the ferrite, and to a lesser extent by after-effect, electrical and mechanical resonances, and hysteresis.

538.221:538.632 1706

Hall Effect and Temperature in Ferromagnetic Conductors—J. P. Jan. (*Helv. phys. Acta*, vol. 25, pp. 677–700; Dec. 15, 1952. In French.) Measurements of the variation of the Hall effect in Fe and Ni are reported for the temperature range −190° to +600°C. The magnetization Hall constant was found to depend mainly on the purity of the material. Graphical comparison is made between the temperature variation curves obtained and results published by various workers.

538.221:621.318.4 1707

Analysis of Measurements on Magnetic Ferrites—C. D. Owens. (Proc. I.R.E., vol. 41, pp. 359–365; March, 1953.) The relations between the magnetic quality factor μQ and the characteristics of coils and transformers are analyzed, and the advantages of using the μQ value of the ferrite as a design parameter are indicated.

538.221:669.14.018.8-131.2 1708

Magnetic Properties of Stainless Steel Wire. Effect of Cold Work—W. Sucksmith. (*Metal Treat.*, vol. 19, pp. 545–546, 549; Dec., 1952.) An account of experiments conducted on wire for magnetic-recording purposes. The increase in coercivity due to heat treatment at 450°–550°C is ascribed primarily to a decrease in size of ferromagnetic inclusions. In cold-worked specimens the coercivity is reduced and longer heat-treatment is required for maximum coercivity to develop.

538.614:538.221 1709

Theory of the Microwave Permeability Tensor and Faraday Effect in Nonsaturated Ferromagnetic Materials—G. T. Rado. (*Phys. Rev.*, vol. 89, p. 529; Jan. 15, 1953.) A calculation is made of the microwave Faraday rotation in a ferromagnetic material without introducing the restriction that the material be magnetized to saturation. See also 1233 of 1952 (Hogan).

538.632/.633 1710

Corbino Effect and Magnetic Variation of Resistance in Bismuth—L. Halpern & K. M. Koch. (*Acta Phys. Austriaca*, vol. 5, no. 1, pp. 129–133; Nov. 1951 & vol. 5, p. 567; June, 1952.) The accuracy of Hall-constant measurements can be increased and information can be obtained about the mechanism of resistance variation in a magnetic field by using specimens of shapes different from the usual strip.

538.652 1711

Reversal of Sign of Magnetostriction by Expansion: Part 2—A. Elsas & E. Vogt. (*Z. Naturf.*, vol. 6a, pp. 233–238; May, 1951.)

546.431-31[535.37+537.58 1712

Luminescence and Thermionic Emission of Barium Oxide—V. L. Stout. (*Phys. Rev.*, vol. 89, pp. 310–314; Jan. 1, 1953.) Two of the six luminescence bands identified varied in intensity with increase of thermionic emission, one decreasing, the other increasing. Peak intensity in both bands varied inversely with temperature.

621.396.6:620.19 1713

Tests relating to the Resistance of Electrical Equipment to Tropical Conditions—A. Delrieu. (*Rev. gén. Élect.*, vol. 61, pp. 551–559; Dec., 1952.) Report of laboratory tests on materials and circuit components.

621.314.632:546.28 1714

Thermal Treatment of Silicon Rectifiers—L. Esaki. (*Phys. Rev.*, vol. 89, pp. 398–399; Jan. 15, 1953.) Measurements were made on Si point-contact rectifiers heated at temperatures between 900° and 1400°C for various periods. With both *p*- and *n*-type Xi, on heating at over 1250°C in vacuo the rectifier property disappears, but is restored by subsequent heating at 1000°C in an oxygen atmosphere at low pressure. Possible mechanisms responsible for the changes are discussed briefly.

621.314.632:546.289 1715

Reverse Characteristics of High-Inverse-Voltage Point-Contact Germanium Rectifiers—J. H. Simpson & H. L. Armstrong. (*Jour. Appl. Phys.*, vol. 24, pp. 25–34; Jan., 1953.) A theoretical investigation is made of the effect of the geometry of the contact and of the high concentration of holes in the "inversion region" on the field at the contact. The latter factor results in a lowering of the effective barrier height for rectifiers made of very pure material. The former factor gives rise to increases in reverse current resulting from image force and tunnel effect at high voltages. Experimentally determined current/voltage characteristics were of the form predicted by the theory.

621.315.61.029.5 1716

Behavior of Insulating Materials at Radio Frequencies—J. J. Chapman, J. W. Dzimianski, C. F. Miller & R. K. Witt. (*Elec. Mfg.*, vol. 48, pp. 107–109, 238; July, 1951.) Data on the breakdown stress, dielectric constant and dissipation factor at frequencies from 60 cps to 18 mc are tabulated for 16 modern materials.

621.315.612.4 1717

Rare Earth Titanates with a Perovskite Structure—J. Brous, I. Fankuchen & E. Banks. (*Acta Cryst., Camb.*, vol. 6, part 1, pp. 67–70; Jan. 10, 1953.) Report of experiments on the production of new materials having interesting dielectric properties. The compounds $EuTiO_3$, $(La,Li)TiO_3$, $(La,Na)TiO_3$, $(La,K)TiO_3$ and $(La,Rb)TiO_3$ having the same crystal structure as $SrTiO_3$ were prepared and their lattice constants determined.

621.315.612.4.011.5 1718

Lattice Constants and Dielectric Properties of Barium-Titanate/Barium-Stannate/Strontium-Titanate Bodies—R. H. Dungan, D. F. Kane & L. R. Bickford, Jr. (*Jour. Amer. Ceram. Soc.*, vol. 35, pp. 318–321; Dec., 1952.) An account, with tabulated results, of investigations of the properties of $BaTiO_3$ ceramics including varying proportions of $BaSnO_3$ and $SrTiO_3$. Substitution of Sn for Ti increases the lattice constant, while substitution of Sr for Ba decreases it. Both substitutions decrease the Curie temperature, which has no direct relation to the lattice constant at room temperature.

621.315.614.6 1719

Electrical Properties of Glass-Fiber Paper—T. D. Callinan, R. T. Lucas & R. C. Bowers (*Elec. Mfg.*, vol. 48, pp. 94–97, 252; Aug., 1951.) Experimental values of dielectric strength, dielectric constant, power and loss factors, and volume resistivity are tabulated for papers made from AAA-superfine glass fibers and for glass-fibre papers impregnated with 10 different varnishes.

621.315.616 1720

Polyvinyl Chloride—A. G. Thomson. (*Elec. Times*, vol. 122, pp. 1157–1160; Dec. 25, 1952.) A review of the properties and applications of PVC, particularly as an insulating material.

621.318.424.042.4.017.3 1721

Alternating-Field Losses in Magnetic Cores with Air Gaps—M. Kornetzki. (*Frequenz*, vol. 6, pp. 313–318; Nov., 1952.) Formulas previously given (3073 of 1950) for the inductance and losses of coils with pot cores are extended so as to apply to coils with an air-gap in the core.

MATHEMATICS

681.142 1722

The Use of a 'Floating Address' System for Orders in an Automatic Digital Computer—M. V. Wilkes. (*Proc. Camb. Phil. Soc.*, vol. 49, part 1, pp. 84–89; Jan., 1953.)

681.142 1723

Modern Mathematical Machines—L. Biermann & H. Billing. (*Naturswissenschaften*, vol. 40, pp. 7–13; Jan., 1953.) Description of the G1 and G2 digital computers at Göttingen.

681.142 1724

Rapid-Access Magnetostatic Store for Electronic Computers—H. Billing. (*Naturwissenschaften*, vol. 40, pp. 49–50; Jan., 1953.) A system using a matrix arrangement of ferrite ring-cores is described.

681.142 1725

Present Development of Programme-Controlled Computers in Germany—G. Overhoff. (*Phys. Blätter*, vol. 9, pp. 31–36; Jan., 1953.) Details are included of electronic machines under development at the Darmstadt Technische Hochschule and in the Max-Planck-Gesellschaft Institute at Göttingen, and of commercial em-relay machines.

681.142 1726

The Numerograph—P. Vauthieu. (*Onde élect.*, vol. 32, pp. 496–499; Dec., 1952.) Description of the general principles of a pulse-operated system of displaying on a CRO successive 5-digit numbers provided by a digital computer, the numbers being then photographed on moving film. Recording speed is about 1000 times that of a teletype machine.

681.142 1727

Numerical Determination of Biharmonic Functions by an Analogue Method using Superposed [resistor] Networks—J. Boscher. (*Comp. Rend. Acad. Sci.* (Paris), vol. 236, pp. 44–46; Jan. 5, 1953.) Description of the network used and of its application to the determination of Airy's function.

681.142:[537.222+538.242 1728

Matrix Storage Systems—J. A. Rajchman. (*Onde élect.*, vol. 32, pp. 479–491; Dec., 1952.) Various es and em methods of digit storage on structures of the matrix type are described, with details of their operation and control systems. See also 2064 of 1951 and 3156 of 1952.

681.142:621.314.7 1729

Typical Block Diagrams for a Transistor Digital Computer—J. H. Felker. (*Elec. Eng.* (N. Y.), vol. 71, pp. 1103–1108; Dec., 1952.) Detailed discussion of digital computer circuits in which transistors can be used with advantage.

MEASUREMENTS AND TEST GEAR

538.71 1730

New Rotating-Iron Magnetometer—H. Gondet. (*Jour. Rech. Center Nat. Rech. Sci.*, pp. 286–291; Dec., 1952.) The instrument comprises three ferite rods, of which two are fixed and aligned while the third rotates in the space between them, round an axis perpendicular to them. The fixed rods carry windings in which is induced an emf whose value depends on the speed of rotation and on the local magnetic field. The possibility of using the instrument in aircraft is discussed.

621.3.018.41(083.74)+621.396.91 1731

Improvements in the N.B.S. Primary Standard of Frequency—(*Tech. News Bull. Nat. Bur. Stand.*, vol. 37, pp. 8–12; Jan., 1953.) The N.B.S. primary frequency standard comprises eight 100-kc quartz-crystal resonators and nine 100-kc crystal-controlled oscillators, three of which are located at the WWV station. The newer oscillators are driven by a current <100 μA and show increased short-time stability and overall reliability. The quartz-crystal resonators are used only once a day as part of a balanced-bridge network for comparison with one of the standard oscillators. Driving current for the resonators is 10 μA. Once a day the frequency of each standard oscillator is compared with that of each crystal resonator and then with one of the standard oscillators as reference. A frequency-difference method is used for the purpose with an electronic frequency counter with a sensitivity of ± 1 part in 10^{10}. Elaborate oven arrangements keep the temperature variations to <0.001°C. Details of a new automatic announcing system for WWV are also given. See also *Radio & Telev. News, Radio-Electronic Engng. Section*, vol. 49, pp. 10–11, 30; Jan., 1953.

621.3.018.41(083.74):529.786 1732

"Geared to Greenwich"—R. S. J. Spilsbury. (*Wireless World*, vol. 59, p. 167; April, 1953.) Authoritative comment on the Rugby MSF standard-frequency service, with particular reference to the transmission of 1 cps impulses. See also 1421 and 1423 of May.

621.317.3.029.64:621.392.5 1733

The Experimental Determination of Linear Quadripoles for Centimeter Wavelengths—H. Oppitz. (*Acta Phys. Austriaca*, vol. 5, pp. 214–236; Dec., 1951.) Weissfloch's transformation law (711, 2083 and 2084 of 1943) for linear reversible loss-free quadripoles is discussed, and a proof is given using quadripole matrices. An experimental method for determining quadripole characteristics, based on this law, requires the use of a terminal piston providing a perfect short-circuit for a coaxial line. An investigation is made of the effect of piston losses on the accuracy of the determinations. A method is described for measuring the apparent impedance of the piston; results are compared with those obtained by the usual method.

621.317.335.3.029.64 1734

A Simple Method for determining the Dielectric Constant of Fluids at Centimetre Wavelengths—F. Reder & E. Hafner. (*Acta Phys. Austriaca*, vol. 5, pp. 189–201; Dec., 1951.) An improved coaxial cylinder method is described. Only a relatively small quantity of the test material is required; the accuracy is to within 0.5%. Results are tabulated for benzene, toluene, carbon tetrachloride and paraffin oil. See also 1664 of 1952 (Ledinegg et al.).

621.317.34:621.396.645 1735

An Instrument for Measuring Complex Voltage Ratios in the Frequency Range 1–100 Mc/s—G. Thirup. (*Philips Tech. Rev.*, vol. 14, pp. 102–114; Sept./Oct., 1952.) Full description of an instrument designed for research on the stability of wide-band feedback amplifiers. The input and output HF voltages are converted to a fixed IF of 0.3 mc and one of the IF voltages is adjusted in amplitude and phase to cancel the other; the phase-shifting device used for this purpose comprises a metal tube containing crossed loops providing a rotating magnetic field, and also a pickup loop. Balance is indicated by the disappearance of a beat note from a loudspeaker. Accuracy is to within 0.2 db in respect of amplitude and 2° in respect of phase angle.

621.317.35:621.397.5 1736

A Television-Waveform Monitor—J. E. Attew. (*Electronic Eng.*, vol. 25, pp. 106–107; March, 1953.) Complete circuit details are given of a monitor for examination of television line, frame and synchronizing-signal waveform. Construction details are included for the delay line used in the pulse-duration calibrator.

621.317.353.3:621.3.018.78 1737

Intermodulation Distortion; Its Significance and Measurement—E. W. Berth-Jones. (*Jour. Brit. I.R.E.*, vol. 13, pp. 57–63; Jan., 1953.) Discussion indicates that in the majority of cases intermodulation testing has little advantage over the simpler total-harmonic testing methods. For the special cases in which intermodulation test methods are justified, great care must be taken in the design of equipment to ensure reasonably accurate results. In particular, phase shifts in filters may affect peak values considerably, and results mean little on an absolute basis unless full details of test conditions are quoted. Typical intermodulation test equipment is described.

621.317.361.029.3 1738

An Accurate Method of Measuring Frequency in the Audio Range—A. F. B. Nickson. (*Jour. Sci. Instr.*, vol. 29, pp. 391–393; Dec., 1952.) The unknown frequency is compared directly with a neighboring frequency given by a VFC locked to a suitable harmonic of a crystal-controlled oscillator. The comparison is effected by means of Lissajous figures on the screen of a CRO.

621.317.373:621.317.755 1739

A Note on Phase-Angle Measurements using a Cathode-Ray Tube—F. A. Benson & M. S. Seaman. (*Electronic Eng.*, vol. 25, p. 100; March, 1953.) A method of eliminating measurement errors due to incorrect location of the horizontal reference line on the CRO screen is described. A double-beam oscillograph is used to generate two ellipses, the intersections of which determine accurately the position of the reference line. See also 1965 of 1950 (Benson & Carter).

621.317.373:621.317.755 1740

Phase-Angle Measurements—F. A. Benson. (*Wireless World*, vol. 59, p. 157; April, 1953.) Comparison of errors due to trace width in three methods of measurement. See also 1965 of 1950 (Benson & Carter).

621.317.373.029.6 1741

Application of the Microwave Homodyne—F. L. Vernon, Jr. (*Trans. I.R.E.*, No. PGAP-4, pp. 110–116; Dec., 1952.) The principle of homodyne detection is explained and its application in the measurement of the phase difference between two microwave signals is described. The method is effective over a wide range of signal amplitudes.

621.317.41 1742

Measurement of the Constants of Ferromagnetic Materials by means of Transmission Lines (80–4000 Mc/s)—A. Hersping. (*Frequenz*, vol. 6, pp. 345–356; Dec., 1952.) A short length of a straight coaxial measurement line is completely filled with the material to be tested, such as a nonmetallic ferrite. The front portion of the line is slotted to permit probe measurements along the line. The ferrite-filled section acts as an attenuator with a complex impedance and propagation constant, formulae for which involve the line parameters and the magnetic and dielectric loss angles. The line is fed through a shielded cable and the permeability, dielectric constant and loss angles are determined from measurements of the no-load and short-circuit impedance of the line. Detailed theory of the method is given. The range 80–600 mc is covered using the Rohde & Schwarz Type-BN3916 measurement line, smaller equipment, details of which are given, being used for the range 600–4000 mc. Measurement results for Ni-Zn and Cu-Zn ferrites are shown graphically.

621.317.42:621.385.833 1743
Pendular System for Electrodynamic Measurement of the Axial Field of a Magnetic Electron Lens—P. Durandeau. (*Comp. Rend. Sci.* (Paris), vol. 236, pp. 366–368; Jan. 26, 1953.) Description of an accurate method based on the displacement of a compensated system of two solenoids.

621.317.421 1744
Null Method for the Precision Measurement of Magnetic Induction—R. Tenzer. (*Arch. Elektrotech.*, vol. 40, pp. 406–421; 1952.) A method developed for investigating the constancy of permanent magnets is described. The voltage pulse generated in a small coil on withdrawing it from the magnet is opposed by another pulse of the same magnitude derived by mutual induction on opening or closing a primary circuit. A fluxmeter rather than a ballistic galvanometer is used as the null instrument. Relevant theory is given and system errors are discussed.

621.317.71 1745
A Direct Current Microampere Integrator—R. N. Schweiger. (*Rev. Sci. Instr.*, vol. 23, no. 12, pp. 735–738; Dec., 1952.) A feedback-stabilized current amplifier feeds the current coil of a modified Type C-6 Thompson watt-hour meter. The no-load speed of this meter is directly proportional to the current supplied, so that the value of the integrated current is given on the scale of a revolution counter operating at nearly zero torque. The nett accuracy is to within about 1% of full scale. Seven ranges are provided, with full-scale readings ranging from 10 μA to 1 mA.

621.317.725 1746
Nonlinearity in a Voltmeter using Cathode Follower and Thermocouple—D. G. Tucker. (*Jour. Sci. Instr.*, vol. 30, pp. 11–13; Jan., 1953.) The arrangement considered comprises a galvanometer connected to a thermocouple whose heater is used as the cathode load of a cathode follower; it is useful for comparing an alternating voltage with a direct-voltage standard. Analysis shows that the effect of valve nonlinearity is usually so small that the calibration error is $<0.1\%$ for a voltage of about 0.8 V.

621.317.73.029.6:621.392.43 1747
New Equipment for Impedance Matching and Measurement at Very High Frequencies—A. Bloch, F. J. Fisher & G. J. Hunt. (*Proc. IEE* (London), part III, vol. 100, pp. 93–99; March, 1953.) A section of low-loss coaxial line, which may be only a third of the length of the equivalent slotted line, is fitted with three fixed probes to measure relative voltage amplitudes. From these ratios an unknown impedance loading the line can be found, either analytically or graphically, each ratio defining a circular locus on the Smith chart. The equipment is particularly suitable for field tests; it has the decided advantage that adjustment of a load to a prescribed value is shown by the simultaneous zero reading of two meters. The frequency range covered is about 3:1. This can be more than doubled if the two outer probes are movable; such an arrangement has the advantage that a single chart can be used for all the frequencies covered.

621.317.733:[621.316.86:537.312.6 1748
Use of Thermistors in a R.F. Bridge for Measurement of Low Admittances—M. Soldi. (*Alta Frequenza*, vol. 21, pp. 243–259; Dec., 1952.) A bridged-T circuit is used, with thermistors as variable resistance standards (see 2134 of 1952). The thermistors are simultaneously regulated and calibrated by means of a special automatic dc bridge. Results obtained with an experimental model confirm the theoretically predicted high sensitivity and good accuracy of the arrangement.

621.317.733:621.316.86:537.312.6 1749
The Design of a Direct-Reading Thermistor Bridge with Temperature Compensation—R. M. Pearson & F. A. Benson. (*Electronic Engng*, vol. 25, pp. 51–57; Feb., 1953.) Characteristic data are given for thermistors of British manufacture, of both bead and disk types. The data are used to design a bridge in which power at a wavelength of 3 cm is measured in terms of the change of resistance of a thermistor on to which the power is directed. Effects due to variations of ambient temperature are balanced out by means of compensating thermistor networks arranged in parallel with the bridge supply source and in series with the meter.

621.317.74:621.397.2 1750
Apparatus for the Measurement of Phase Delay in Television Transmission Circuits and in Associated Equipment—C. W. Goodchild & R. C. Looser. (*Proc. IEE* (London), part IIIA, vol. 99, no. 20, pp. 788–795. Discussion, pp. 860–866; 1952.) A waveform rich in harmonics of a convenient fundamental frequency is applied to the circuit under test, the output from which is compared with a similar reference waveform, of opposite polarity, by means of a calibrated delay unit. The frequency range covered is 100 kc—10 mc. For delays <1 μs the error is $<\pm 0.01$ μs.

621.317.76.089.6 1751
Wide-Range Frequency Calibrator—J. F. Sterner. (*Radio & Telev. News, Radio-Electronic Eng. Section*, vol. 49, pp. 12–13, 31; Jan., 1953; *Proc. NEC* (Chicago), vol. 8, pp. 831–835; 1952.) Description of simple equipment providing subharmonics and harmonics of a 2.5-mc crystal throughout the range 0.25–250 mc. An *LC* multivibrator, locked to the crystal-controlled oscillator, provides harmonics of its 0.25 mc fundamental frequency whose amplitudes are increased by means of a 1-mc "bumper" circuit in the cathode lead.

621.317.784.029.51 1752
High-Frequency Power Meter with Dry Rectifier—H Wilde. (*Arch. Tech. Messen*, pp. 5–6; Jan., 1953.) Description of an instrument using a dynamometer type of indicator, with phase control of the rectified voltages applied to the coils. The frequency limit is about 200 kc; power consumption is <0.2 W on the lowest power range of 0–8 W.

621.317.79:621.397.8 1753
A Variable-Definition Camera Channel for the Appraisal of Television Standards—A. V. Lord & C. B. B. Wood. (*Proc. IEE* (London), part IIIA, vol. 99, no. 20, pp. 811–820; 1952. Discussion, pp. 860–866.) Description of equipment which can be switched rapidly between six preselected line-scanning standards in the range of line frequency 10–32 kc, the frame frequency in all cases being that of the mains. The more interesting units are described in detail and results obtained with the equipment are reported.

621.397.2.001.4 1754
The Testing of Television Transmission Systems by means of Square Waves—J. Müller. (*Funk u. Ton*, vol. 6, pp. 617–731; Dec., 1952.) Description of the method, with two practical examples illustrating the connection between transient response and transfer function. See also 209 and 1879 of 1952.

621.397.24.001.4 1755
The Specification and Testing of Television Wire-Broadcasting Systems—F. Hollinghurst & D. S. Tod. (*Proc. IEE* (London), part IIIA, vol. 99, no. 20, pp. 680–695; 1952. Discussion, pp. 757–760.) Technical conditions and recommended standards of performance specified for such systems are discussed and test methods described. The main features of eight experimental or working systems are tabulated and results of performance tests on four systems are presented.

OTHER APPLICATIONS OF RADIO AND ELECTRONICS

534.321.9:620.179.1 1756
Efficient Small Apparatus for Ultrasonic Testing of Materials with Barium-Titanate Oscillator—V. Met & E. Skudrzyk. (*Elektrotech. u. Maschinenb.*, vol. 69, pp. 519–523; Dec. 1, 1952.) Description and circuit details of equipment including a specially damped $BaTiO_3$ disk operated below its natural frequency, pulse recurrence frequencies ranging from 25 to 200 /sec.

534.321.9:639.245.1 1757
Ultrasonic Equipment for Locating Whales—(*Engineering* (London), vol. 175, pp. 90–91; Jan. 16, 1953.) Pulse-reflection apparatus is described using a narrow horizontal beam with a maximum range of about 2000 yards. The generator is of magnetostriction type, operating at 14 or 25 kc.

535.33.071:621.383.4 1758
A Simple High-Speed Spectrometer for the Infrared Region—D. A. H. Brown & V. Roberts. (*Jour. Sci. Instr.*, vol. 30, pp. 5–8; Jan., 1953.) A single-prism spectrometer is described which uses a rapid-response photoconductive detector together with CRO presentation at a repetition rate of 150 per sec. Using a PbTe cell, the long-wave limit is about 5.5 μ.

535.822.9:621.397.611.2 1759
The Flying-Spot Microscope—F. Roberts & J. Z. Young. (*Proc. IEE* (London), part IIIA, vol. 99, pp. 747–757; 1952. Discussion, pp. 757–760.) For another account see 1733 of 1951.

621.316.7 1760
Calculation of Control Systems having Given Limits of Control Error—D. Ströle. (*Arch. elekt. Übertragung*, vol. 7, pp. 37–46 & 107–116; Jan. & Feb., 1953.) The criteria for assessing a control system are that the damping and the maximum and final deviations of the system under control shall not exceed given limits. The problem is treated in terms of frequency response. A practical method of designing the control system is developed and is illustrated by means of two examples.

621.316.7 1761
Stabilization of Nonlinear Feedback Control Systems—R. L. Cosgriff. (Proc. I.R.E., vol. 41, pp. 382–385; March 1953.)

621.317.083.7 1762
Radio Telemetering—E. D. Whitehead & J. Walsh. (*Proc. IEE* (London), part III, vol. 100, pp. 45–56; March, 1953. Discussion, pp. 57–59.) Basic principles of present-day telemetry systems are discussed, together with the characteristics of various types of modulation and methods of multiplexing. Particular systems are outlined and a 6-channel frequency-multiplex fm/am system developed for aerodynamic research is described in some detail.

621.383.001.8:778.37 1763
An Industrial Instrument for the Observation of Very-High-Speed Phenomena—M. S. Richards. (*Proc. IEE* (London), part IIIA, vol. 99, no. 20, pp. 729–746; 1952. Discussion, pp. 757–760.) Detailed description of equipment designed in conjunction with an experimental image-converter tube. Repetitive exposures down to 1 μs are available whose repetition rate can be varied between 12/sec and 10^5/sec for stroboscopic viewing. Single exposures down to 0.05 μs, for recording transient phenomena, can also be obtained.

621.384.711/.612 1764
Synchrocyclotron for 450-MeV Protons—H. L. Anderson, J. Marshall, L. Kornblith, Jr., L. Schwarcz & R. Miller. (*Rev. Sci. Instr.*, vol. 23, pp. 707–728; Dec., 1952.) Detailed description of the particle accelerator recently completed at the Institute for Nuclear Studies, Chicago University.

621.384.611 1765

Electric Fields within Cyclotron Dees—R. L. Murray & L. T. Ratner. (*Jour. Appl. Phys.*, vol. 24, pp. 67–69; Jan., 1953.)

621.384.622.1 1766

A New Focusing Principle applied to the Proton Linear Accelerator—J. S. Bell. (*Nature* (London), vol. 171, pp. 167–168; Jan. 24, 1953.) A modification of the drift tube is described by which suitable electric or magnetic fields can be applied transverse to the particle motion so that particles converge strongly in one direction and diverge in the direction at right angles. Over-all focusing results if the field directions are interchanged periodically along the accelerator. See also 1455 of May (Blewett).

621.385.83:538.691 1767

Determination of an Electron Trajectory by Successive Integrations—E. Durand. (*Comp. Rend. Acad. Sci.* (Paris), vol. 236, pp. 364–366; Jan. 26, 1953.) A method of integration of second-order linear equations is adapted for systematic calculations in electron optics.

621.385.833 1768

The Scanning Electron Microscope and the Electron-Optical Examination of Surfaces—D. McMullan. (*Electronic Eng.*, vol. 25, pp. 46–50; Feb., 1953.) A conventional two-stage es electron microscope has been modified to operate as a scanning microscope by removal of the projector lens and replacement of the fluorescent screen by a unit comprising deflection coils, es lens, specimen stage and electron multiplier; the picture is reconstituted in a separate CR tube. For direct viewing, the system uses 405 lines (interlaced) per picture and about 0.9 pictures/sec; for recording, with beam current reduced to give maximum resolving power, the system uses 550 lines per picture and 1 picture in 300 sec. It is possible to obtain pictures of surfaces directly without making replicas.

621.385.833 1769

Electrostatic Lenses for Focusing Very-High-Energy Particles—M. Y. Bernard. (*Comp. Rend. Acad. Sci.* (Paris), vol. 236, pp. 185–187; Jan. 12, 1953.) The type of lens described, which is similar to that proposed recently by Courant, Livingston & Snyder (1454 of May), uses two sets of electrodes in line. Each set comprises four nearly quadrantal sections of a cylinder, two opposite sections being maintained at a positive potential and the other two at an equal negative potential. One set is rotated 90° with respect to the other. With such systems, ions with energies of several megavolts can be focused, using very much lower voltage sources.

621.385.833 1770

Experimental Study of Electrostatic Immersion Objective with Plane Electrodes: Extractor Field E_0 under Condition of Focusing. Geometrical Aberrations off the Axis—A. Septier. (*Comp. Rend. Acad. Sci.* (Paris), vol. 236, pp. 58–60; Jan. 5, 1953.)

621.385.833:061.3 1771

Summarized Proceedings of a Conference on Electron Microscopy—Bristol, September 1952—V. E. Cosslett, J. Nutting & R. Reed. (*Brit. Jour. Appl. Phys.*, vol. 4, pp. 1–5; Jan., 1953.) Summaries are given of papers and discussion on design, operating technique and applications.

PROPAGATION OF WAVES

538.566.029.45/.51:551.594.6 1772

The Propagation of Very Long Electromagnetic Waves and of [waves due to] Lightning Discharges round the Earth—W. O. Schumann. (*Z. angew. Phys.*, vol. 4, pp. 474–480; Dec., 1952.) See 802 of March.

621.396.11 1773

Ionospheric Propagation—R. Gea Sacasa. (*Rev. Telecommunicación* (Madrid), vol. 8, pp. 2–10; Dec., 1952. In Spanish, French and English.) Documents discussed at Stockholm in May 1952 by the C.C.I.R. committee on ionospheric propagation are analyzed in detail to show that the accuracy of predictions made by the "Spanish method" (3536 of 1952) compares favorably with that of predictions made by British and U. S. methods.

621.396.11 1774

Investigations of the Propagation of Space Waves: Part 2—W. Budde. (*Z. Naturf.*, vol. 6a, pp. 238–242; May, 1951.) Measurements made during the period October 1944 to January 1945 over the path Ismaning (Munich)–Kölby (Denmark) are discussed; the frequency used was 9.83 mc. Short-term fluctuations of azimuth angle were observed. The fluctuations decreased from a fairly high early-morning value to a minimum around midday and then increased to a maximum during the afternoon, decreasing again in the early evening. No seasonal variation of the mean fluctuations was observed.

621.396.11 1775

Determination of the Sense of Polarization of the Magneto-Ionic z-Component—B. Landmark. (*Tellus*, vol. 4, pp. 319–323; Nov., 1952.) See 2867 of 1952.

621.396.11 1776

The Diffraction of Radio Waves by the Curvature of the Earth—M. H. L. Pryce. (*Advances Phys.*, vol. 2, pp. 67–95; Jan. 1953.) A simplified approximate derivation is given of the field at moderate heights and distances due to an oscillating dipole at moderate height, taking into account the curvature and electrical constants of the earth. The treatment is approximately equivalent to assuming the earth to be flat and the wave path to be curved upwards, and is mathematically convenient because Fourier integrals can be used instead of expansions in Legendre functions. The method applies to both vertically and horizontally polarized waves.

621.396.11 1777

Tables of Functions occurring in the Diffraction of Electromagnetic Waves by the Earth—C. Domb. (*Advances Phys.*, vol. 2, pp. 96–102; Jan., 1953.) In a previous paper [800 of 1948 (Domb & Pryce)] curves and formulae were given which enabled field strength to be calculated with fair accuracy; the approximation of the first term of the differential series was used for the region well beyond the optical range. Details are now given of relevant tables of functions to enable more accurate calculations to be made and the region of validity of the one-term approximation to be assessed. See also 1776 above.

621.396.11:551.510.535 1778

Effect of the Geomagnetic Field on the Absorption of Short Waves in the Ionosphere (Vertical Incidence)—Argence, Rawer & Suchy. (See 1678.)

621.396.11:551.510.535 1779

The Reflection and Absorption of Radio Waves in the Ionosphere—Piggott. (See 1679.)

621.396.11:551.510.535 1780

Gradient Reflections from the Atmosphere—J. Feinstein. (*Trans. I.R.E.*, pp. 2–13; Dec., 1952.) Analysis is presented showing the difference between (*a*) the effect on the field far beyond the horizon of a refractive-index gradient with no discontinuities in the derivatives of any order, and (*b*) the effect of a gradient having a discontinuity in a particular derivative. A theory of scattering from regions of random gradient of refractive index is developed, under the assumption of complete horizontal stratification of the atmosphere.

621.396.11.029.51/.53 1781

A Review of Present Knowledge of the Ionospheric Propagation of Very-Low, Low- and Medium-Frequency Waves—F. A. Kitchen, B. G. Pressey & K. W. Tremellen. (*Proc. IEE* (London), part III, vol. 100, pp. 100–108; March, 1953.) Observations at frequencies <3 mc and for ranges mainly <500 km are reviewed. The results for frequencies <300 kc are summarized under the headings of field strength, phase and polarization measurement, the effects of ionospheric disturbances, the effects of local ionospheric characteristics, and theoretical studies. Propagation investigations on medium frequencies prior to 1937 were adequately summarized in an I.R.E. report (27 of 1939), so that only work done since that date is considered here. Present knowledge of the subject is summarized and suggestions are made for further study. 70 references.

621.396.11.029.51 1782

The Measurement of the Phase Velocity of Ground-Wave Propagation at Low Frequencies over a Land Path—B. G. Pressey, G. E. Ashwell & C. S. Fowler. (*Proc. IEE*, part III, vol. 100, pp. 73–84; March, 1953.) An account of measurements of the change of phase of a 127.5-kc wave with distance along the irregular 177-km land path between the Decca stations at Lewes (Sussex) and Warwick. Mobile equipment was used at 25 points along the path to measure the phase difference of the signals from the two transmitters. The results (accurate to within 0.25°) were used to plot a curve showing the deviation of the measured phase difference from that calculated on the assumption of a propagation velocity equal to that in free space. The mean velocity deduced for the path was 299 230 ± 12 km/s. No definite evidence was found of any ground-contour effect on the phase, but the effect of the nature of the ground was very marked, a high velocity being obtained over ground of good conductivity and a low velocity over ground of poor conductivity.

621.396.11.029.55(98) 1783

Ionospheric Propagation of Decameter Waves in the Arctic Polar Regions—J. Bouchard. (*Comp. Rend. Acad. Sci.* (Paris), vol. 236, pp. 220–222; Jan. 12, 1953.) Discussion of reception in France of signals mainly from stations on the Pacific coast of North America, the frequencies concerned ranging from 12 to 17 mc. Distortion on these frequencies is at times so great that the signals are unreadable. The distortion appears to be due to ionospheric turbulence in the arctic polar regions, and related to geomagnetic disturbance. The distortion of signals whose transmission paths involve reflection at points in the arctic regions can be attributed to fluctuations of the critical frequency at the reflection points. In some cases, when the signals follow a great-circle path with a considerable length in the arctic regions, similar distortion of signals from the antipodes occurs, but when the signals travel by other paths no great distortion is observed. Correlation has been established between the received field-strength and distortion magnitude and the data on geomagnetic variations published by the French Ionospheric Bureau, and it is known that the corresponding variations in the zone of maximum auroral activity are 4 or 5 times greater than in France.

621.396.11.029.6:551.510.52 1784

Meteorological Effects on V.H.F. Propagation—K. Toman, W. G. Albright & E. C. Jordan. (*Trans. I.R.E.*, pp. 20–30; Dec., 1952.) Continuous records of the signal strength of several fm and TV stations in the Chicago area have been obtained during a period of 18 months at Urbana, Illinois, about 127 miles away. Correlation is discussed between the observed signal strengths and meteorological data obtained at two radiosonde stations along the transmission path. Low values of signal strength are obtained when the distribution of the effective dielectric constant ϵ of the troposphere is nearly linear, with a gradient corresponding to a well-mixed atmosphere. Medium and high signal levels result from larger surface gradients of ϵ and from larger

gradients at certain heights above ground. Very high signal levels are obtained when the trapping conditions of duct propagation are satisfied.

621.396.11.029.63 1785

Propagation Characteristics of Microwave Optical Links—L. G. Trolese, J. P. Day & R. U. F. Hopkins. (*Trans. I.R.E.*, pp. 31–36; Dec., 1952.) A report of tests, at frequencies in the band 1.7–1.85 kmc, on two paths near San Francisco, the transmitter being on Mt. Diablo at a height of 3800 ft and the receivers respectively at heights of 7–65 ft and 165 ft above sea level. Owing to the height of the transmitter, the path difference between the direct and the ground-reflected component varies rapidly with the height of the receiving antenna, so that closely spaced maxima and minima occur in the signal-strength antenna-height curves. The measure of the path difference in wavelengths also varies rapidly with frequency, so that the maxima and minima for frequencies of 1.7 and 1.85 kmc do not correspond, an antenna at a height of 55 ft giving maximum signals on 1.7 kmc and minimum signals on 1.85 kmc, essentially the same response on the two frequencies being obtained for an antenna height of 7 ft, where the first maximum occurs for both frequencies and for which less fading is observed.

621.396.11.029.63 1786

Variation of Field Intensity over Irregular Terrain within Line of Sight for the U.H.F. Band—H. Fine. (*Trans. I.R.E.*, no. PGAP-4, pp. 53–65; Dec., 1952.) Statistical analysis of available data from field-strength surveys enabled empirical propagation formulas to be deduced for the whole UHF television band from 300 to 900 mc to assist the Federal Communications Commission in the problem of frequency allocation for UHF television broadcasting stations.

621.396.11.029.65/.65 1787

Microwave Radio Reflection from Ground and Water Surfaces—A. W. Straiton. (*Trans. I.R.E.*, pp. 37–45; Dec., 1952.) Reflection measurements for wavelengths from 0.86 to 26.5 cm and angles within 5° of grazing incidence showed that the reflection coefficient increased with wavelength and decreased with increase of the angle between the beam direction and the ground or water surface. The 0.86-cm signals were very sensitive to roughness of the reflecting surface. The reflection coefficient was greater for horizontal than for vertical polarization.

RECEPTION

621.396.4:621.396.619.16:621.396.621 1788

Channel Separation in Pulse-Phase Modulation (P.P.M.)—K. Steinbuch. (*Fernmeldetech. Z.*, vol. 5, pp. 535–538; Dec., 1952.) An outline description of separations for multichannel ppm telephony systems, and an examination of their relative cost.

621.396.621.029.62:621.396.82 1789

Noise Performance of V.H.F. Receivers—E. G. Hamer. (*Electronic Eng.*, vol. 25, pp. 68–71; Feb., 1953.) The frequency distribution of different types of noise is shown graphically, and receiver design is discussed in relation to the reduction particularly of man-made interference and of noise inherent in the receiving system itself, including the aerial. A convenient method of assessing receiver noise performance makes use of a diode as a calibrated noise generator; a miniature diode with associated disk resistor for measurements at frequencies up to 500 mc is illustrated. The additional cost of a special low-noise-factor design may be justified for services operating at frequencies >200 mc.

621.396.621.54.029.64:621.396.822 1790

The Noise Factor of Centimetric Superheterodyne Receivers—J. H. Evans. (*Electronics Eng.*, vol. 25, pp. 98–100; March, 1953.) The noise contributions from the various units of a receiver comprising a crystal frequency changer, klystron local oscillator, and IF amplifier, are discussed and curves are given which show the effect on the receiver noise factor of the noise in the local oscillator and the IF amplifier. Methods of reducing local-oscillator noise are noted and their attendant disadvantages are considered briefly.

621.396.622.63:621.396.621.54 1791

Harmonic Mixing and Distortion with Crystal Diodes—H. F. Mataré. (*Arch. elekt. Übertragung*, vol. 7, pp. 1–15; Jan., 1953.) Basic theory is outlined for heterodyning with oscillator harmonics and for the distortion resulting from curvature of the diode characteristic. The principal properties of mixers, viz. slope of rectifier characteristic, conversion slope and optimum conversion efficiency, are shown in families of curves for two basic forms of presentation of characteristics. Distortion may be caused by pure impedance variations. From the curves it is possible to estimate the losses with harmonic mixing, on the efficiency in the presence of distortion. In this respect Ge diodes are better than Si diodes. See also 2824 of 1951.

STATIONS AND COMMUNICATION SYSTEMS

621.39.001.11 1792

Technical Characteristics related to Information. Application to Telecommunications and [radar] Detection—J. Maillard. (*Onde élect.*, vol. 32, pp. 500–514; Dec., 1952.) The terms "quantity of information" and "rate of information" are defined and basic relations between them are discussed. These relations enable comparison to be made between the efficiency of the different methods used for the transmission of information, in particular, between the different methods of modulation, whose advantages and disadvantages are here discussed. The use of cm or acoustic waves for the detection of objects is also considered in the light of information theory. The analysis indicates that though fm equipment appears to have theoretical advantages, pulse equipment has in most cases technical and practical advantages.

621.396.41:621.396.619.16 1793

Time-Division Multiplex Systems—J. E. Flood. (*Electronic Eng.*, vol. 25, 302, pp. 2–5, 58–63, 101–106 & 146–150; Jan.–April, 1953.) A series of articles forming an introduction to the subject. Part 1 describes different forms of pulse modulation which can be used and discusses features common to different time-division multiplex systems. Part 2 deals in detail with pam, part 3 with pwm and ppm, and part 4 with pcm. 94 references.

621.396.44:621.315.052.63:621.396.822 1794

The Reduction of Radiation from Carrier Communication Circuits on Overhead Power Lines—E. P. L. Westell (*Jour. Instn. Eng.* (Australia), vol. 24, pp. 213–218; Dec., 1952. Discussion, pp. 218–219.) An account of measurements of noise voltages on (*a*) a single-channel am carrier system on a 132-kV power line, (*b*) a multichannel ssb suppressed-carrier system, with suggestions as to practical means of reducing the RF interference from such systems.

621.396.5:621.396.8 1795

150–370 Mc/s Performance Tests—W. R. Young, Jr. (*Commun. Eng.*, vol. 13, pp. 15–18, 34; Jan./Feb., 1953.) See 823 of March.

621.396.65:621.396.8 1796

Intermodulation Interference in Radio Systems—W. C. Babcock. (*Bell Sys. Tech. Jour.*, vol. 32, pp. 63–73; Jan., 1953.) Formulas are derived for the number of third- and fifth-order intermodulation products liable to be formed within a continuous frequency band comprising a number of channels. Calculations are made of the probability of encountering interference in channels selected at random from this band, and of the number of interference-free channels that can be obtained by careful selection.

621.396.65:621.396.93 1797

Frequency Economy in Mobile-Radio Bands—K. Bullington. (*Bell Sys. Tech. Jour.*, vol. 32, pp. 42–62; Jan., 1953.) Factors affecting the suitability of different channels for mobile radio services are discussed, and estimates are made of the number of usable channels per mc for some present and proposed methods of operation, taking into account the possibilities of geographical and operational corrdination as well as circuit selectivity.

621.396.933:621.396.82 1798

Ground-to-Air Cochannel Interference at 2.9 kMc/s—P. L. Rice, W. V. Mansfield & J. W. Herbstreit. (*Trans. I.R.E.*, pp. 1–10; Dec., 1952.) Estimates are made of the average interference—limited coverage to be expected for a ground station using a Bendix Type-ASR-1 antenna with vertical polarization and operating at 2.9 kmc. Coverage is defined in terms of protection ratios of 0, 6, 12, and 18 db with respect to interfering transmissions from a similar station 10, 50, 100 or 150 miles distant.

621.396.97+621.397.61].029.62:061.3 1799

The Technical Principles of the Allocation of Frequencies at the European Broadcasting Conference of 1952 in Stockholm—F. Kirschstein. (*Fernmeldetech. Z.*, vol. 5, pp. 563–567; Dec., 1952.) For other accounts see 3560 of 1952.

SUBSIDIARY APPARATUS

621–526 1800

The Principle of a Servo-Type Mechanism requiring variable Elements—R. Drenick. (Proc. I.R.E., vol. 41, pp. 373–377; March, 1953.)

621–526:621.316.7 1801

The Analysis of Sampled-Data Systems—J. R. Ragazzini & L. A. Zadeh. (*Elec. Eng*, (N.Y.), vol. 71, p. 1102; Dec., 1952.) Digest only. The Laplace and Fourier transform methods of analysis for sampled-data systems are unified and extended. Formulas representing the input-output relations of such systems in the frequency domain are derived.

621.314.634.011.4 1802

Capacitance of Selenium Rectifiers—W. Oldekop. (*Z. Phys.*, vol. 134, pp. 66–77; Dec. 17, 1952.) In ac measurements on Se rectifiers, a temperature-dependent phase shift between current and voltage is produced. Representation of the rectifier by an equivalent circuit consisting of a resistor and parallel capacitor affords a satisfactory explanation of this. Discussion shows that a negative component of capacitance is concerned which decreases with decreasing current and with increasing frequency. The abnormal decrease of capacitance with high reverse voltages observed by Hoffmann (941 of 1951) is in agreement with this. See also 3566 of 1952 (Schottky).

621.316.722.621.311.6:621.387.422 1803

A Corona Stabilizer E.H.T. Supply for Proportional Counters—P. Holton & J. Sharpe. (*Electronic Eng.*, vol. 25, pp. 63–65; Feb., 1953.)

621.316.722.1 1804

An Electric Control Device—W. Hartel. (*Elektrotech. Z., Edn. A*, vol. 73, pp. 769–771; Dec. 11, 1952.) Description of a high-precision voltage regulator suitable for a rotary generator.

621.316.722.1 1805

Cold-Cathode Voltage Stabilizer—G. O. Crowther. (*Electronic Eng.*, vol. 25, p. 127; March, 1953.) Comment on 554 of February (Goulding).

TELEVISION AND PHOTOTELEGRAPHY

621.397.2:621.317.74 1806

Apparatus for the Measurement of Phase Delay in Television Transmission Circuits and in Associated Equipment—Goodchild & Looser. (See 1750.)

621.397.2.001.4 1807

The Testing of Television Transmission Systems by means of Square Waves—Müller. (See 1754.)

621.397.24 1808

Television Distribution by Wire—P. Adorian. (*Proc. IEE* (London), part IIIA, vol. 99, pp. 665–672; 1952. Discussion, pp. 757–760.) Discussion of systems particularly suitable for densely populated urban areas. Distribution on screened quad cable and coaxial cable is mainly considered. Typical transmitting and receiving systems are described.

621.397.24.001.4 1809

The Specification and Testing of Television Wire-Broadcasting Systems—Hollinghurst & Tod. (See 1755.)

621.397.26:621.396.65 1810

Directional Radio Links on Ultra-short Waves for Television Programme Exchange with Berlin—W. Scholz. (*Fernmeldetech. Z.*, vol. 5, pp. 539–544; Dec., 1952.) An account of the planning and design of the Berlin-Höhbeck-Hamburg relay system, including test measurements of field strengths in the 174–216 mc band. For the Berlin-Höhbeck 136-km link, antenna systems comprise 30 units mounted on a 150-m mast, each unit consisting of 8 horizontal dipoles. The 10-kW Berlin and 1-kW Höhbeck transmitters use negative a.m. The attenuation of the antenna feeders, which are 360-m coaxial lines of brass with polystyrene-disk insulation, is 1.4 db at 175 mc and 1.8 db at 240 mc.

621.397.26:621.396.72 1811

Television "Booster" Stations—P. J. Harvey. (*Wireless World*, vol. 59, pp. 148–152; April, 1953.) Discussion, based on experimental investigations, of the operation of satellite stations in fringe areas, receiving the normal broadcast transmission and reradiating locally on suitable frequencies. Circuit arrangements for 10–250-W vision and 5–50-W sound transmitters are outlined. In the case of retransmission at uhf the expense of converters in domestic receivers would be largely offset by the saving on preamplifiers and special aerials. Initial and maintenance costs of a typical unattended station are estimated and administrative aspects of the system are considered.

621.397.335:538.88 1812

A Precision Synchronizing System for Large-Screen Television Equipment—A. W. Keen. (*Proc. IEE* (London), part IIIA, vol. 99, pp. 696–707; 1952. Discussion, pp. 757–760.) A description is given of a complete system developed for experimental cinema equipment. It provides, under local control, line- and frame-trigger and black-level-clamp switching-pulse waveforms, all of which are derived from a type of automatic phase follower and are therefore substantially unaffected by interference or all but the most severe degradation of the signal. Automatic interlacing is introduced, with fine manual control of interframe spacing to eliminate the mean interlace error. Schematic diagrams are given of all the main sections of the equipment, which was designed for 625/50 European standard, with negative modulation. Since the method adopted is practically equivalent to regeneration of the synchronizing signal, it would appear to be adaptable to other problems, particularly in network repeater stations.

621.397.5:535.62/.65 1813

A Survey of the Methods and Colorimetric Principles of Colour Television—J. E. Benson. (*Jour. Brit. I.R.E.*, vol. 13, pp. 9–49; Jan., 1953. Reprinted from *Proc. IRE* (Australia), vol. 12, pp. 201–205 & 237–258; July & Aug., 1951.) The historical development of color television is reviewed and the basic requirements of a satisfactory system are discussed. A detailed account is given of the principles of color specification, measurement and calculation, using the concept of color space as a means of explaining the algebraic development of the trichromatic theory of color representation, and leading to an explanation of the origin and principal characteristics of the chromaticity diagram of the International Commission on Illumination. An outline is given of the principles of three-color reproduction in television. About 140 references.

621.397.5:535.623/.624 1814

Some Fundamental Aspects of Colour Television—W. N. Sproson, M. Gilbert & W. West. (*Proc. IEE* (London), part IIIA, vol. 99, pp. 842–853; 1952. Discussion, pp. 860–866.) A review of the physical and physiological factors relevant to the analysis and synthesis of television pictures in color.

621.397.5:535.623/.624 1815

Compatible Systems of Colour Television—G. Valensi. (*Ann. Télécommun.*, vol. 7, pp. 439–458 & 482–496; Nov. & Dec., 1952.) The concept of compatibility, as applied to a system of television in color, is defined, and the specification of colors by defining the trichromatic coefficients, the dominant wavelength, and colorimetric purity factor, is described. Some physiological characteristics concerned in color vision are discussed briefly. Two only of the numerous methods of realizing television in color are described: (*a*) a system using the electrical double-refraction properties of a Kerr cell in the receiving system; (*b*) an entirely electronic system. Discussion indicates a possible reduction of the total bandwidth required for the transmission of color-television signals. Two of the compatible systems developed in the U.S.A. are also described: the R.C.A. system with dot interlacing of the image, and the N.T.S.C. system using line interlacing.

621.397.5:535.623 1816

Colorimetric Analysis of Gamma-Corrected Shunted-Monochrome Simultaneous Colour Television Systems—D. C. Livingston. (*Sylvania Technologist*, vol. 6, pp. 13–17; Jan., 1953.) A formula is developed for use in analyzing the colorimetric properties of color-television systems; in a subsequent paper the method is to be applied to an analysis of the color system used by the U. S. N.T.S.C. for field testing.

621.397.5:535.623(083.71) 1817

Standards on Television: Definitions of Color Terms, Part 1, 1953—(Proc. *I.R.E.*, vol. 41, pp. 344–347. March, 1953.) Standard 53 IRE 22. S1.

621.397.5:535.65 1818

Colour Television: Some Subjective and Objective Aspects of Colour Rendering—G. T. Winch. (*Proc. IEE* (London), part III A, vol. 99, pp. 854–860; 1952. Discussion, pp. 860–866.)

621.397.5:621.317.35 1819

A Television-Waveform Monitor—Attew. (See 1736.)

621.397.5:621.396 1820

Television as a Communication Problem—L. C. Jesty. (*Proc. IEE* (London), part IIIA, vol. 99, no. 20, pp. 761–770; 1952. Discussion, pp. 860–866.) A survey of the art of television communication and discussion of possible lines of development. 26 references.

621.397.6 1821

Signal Corps Mobile Television System—J. S. Auld. (*Jour. Soc. Mot. Pict. Telev. Engs.*, vol. 59, pp. 462–469; Dec., 1952.) Brief description of a complete microwave system operating over distances up to 20 miles. All equipment for transmission, reception, recording and power supply is housed in five vehicles.

621.397.6:535.623 1822

Generation of N.T.S.C. Color Signals—J. F. Fisher. (Proc. I.R.E., vol. 41, pp. 338–343; March, 1953.) Equipment is described for generating a composite compatible color signal in accordance with the N.T.S.C. specifications discussed previously [1750 of 1952 (Hirsch et al.)]. A flying-spot system is used which yields voltages proportional to the tristimulus values of the C.I.E. system; these are corrected to suit the red, green and blue channels by a process of electronic addition and subtraction termed "matrixing." An indication is given of modifications made to the signal specification in the light of the results of the field tests carried out during 1951 and 1952.

621.397.6:621.317.74 1823

Test Equipment for Television Transmission Circuits—S. H. Padel, A. R. A. Rendall & S. N. Watson. (*Proc. IEE* (London), part IIIA, vol. 99, No. 20, pp. 821–833; 1952. Discussion, pp. 860–866.) The standard of performance of a complete television transmission system is considered, and definite limits are suggested for distortion of amplitude and phase, with respect to frequency, noise and linearity. Descriptions are given of instruments designed to measure amplitude and phase distortions; these are (*a*) video-frequency oscillator, (*b*) video-frequency amplifier detector, (*c*) test-pulse generator, (*d*) waveform monitor, (*e*) group-delay measurement equipment. Applications of these instruments are discussed.

621.397.61/.62 1824

Compressed Television—Radionyme. (*Télévision*, pp. 259–260, 274; Nov., 1952.) The principles of various techniques developed by Toulon for reducing the bandwidth required for a vision channel are outlined. Combinations of vertical and horizontal interlacing can be used in conjunction with storage devices at the receiver. By using picture-difference transmission the bandwidth required for a radio link can be reduced to 1 mc for a system normally occupying 14 mc. Magnetic-drum and phosphorescent-film devices for storing the picture signals are described.

621.397.61/.62 1825

Saving Television Bandwidth—(*Wireless World*, vol. 59, pp. 158–162; April, 1953.) Methods proposed for reducing the bandwidth required for the vision channel are reviewed. These include prediction techniques for reducing redundancy in successive images or elements, variable-velocity scanning, decreasing the picture frequency and other methods of exploiting limitations in visual acuity.

621.397.61 1826

A Gamma-Control Circuit using Crystal Diodes—L. Lax & D. Weighton. (*Proc IEE* (London), part IIIA, vol. 99, pp. 804–810; 1952. Discussion, pp. 860–866.) A basic bridge-type circuit is described which meets the requirements of gamma-control circuits more nearly than those using thermionic tubes as nonlinear elements. A practical circuit with a high degree of dc stabilization is also described.

621.397.61.029.62:061.3 1827

The Stockholm Plan—*Télévision*, pp. 296–300; Dec., 1952.) Details of French television transmissions based on the frequency allocations of the 1952 Stockholm Conference.

621.397.611.2 1828

The Mechanism of Signal Generation in Storage-Type Television Camera Tubes—R. Theile. (*Jour. Telev. Soc.*, vol. 6, pp. 457–477; Oct./Dec., 1952.) The principles of operation of the iconoscope, image iconoscope, orthicon

and image orthicon are described in detail. Charge-storage action and target-stabilization processes are discussed with reference to storage efficiency and transfer characteristic. Two methods of deriving the signal current are described and the signal/noise ratios in the two cases are compared; at low light intensities a better ratio is maintained with preamplification by secondary-emission multiplication. Operational features of the four tubes and improvements in design are discussed, particularly the photoelectron-stabilization and pulsed-biasing techniques applied to the image iconoscope, and performance characteristics directly dependent on the mechanism of signal generation in the four types of tube are compared.

621.397.611.2 1829

Generation of Signals in Television Camera Tubes: Part 1—Fundamentals of the Transformation of the Optical Image into a Charge Image used for Signal Generation—R. Theile. (*Arch. elekt. Übertragung*, vol. 7, pp. 15–27; Jan., 1953.) See 1828 above.

621.397.611.2:778.53 1830

The Electronic Camera in Film-Making—N. Collins & T. C. Macnamara. (*Proc. IEE* (London), part IIIA, vol. 99, no. 20, pp. 673–679; 1952. Discussion, pp. 757–760. *Jour. Soc. Mot. Pict. Telev. Engs.*, vol. 59, pp. 445–457; Dec., 1952. Discussion, pp. 458–461.) Limitations of the cinematograph camera are reviewed and the advantages of the use of several electronic cameras, with the attendant possibilities of image distribution for control purposes, are discussed. See also *Wireless World*, vol. 59, pp. 153–156; April, 1953.

621.397.62 1831

Television Sound Reception. The Critical Capacitance-Coupling System—S. L. Fife. (*Electronic Eng.*, vol. 25, pp. 114–117; March, 1953.) In receivers with common RF and (sometimes) IF stages for the vision and sound signals, it has been found advantageous to use critical coupling, by means of capacitors of the order of 1 pF, in the succeeding sound-channel IF amplifier. Suitable IF circuits are shown. The use of an intercarrier FM sound circuit in television receivers for the American and European line standards is also considered briefly.

621.397.62:621.396.665 1832

Television-Receiver A.G.C. Systems—E. S. White. (*Electronics*, vol. 26, pp. 146–149; March, 1953.) Discussion of the operation of seven AGC circuits commonly used in television receivers, and of design factors important for obtaining an efficient low-noise circuit.

621.397.62:621.396.666 1833

Vision AGC—(*Wireless World*, vol. 59, pp. 173–174; April, 1953.) Description of the "automatic picture control" system which operates on the black-level signal following each line-synchronizing pulse.

621.397.621.2 1834

Some Factors in the Design of Deflecting Coils for Cathode-Ray Beam Systems—E. W. Bull. (*Proc. IEE* (London), part IIIA, vol. 99, no. 20, pp. 771–706; 1952. Discussion, pp. 860–866.) Conditions for the optimum field distribution are determined for a deflecting-soil system and practical arrangements are briefly described.

621.397.621.2:535.88 1835

Some Aspects of a Cathode-Ray-Tube Projector for Large-Screen Television in Cinemas—E. D. McConnell. (*Proc. IEE* (London), part IIIA, vol. 99, pp. 708–720; 1952. Discussion, pp. 757–760.) An account of the development of a large-screen projector system using a Schmidt optical system with a 9-in. CR tube which has a back-aluminized screen. Details of the design of the tube and optical system are discussed.

621.397.621.2:621.396.615.17 1836

Timebase Circuits—Bähring. (See 1631.)

621.397.645:621.397.822 1837

Fluctuation Noise in Television-Camera Head Amplifiers—I. J. P. James. (*Proc. IEE* (London), part IIIA, vol. 99, no. 20, pp. 796–803; 1952. Discussion, pp. 860–866.) An improvement in signal/noise ratio for the higher video frequencies is obtained with a modified input circuit for an amplifier used with a pickup tube of the C.P.S. emitron type. A method of equalizing the frequency/amplitude response of the modified circuit is described. An improvement of picture quality is obtained, particularly when aperture correction is applied.

621.397.645.018.424 1838

Some Factors in the Design of Wide-Band Amplifiers for Television—W. S. Percival. (*Proc. IEE* (London), part IIIA, vol. 99, no. 20, pp. 834–841; 1952. Discussion, pp. 860–866.)

621.397.645.029.62 1839

Fundamental Problems of H.F. and I.F. Amplifiers for TV Reception: Part 1—Gain and Bandwidth—Uitjens. (See 1639.)

621.397.645.029.62:621.397.822 1840

Fundamental Problems of H.F. and I.F. Amplifiers for TV Reception: Part 2—Noise Uitjens. (See 1640.)

621.397.8:535.735 1841

An Investigation of the Phenomenon of Flicker and a Possible Explanation of an Observed Resonance Effect—H. de Lange Dzn. (*Tjidschr. ned. Radiogenoot.*, vol. 18, pp. 1–31, Discussion, pp. 31–32; Jan., 1953.) The dependence on frequency and mean brightness of the ability of the eye to perceive rapid variations of brightness can be explained by assuming that the physiological system transmitting the visual impressions from the retina to the brain includes a low-pass filter. The problem can then be examined in the frequency domain, using Fourier analysis. An important parameter is the ripple ratio r, defined as the ratio of the amplitude of the first Fourier component to the mean brightness. At high brightness levels a resonance effect occurs at about 9 cps; under these conditions the value of r at which flicker disappears is $<1.35\%$. The results are consistent with the presence in the physiological system of a feedback mechanism having a time delay of about 1/80 sec.

621.397.8:621.317.79 1842

A Variable-Definition Camera Channel for the Appraisal of Television Standards—Lord & Wood. (See 1753.)

621.397.828 1843

Reduction of Pulse Interference in Television Receiving Systems—A. W. Keen. (*Jour. Brit. I.R.E.*, vol. 13, pp. 51–55; Jan., 1953.) A method of interference reduction, known as "black spotting," which has been used in receivers designed for reception of British positive-modulation transmissions (405/50 standard), is discussed. Existing circuit techniques are reviewed and a more detailed description is given of examples chosen to illustrate the particular suitability of the cathode-coupled-pair type of amplifier as a basis for improved circuit arrangements.

621.397.9 1844

Industrial and Professional Applications of Television Technique—R. C. G. Williams. (*Proc. IEE* (London), part IIIA, vol. 99, no. 20, pp. 651–664; 1952. Discussion, pp. 757–760.) A survey of British developments.

621.397.9:617(07) 1845

An Application of Television to the Demonstration of Operative Surgery—G. C. Newton & H. J. B. Atkins. (*Proc. IEE* (London), part IIIA, vol. 99, no. 20, pp. 721–728; 1952. Discussion, pp. 757–760.) Description of the equipment used at Guy's Hospital, London, and discussion of the value of television as a teaching aid and of the possibilities for its future development, based on extensive experience with the equipment. See also 3276 of 1949.

TRANSMISSION

621.396.619.23 1846

Serrasoid Modulation—E. Paulsen. (*Frequenz*, vol. 7, pp. 14–18; Jan., 1953.) An explanation is given of the operation of the serrasoid modulator [342 of 1949 (Day)], with particular reference to the capacitor charge and discharge phenomena in the modulation section, which have a great influence on the attainable frequency swing and the incidental a.m. See also 3267 (Gundlach) and 3589 (Bünemann & Pethke) of 1952.

621.396.3:621.396.61 1847

Rounding of Signals by a Filter in a Radiotelegraphy Transmitter—A. Tchernicheff. (*Ann Télécommun.*, vol. 7, pp. 513–516; Dec., 1952.) Results are given of measurements carried out on a transmitter in which a low-pass filter is used to reduce the transmission bandwidth. The frequency spectra of rectangular signals and of signals filtered by means of filters with cut-off frequencies of 75 cps and 100 cps are compared. Measurements of the telegraphy distortion were made by a stroboscopic method using a CRO.

TUBES AND THERMIONICS

537.533:621.396.822 1848

Noise Analysis of a Single-Velocity Electron Gun of Finite Cross Section in an Infinite Magnetic Field—H. E. Rowe. (*Trans. I.R.E.* pp. 36–46; Jan., 1953.) The various sinusoidal modes of propagation of a finite accelerated electron beam, converging or parallel, are investigated and boundary conditions for matching at the cathode and at the anode are considered. An idealized model is analyzed in which an infinite magnetic field parallel to the axis of the beam prevents all transverse motion of the electrons both in the drift space and in the electron gun. Only a summary of the analysis is presented. The results are applied to numerical calculations for seven different guns, for which noise-standing-wave curves are given for different anode voltages and, in the case of converging beams, for different angles of convergence. These curves show that for beams of the same total current and radius in the drift space, a converging-beam gun has a lower swr than a parallel-beam gun. Reduction of the beam radius, keeping beam voltage and current constant, reduces the level of the maxima while increasing the swr, thus further reducing the minima of the noise standing wave.

621.314.632 1849

Germanium Diodes Sealed in Glass—J. W. Dawson. (*Sylvania Technologist*, vol. 6, pp. 1–4; Jan., 1953.) To prevent the entry of moisture into the diodes they may be sealed either in glass or in ceramic cartridges filled with wax. Humidity-exposure tests indicate that the glass-cartridge assembly is the more effective in maintaining the diode characteristics stable.

621.314.7+621.314.632 1850

Germanium in Telecommunications Technique—M. C. Weill. (*Onde élect.*, vol. 33, pp. 15–26; Jan., 1953.) A review of the many uses of Ge rectifiers and transistors.

621.314.7.001.8 1851

Properties and Utilization of Transistors—J. M. Moulon. (*Onde élect.*, vol. 33, pp. 27–35; Jan., 1953.) A review of the characteristics of point-contact and p-n junction transistors and of their applications in amplifiers, negative-impedance repeaters, gating circuits, etc.

621.383+621.314.63 1852

Height of the Potential Barrier in Barrier-

Layer Cells—M. S. Ridout. (*Nature* (London), vol. 171, p. 219; Jan. 31, 1953.) If the barrier height is assumed to have a normal distribution about a mean value and to have a standard deviation, the equation relating zero-voltage resistance to temperature can be recast in a form which in general fits well the experimental results of Billig & Ridout (3135 of 1951) for Se, Ge and Si rectifiers and for Se photocells.

621.383.27 1853

Development and Use of Electron-Multiplier Photocells—A. Lallemand. (*Onde élect.*, vol. 32, pp. 492–495; Dec., 1952.) The general principles of construction of electron-multiplier photocells are discussed, with illustrations of the actual construction of cells with 7 and 19 stages respectively.

621.385:621.3.018.78 1854

Parasitic Effects and Distortion due to Curvature of Valve Characteristics—G. B. Dammers, J. Haantjes, J. Otte & H. Van Suchtelen. (*Philips tech. Commun., Aust.*, no. 7, pp. 3–26; 1952.) Reprint from "Applications of the Electronic Tube in Radio Receivers and Amplifiers" (991 of 1950).

621.385.029.63/.64 1855

Phase Distortion in Amplification by means of Traveling-Wave Valves—L. Brück. (*Arch. elekt. Übertragung*, vol. 7, pp. 28–36; Jan., 1953.) Reflections and dispersion introduced by the delay line give rise to a variation of the group transit time over the pass band which is of particular importance in wide-band amplifiers for multichannel radio links. An approximate determination is made of the distortion factor for fm signals. For a tube with a helix, distortion due to dispersion is negligible compared with that due to mismatching. Methods of reducing the latter are discussed.

621.385.029.64 1856

Space-Charge-Wave Amplifier Tubes, Basic Principles of Operation—R. G. E. Hutter. (*Sylvania Technologist*, vol. 5, pp. 94–99, Oct., 1952 & vol. 6, pp. 6–12; Jan., 1953.) The performance of space-charge-wave tubes (i.e. traveling-wave tubes, electron-wave tubes, single-stream electron-wave tubes etc.) is analyzed by considering them as composed of basic regions, viz., gaps between apertured electrodes, drift regions and slow-waveguide regions. A general electronic theory applicable to all the regions is developed. The circuit problem is discussed, first in general and then for each region, The combined electronic and circuit relations are derived.

621.385.032.216 1857

Thermionic Emission from Oxide-Coated Tungsten Filaments—C. P. Hadley. (*Jour. Appl. Phys.*, vol. 24, pp. 49–52; Jan. 1953.) An experimental investigation including (*a*)observations with a phosphor-coated tube of emission distribution, (*b*) retarding-field measurements, (*c*) accelerating-field measurements, and (*d*) X-ray diffraction study of the coating.

621.395.032.216 1858

The Effect of Impurity Migrations on Thermionic Emission from Oxide Cathodes—I. E. Levy. (Proc. I.R.E., vol. 41, pp. 365–368; March, 1953.) Emission measurements were made using diodes (*a*) similar to the A.S.T.M. standard, and (*b*) with specially purified materials. Results indicate the dependence of the work function on impurities migrating from parts of the tube other than the cathode.

621.385.032.216:537.311.33 1859

Semiconductors and Oxide Cathodes—R. Bourion. (*Onde élect.*, vol. 33, pp. 36–39; Jan., 1953.) Electron emission from semiconductors in vacuo is discussed in relation to Fermi energy levels. Reasons are given for considering that the active material in an oxide cathode is an excess semiconductor. Experimental results support this view, but the complex effects observed in oxide cathodes cannot be adequately explained by this simple theory.

621.385.032.8 1860

Vacuum-Tube Sockets for Industrial Equipment—W. Clarkin & L. F. Biosca. (*Elec. Mfg.*, vol. 48, pp. 72–77. 218; July, 1951.) A review of available types of wafer and moulded sockets suitable for receivers, and also for heavy-duty industrial service and for applications requiring low leakage, low loss, and reliable operation under vibration and humid conditions.

621.385.2 1861

Schottky's Equation for Thermal Electron Emission—H. Bonifas. (*Rev. gén. Élect.*, vol. 61, pp. 539–540; Nov., 1952.) An error in the development of this equation is pointed out, and a corrected formula is given for the anode current of a diode operating at constant temperature.

621.385.2 1862

Extension of the Planar Diode Transit-Time Solution—W. E. Benham. (Proc. I.R.E., vol. 41, pp. 395–396; March, 1953.) Comment on 497 of 1950 (Begovich).

621.385.2:537.533 1863

Electron-Gas Equations for Electron Flow in Diodes—H. Poritsky. (*Trans. I.R.E.*, pp. 60–84; Jan., 1953.) Analysis is presented which shows that Langmuir's results relative to the electron current in a diode can be recast in a form involving the concepts of electron gas. Examination of the discrepancies between Langmuir's results and those of Hahn (566 of 1949) indicates that they are due to somewhat arbitrary assumptions made by Hahn, and that the discrepancies disappear when these assumptions are properly modified. Langmuir's planar-diode equations, when put into a form involving gas motion, thus yield results identical with those obtained from analysis of the electron motion.

621.385.2:621.396.822 1864

Noise in Thermionic Valves—J. H. Fremlin. (*Proc. IEE* (London), part III, vol. 100, pp. 91–92; March, 1953.) The relation between Nyquist's formula for the mean square noise voltage generated by a resistive circuit and the formula for the fluctuation current in a temperature-limited diode is discussed. In the practical space-charge-limited case the thermodynamical approach is of little assistance; an explanation of this is given.

621.385.3 1865

Inherent Feedback in Triodes—H. Stockman. (*Wireless Eng.*, vol. 30, pp. 94–96; April, 1953.) The triode is considered as an infinite-impedance pentode, with the effect of the anode on the field at the cathode represented by negative feedback. By means of this transformation practical formulae are obtained for the triode circuit from conventional feedback theory.

621.385.3/.5].012 1866

The Effect of Filament Voltage upon Vacuum Tube Characteristics—A. J. Winter. (*Trans. I.R.E.*, pp. 47–59; Jan., 1953.) Operation of tubes with reduced filament voltages is discussed. By using the concept of an image cathode, located behind the real cathode at the position from which the electrons appear to be emitted, the principles of electrostatics can be applied to determine the effect of lowered cathode temperature on the amplification factor. Curves for a Type-6C4 triode and a Type-6AG5 pentode illustrate the fact that a higher gain can be obtained with a lower filament voltage. A 50% increase of gain has been obtained by reducing the filament voltage from 6.3 V to 3.0 V.

621.385.5.032.212 1867

A Ten-Stage Cold-Cathode Stepping Tube—D. S. Peck. (*Elec. Eng.* (N.Y.), vol. 71, pp. 1136–1139; Dec., 1952.) Description of the construction and operating characteristics of the Western Electric Type-6167 decade counter tube, which is capable of operating at pulse rates up to about 2000/sec.

621.385.832 1868

Single-Gun Storage Tube Writes, Reads and Erases—R. C. Hergenrother & A. S. Luftman. (*Electronics*, vol. 26, pp. 126–130; March, 1953.) An article based on a 1952 National Electronics Conference paper (*Proc. nat. Electronics Conf., Chicago*, 1952, Vol. 8, pp. 543–552). Improvements effected in an earlier model [2942 of 1950 (Hergenrother & Gardner)] are described which permit storage of charges for periods as long as a week with little loss and up to 27,000 play-backs with little effect on the storage pattern. Typical applications are noted.

621.385.832:621.397.62:535.37 1869

Phosphors for Television Cathode-Ray Tubes—H. G. Jenkins. A. H. McKeag & E. E. Welch. (*Proc. IEE* (London), part IIIA, vol. 99, no. 19, pp. 542–550. 1952. Discussion, pp. 571–576.) The development of television CR-tube screens and phosphors is reviewed, the theory of luminescence outlined, the preparation of the principal television-tube phosphors described and their characteristics noted. 44 references.

621.385.832.002.2:621.397.62 1870

Some Aspects of Modern Cathode-Ray-Tube Manufacture—L. J. Bayford. (*Proc. IEE* (London), part IIIA, vol. 99. no. 19, pp. 514–523; 1952. Discussion, pp. 571–576.) An account of the more important processes in the manufacture of aluminized television CR tubes, including descriptions of (*a*) a semi-automatic method of screen deposition, with film forming before screen drying, (*b*) the pipette specially designed to facilitate the continuous production of nitrocellulose films on fluorescent screens prior to aluminizing.

621.387:621.316.722.1 1871

Voltage-Regulator Tubes—W. Kiryluk. (*Electronic Eng.*, vol. 25, p. 83; Feb., 1953.) A method is outlined for determining the dynamic characteristics, from which the best operating point for each tube can be rapidly found.

621.396.615.14:621.385.029.6 1872

Traveling-Wave-Tube Oscillators—H. R. Johnson & J. R. Whinnery. (*Trans. I.R.E.*, pp. 11–35; Jan., 1953.) Analysis is presented for a type of oscillator comprising a traveling-wave tube with feedback via an external path including a cavity resonator of the transmission-line type. The analysis indicates that a tuning range of 4–8% should be obtainable by variation of the helix voltage. A range of 4.5% has been obtained experimentally, the center frequency being 2.72 mc and power output 0.3 W. Theory shows that the valve used should be short, with a high gain per unit length.

MISCELLANEOUS

061.3:621.39 1873

1953 I.R.E. National Convention, 23rd–26th March—(Proc. I.R.E., vol. 41, pp. 401–427; March, 1953.) Summaries are given of the papers presented.